Quinolone drugs: investigating pathways of DNA damage repair and antibiotic resistance

Isabel Díez Santos

A thesis submitted to the University of East Anglia for the degree of Doctor of Philosophy

John Innes Centre

Norwich, UK

May 2022

Abstract

Quinolones are widely used antibiotics that target bacterial topoisomerases. These are essential enzymes that modify the topology of DNA by making double-strand breaks (DSBs). Quinolones bind to topoisomerase-DNA complexes trapping the topoisomerases on the DNA. This causes bacterial death due to the formation of DSBs. But when the levels of quinolones are not high enough to kill bacteria, they can lead to the acquisition of antibiotic resistance (AR) to quinolone and non-quinolone antibiotics.

The link between the mechanism of action of quinolones and the acquisition of AR is not clear. In this work I have investigated whether quinolone-induced antimicrobial resistance (QIAR) depended on the repair of quinolone-induced DNA damage. I have explored different pathways of repair and found that the protease Lon, the nuclease Exo VII, and the recombinase RecBCD might work together to, first, digest part of the trapped topoisomerase, then remove the topoisomerase from the DNA and finally to repair the DSB. I have also shown that the quinolone ciprofloxacin induced resistance to several non-quinolone antibiotics, such as chloramphenicol. This ciprofloxacin-induced chloramphenicol resistance was due to mutations (i.e., mutations in *marR* or amplifications of *mdfA*) that depended on the SOS response, a bacterial response to DNA damage. However, this QIAR phenomenon was not solely dependant on Exo VII, one of the proteins involved in the repair of quinolone-induced DNA damage, suggesting that QIAR can be caused by an alternative pathway of DNA repair.

These findings may aid our understanding of how quinolones kill bacteria and induce mutations. They may have implications in the use of quinolones, as targeting the SOS response would improve quinolone activity and prevent QIAR. Still, further studies on the biological and clinical implications of QIAR are needed.

Statement

The work submitted within this thesis is entirely my own, except where due reference has been paid, and has not been submitted to this or any other university as part of any degree.

Contents

List of Figures

List of Tables

Acknowledgements

This project began four years ago, when I joined a PhD programme at the John Innes Centre. At that time, I did not know very well what I was going to do or how I was going to do it. I was just excited. Four years later, I look back at that moment and I feel grateful to myself for deciding to embark on this PhD, but, above all, for having been given the opportunity to do it.

Many people have been key in this journey and Tony Maxwell, my supervisor, is one of them. Thank you, Tony, for your constant support, your kindness, and your dad jokes. You've been a fantastic boss and a role model to follow.

I would also like to thank my secondary supervisor Mark Webber, and the rest of the members of my PhD committee (Tung Le, Bernardo Clavijo and Tash Bush) for all the advice and support they have provided. Additionally, I would like to thank BBSRC, the GSO, and the JIC, for funding this PhD and the 3-month placement I did in Pwani University (Kenya), that was one of the best experiences of my life.

Four people have read this thesis before being submitted: Tony, Tash, Emil and Nef. All your comments have been really helpful, and I would like to thank you for that.

This journey would have been much less exciting without some wonderful people. A big thank you to all the members of Tony's lab, especially Lesley, Tash, Nidda, Judit, Adam, Harriet, and Vicky for helping me in the lab and for making me laugh. Thank you, also, to the Spanish community in Norwich (Lola, Pablo, Abraham, Alba, Roger, Juan Carlos…) and to Basti for making me feel at home. And finally, thank you to my beach squad: Raf, Lira and Mimi. You have been the best PhD buddies I could have ever found.

También me gustaría agradecer a mis padres, a mi hermana y a mi cuñado su apoyo constante durante estos cuatro años. Papá, mamá, a pesar de no entender lo que hago, siempre me habéis apoyado en mi carrera. (Y ya veis, ¡estoy entregando la tesis a tiempo!).

Por último, quiero dedicar esta tesis a Nef, por acompañarme en los buenos y malos momentos y por ayudarme a ser una mejor científica y persona.

Chapter 1:

1 General introduction

Sections of this chapter are adapted from: Bush, N.G., Diez-Santos, I., Abbott, L. R., & Maxwell, A. *Quinolones: Mechanism, lethality and their contributions to antibiotic resistance.* Molecules, 2020. **25**(23) (Appendix IV).

1.1 Antibiotic resistance (AR)

Antibiotics are essential drugs used to treat and prevent bacterial infections. Most of the antibiotics are produced by bacterial and fungal species (e.g., *Streptomyces* and *Penicillium*) to combat the presence of other bacteria. A few of them, like the quinolone drugs, were synthesised in the lab and proved to be successful in killing bacteria. But bacteria, like any living organism, can adapt to new environments (e.g., the presence of an antibiotic) by developing defence mechanisms against it. This ability of bacteria to develop defence mechanisms to survive the effects of an antibiotic is called antibiotic resistance (AR).

1.1.1 AR is a global issue

Since antibiotics were first used in therapy in the 1940s, a growing number of pathogenic bacteria have evolved mechanisms of AR and have disseminated them to other bacteria. AR is a natural process that was thought to be negligible [1]. However, in the last 50 years, the appearance of multidrug-resistant bacteria and the rapid emergence of AR in microbes to almost all the antibiotics we use, have raised worldwide concern [2]. Several studies have signposted the overuse of antibiotics in medicine and agriculture and the lack of new antibiotics as the main causes of this antibiotic crisis [3]. According to the World Health Organization [4], almost every country in the world has observed high rates of AR in bacteria that cause common infections; and the trend has been predicted to rise (**Figure 1.1**). In fact, an independent review on antimicrobial resistance estimated that the annual deaths caused by antimicrobial-resistant pathogens would increase from 700,000 to 10 million by 2050 [5].

Understanding how bacteria become resistant to antibiotics and how they were selected for such resistance, is, therefore, crucial for developing new or alternative therapies to treat infectious diseases.
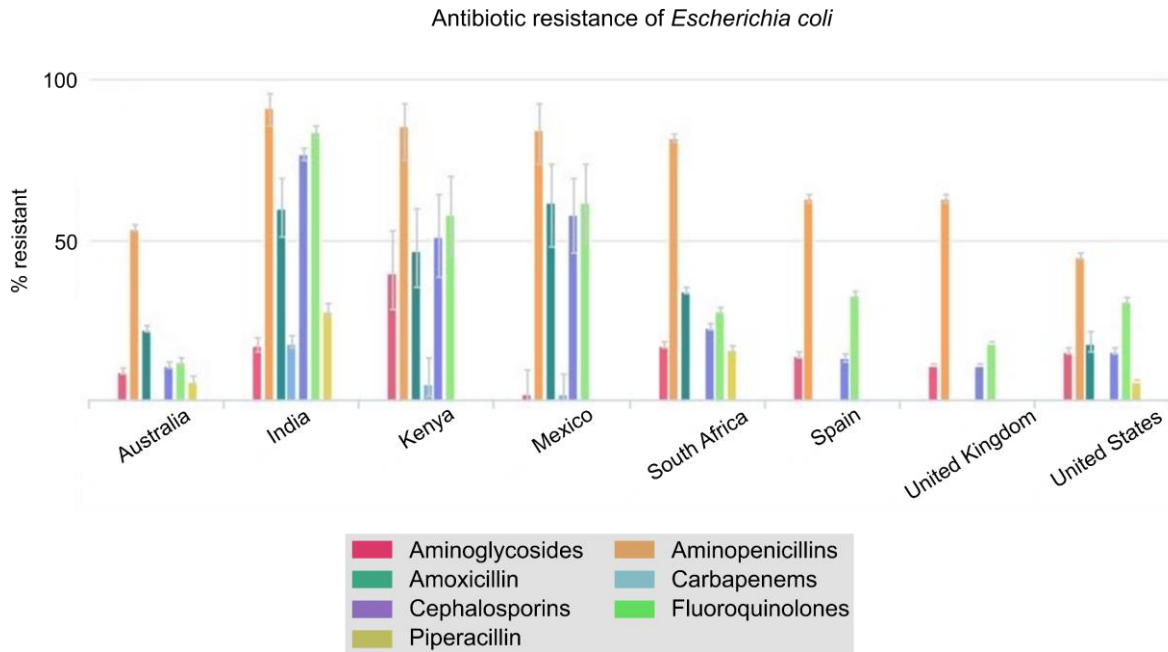
Figure 1.1. Percentage of *Escherichia coli* isolates resistant to different antibiotics in several countries in 2017. Figure obtained from The Center for Disease Dynamics, Economics & Policy. ResistanceMap: Antibiotic Resistance. 2021. https://resistancemap.cddep.org/AntibioticResistance.php. Date accessed: Jul 31, 2021.

1.1.2 How antibiotics kill bacteria

To understand how bacteria become resistant to antibiotics, we need to know how antibiotics work. Antibiotics interact with specific components of the bacterial cell (also called targets). This interaction does not kill the cell but can lead to downstream processes that are the ultimate cause of the bacterial death. Therefore, it is important to distinguish between how antibiotics interact with the cell causing an immediate effect (the mechanism of action) and the downstream processes that cause the bacterial death (the bactericidal action) [6].

Broadly, clinically-used antibiotics have four mechanisms of action: alteration of the cell envelope, inhibition of the synthesis of the nucleic acids, inhibition of the synthesis of the proteins, and inhibition of metabolic pathways (**Figure 1.2**) [7]. The cell envelope is the barrier that limits the contents of the bacterial cell from the outside. Depending on the composition of the cell envelope, bacteria can be divided into Gram-positive bacteria (that have a lipid membrane covered by layers of a polymer called peptidoglycan) and Gram-negative bacteria (that have an additional outer membrane). The cell envelope shapes the cell and controls the transport of molecules to or from the inside of the cell. The nucleic acids (RNA and DNA) are biomolecules that contain the information to make proteins,

which are another type of biomolecules in charge of most of the functions of the cell. Proteins are part of metabolic pathways in which they catalyse the chemical reactions occurring within the cell. They can also have other functions such as providing structure and support for cells or transporting other molecules throughout the body. These biomolecules are essential in bacteria and in any other living organism. However, some specific components are only present in bacteria or are different from the ones of other organisms. These components that distinguish the bacterial cell from other organisms, can be targeted by antibiotics (**Table 1.1**). For example, some proteins involved in the synthesis of peptidoglycan (a polymer that is only present in the bacterial envelope) are targeted by the antibiotic ampicillin. Another example of an antibiotic target is the bacterial ribosome that is different from the ribosomes of other organisms and that is targeted by molecules such as kanamycin, tetracycline, streptomycin, and chloramphenicol.
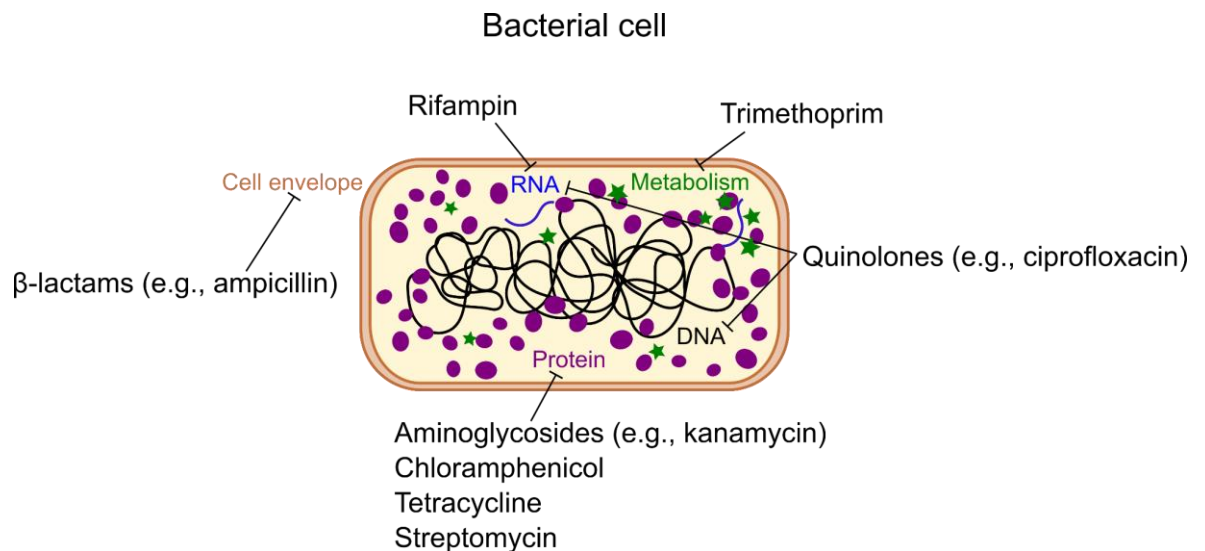
Figure 1.2. Different antibiotics and their mechanisms of action. β-lactams inhibit the synthesis of the cell envelope; aminoglycosides, chloramphenicol, and tetracycline, inhibit the synthesis of proteins; rifampin inhibits the synthesis of RNA; quinolones inhibit the synthesis of DNA and RNA; and trimethoprim inhibits the folic acid metabolism pathway.

Clinically relevant antibiotics can be classified into bactericidal or bacteriostatic depending on the rate at which they kill bacteria [8]. Bacteriostatic antibiotics kill at low rates, whereas bactericidal antibiotics kill at greater but substantially different rates [6]. Targeting protein synthesis, for example, can have either a bacteriostatic or a bacteriolytic effect [9], making it difficult to determine what makes an antibiotic bactericidal or bacteriostatic.

Ultimately, the mechanisms of action of all the antibiotics converge into two bactericidal actions: the disruption of the cell envelope or the loss of the genetic integrity of the cell [6].

Antibiotics that affect the cell envelope or the synthesis of proteins are thought to ultimately kill the cells by disrupting the cell envelope (**Table 1.1**). How this happens has only been recently shown in the case of β-lactams (antibiotics that target the cell envelope) [10]. β-lactams affect the balance between the synthesis and hydrolysis of peptidoglycan which leads to the appearance of holes in the cell envelope. These holes disrupt the cell envelope causing the loss of the internal turgor pressure and the dissipation of the content of the cell which inevitably kills it. In the case of antibiotics affecting the synthesis of DNA (this includes quinolones and trimethoprim), it is thought that their bactericidal action is due to the loss of the genetic integrity of the cell. Trimethoprim binds to dihydrofolate reductase which inhibits the production of an essential precursor for the synthesis of thymidine, a precursor of DNA. The inhibition of DNA synthesis is thought to provoke, somehow, DNA damage [11]. This is better understood with quinolones, which have been found to trigger a stress response in the cell that leads to breaks in the DNA [12]. If these DNA breaks are not repaired, the cell cannot perform most of its vital functions and ultimately dies.

Table 1.1. Examples of antibiotics used in this thesis and their classification based on their cellular targets, mechanisms of action, and bactericidal actions.

Antibiotic	Cellular target	Mechanism of action	Bactericidal action
Ampicillin	Penicillin-binding proteins	Inhibition of cell envelope synthesis	Disruption of the cell envelope [10]
Ciprofloxacin	Topoisomerase	Inhibition of DNA synthesis	Loss of the genetic integrity [13]
Trimethoprim	Dihydrofolate reductase	Inhibition of folic acid metabolism	Loss of the genetic integrity? [6]
Kanamycin	30S ribosomal subunit	Inhibition of protein synthesis	Disruption of the cell envelope? [6]
Tetracycline	30S ribosomal subunit	Inhibition of protein synthesis	Disruption of the cell envelope? [6]
Streptomycin	30S ribosomal subunit	Inhibition of protein synthesis	Disruption of the cell envelope? [6]
Rifampin	RNA polymerase	Inhibition of RNA synthesis	Disruption of the cell envelope? [6]
Chloramphenicol	50S ribosomal subunit	Inhibition of protein synthesis	Disruption of the cell envelope? [6]

The link between the mechanisms of action and the bactericidal action of antibiotics is not clear for most of the antibiotics. Of particular interest for this thesis is the case of quinolones that somehow kill bacteria by affecting their genetic integrity after they bind to topoisomerase proteins. This will be discussed in section 1.2.4.

1.1.2.1 Accumulation of reactive oxygen species (ROS): a common mechanism of action that leads to the loss of genetic integrity?

In 2007, Kohanski et al. [14] proposed a common mechanism of action for some antibiotics. They suggested that quinolones, β-lactams, and aminoglycosides killed bacteria by stimulating the production of reactive oxygen species (ROS). These are reactive molecules and free radicals derived from molecular oxygen. Some examples of ROS are hydrogen peroxide (H_2O_2), superoxide radicals ($\bullet O_2^-$), and hydroxyl radicals ($\bullet OH$). ROS are formed during aerobic respiration and cause mutations and DNA breaks when they react with the DNA [15]. Therefore, their accumulation can lead to the loss of the genetic integrity and the death of the cell.

Kohanski's hypothesis was contradicted by several studies that either did not show a correlation between ROS and antibiotic lethality or criticised the methodology of the experiments [16-18]. But in recent years, most studies have supported the ROS hypothesis, as it has been shown that antibiotics induce the formation of ROS, that the amount of ROS correlated with the lethality of the antibiotics and that the inhibition of ROS blocked the lethality of the antibiotics [11, 19-24]. However, we still do not know how antibiotics cause ROS. Some researchers proposed that antibiotics alter the cellular membrane, which stimulates the aerobic respiration and therefore the formation of ROS [25]. Thus, it seems that ROS do participate in the lethality of antibiotics, but it is not clear how.

1.1.3 How bacteria become resistant to antibiotics

Antibiotics can be lethal for bacteria unless bacteria have mechanisms of AR. How bacteria are able to resist antibiotics depends on the ability of bacteria to incorporate and spread AR factors, the presence of AR factors in bacterial cells, the selection of AR and the induction of AR.

1.1.3.1 Genetic mechanisms of AR

Bacteria can modify their genomes to become resistant to antibiotics. Mutations can occur in the bacterial DNA which can lead to AR if they affect, for example, how the antibiotic interacts with its target. Moreover, external DNA containing antibiotic resistance determinants can be acquired through horizontal gene transfer (HGT) [26]. HGT, which is the movement of genetic material between two microorganisms that are not parent and offspring, can lead to the movement of AR factors across different bacteria. HGT genetic exchanges occur by transformation (incorporation of extracellular DNA), transduction (injection of DNA from a virus) and conjugation (transfer of DNA from one bacterium to

another). Bacteria can incorporate or disseminate AR determinants by HGT which is one of the main reasons for the spread of multidrug resistance and the dissemination of AR in clinical environments [27].

1.1.3.2 Molecular mechanisms of AR

At a molecular level, bacteria have three main mechanisms to overcome the activity of antibiotics (**Figure 1.3**): the modulation of cell envelope permeability to antibiotics, the modification of the antibiotic cellular target, and the inhibition or inactivation of the antibiotic [28]. Bacteria can also survive transient exposure to antibiotics by not growing nor replicating during treatment [29]. This ability to survive antibiotics is called tolerance (when it refers to a whole population of bacteria) or persistence (if it refers to a subpopulation of bacteria and it is not inherited) [30].
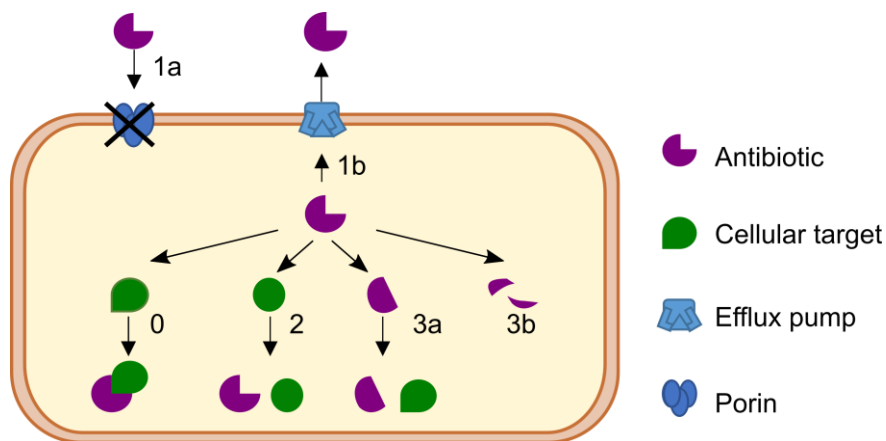
Figure 1.3. Molecular mechanisms of AR. In a susceptible (non-resistant) bacterium, the antibiotic binds to its target (0). To prevent antibiotic activity, bacteria have developed 3 different mechanisms of AR. The first mechanism of AR is the reduction of the presence of the antibiotic inside the cell by decreasing the expression of porins (1a) or by upregulating efflux pumps (1b). The second mechanism is the modification or protection of the antibiotic target so that the antibiotic cannot bind to it (2). The last mechanism is the modification (3a) or destruction (3b) of the antibiotic.

Bacteria can reduce the penetration of most types of antibiotics, including quinolones, β-lactams, and aminoglycosides, by decreasing the expression of porins and/or increasing the number of efflux pumps [31, 32]. Porins and efflux pumps are proteins embedded in the cell envelope that can transport antibiotics to the inside (in the case of porins) or to the outside of the cell (in the case of efflux pumps). Thus, having less porins decreases the uptake of the drug whereas having more efflux pumps increases the expulsion of the drug. For instance, *Escherichia coli* (*E. coli*), the most studied Gram-negative bacterium, can be

resistant to quinolones if it has mutations in the transcription regulators that control the expression of the porins and efflux pumps [33].

Another molecular mechanism of AR is the modification of the antibiotic target in a way that prevents the drug from binding its target. This can be done by having mutations in the target or by protecting the target from the antibiotic using another molecule. For example, a mutation in a topoisomerase (the target of quinolones) prevents the quinolone from binding its target causing quinolone resistance [34]. The activity of quinolones is also inhibited when bacteria produce the protein MfpA that binds to the topoisomerase preventing the binding of the quinolone [35].

Apart from altering the cell wall permeability and the antibiotic target, bacteria can also modify the antibiotic to avoid its activity. Bacteria have enzymes that inactivate antibiotics by adding specific chemical groups (mainly acetyl, phosphoryl and adenyl groups) and hydrolytic enzymes that destroy the drugs. One example of resistance via the modification of the drug, is the enzyme Aac(6′)-Ib-cr, an acetyltransferase that modifies quinolone drugs, decreasing their effectiveness [34]. On the other hand, penicillinase, an enzyme that breaks penicillin, is a typical example of an enzyme that can destroy an antibiotic [2].

1.1.3.3 Selection of AR

Antibiotics act as an environmental pressure on bacteria. They are important selectors of AR that can influence the presence and abundance of antibiotic-resistant bacteria in populations [36].

Depending on the concentration of antibiotics, antibiotic-resistant bacteria are selected in different ways (**Figure 1.4**). At lethal concentrations, all bacteria except the intrinsically antibiotic-resistant strains die, and, therefore, only bacteria that are resistant to lethal concentrations of antibiotics are selected (or enriched) in the population [1]. Sublethal concentrations of drugs can also select for AR [1, 37, 38] by enriching pre-existing resistant bacteria [39] or by enriching induced resistant bacteria [40]. Because bacteria are frequently exposed to low levels of antibiotics in their natural environment (produced by other organisms or as a residue from human production) and in our bodies, it is likely that low levels of antibiotics have an important role in the extensive emergence of AR.
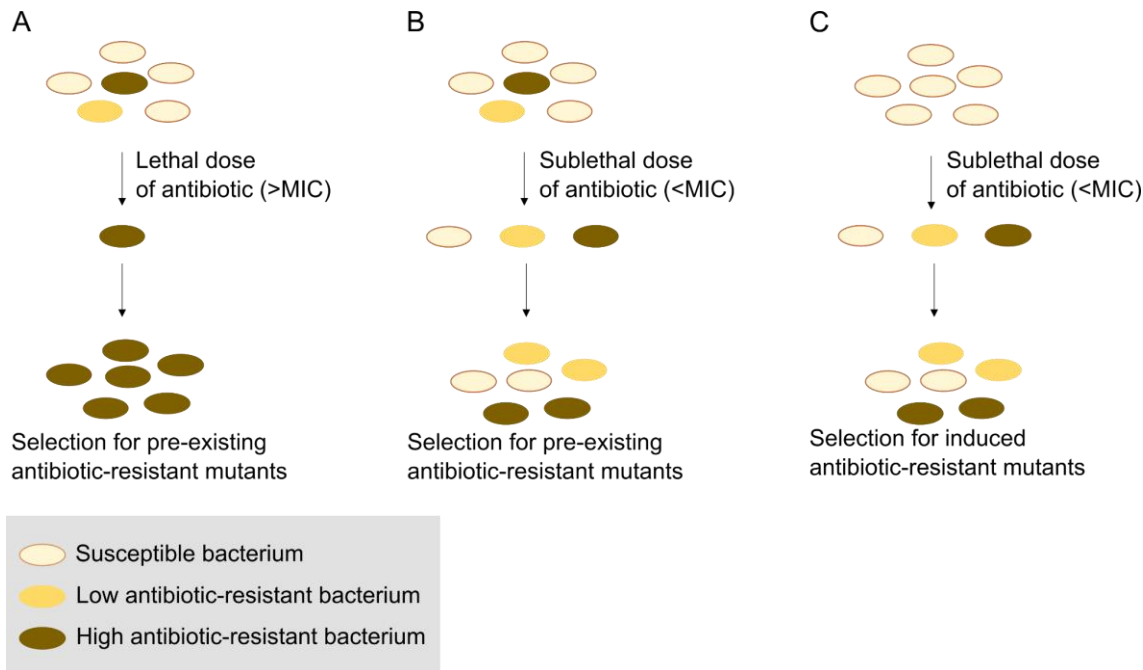
Figure 1.4. AR selection at different concentrations of antibiotics. A) When an initial population containing antibiotic-resistant bacteria are exposed to lethal (high) concentrations of antibiotics, only the high antibiotic-resistant colonies survive and are eventually enriched (selected) in the population. B) If the same initial population as in A) is administered sublethal concentrations of antibiotics; susceptible, low, and high antibiotic-resistant bacteria survive and are selected. C) In an initial population containing no pre-existing antibiotic-resistant bacteria, sublethal antibiotic concentrations can induce the emergence of low and high antibiotic-resistant bacteria that are eventually selected. The MIC refers to the minimum inhibitory concentration of an antibiotic necessary to inhibit the growth of bacteria. Concentrations below the MIC (<MIC) are considered sublethal whereas concentrations over the MIC (>MIC) are considered lethal.

But does AR occur randomly or is it induced by the antibiotic action? If AR occurs randomly, in an initial antibiotic-susceptible population, a few cells spontaneously become antibiotic-resistant before the addition of the antibiotic and will be enriched in the presence of the drug. On the other hand, if AR is induced by the antibiotic, in an initial antibiotic-susceptible population, a few colonies will become antibiotic-resistant because of the antibiotic action, and will also be selected by the presence of the antibiotic [38]. To test the random and induced hypothesis, Luria and Delbruck [41] designed an experiment with bacteria and viruses in which they recorded the proportion of resistant bacteria that would survive the attack of a virus. If the random hypothesis was true, the fluctuations of numbers of resistant bacteria should be large, as the number of resistant colonies would depend on the time when the mutation happened, whereas under the antibiotic-induced

hypothesis, smaller fluctuations would be expected. They found that the proportion of resistant strains varied greatly from day to day, indicating that mutations occurred spontaneously and, therefore, were not induced by the virus. This experiment, along with others [42, 43] supported the idea that antibiotics did not induce AR and that the exposure to antibacterial agents resulted in the selective enrichment of pre-existing resistant strains. However, as we will discuss later in more detail, other studies later found that certain antibiotics can induce antibiotic-resistant mutations, HGT or recombination events that result in AR.

1.1.3.4 Induction of AR

In the previous section, I have mentioned that sublethal concentrations of antibiotics can select for pre-existing and induced mutants at the expense of their susceptible counterparts. The presence of pre-existing mutants can be explained by random mutations; however, the existence of induced mutants indicates that antibiotics might also cause AR. Several groups have suggested that antibiotics activate stress responses that lead to mutations. If these mutations affect the antibiotic action, they can ultimately give rise to AR [44]. Four mechanisms that explain antibiotic-induced resistance have been proposed: *i*) the emergence of persisters, *ii*) HGT events, *iii*) the stimulation of recombination and *iv*) the enhancement of mutagenesis.

1.1.3.4.1 Emergence of persisters

Persisters are cells that can survive lethal concentrations of antibiotics without changing their DNA. How persisters manage to survive the antibiotic action is not clear, though it has been suggested that they can inactivate the drug target or lower the drug uptake [45]. Dorr, Lewis and Vulic [46] showed that low levels of quinolones induced the formation of persisters by activating a stress response and DNA repair pathways. Also, Barrett et al. [47] found that quinolones induced a stress response in persisters that accelerated the acquisition of resistance to unrelated antibiotics like rifampin. Therefore, alterations in the metabolism of bacteria caused by quinolones can influence later modifications in their DNA that can cause AR.

1.1.3.4.2 HGT events

HGT processes are also induced by low levels of antibiotics like quinolones and trimethoprim. Such genetic variations can increase the bacterial virulence as well as the dissemination of AR [48-50]. For example, ciprofloxacin has been found to induce the transfer of mobile conjugative elements that encode genes conferring resistance to chloramphenicol, trimethoprim and other antibiotics [49]. However, another study has claimed that the contribution of low levels of antibiotics to the promotion of HGT-mediated

AR has been overestimated [51]. Thus, the effect of antibiotics on HGT needs to be further studied.

1.1.3.4.3 Stimulation of recombination

Recombination is the rearrangement of genetic material in the cell. It can happen, for example, when segments of DNA are moved from one place to another within the genome. Those segments of DNA, also called integrons, can have AR genes. Depending on their position in the genome, those AR genes can be transcribed at different rates, which in turns affects how resistant to an antibiotic the bacterium is [52]. Antibiotics have been shown to affect the recombination of integrons. Hocquet et al. [53] investigated a high level β-lactam-resistant strain of *Pseudomonas aeruginosa* isolated from a patient treated with the antibiotic metronidazole (an antibiotic that inhibits DNA synthesis). They observed that the high level β-lactam-resistant strain had an integron-mediated rearrangement of β-lactamase genes. Also, they demonstrated that metronidazole treatment could cause the re-arrangement of β-lactamases encoded by integrons resulting in bacterial resistance to β-lactams. This study was carried out with high levels of antibiotics, however, there is also evidence that sublethal concentrations of quinolones can stimulate recombination in *E. coli* [54] albeit it has not been linked to the acquisition of AR.

Another type of recombination, illegitimate recombination (IR), might also play a role in AR. IR is a type of recombination that, contrary to homologous recombination, occurs between DNA strands that share little or no homology. Topoisomerases are thought to cause IR events that could result in small deletions, insertions, duplications and translocations, although the mechanism(s) are not fully understood [55]. Thus, it is plausible that one of the mechanisms by which quinolones induce the acquisition of AR is by promoting IR events. For instance, Cirz et al. [56] attributed the existence of small deletions after sublethal ciprofloxacin treatment to an IR pathway. However, the potential role of IR in quinolone-induced antibiotic resistance has not yet been proven.

1.1.3.4.4 Enhancement of mutagenesis

The frequency of observed antibiotic-resistant mutants and the rate at which mutation events arise are increased by the action of some antibiotics like quinolones, aminoglycosides, glycopeptides or β-lactams [57]. When different bacterial species were exposed to low levels of such drugs the mutation frequencies and rates were increased in comparison with the cells left untreated [58-60]. In particular, quinolones, which are the focus of the present project, seem to have a higher mutagenic effect than other types of antibiotics and have been shown to promote AR by mutagenic mechanisms.

1.2 Quinolones

1.2.1 Story of quinolones

In 1962, the chemist Lester Mitscher found a compound during the production of the antimalarial agent chloroquine that had antimicrobial activity. This compound was used to synthesise the first quinolone: nalidixic acid [61] (**Figure 1.5**). The 1st generation of quinolones, that included nalidixic acid and oxolinic acid among others, were active against Gram-negative bacteria and were used to treat urinary tract infections (UTIs) [62]. To improve the spectrum of activity of quinolones, a fluorine atom was added on carbon 6 of the quinolone scaffold, producing a fluoroquinolone. This modification made quinolones active against some Gram-negative and Gram-positive bacteria. 2nd, 3rd, and 4th generation quinolones (all of them fluoroquinolones) had additional modifications that made them active against more bacterial species and less toxic for humans. One of those fluoroquinolones, ciprofloxacin, is currently used to treat UTIs, febrile neutropenia, cholera, osteomyelitis, prostatitis, and septicaemia, and is one of the most used antibiotics worldwide [63].
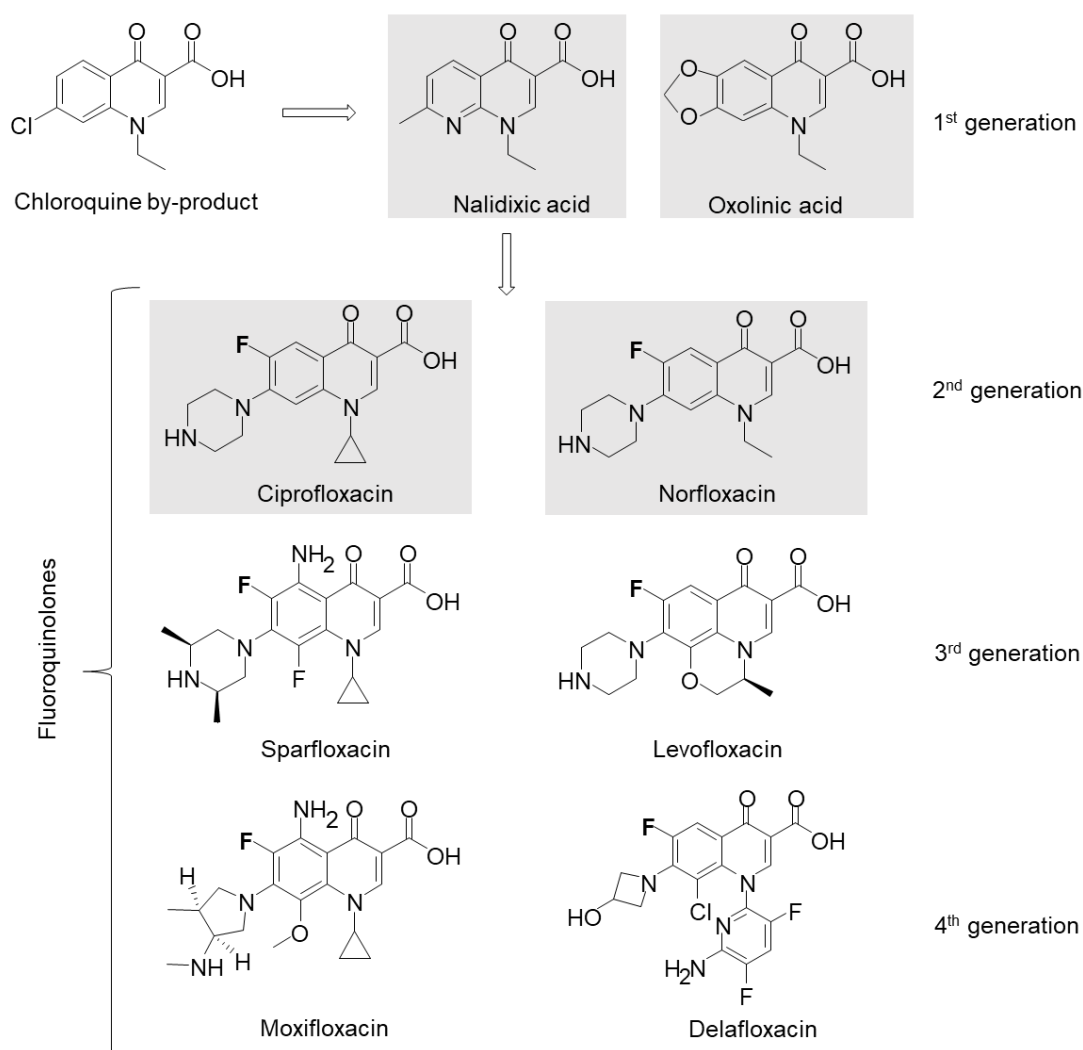
Figure 1.5. Chemical structures of several quinolones in the order in which they were synthesised. The chloroquine by-product was used as a lead compound to synthesise nalidixic acid, the first quinolone. 2nd, 3rd, and 4th generation quinolones have a fluorine atom in carbon 6 and are classified as fluoroquinolones. The grey squares highlight the quinolones that were investigated in this thesis.

1.2.2 Quinolones' target: type II topoisomerases

Quinolones target bacterial DNA topoisomerases. These are proteins that, like "cellular engineers", modify the topology of DNA (i.e., how relaxed, supercoiled, knotted and/or catenated the DNA is) [64] (**Figure 1.6**).

The topology of DNA plays an important role in several essential cellular processes. For example, when the DNA is copied (a process known as replication), the strands of the DNA need to be separated. This creates a structure called replication fork with positive

supercoils in front of it and precatenates behind it. If too much positive supercoiling builds up, the proteins involved in the replication of the DNA cannot progress, and the DNA cannot be synthesised. The same happens when the DNA needs to be transcribed into RNA (a process called transcription). The separation of the DNA strands creates a transcription bubble structure with positive supercoils in front of it and negative supercoils behind it. Too much positive supercoiling inhibits transcription and therefore the production of RNA [65].
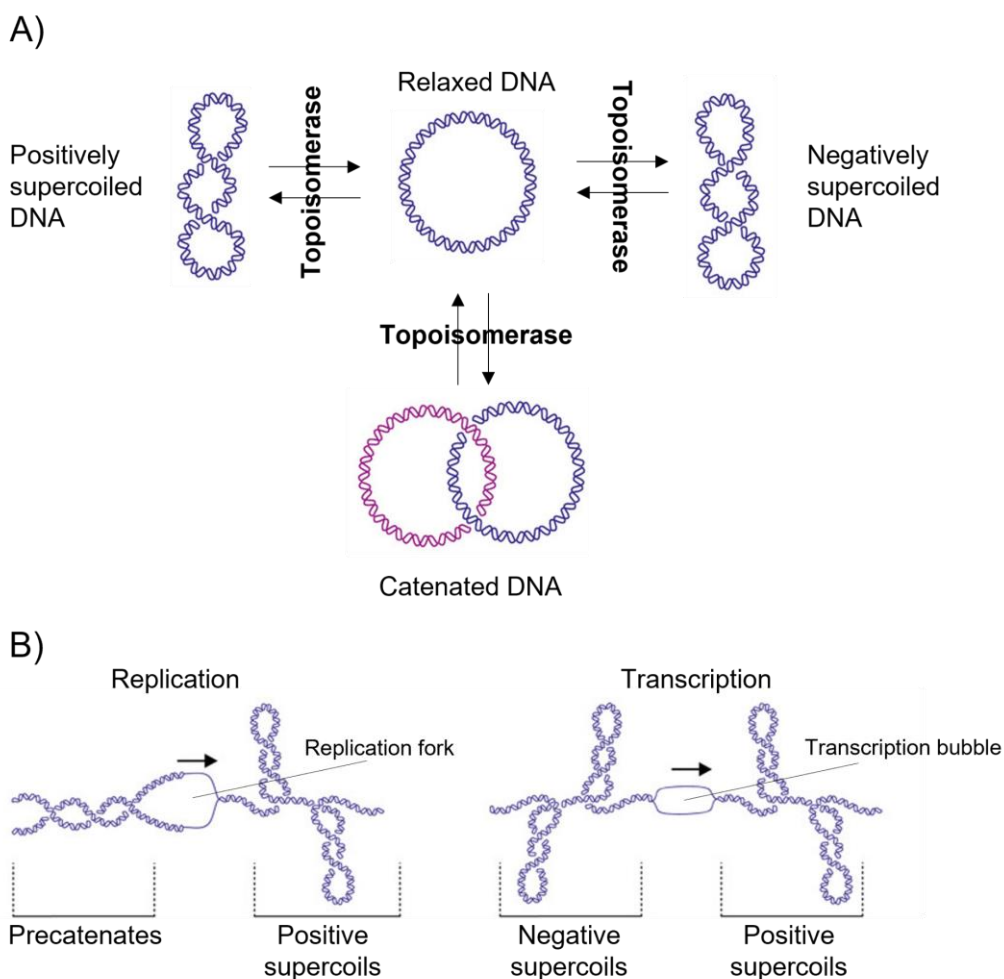
Figure 1.6. Topological states of the DNA. A) Topoisomerases can modify the topology of the DNA by relaxing, supercoiling, catenating or decatenating the DNA. B) During replication and transcription, the DNA suffers topological changes before and after the location where the replication or the transcription are happening. Figure adapted from [64] with permission.

Topoisomerases can be divided into type I or type II depending on whether they make a single- or a double-strand break in the DNA, respectively. As quinolones target type II topoisomerases, I will focus on type II topoisomerases. *E. coli* has two type II

topoisomerases: DNA gyrase (gyrase) and topoisomerase IV (topo IV). Gyrase and topo IV can relax and decatenate DNA, although topo IV is preferentially a decatenase. Gyrase is unique in that it is the only topoisomerase that can introduce negative supercoils, which is important for the initiation of DNA replication and transcription [66]. Gyrase is ubiquitous and essential in bacteria, but not in humans, making it an ideal target for antibiotics. Nonetheless, gyrase is found in plants and plasmodial parasites. In humans and other eukaryotes, DNA topoisomerase II (topo II) is a comparable enzyme, but it differs enough from bacterial gyrase and topo IV to allow these enzymes to be targeted selectively [34].

Gyrase and topo IV are heterotetramers; that is, formed of four separate subunits (two subunits X and two subunits Y). Gyrase is composed of two GyrA and two GyrB, and topo IV is composed of two ParC and two ParE. Type II topoisomerases have a complex reaction cycle (**Figure 1.7**). They bind two pieces of DNA: a G (or Gate) segment and a T (or Transported) segment. The enzyme cleaves the G segment in both strands of DNA, leaving a four-base-pair staggered break. To make this double-strand break (DSB), the topoisomerase binds covalently to the DNA using a tyrosine residue from each GyrA or ParC subunit. This reaction intermediate, with the enzyme covalently linked to broken DNA, is referred to as the cleavage complex. Once the DSB in the G segment is made, the topoisomerase passes the T segment, re-ligates the DSB and releases the T segment.
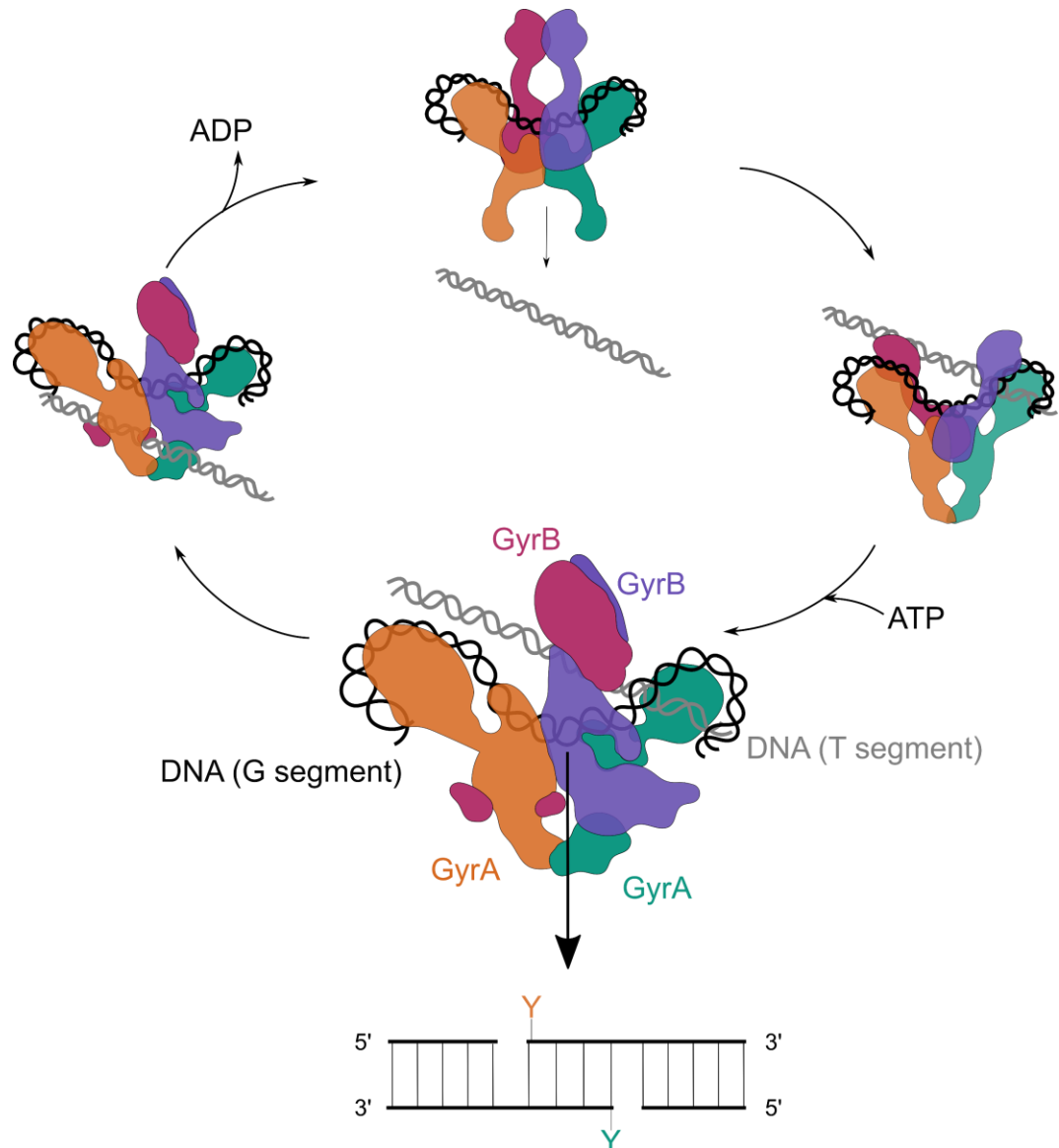
Figure 1.7. Gyrase reaction cycle. Gyrase is represented with a cartoon based on a cryo-electron microscopy structure of the complete *E. coli* gyrase (PDB 6RKW) [67]). Gyrase is composed of two GyrA subunits (pictured in orange and in green) and two GyrB subunits (pictured in pink and purple). Gyrase binds to a piece of DNA (G segment, in black) and captures another piece of DNA (T segment, in grey) by opening the GyrB subunits. Upon binding to ATP, the GyrB subunits close, and gyrase binds covalently to the G segment through a catalytic tyrosine (Y) residue from each GyrA. The binding of gyrase to the DNA causes a transient double-strand break (DSB) in the G segment. Gyrase uses that DSB to pass the T segment through the G segment and then religates the break. The T segment is then released by opening the GyrA subunits and the cycle can start again.

Quinolones interact with both subunits of the topoisomerase (GyrA and GyrB in the case of gyrase, or ParC and ParE in the case of topo IV) as well as the DNA (**Figure 1.8**) [68, 69]. The interaction between the quinolone and the topoisomerase-DNA complex is based on a water-metal ion bridge in which specific serine and acidic residues from the topoisomerase have a key role.

A)

B)

Intercalation of quinolones in the DNA

C)

Interaction of a quinolone with topo IV and the DNA
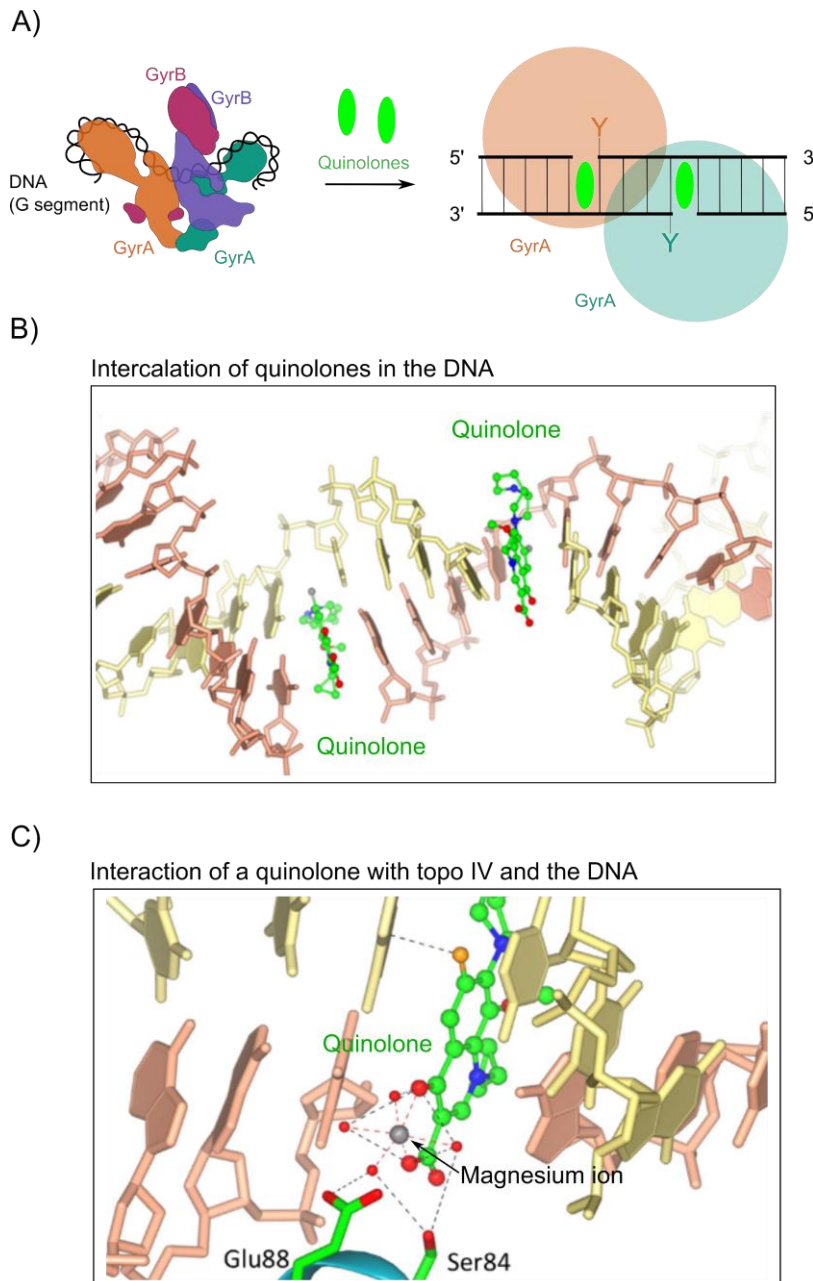
Figure 1.8. Interaction of quinolones with a topoisomerase-DNA complex. A) Schematic representation of gyrase and the location where quinolones intercalate in the DNA. B) Detail of the fluoroquinolone moxifloxacin (ball and stick, green carbons) partially intercalated into the DNA bases at the break sites, spaced 4-bp apart (PDB 2XKK). C) Detail of the interaction of moxifloxacin (ball and stick, green carbons) with topo IV and the

DNA (PDB 2XKK). A magnesium ion coordinates the interaction between the quinolone and the topoisomerase through a water bridge.

Quinolones intercalate between DNA bases at the DNA-cleavage site (where the topoisomerase breaks the DNA) so that there is one quinolone per break. The presence of the quinolones at the DNA-cleavage site physically blocks the religation of the DNA and stabilises the state of the topoisomerase in which it is covalently bound to the DNA [70]. Thus, in the presence of quinolones, the topoisomerase remains trapped on the DNA.

1.2.3 Quinolones' mechanism of action

The immediate consequence of quinolones trapping the topoisomerase on the DNA (or the mechanism of action of quinolones) is the inhibition of the synthesis of DNA and RNA [71, 72]. Because the topoisomerase is stuck on the DNA, the DNA strands cannot be separated, and the replication and transcription cannot proceed [73, 74]. The blockage of replication or transcription inhibits the synthesis of DNA or RNA, respectively. This inhibits the growth of the bacteria; however, it does not affect the lethality of quinolones [75, 76]. Hence, the bactericidal action of quinolones is due to downstream factors.

1.2.4 Quinolones' bactericidal action

Quinolones induce DNA breaks [77, 78], that correlate with their bactericidal action [75, 79]. Also, quinolones induce stress responses that are activated by the presence of DNA damage [80]. Thus, it is believed that quinolones kill by inducing DNA breaks which cause the loss of the genetic integrity of the bacterium. However, the origin (or origins) of those DNA breaks it is not clear yet (**Figure 1.9**).
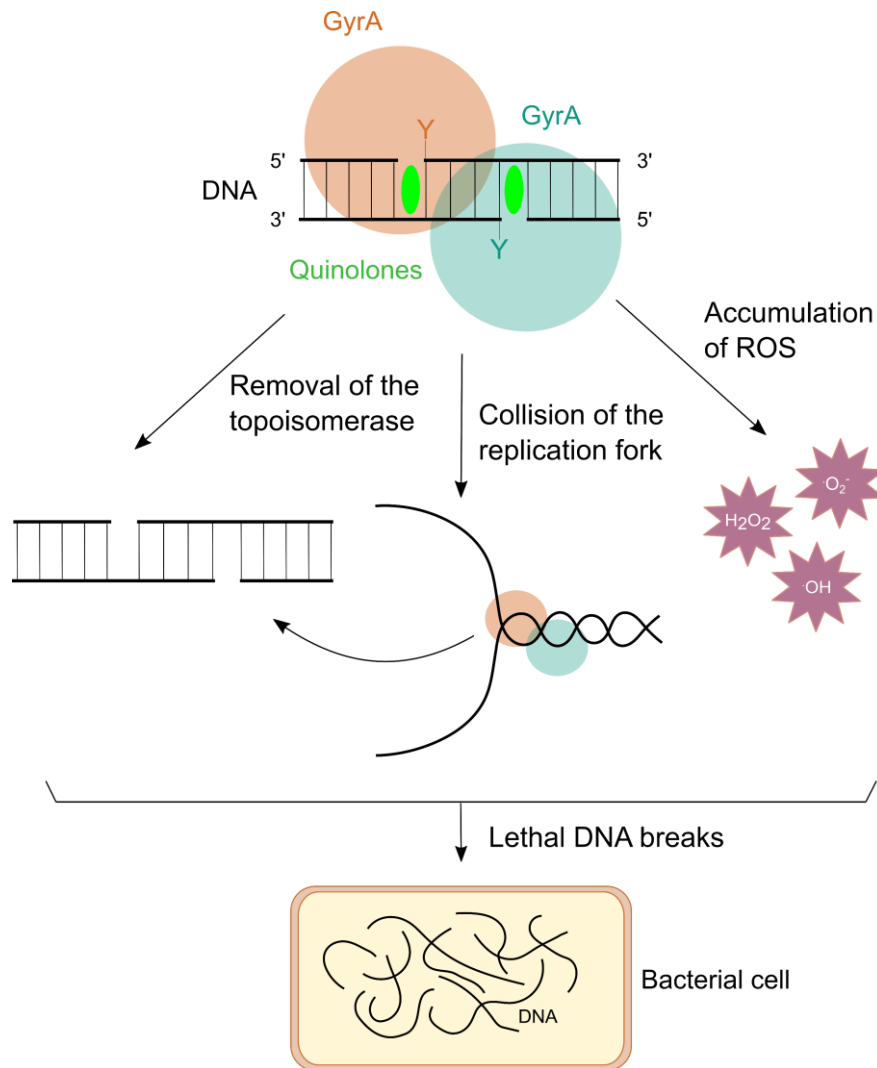
Figure 1.9. Potential origins of the quinolone-induced lethal DNA breaks. Quinolones lead to lethal DNA breaks after they bind to topoisomerase-DNA complexes. The origin of those lethal breaks might be the removal of the trapped topoisomerase from the DNA, which reveals a DSB, the collision of the replication fork with the trapped topoisomerase or the accumulation of ROS.

Several groups have tested whether the origin of the quinolone-induced DNA breaks is the DSB made by the topoisomerase [12, 75, 79]. But that DSB is only exposed in 0.1% of trapped topoisomerases [81], suggesting that it is "hidden" in the topoisomerase. Thus, the topoisomerase needs to be removed from the DNA so that the DSB can be exposed. Depending on the quinolone there are three pathways in which a poisoned topoisomerase can be removed from the DNA [82]. First generation quinolones, such as oxolinic or nalidixic acid, are not lethal in the presence of a protein-synthesis inhibitor (e.g., chloramphenicol) or under anaerobic conditions, and therefore, they belong to the protein synthesis, aerobic-dependent pathway. Norfloxacin, a 2nd generation quinolone, is not

lethal in the presence of chloramphenicol, but it is lethal under anaerobic conditions and, thus, belongs to the protein synthesis-dependent, aerobic-independent pathway. Ciprofloxacin, a 2nd generation quinolone, and other 2nd and 3rd generation quinolones are lethal regardless of protein synthesis or aerobiosis, so they belong to the protein synthesis, aerobic-independent pathway [75, 82]. In principle, trapped topoisomerases could be removed by a protein (e.g., either a nuclease that cleaves next to the topoisomerase-DNA bond, a protease that processes the topoisomerase or a protein that specifically breaks the bond between the gyrase and the DNA) or by the dissociation of the gyrase subunits. For the 1st generation quinolones that belong to the protein synthesis-dependent pathway, it is expected that said protein would be needed to be lethal. Whereas fluoroquinolones like ciprofloxacin, which are lethal regardless of continued protein synthesis, might be lethal due to dissociation of the gyrase subunits.

Other groups have tested if the origin of quinolone-induced DNA damage was the collision of the replication fork with the trapped topoisomerase [83, 84]. They found DNA breaks but only after the topoisomerase had been removed from the DNA. This is different to what was seen with drugs that trap eukaryotic topoisomerases on the DNA. Camptothecin, a stabiliser of the eukaryotic topoisomerase I, causes the formation of DSBs when the replication fork collides with the cleavage complex [85-87]. A similar situation might happen with topo II-DNA cleavage complexes. For instance, m-AMSA, an inhibitor of topo II, is less lethal in the presence of a DNA synthesis inhibitor. This indicates that its lethality depends on the replication of DNA [88].

Another explanation for the origin of quinolone-induced DNA breaks is the accumulation of ROS. Several groups have shown a correlation between quinolone lethality and the accumulation of ROS [75, 89, 90]. They have done this by measuring levels of ROS and lethality after treating cells with quinolones and inhibitors of ROS or using strains overproducing or lacking enzymes that regulate oxidative stress. For example, Dwyer et al. [19] showed that, after norfloxacin treatment, ROS-related genes were upregulated, there was an increase in •OH and no killing was observed when a ROS neutralizer was used. However, Liu et al. [16] showed that quinolones did not increase the levels of ROS, and Keren et al. [17] found no correlation between ROS formation and quinolone lethality. The disparities between these results and the ones from Dwyer et al. [19] were addressed in an exhaustive review (see [91]), and since then, several studies have shown that ROS account, at least in part, for the lethality of all quinolones [23, 24]. The ROS theory is also supported by the fact that a co-treatment with DMSO (an inhibitor of ROS) suppressed the number of ciprofloxacin-induced DSBs [78]. ROS can convert single-stranded DNA breaks into double-stranded breaks [92] and that the accumulation of ROS can be self-amplifying

[23]. Thus, it is possible that the accumulation of ROS causes lethal DNA breaks, although as I mentioned before (section 1.1.2.1), how quinolones induce ROS is not well understood.

1.2.5 Repair of quinolone-induced DNA damage

Quinolones cause DNA damage that can be repaired [93]. This repair was shown in two studies that measured the density of the cell or the formation of DNA breaks in bacteria during quinolone treatment and after removing the quinolone. In the first study they found that the removal of the quinolone caused an increase in the cell density. This suggests that DNA breaks were resealed, as the longer the DNA is, the more viscous the solution is [79]. In the second study they observed that the DNA of quinolone-treated cells was less fragmented after the quinolone was removed [94].

Because the origin of quinolone-induced DNA damage is not well understood, it is difficult to explain how bacteria can repair this damage. Also, it is likely that DNA damage from different origins is repaired in different ways. However, we know that several DNA repair proteins are involved (as their absence make cells more sensitive to quinolones) and that several stress responses are activated [46, 95].

For example, the deletion of the genes *recA/B/C/D/G/N* or *uvrB*, makes bacteria hypersensitive to quinolones [96, 97]. RecA/B/C/D/G/N are proteins that repair DSBs through the homologous recombination (HR) pathway, whereas UvrB participates in the nucleotide excision repair pathway (NER) [98]. The HR and NER pathways have been shown to participate in the repair of proteins irreversibly trapped on the DNA [99]. The expression of those DNA repair proteins is controlled by a general stress response called the SOS response (**Figure 1.10**). This is the bacterial response to DNA damage, and it is regulated by RecA and LexA [100]. In the absence of DNA damage, LexA represses the transcription of the SOS genes. But in the presence of DNA damage, RecA is activated and LexA is degraded. As a result, LexA is no longer able to repress the transcription of the SOS genes. All quinolones activate the SOS response; however, it is not the sole stress response that quinolones trigger. Pribis et al. [77] discovered that when a subpopulation of cells is exposed to sublethal ciprofloxacin, they experience SOS and the formation of ROS, which activates the sigma S response. This is a broad stress response that controls the expression of hundreds of genes, including DNA repair genes. All these stress reactions result in the repair of DNA breaks by error-free (HR or NEB, for example) or error-prone (translesion synthesis, for example) DNA damage repair processes [100].

Error-free repair pathways do not result in mutations, but error-prone repair pathways do which is why it has been hypothesised that quinolones can be mutagenic [44].
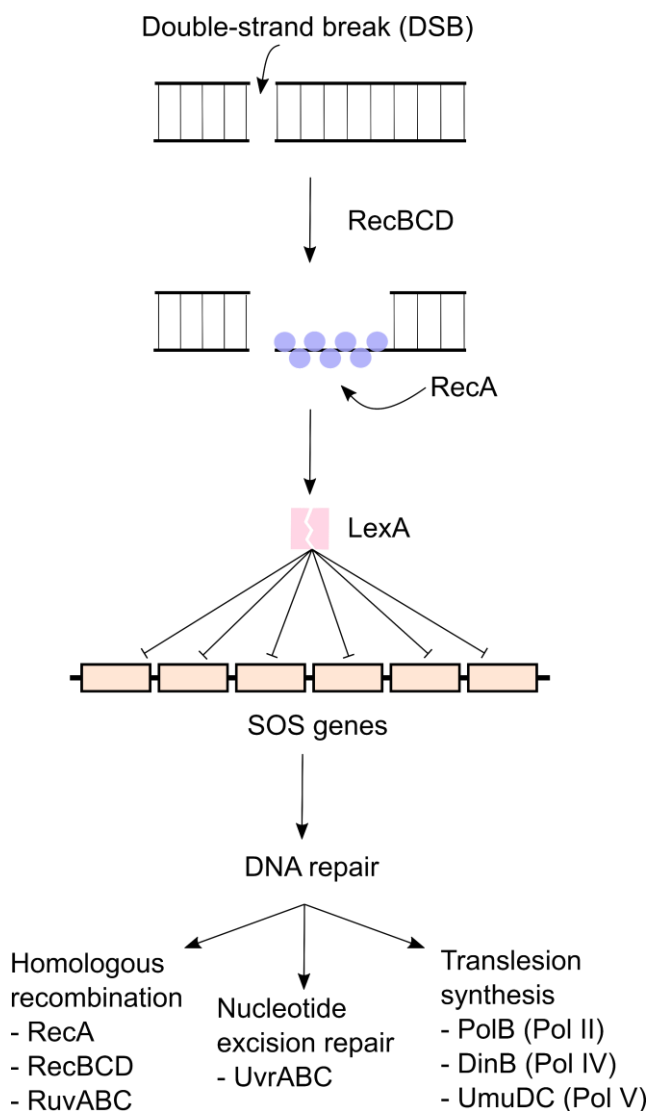
Figure 1.10. The SOS response. RecBCD binds to a double-strand break and digests one of the strands. RecA loads on the single-stranded DNA which leads to the auto-cleavage of LexA. As a result, LexA stops repressing the SOS genes, which activates the transcription of genes involved in DNA repair.

1.2.6 Quinolone-induced antimicrobial resistance (QIAR)

Treatments with low levels of quinolones have been shown to increase mutation, recombination, and persister formation rates, often leading to an increase in the frequency of resistance to non-quinolone antibiotics [46, 54, 58, 101-104]. This ability of quinolones to induce antibiotic resistance has been named quinolone-induced antimicrobial resistance (QIAR) [55]. Despite the increasing number of articles that have studied the

QIAR phenomenon and its potential importance in antibiotic treatment, the mechanisms by which quinolones induce QIAR are not well known. Because most of the proposed mechanisms of QIAR are associated with the SOS response or the accumulation of ROS, I have classified them based on which of those cellular responses was predominant.

1.2.6.1 The role of the SOS response on QIAR

The relationship between quinolones and SOS induction has been investigated by several groups. Through transcriptome analysis, the upregulation of SOS-related genes after treatment with high levels of ciprofloxacin has been oberved in *E. coli* [105], *Salmonella* [106] and *Pseudomonas aeruginosa* [101]. Moreover, subinhibitory concentrations of ciprofloxacin also increased the transcription of SOS genes [107]. Other studies have shown that the transcription of *recA* is rapidly increased after being treated with quinolones, however, this increase was mantained for a short period of time [108, 109].

The specific role of RecA and LexA in quinolone mutagenesis has been largely studied. Several studies have compared the the mutation frequencies or rates of a RecA deficient mutant (Δ*recA*) and a LexA mutant unable to be degraded, with the ones of the wild type [110]. Because of the function of RecA and LexA in the SOS pathway (**Figure 1.10**), the absence of RecA and the lack of LexA autocleavage should prevent, in different ways, the initiation of the SOS response. Thus, if the induction of the SOS response is necessary for QIAR, RecA and LexA mutants should show a decrease in the AR mutation frequency or rate. Wang et al. [108] reported a lower ciprofloxacin-resistance mutation frequency in the *recA* mutant compared to the WT after ciprofloxacin exposure. Consistent with this result, Thi et al. [107] reported a decrease in the mutation frequency that led to rifampin and fosfomycin resistance after quinolone treatment when comparing the *recA* mutant with the WT. On the other hand, Cirz et al. [56] carried out *in vivo* studies in which they injected mice with LexA-defective *E. coli*. They found that no ciprofloxacin-resistant mutants were induced in the LexA-defective strains whereas ciprofloxacin-resistant clones were seen in the WT bacteria. Similar results were obtained when looking at ciprofloxacin mutation frequencies in a *lexA* mutant and WT *in vitro*. Moreover, Torres-Barcelo et al. [109] showed that the *lexA* mutant had a slight increase in fitness compared to the WT, and that the mutation rate in the presence of ciprofloxacin was higher in the WT compared to the *lexA* mutant.

Several groups have shown that the QIAR mutations were caused by SOS-activated polymerases [56, 77]. The SOS response activates the transcription of the polymerases *polB* (Pol II), *dinB* (Pol IV) and *umuDC* (Pol V) which can make mutations when repairing DNA breaks. However, Song et al. [111] found that the mutation frequencies of rifampin-

resistant mutants obtained after low levels of ciprofloxacin treatment did not depend on the SOS-activated polymerases, suggesting that SOS-induced polymerases might not be involved in QIAR.

1.2.6.2 The role of ROS on QIAR

Another stress-response pathway that have been associated with the quinolone action, is the oxidative stress. Quinolones are known to induce the formation of ROS (see section 1.2.4), which have been linked to the mutagenic effect of quinolones [112]. This was tested by Kohanski et al. [90] by exposing *E. coli* to sublethal concentrations of norfloxacin under different levels of oxidative stress. They showed that there was an increase in AR mutation rate that correlated with the level of oxidative stress. This piece of work though, has been questioned by other groups that have not found a relationship between low levels of quinolones and ROS mutagenesis [17, 113]. Hence, the role of ROS on QIAR needs to be further investigated.

1.3 Project aims

Quinolones are widely used antibiotics that can induce resistance to other antibiotics. However, the molecular mechanism of quinolone-induced antimicrobial resistance (QIAR) is not fully understood. QIAR is thought to be a consequence of the repair of quinolone-induced DNA damage, although the mechanism of this repair is not known. Thus, the aims of this thesis were to understand how bacteria repair quinolone-induced DNA damage and how this damage leads to antibiotic resistance. My hypothesis was that quinolones caused DNA breaks that activated repair responses able to make mutations conferring antibiotic resistance (**Figure 1.11**). To test this hypothesis, I have investigated how quinolones repair DNA breaks (Chapter 3, 4 and 5), and if this repair was involved in QIAR (Chapter 5). I have also tested if QIAR could happen in an animal model (Chapter 6). The results, limitations and implications of these chapters were further discussed in Chapter 7.
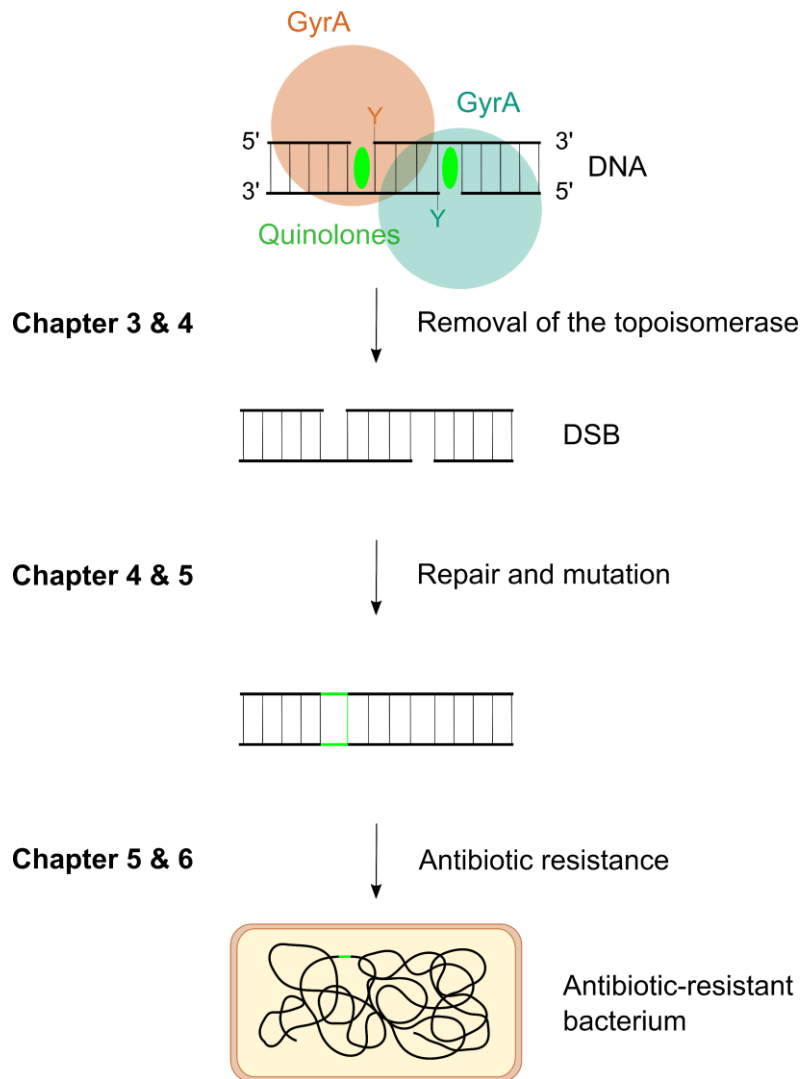
Figure 1.11. Hypothesis of this thesis. The removal of a quinolone-stabilised topoisomerase from the DNA reveals a double-strand break (DSB). The repair of this DSB by the bacterium can lead to mutations. If these mutations affect the action of an antibiotic, the bacterium becomes antibiotic-resistant. These statements were investigated in Chapters 3-6.

Chapter 2:

2 Materials and methods

2.1 Materials

2.1.1 Bacterial and bacteriophage strains, plasmids, and growing conditions

Escherichia coli (*E. coli*) strains, including the wild type [110] strains *E. coli* MG1655 (RefSeq accession no. NC_000913.3) and BW25113 (RefSeq accession no. CP009273.1) were grown in Luria-Bertani (LB) medium (10 g/L NaCl, Sigma; 10 g/L tryptone, Oxoid; 5 g/L yeast extract, Oxoid) supplemented with 1.5% w/w agar (Formedium) when indicated. When bacteria were transformed with DNA, they were grown on Super Optimal broth with Catabolite repression (SOC) medium made by the John Innes Centre Media Kitchen facility (5 g/L yeast extract, 20 g/L tryptone, 0.58 g/L NaCl, 0.186 g/L KCl, 2.03 g/L MgCl$_2$, 2.46 g/L MgSO$_4$, 3.6 g/L glucose). Bacterial cells were incubated at 37°C with agitation (when using liquid medium) or without agitation (when using medium supplemented with agar). To distinguish *E. coli* cells from Enterococci, cells were grown on MacConkey agar (Sigma).

Enterococcus gallinarum (*En. gallinarum*) and *Enterococcus faecalis* (*En. faecalis*) were grown on Brain Heart Infusion (BHI) media (Sigma) with or without 1.5% w/w agar (Formedium) at 37°C without agitation. Enterococcus selective media (Sigma) was used to distinguish *Enterococcus* strains from *E. coli* cells.

E. coli bacteriophage P1 (ATCCr 25404-B1^{tm}) was propagated as stated by Thomason et al. [114] and stored at 4°C.

For a complete list of all the bacterial and phage strains and plasmids see **Table 2.1**.

Table 2.1. List of bacteria, phages, and plasmids used in this thesis.

E. coli strain	Relevant features	Source
MG1655 WT	K-12 F⁻ λ⁻ *ilvG*- *rfb*-50 *rph*-1	*E. coli* Genetic Stock Centre
BW25113 WT	K-12 F⁻ λ⁻ Δ(*araD-araB*)*567* Δ(*rhaD-rhaB*)*568* Δ*lacZ4787* (::rrnB-3) *hsdR514 rph-1*	*E. coli* Genetic Stock Centre

BL21(DE3)pLysS	F− *omp*T *hsd*S$_B$ (r$_B^-$, m$_B^-$) *gal dcm* (DE3) pLysS(Cam^R)	Thermo Fisher
BL21 Star (DE3)	F− *omp*T *hsd*S$_B$ (r$_B^-$, m$_B^-$) *gal dcm rne*131 (DE3)	Thermo Fisher
Stellar	F− λ− Δ(*mrr* - *hsdRMS* - *mcrBC*) Δ*mcrA*	Takara Bio
EcNR2	MG1655 *bla bio* Red1 *mutS*– Cam^R	Addgene
BW25113 *xthA*::Kan^R (strain 1)	*xthA*::Kan^R (strain 1)	Keio collection
BW25113 *yafD*::Kan^R (strain 1)	*yafD*::Kan^R (strain 1)	Keio collection
BW25113 *yafD*::Kan^R (strain 2)	*yafD*::Kan^R (strain 2)	Keio collection
BW25113 *ybhP*::Kan^R (strain 2)	*ybhP*::Kan^R (strain 2)	Keio collection
BW25113 *ybhP*::Kan^R (strain 3)	*ybhP*::Kan^R (strain 3)	Keio collection
MG1655 *xthA*::Kan^R	*xthA*::Kan^R	This project
MG1655 *ΔxthA*	*ΔxthA*	This project
MG1655 *yafD*::Cam^R	*yafD*::Cam^R	This project
MG1655 *ybhP*::Kan^R	*ybhP*::Kan^R	This project
MG1655 *ΔxthA yafD*::Cam^R	*ΔxthA yafD*::Cam^R	This project
MG1655 *ΔxthA ybhP*::Kan^R	*ΔxthA ybhP*::Kan^R	This project
MG1655 *yafD*::Cam^R *ybhP*::Kan^R	*yafD*::Cam^R *ybhP*::Kan^R	This project
MG1655 *ΔxthA ybhP*::Kan^R *yafD*::Cam^R	*ΔxthA ybhP*::Kan^R *yafD*::Cam^R	This project
MG1655 *recA*::Kan^R	*recA*::Kan^R	Susan Rosenberg (Baylor College of Medicine)
BW25113 *recB*::Kan^R	*recB*::Kan^R	Keio collection
EcNR2 *clpP*::Kan^R	*clpP*::Kan^R	This project
MG1655 *ΔclpP*	*ΔclpP*	This project
EcNR2 *sbcCD*::Kan^R	*sbcCD*::Kan^R	This project
MG1655 *ΔsbcCD*	*ΔsbcCD*	This project
MG1655 *ΔsbcCD clpP*::Kan^R	*ΔsbcCD clpP*::Kan^R	This project
MG1655 *xseA*::Kan^R	*xseA*::Kan^R	This project
MG1655 *ΔxseA*	*ΔxseA*	This project
MG1655 *ΔxseA sbcCD*::Kan^R	*ΔxseA sbcCD*::Kan^R	This project
BW25113 *lon*::Kan^R (strain 1)	*lon*::Kan^R (strain 1)	Keio collection
MG1655 *lon*::Kan^R	*lon*::Kan^R	This project
MG1655 *Δlon*	*Δlon*	This project
MG1655 *ΔxseA Δlon*	*ΔxseA Δlon*	This project
MG1655 *ΔxseA recB*::Kan^R	*ΔxseA recB*::Kan^R	This project
Gam	MG1655 Gam Cam^R	Susan Rosenberg (Baylor College of Medicine)

Gam-GFP	MG1655 Gam-GFP Cam^R	Susan Rosenberg (Baylor College of Medicine)
Gam-GFP *xseA*::Kan^R	*xseA*::Kan^R	This project
MG1655 *dinB*::Kan^R	*dinB*::Kan^R	This project
MG1655 Δ*dinB*	Δ*dinB*	This project
MG1655 *polB*::Kan^R	*polB*::Kan^R	This project
MG1655 Δ*polB*	Δ*polB*	This project
MG1655 *umuD*::Kan^R	*umuD*::Kan^R	This project
MG1655 Δ*umuD*	Δ*umuD*	This project
MG1655 Δ*dinB* *polB*::Kan^R	Δ*dinB polB*::Kan^R	This project
MG1655 Δ*dinB* Δ*polB*	Δ*dinB* Δ*polB*	This project
MG1655 Δ*dinB* *umuD*::Kan^R	MG1655 Δ*dinB umuD*::Kan^R	This project
MG1655 Δ*dinB* Δ*umuD*	Δ*dinB* Δ*umuD*	This project
MG1655 Δ*polB* *umuD*::Kan^R	Δ*polB umuD*::Kan^R	This project
MG1655 Δ*polB* Δ*umuD*	Δ*polB* Δ*umuD*	This project
MG1655 Δ*dinB* Δ*polB* *umuD*::Kan^R	Δ*dinB* Δ*polB umuD*::Kan^R	This project
MG1655 Δ*dinB* Δ*polB* Δ*umuD*	Δ*dinB* Δ*polB* Δ*umuD*	This project
MG1655 *marR*::Kan^R	*marR*::Kan^R	This project
MG1655 Δ*marR*	Δ*marR*	This project
MG1655 *marR170*	*marR170*	This project
BW25113 Δ*e14*	Δ*e14*	NCTC
EcNR2 *lit*::Kan^R	*lit*::Kan^R	This project
MG1655 *lit*::Kan^R	*lit*::Kan^R	This project
EcNR2 *ymfM*::Kan^R	*ymfM*::Kan^R	This project
MG1655 *ymfM*::Kan^R	*ymfM*::Kan^R	This project
EcNR2 *lexA*(S119A)	*lexA*(S119A) Kan^R	This project
MG1655 *lexA*(S119A)	*lexA*(S119A) Kan^R	This project
29-1	29-1 ST469 Phylo B1	Ebenezer Foster-Nyarko (QIB)
H-18-2	H-18-2 ST9281 Phylo B1	Ebenezer Foster-Nyarko (QIB)
H-21-1	H-21-1 ST58 Phylo A	Ebenezer Foster-Nyarko (QIB)
H-21-4	H-21-4 ST540 Phylo B1	Ebenezer Foster-Nyarko (QIB)
Enterococci	**Relevant features**	**Source**
En. gallinarum	Not resistant to ciprofloxacin	Harriet Gooch (JIC)
En. faecalis	Not resistant to ciprofloxacin	Harriet Gooch (JIC)
Bacteriophage	**Relevant features**	**Source**
E. coli bacteriophage P1 (ATCCr 25404-B1^{tm})	Wild type, non-lysogenic	Jessica Blair (Institute of Microbiology and Infection, University of Birmingham)
Plasmid	**Relevant features**	**Source**
pUC19	Amp^R	Sigma

pKD4	Kan^R, FRT sites	*E. coli* Genetic Stock Center
pKD3	Cam^R, FRT sites	*E. coli* Genetic Stock Center
pKD46	Amp^R, λRed genes (*exo*, *beta*, *gam*), pBAD promoter, *repA101ts*	*E. coli* Genetic Stock Center
pCP20	*FLP* Amp^R Cam^R *repA101ts*	*E. coli* Genetic Stock Center
pCS6	T7 RNA polymerase under pBAD promoter, Spec^R	Thomas Germe (JIC)
pET28-MHL	*sacB* under T7-lacO promoter, HIS6, Kan^R	Lab stock
pET28-TDP2	*TDP2*	Nick Burton (Inspiralis)
pET28-YafD	*yafD*	This project
pET28-YbhP	*ybhP*	This project
pET28-XthA	*xthA*	This project
pOPINF	HIS6-3C	Neftaly Cruz Mireles (TSL)
pOPINJ	HIS6-GST-3C	Neftaly Cruz Mireles (TSL)
pOPINM	HIS6-MBP-3C	Neftaly Cruz Mireles (TSL)
pOPINS	HIS6-SUMO-3C	Neftaly Cruz Mireles (TSL)
pOPINJ-TDP2	*TDP2*	This project
pOPINM-TDP2	*TDP2*	This project
pOPINS-TDP2	*TDP2*	This project
pOPINJ-YafD	*yafD*	This project
pOPINM-YafD	*yafD*	This project
pOPINS-YafD	*yafD*	This project
pOPINF-Lon	*lon*	This project
pOPINM-Lon	*lon*	This project
pBAD322-K	Empty vector, pBAD promoter	Mark Dillingham (University of Bristol)
pBAD322-GamL	*gamL*	Mark Dillingham (University of Bristol)
pBAD322-GamS	*gamS*	Mark Dillingham (University of Bristol)
eGFP-pBAD	eGFP tag, pBAD promoter	Addgene
DsRed2-pBAD	DsRed2 tag, pBAD promoter	Addgene
eGFP-pBAD-RecB	*recB*	This project
DsRed2-pBAD-RecB	*recB*	This project

Kan^R- kanamycin resistance, Amp^R- ampicillin resistance, Cam^R- chloramphenicol resistance, Spec^R- spectinomycin resistance, FRT- flippase recognition target, *FLP* - flippase.

2.1.2 Oligonucleotides

Oligonucleotides (Appendix I, **Table I**) were purchased from Sigma-Aldrich. All primers were designed using the software Benchling.

2.1.3 Antibiotics

Antibiotics (**Table 2.2**) were stored as recommended by the manufacturer's instructions. For the preparation of the stock concentrations, the appropriate amount of each antibiotic was measured in a precision balance, dissolved in the required solvent and filter sterilised. Antibiotics stocks were kept at -20°C and were thawed once.

Table 2.2. List of antibiotics, their solvents and stock concentrations.

Antibiotic	Solvent	Stock concentration (mg/mL)	Manufacturer
Ampicillin	H_2O	100	Sigma
Chloramphenicol	70% Ethanol	30	Sigma
Ciprofloxacin	H_2O	10	Sigma
Doxycycline	DMSO	100	Alfa Aesar
Kanamycin	H_2O	50	Sigma
Mitomycin C	H_2O	0.4	Sigma
Nalidixic acid	H_2O	50	Sigma
Norfloxacin	DMSO	5	Sigma
Oxolinic acid	H_2O 0.5 M NaOH	50	Sigma
Oxytetracycline	Ethanol	15	Sigma
Spectinomycin	H_2O	50	Sigma
Streptomycin	H_2O	15	Sigma
Tetracycline	Ethanol	15	Sigma
Trimethoprim	H_2O	10	Sigma

2.1.4 Enzymes, buffers and reagents for topoisomerase assays

E. coli gyrase, the supercoiled and relaxed DNA and the buffers used in the topoisomerase assays were purchased from Inspiralis. Exceptionally, GyrA and GyrB purified by Natassja Bush were used in the experiment in section 4.2.2.4. Proteinase K (Sigma), SDS, ATP (Sigma), EDTA, STEB (100 mM Tris.HCl pH 8.0, 40% (v/v) sucrose, 100 mM EDTA, 0.5 mg/mL Bromophenol Blue) and chloroform/isoamyl alcohol were used when indicated.

2.1.5 Buffers for protein purification

For Exo III purification:

Buffer A	50 mM Tris pH 8.0, 100 mM NaCl, 1 mM 2-Mercaptoethanol, 10% glycerol
Buffer B	50 mM Tris pH 8.0, 100 mM NaCl, 1 mM 2-Mercaptoethanol, 10% glycerol, 1M imidazole
Dialysis buffer	50 mM Tris pH 8.0, 100 mM NaCl, 1 mM 2-Mercaptoethanol, 10% glycerol
Buffer AQ	50 mM Tris pH 8.0, 100 mM NaCl, 1 mM 2-Mercaptoethanol, 10% glycerol

| Buffer BQ | 50 mM Tris pH 8.0, 100 mM NaCl, 1 mM 2-Mercaptoethanol, 10% glycerol, 1M imidazole |

For YbhP and YafD purification:

Buffer A	20 mM Tris pH 8.0, 500 mM NaCl, 0.2 mM 2-Mercaptoethanol, 5% glycerol
Buffer B	20 mM Tris pH 8.0, 500 mM NaCl, 0.2 mM 2-Mercaptoethanol, 5% glycerol, 1M imidazole
Dialysis buffer	20 mM Tris pH 8.0, 100 mM NaCl, 0.2 mM 2-Mercaptoethanol, 5% glycerol
Buffer AQ	20 mM Tris pH 8.0, 100 mM NaCl, 0.2 mM 2-Mercaptoethanol, 5% glycerol
Buffer BQ	20 mM Tris pH 8.0, 100 mM NaCl, 0.2 mM 2-Mercaptoethanol, 5% glycerol

For TDP2 purification:

Buffer A	50 mM Tris pH 8.0, 100 mM NaCl, 1 mM 2-Mercaptoethanol, 10% glycerol
Buffer B	50 mM Tris pH 8.0, 100 mM NaCl, 1 mM 2-Mercaptoethanol, 10% glycerol, 1M imidazole
Chaperone buffer	50 mM Tris pH 8.0, 50 mM KCl, 20 mM $MgCl_2$
Chaperone buffer + ATP	50 mM Tris pH 8.0, 50 mM KCl, 20 mM $MgCl_2$, 5 mM ATP
Dialysis buffer	50 mM Tris pH 8.0, 100 mM NaCl, 0.2 mM 2-Mercaptoethanol, 10% glycerol
Buffer AQ	50 mM Tris pH 8.0, 100 mM NaCl, 0.2 mM 2-Mercaptoethanol, 10% glycerol
Buffer BQ	50 mM Tris pH 8.0, 1 M NaCl, 0.2 mM 2-Mercaptoethanol, 10% glycerol

For Lon purification:

Buffer A	20 mM Tris pH 8.0, 200 mM NaCl, 1 mM 2-Mercaptoethanol, 10% glycerol
Buffer B-MBP	20 mM Tris pH 8.0, 200 mM NaCl, 1 mM 2-Mercaptoethanol, 10% glycerol, 10 mM maltose
Buffer B-His	20 mM Tris pH 8.0, 200 mM NaCl, 1 mM 2-Mercaptoethanol, 10% glycerol, 1 M imidazole
Dialysis buffer	20 mM Tris pH 8.0, 200 mM NaCl, 1 mM 2-Mercaptoethanol, 10% glycerol
Buffer AQ	20 mM Tris pH 8.0, 200 mM NaCl, 1 mM 2-Mercaptoethanol, 10% glycerol
Buffer BQ	20 mM Tris pH 8.0, 1 M NaCl, 1 mM 2-Mercaptoethanol, 10% glycerol

2.1.6 Rearing of *Galleria mellonella*

Galleria mellonella larvae and eggs were obtained from the John Innes Centre Entomology and Insectary Platform. Colonies were kept in the dark at 37°C in large Petri dishes packed with food (**Figure 2.1**). When the larvae started to pupate, they were moved to empty boxes in which the moths could lay the eggs. The eggs were then placed on fresh food.

Figure 2.1. *Galleria mellonella* larvae fed on artificial food.

The artificial diet medium was prepared by mixing and autoclaving the dry ingredients, and then mixing them with UV-irradiated wet ingredients. Fresh food was made every two months.

The dry ingredients were:

- 200 g milk powder (Dried Skimmed Milk Powder, Marvel)
- 200 g wholemeal flour (Strong Stoneground 100% Wholemeal Flour, Sainsbury's)
- 100 g yeast powder (Merck)
- 100 g wheat germ (Neal's Yard Wholefoods Natural Wheatgerm)
- 400 g bran (Neal's Yard Wholefoods Natural Wheat Bran)

The wet ingredients were:

- 300 mL honey (clear honey, Sainsbury's)
- 400 mL glycerol (Sigma)

2.2   Methods

2.2.1   Bioinformatics

2.2.1.1   Analysis of *E. coli* genomes

Sixteen *E. coli* strains were sent for whole-genome sequencing to Microbes NG or the QIB facilities (**Table 2.3**). All the strains were sequenced using Illumina and two of them were also sequenced using Nanopore. The sequences were analysed using the High Performing Computing cluster at the Norwich Bioscience Institutes.

Table 2.3. List of samples sent for whole-genome sequencing.

Sample name	Sequencing company	Sequencing method
dinB_CamR	MicrobesNG	Illumina and Nanopore
dinB_noCamR	MicrobesNG	Illumina and Nanopore
dinBpolB	MicrobesNG	Illumina
dpu_CamR	MicrobesNG	Illumina
dpu	QIB facilities	Illumina
dpu_noCamR	MicrobesNG	Illumina
lexA	MicrobesNG	Illumina
mito_1_CamR	QIB facilities	Illumina
mito_2_CamR	MicrobesNG	Illumina
mito_2_noCamR	MicrobesNG	Illumina
wt_1_CamR	MicrobesNG	Illumina
wt_2_1_CamR	QIB facilities	Illumina
wt_2_2_CamR	QIB facilities	Illumina
wt_2_3_CamR	QIB facilities	Illumina
wt_2_noCamR	QIB facilities	Illumina
wt	MicrobesNG	Illumina

For the samples that were sequenced at the QIB facilities, I trimmed the only Illumina adapter sequence that I could find (the Nextera adapter sequence) when sorting with `grep` using `cutadapt-1.9.1`. The same command was used for trimming low quality reads and reads below 50 bp:

#Source software from catalogue.

```
source cutadapt-1.9.1
```

#Trimming of the adapter sequence, low quality reads and reads < 50 bp.

```
cutadapt -q 30 -m 50 -a adapter_sequence -o "R1_trimmed.fastq" -p
"R2_trimmed.fastq" "R1_fastq" "R2_fastq"
```

The quality of all the reads was checked with `fastqc-0.11.3`.

The software `snippy-4.2.1` was used to find SNPs and indels by comparing the reads of the samples to the reference genome (NC_000913.3):

```
#Source software from catalogue.
source jre-7.21 samtools-1.9 snippy-4.2.1
#Run snippy command.
snippy --outdir <name of the directory snippy will create to put
the files> --ref <file with reference genome> --R1
sample1_R1_trimmed.fastq.gz -R2 sample2_R2_trimmed.fastq.gz
```

For the alignment of short reads:

```
#Source software from catalogue.
source bwa-0.7.17 samtools-1.9
#First index your reference genome.
bwa index reference_genome.fna
#Mapping of the R1 and R2 reads of sample 1 to the indexed reference genome to obtain
a SAM file.
bwa mem -t 8 reference_genome.fna sample1_R1_trimmed.fastq.gz
sample1_R2_trimmed.fastq.gz -o sample1.sam
#Creating a BAM file from the SAM file.
samtools view -b -o sample1.bam sample1.sam
#Sorting the BAM file.
samtools sort -o sample1.sort.bam sample1.bam
#Indexing the BAM file.
samtools index sample1.sort.bam
```

For the alignment of long reads:

```
#Source software from catalogue.
source minimap2-2.8 samtools-1.9
#Mapping of the reads of sample 1 to the indexed reference genome to obtain a SAM file.
minimap2 -t 6 -ax map-ont reference_genome.fna sample1.fastq >
sample1.sam
```

Then create, sort, and index a BAM file with samtools as in the alignment of short reads.

For the coverage analysis I aligned the reads to the reference genome (NC_000913.3) and then used the `bedtools genomecov` commands written by Luis Yanes (Earlham Institute):

#Source software from catalogue.

```
source bedtools-2.27.1
```

#To find deletions I looked for regions with low coverage (coverage <5 in a region size >50).

```
bedtools genomecov -bga -ibam sample1.sort.bam | awk '$4 <
MIN_COVERAGE' | bedtools merge -i - | awk '($3-$2)>MIN_REGION_SIZE
{print $0,$3-$2}' > name_ouput_file.bed
```

#To find amplifications I looked for regions with increased coverage (coverage >100 in a region size >500).

```
bedtools genomecov -bga -ibam sample1.sort.bam | awk '$4 >
MIN_COVERAGE' | bedtools merge -i - | awk '($3-$2)>MIN_REGION_SIZE
{print $0,$3-$2}' > name_output_file.bed
```

#To calculate the average coverage and standard deviation of each alignment I used the following command (https://www.biostars.org/p/5165/#67920).

```
samtools depth sample1.sort.bam  |  awk '{sum+=$3; sumsq+=$3*$3}
END { print "Average = ",sum/NR; print "Stdev = ",sqrt(sumsq/NR -
(sum/NR)**2)}'
```

To visualise the alignment as well as to confirm the presence of the SNPs, indels, deletions and amplifications, I used `IGV 2.7.2`.

2.2.2 Cloning

The cloning techniques were mainly used to introduce mutations in *E. coli* cells and to clone genes in expression vectors. Before describing how each *E. coli* mutant and expression vector were generated, I will explain each individual cloning technique.

2.2.2.1 Plasmid extraction and quantification of DNA

To extract plasmids from *E. coli* cells, I used the QIAprep Spin Miniprep Kit (QIAGEN). After the extraction, the quality and concentration of the DNA were determined using a Nanodrop (Nanodrop One, Thermo Scientific).

2.2.2.2 Genomic DNA extraction

To extract *E. coli* genomic DNA, two protocols were used: the QIAGEN Genomic DNA 20G kit (as instructed by the manufacturer) and a *Streptomyces* modified protocol. The latter method was adapted from the isolation of genomic DNA protocol detailed in [115]. A 15 mL tube containing 10 mL overnight culture was centrifuged at 3,000 g for 15 min. The

supernatant was removed and 5 mL of SET buffer (75 nM NaCl, 25 mM EDTA pH 8.0, 20 mM Tris.HCl pH 7.5) was added. Cells were gently resuspended and 10 µL of RNase (4 mg/mL) and 40 µL of lysozyme (50 mg/mL) were added to the sample. The tubes were mixed by inversion and incubated 1 h at 37°C. 28 µL of proteinase K (20 mg/mL) and 120 µL of 10% SDS were added, mixed by inversion and incubated at 55°C for 3 h inverting the tubes every hour. 800 µL of 5 M NaCl was added, mixed by inversion, and let to cool to 37°C. In the fume hood, I added 1 mL of chloroform and left the tubes in a rotating mixer at room temperature for 30 min. The tubes were centrifuged at 4,000 g for 20 min. Using 1 mL cut tips, I transferred the top layer of liquid to another 15 mL tube in which I added the same volume of isopropanol and I mixed by inversion. The visible DNA was fished with a sealed Pasteur pipetted and transferred to an Eppendorf filled with 70% ethanol. The ethanol was then removed and air dried. The pellet with the DNA was resuspended in 100-500 µL of TE buffer (10 mM Tris.HCl, 1 mM EDTA•Na$_2$).

2.2.2.3 PCR

Phusion^{TM} High-Fidelity DNA Polymerase (Thermofisher) was used to amplify DNA for cloning experiments. PCR was carried out in a final volume of 25-50 µL containing 1x Phusion 5x buffer, 0.02 U/µL of Phusion^{TM} High-Fidelity DNA Polymerase, 200 µM of dNTPs, 0.5 µM of each oligonucleotide, 0.2 ng/µL of template DNA and the corresponding volume of Milli-Q H$_2$O. The thermal cycler program was set as follows: 1) 95°C for 7 s, 2) 94°C for 15 s, 3) 56°C for 30 s, 4) 72°C for 15-30 s per kilobase, 5) repeat steps 2-4 for a total of 30 cycles, 6) 72°C for 10 min. If a gradient PCR was carried out, the annealing temperature was set up from 60-80°C.

When high sequence fidelity was not necessary, such as when screening plasmids, colonies and extracted chromosomal DNA, GoTaq polymerase (Promega) was used. PCR was carried out in a final volume of 25 µL containing 12 µL GoTaq™ Green mix, 0.2 µM of each oligonucleotide and between 10 and 100 ng of template DNA. The PCR machine was programmed as follows: 1) 90°C for 5 mins, 2) 94°C for 20 s, 3) 56°C for 20 s, 4) 72°C for 1 min per kilobase, 5) Repeat steps 2-4 for a total of 30 cycles, 6) 72°C for 5 min.

To purify PCR fragments, a PCR clean-up kit (New England Biolabs) was used following the manufacturer's instructions.

2.2.2.4 Gel electrophoresis

Samples were loaded in 1% (w/v) agarose gels made in TAE buffer (40 mM Tris-Base, 20 mM Acetic Acid, 1 mM Disodium EDTA) and run for ~45 min at 120 V. The gel was

stained in a 1 µg/mL ethidium bromide bath for 10 min and visualised using a Syngene G:BOX Gel Doc system.

2.2.2.5 Electrocompetent cells and bacterial transformation

To obtain *E. coli* electrocompetent cells, 500 µL of an overnight *E. coli* culture were poured into a flask with 50 mL of LB and incubated until OD_{600} = 0.4-0.5. This was done at 37°C if the cells were going to be transformed with a plasmid or at 30°C if the cells were going to be transformed with double-stranded DNA (dsDNA). In the latter situation, *E. coli* cells contained the thermosensitive plasmid pKD46 that expresses the λRed proteins. To induce the expression of the λRed proteins, once the culture reached OD_{600} = 0.4-0.5, I added 20 mM of arabinose (Sigma) and incubated for 10-15 min. The culture was then placed on ice for 5 min, and centrifuged at 7,000 x g for 7 min. The pellet was resuspended in ice-cold water and centrifuged as in the previous step. This was done twice. The final pellet was resuspended in 1 mL of ice-cold water and centrifuged at 13,000 x g for 1 min.

To transform electrocompetent *E. coli* cells, dsDNA (10-100 ng) or plasmid DNA (1-10 ng) was added to 50 µL of cells and the sample was electroporated at 1,800 V. After the electroporation, 1 mL of SOC was added to the cuvette and then transferred to a tube containing 2 mL of SOC. The tube was incubated for 3-24 h at 30°C. 100 µL of the transformed cells were plated on plates supplemented with the corresponding antibiotic (e.g., 100 µg/mL ampicillin, 50 µg/mL kanamycin, or 30 µg/mL chloramphenicol). The plates were incubated overnight at 37°C or at 30°C if a thermosensitive plasmid was used.

2.2.2.6 Double-stranded DNA (dsDNA) recombineering

To introduce mutations in the *E. coli* genome, I used the double-stranded DNA (dsDNA) recombineering protocol adapted from Datsenko & Wanner [116].

First, I did a PCR to generate a dsDNA fragment containing an antibiotic resistance cassette with the FLP recognition target (FRP) sites flanked by a homologous region of the target DNA sequence. To do this, I used a set of primers (e.g., YafD-pKD4_FW & YafD-pKD4_RV) containing ~50 nucleotides (nt) homologous to the downstream or upstream sequence of the target DNA sequence I wanted to delete and 20 nt of the priming site 1 or 2 of the plasmid pKD4 or pKD3. I also constructed primers that flanked the target DNA sequence (e.g., YafD-H1_FW & YafD-H2_RV) to confirm the mutation of the target DNA sequence. pKD4 (that contained a Kan^R cassette) or pKD3 (that contained a Cam^R cassette) was used as the template DNA in this PCR reaction. All primers are

listed in Appendix I, **Table I**. Because the primers used in this reaction were long (60-70 base pairs (bp)) gradient PCRs were carried out in most of the cases to find the optimal conditions for amplifying the dsDNA substrate. Once the substrate was amplified and cleaned (for details see section 2.2.2.3), it was sent for Sanger sequencing (Eurofins Genomics) to confirm that the sequence was correct.

Electrocompetent *E. coli* cells containing pKD46 were transformed with the PCR-amplified dsDNA fragment. *E. coli* pKD46 cells express the λRed proteins (λGam, Exo and Beta) which catalyse the homologous recombination of the substrate with the target DNA sequence. The colonies that had the target DNA sequence replaced with the dsDNA substrate were then selected on kanamycin or chloramphenicol plates depending on the antibiotic resistance cassette that was introduced. Positive colonies were then confirmed by PCR.

2.2.2.7 P1 transduction

To move segments of the *E. coli* genome from one strain to another, I used a P1 transduction protocol based on Thomason et al. [114]. P1 bacteriophage was used to infect the strain that contained the DNA sequence of interest (e.g., *marR*::Kan^R). The P1 bacteriophage with the DNA of interest was extracted and used to transduce the DNA of interest into the target strain (e.g., a WT strain). The transductants were checked by PCR.

2.2.2.8 FLP recombination

To remove the Kan^R or Cam^R cassette from the mutants made by dsDNA recombineering or P1 transduction, I used the FLP recombination protocol from Datsenko & Wanner [116]. Basically, the mutants were made electrocompetent and then transformed with the plasmid pCP20. The transformants were then grown overnight at 45°C to induce FLP expression and select for the loss of pCP20. Single candidate recombinants were plated and screened for genomic recombination and plasmid loss.

2.2.2.9 Construction of the deletion mutants

The mutants created in this project (**Table 2.1**) were built using the dsDNA recombineering, P1 transduction and/or FLP removal protocols mentioned above. The specific cloning protocol used for each mutant is detailed in **Table 2.4**. The primers are listed in Appendix I, **Table I**.

Table 2.4. List of mutants generated in this project and the cloning technique used.

Mutant	Cloning technique
MG1655 *xthA*::Kan^R	P1 transduction of BW25113 *xthA*::Kan^R (strain 1) into MG1655
MG1655 Δ*xthA*	Removal of the Kan^R cassette of MG1655 *xthA*::Kan^R strain with FLP recombination
MG1655 *yafD*::Cam^R	dsDNA recombineering
MG1655 *ybhP*::Kan^R	dsDNA recombineering
MG1655 Δ*xthA yafD*::Cam^R	P1 transduction of *yafD*::Cam^R into Δ*xthA*
MG1655 Δ*xthA ybhP*::Kan^R	P1 transduction of *ybhP*::Kan^R into Δ*xthA*
MG1655 *yafD*::Cam^R *ybhP*::Kan^R	P1 transduction of *ybhP*::Kan^R into *yafD*::Cam^R
MG1655 Δ*xthA ybhP*::Kan^R *yafD*::Cam^R	P1 transduction of *yafD*::Cam^R into Δ*xthA ybhP*::Kan^R
EcNR2 *clpP*::Kan^R	dsDNA recombineering
MG1655 Δ*clpP*	P1 transduction of EcNR2 *clpP*::Kan^R into MG1655
EcNR2 *sbcCD*::Kan^R	dsDNA recombineering
MG1655 Δ*sbcCD*	P1 transduction of EcNR2 *sbcCD*::Kan^R into MG1655
MG1655 Δ*sbcCD clpP*::Kan^R	dsDNA recombineering of MG1655 Δ*sbcCD*
MG1655 *xseA*::Kan^R	dsDNA recombineering
MG1655 Δ*xseA*	Removal of the Kan^R cassette of MG1655 *xseA*::Kan^R strain with FLP recombination
MG1655 Δ*xseA sbcCD*::Kan^R	dsDNA recombineering of MG1655 Δ*xseA*
MG1655 *lon*::Kan^R	P1 transduction of BW25113 *lon*::Kan^R (strain 1) into MG1655 dsDNA recombineering
MG1655 Δ*lon*	Removal of the Kan^R cassette of MG1655 *lon*::Kan^R strain with FLP recombination
MG1655 Δ*xseA lon*::Kan^R	dsDNA recombineering
MG1655 Δ*xseA* Δ*lon*	Removal of the Kan^R cassette of MG1655 Δ*xseA lon*::Kan^R strain with FLP recombination
MG1655 Δ*xseA recB*::Kan^R	dsDNA recombineering of MG1655 Δ*xseA*
Gam-GFP *xseA*::Kan^R	P1 transduction of *xseA*::Kan^R into Gam-GFP
Gam-GFP *clpP*::Kan^R	P1 transduction of *clpP*::Kan^R into Gam-GFP
MG1655 *dinB*:: Kan^R	dsDNA recombineering
MG1655 Δ*dinB*	Removal of the Kan^R cassette of MG1655 *dinB*::Kan^R strain with FLP recombination
MG1655 *polB*::Kan^R	dsDNA recombineering
MG1655 Δ*polB*	Removal of the Kan^R cassette of MG1655 *polB*::Kan^R strain with FLP recombination
MG1655 *umuD*::Kan^R	dsDNA recombineering
MG1655 Δ*umuD*	Removal of the Kan^R cassette of MG1655 *umuD*::Kan^R strain with FLP recombination
MG1655 Δ*dinB polB*::Kan^R	dsDNA recombineering of MG1655 Δ*dinB*
MG1655 Δ*dinB* Δ*polB*	Removal of the Kan^R cassette of MG1655 *polB*::Kan^R strain with FLP recombination
MG1655 Δ*dinB umuD*::Kan^R	P1 transduction of *umuD*::Kan^R into MG1655 Δ*dinB*

MG1655 Δ*dinB* Δ*umuD*	Removal of the Kan^R cassette of MG1655 *umuD*::Kan^R strain with FLP recombination
MG1655 Δ*polB* *umuD*::Kan^R	dsDNA recombineering of MG1655 Δ*polB*
MG1655 Δ*polB* Δ*umuD*	Removal of the Kan^R cassette of MG1655 *umuD*::Kan^R strain with FLP recombination
MG1655 Δ*dinB* Δ*polB* *umuD*::Kan^R	dsDNA recombineering of MG1655 Δ*dinB* Δ*polB*
MG1655 Δ*dinB* Δ*polB* Δ*umuD*	Removal of the Kan^R cassette of MG1655 *umuD*::Kan^R strain with FLP recombination
MG1655 *marR*::Kan^R	dsDNA recombineering of MG1655
MG1655 Δ*marR*	Removal of the Kan^R cassette of MG1655 *marR*::Kan^R strain with FLP recombination
MG1655 *marR170*::Kan^R	dsDNA recombineering of MG1655
MG1655 *marR170*	Removal of the Kan^R cassette of MG1655 *marR170*::Kan^R strain with FLP recombination
EcNR2 *lit*::Kan^R	dsDNA recombineering
MG1655 *lit*::Kan^R	P1 transduction of *lit*::Kan^R into MG1655
EcNR2 *ymfM*::Kan^R	dsDNA recombineering
MG1655 *ymfM*::Kan^R	P1 transduction of *ymfM*::Kan^R into MG1655

2.2.2.10 Introduction of a point mutation (*lexA*(S119A) mutant)

To build the *lexA*(S119A) mutant, I used some of the cloning techniques mentioned above. Because of the numerous steps it took me to build this mutant, I have detailed them below (**Figure 2.2**).

First, I constructed a pUC19-lexA plasmid with the *lexA*(S119A) mutation. To do this, I cloned four different fragments (A1, A2, B1 and B2) into a pUC19 plasmid. A1 contained 15 bp of pUC19, 50 bp upstream the *lexA* codon 119, and codon 119 with a mutation (T→G in position 355). The mutation in codon 119 changed it from being translated to Serine (TCG) to Alanine (GCG). A2 contained the last 15 bp of A1, and the sequence from codon 119 to the end of the *lexA* open reading frame. B1 contained the last 15 bp of A2 and a Kan^R cassette flanked by FRT sites. B2 contained the last 15 bp of B1, 50 bp downstream *lexA*, and 15 bp of pUC19. A2 was obtained by PCR amplifying the chromosome of *E. coli* MG1655 using primers lexA.A2_FW and lexA.A2_RV. B1 was obtained by PCR-amplifying a pKD4 vector using primers lexA.B1_FW and lexA.B1_RV. A1 and A2 were fused into an A fragment by using primers lexA.A1_FW and lexA.A2_RV. B1 and B2 were fused into a B fragment by using primers lexA.B1_FW and lexA.B2_RV. Fragments A and B were cloned by In-Fusion (Takara Bio) into a pUC19 vector linearised with SfoI (New England Biolabs). All fragments were purified with a PCR clean-up kit (Takara Bio) before being used in any cloning reaction. Stellar cells were transformed with the pUC19 vector containing *lexA*(S119A) cassette as stated by Takara Bio. Colonies that

were both ampicillin- and kanamycin-resistant were selected, grown, miniprepped, and checked for the presence of the *lexA*(S119A) cassette by PCR using primers pUC19.lexA_FW and pUC19.lexA_RV. A pUC19 plasmid containing the *lexA*(S119A) cassette was sent for sequencing to confirm the presence of the *lexA* mutation, and then used as a template to amplify the *lexA*(S119A) cassette using primers pUC19.lexA_FW and pUC19.lexA_RV. The *lexA*(S119A) cassette was transformed into electrocompetent *E. coli* MG1655 cells, but all the kanamycin-resistant colonies obtained were false positives. Because of the presence of false positives, the *lexA*(S119A) cassette was split in two fragments (lexA1 and lexA2) using primer lexA_A_H1KanR_FW and lexA_A_H1KanR_RV to amplify lexA1, and primer lexA_B_H2KanR_FW and lexA_B_H2KanR_RV to amplify lexA2. Fragment lexA1 had half of the Kan^R cassette, and thus, only the cells that incorporated both fragments lexA1 and lexA2 could have the whole Kan^R cassette and be resistant to kanamycin. The lexA1 and lexA2 fragments were transformed into electrocompetent *E. coli* MG1655 cells, but no kanamycin-resistant colonies were obtained. Because of the lack of colonies, I used *E. coli* EcNR2 cells that had a higher recombination rate. The lexA1 and lexA2 fragments were transformed into electrocompetent *E. coli* EcNR2 cells as in [117], and a kanamycin-resistant colony was sent for sequencing to confirm the presence of the *lexA*(S119A) cassette. To move the *lexA*(S119A) mutation from EcNR2 cells to MG1655 cells, I used P1 transduction. Briefly, I made a P1 lysate of EcNR2 cells containing the *lexA*(S119A) cassette, and I transduced MG1655 cells with it. Kanamycin-resistant colonies were checked by PCR and then sent for whole-genome sequencing to confirm the *lexA*(S119A) mutation.
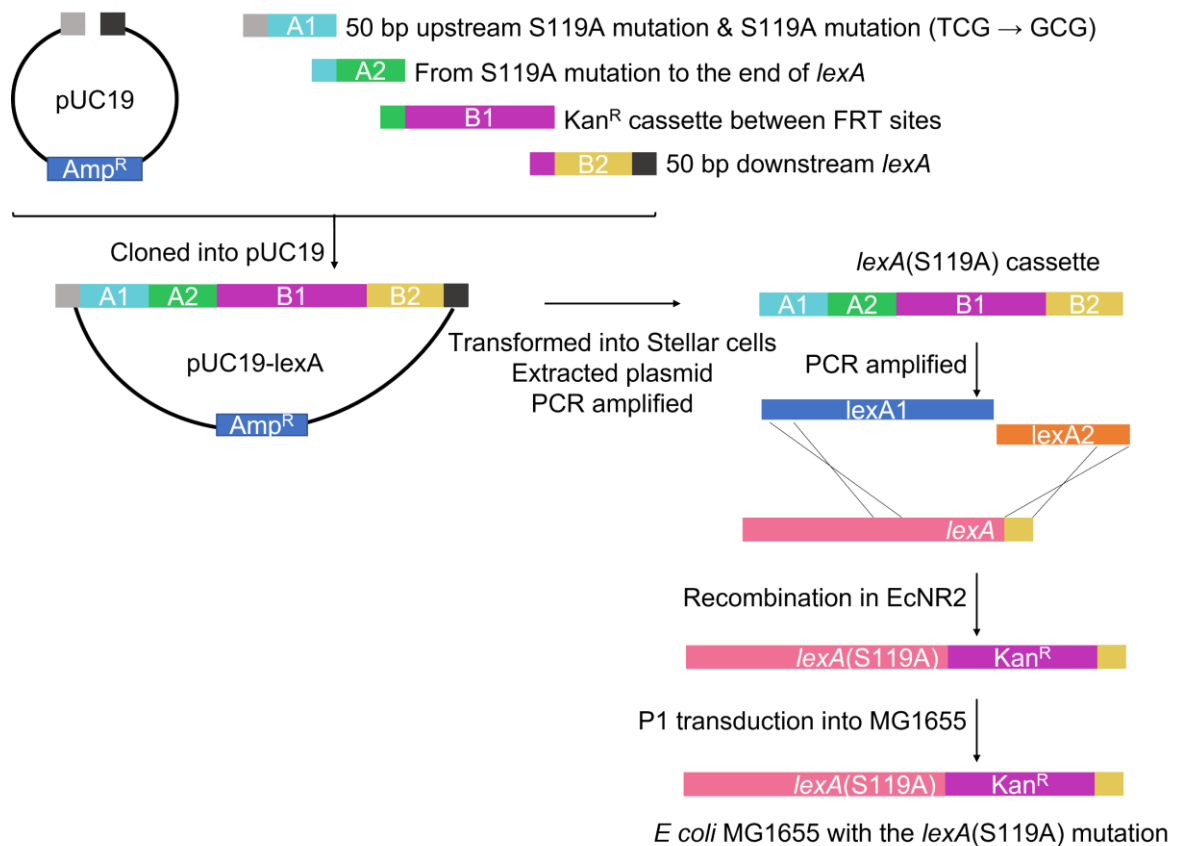
Figure 2.2. Cloning steps to construct the *E. coli* MG1655 *lexA*(S119A) mutant. A cassette containing the *lexA*(S119A) mutation and a kanamycin resistance (Kan^R) fragment was introduced into a pUC19 plasmid. The pUC19-lexA plasmid was used as a template to amplify the lexA1 and lexA2 fragments which were introduced into *E. coli* EcNR2 cells. The *lexA*(S119A) cassette was then moved into *E. coli* MG1655 cells by P1 transduction.

2.2.2.11 Plasmid cloning

To clone *yafD*, *ybhP*, *xthA*, *TDP2* and *lon* into a pET28-MHL or a pOPIN vector, an In-Fusion® HD Cloning Kit (Takara Bio) was used. First, 2-4 μg of pET28-MHL or pOPIN were digested with BseRI (New England Biolabs), in the case of pET28-MHL, or KpnI and HindIII (Roche), in the case of pOPIN, for 1 h. The digestion product was run in an agarose gel and extracted from the gel using a PCR clean-up kit (Takara Bio). A fragment containing the gene of interest plus 15 bp in the 5′ and 3′ ends that were complementary to the ends of the linearised vector, was amplified by PCR using *E. coli* MG1655 genomic DNA as the template (see primers in Appendix I, **Table I**) and purified using a PCR clean-up kit. To ligate the linearised vector with the *yafD*/*ybhP*/*xthA*/*TDP2*/*lon* inserts, the In-Fusion HD Enzyme Premix was used as stated by the manufacturer. The In-Fusion

product was used to transform Stellar™ Competent Cells (Takara Bio) following the manufacturer's recommendations.

To clone *recB* in DsRed2-pBAD or eGFP-pBAD, I followed the same process as mentioned above with one exception; DsRed2-pBAD or eGFP-pBAD were digested with EcoRI (Roche).

2.2.3 Protein expression and purification

2.2.3.1 Cell lysates

A colony of *E. coli* was grown overnight in 5 mL LB at 37°C. 50 µL of the overnight culture was added into 5 mL of LB and grown for 3.5 or 6.5 h to have logarithmic or stationary cultures, respectively. When indicated, the cultures were treated with 0.4 or 100 µg/mL of oxolinic acid. Cells were harvested by centrifugation at 3,000 g for 10 min. The pellet was resuspended in 100 µL of 50 mM Tris.HCl pH 8.0 and 10 µL of 100 mg/mL lysozyme. The samples were frozen in liquid N_2 and slowly thawed on ice. The last step was repeated twice. Then the lysates were centrifuged at maximum speed for 30 min at 4°C. The supernatant was frozen in liquid N_2 and kept at -80°C.

2.2.3.2 Sodium dodecyl-sulphate polyacrylamide gel electrophoresis (SDS-PAGE)

Protein samples were mixed with 4x loading buffer (Thermofisher) to make a final volume of 50 µL and boiled for 5 min. 3 µL of a protein ladder (Color Protein Standard Broad Range, New England Biolabs) and 15 µL of each protein sample were loaded on 12% SDS-PAGE pre-cast gels (Thermofisher) and run at 180 V for 45 min. The protein bands were observed using InstantBlue® (Abcam).

2.2.3.3 Small scale protein expression

50 µL of an overnight culture was grown in 5 mL LB until $OD_{600} = 0.5$ and then grown for the desired amount of time with or without IPTG. 500 µL of the culture was lysed with small glass beads. Then the lysate was centrifuged for 2 min at 13,000 g. The supernatant of the lysate was centrifuged for 2 min at 13,000 g. The pellet of the resulting supernatant and the was resuspended in 50 µL. The resuspended pellet, 50 µL of the culture and 50 µL of the supernatant were mixed with 12.5 µL of 4x loading buffer and boiled before being loaded in an SDS-PAGE gel.

2.2.3.4   Large scale protein expression

10-20 mL of an overnight culture was grown in 1 L LB until OD_{600} = 0.5. Then it was added 0.5-1 mM IPTG and grown for 1-24 h at 18°C, 28°C or 37°C. The culture was centrifuged for 10 min at 5,000 g and the pellet was resuspended in 10-15 mL of buffer A (see section 2.1.5). The resuspended cells were disrupted using an Avestin High Pressure Homogeniser. After disruption, cells were centrifuged at 19,000 g for 1 h at 4°C.

2.2.3.5   Protein purification

To purify protein, I used the protein purification system AKTA Unicorn (Cytiva), and the buffers mentioned in section 2.1.5. To check each purification step, the protein samples were run on an SDS-PAGE gel as shown in section 2.2.3.2.

For affinity chromatography, I used three different strategies depending on the protein I wanted to purify (see section 3.2.2.5). In the first strategy, I loaded the supernatant of lysed cells onto a HisTrap FF 5 mL column (GE Healthcare) using 98% of buffer A and 2% of buffer B. The histidine-tagged protein was eluted using an imidazole gradient which was generated by slowly increasing buffer B concentration from 2% to 100%. For the second strategy, I used an MBPTrap HP 5 mL column (Cytiva). The MBP-tagged protein was eluted using a maltose gradient which was generated by slowly increasing buffer B-MBP concentration from 2% to 100%. For the third strategy, the supernatant of the lysed cells was loaded onto a HisTrap FF 5 mL column (GE Healthcare). The column was washed with buffer A and equilibrated with the chaperone buffer. Then the column was washed with chaperone buffer + ATP using 20 times the volume of the column and a flow rate of 20 mL/min. Buffer A was used to equilibrate the column before doing an imidazole gradient by slowly increasing buffer B concentration from 2% to 100%.

For the dialysis, the best purified fractions were added into a dialysis bag (SnakeSkin™ Dialysis Tubing, 10K MWCO, 22 mm, Thermofisher Scientific) and placed inside a beaker with 3 L of dialysis buffer. The buffer was shaken with a magnetic shaker at 4°C overnight.

To digest the His-MBP tag, 3C protease (Thermofisher) was used as stated by the manufacturer.

For anion exchange chromatography, the dialysed sample was loaded onto a HiTrap Q HP 5 mL column (GE Healthcare) using 100% buffer AQ. The sample was eluted using a NaCl gradient generated by slowly increasing buffer BQ concentration to 100%.

If the protein needed to be concentrated, a Merck Millipore Amicon™ Ultra-2.0 Centrifugal Filter Unit was used. Protein samples were centrifuged at 6,500 g for 30-60 min at 4°C.

For gel filtration calibration, I used a kit from GE Healthcare containing blue dextran, ovalbumin and conalbumin following the manufacturer's instructions. For gel filtration chromatography, 500 µL of purified fractions were loaded on a Superdex 75 Increase 10/300 GL column (GE Heathcare) using buffer AQ.

To measure the protein concentration, I used the absorbance at 280 nm method from Nanodrop (Nanodrop One, Thermo Scientific).

To measure the purity of the bands, I used ImageJ. I selected the lane of interest, then I used the "Analyze > Gels > Plot lines" function to measure the density of each band. With this information I divided the background-corrected density of the protein band by the background-corrected density of the whole lane and multiplied by 100 to get % purity.

2.2.3.6 Western blot

Proteins were separated by SDS-PAGE and transferred onto a polyvinylidene difluoride membrane using a Trans-Blot turbo transfer system (Bio-Rad) at 20 V, 2.5 mA, for 15 min. After the transfer, the membrane was briefly washed with Ponceau S (Sigma) then rinsed with ultrapure MilliQ H_2O. The membrane was blocked in TBS-T (50 mM Tris.HCl pH 7.6, 150 mM NaCl, 0.1% Tween-20) with 5% milk solids (Marvel Dry Skimmed Milk powder) for 10 min before incubating at 4°C overnight with monoclonal antibody (anti-GyrA-CTD – 4D3; a gift from Alison Howells, Inspiralis) diluted 1/1,000 in TBS-T 5% milk. The membrane was then rinsed briefly with TBS-T before washing three times with TBS-T for 10 min each at room temperature. The membrane was then incubated at room temperature for 1 h with secondary antibody (diluted 1/5,000 in TBS-T 1% milk); rabbit polyclonal antimouse-HRP conjugate (Dako). This was then washed as described above. The membrane was flooded with Pierce™ ECL Western Blotting Substrate and left for 1 min at room temperature before imaging in ImageQuant™ LAS 500.

2.2.4 Gyrase assays

For the supercoiling assay, I incubated gyrase with 500 ng of relaxed pBR322 plasmid for 30 min at 37°C in the presence or absence of 10 µg/mL ciprofloxacin as stated by the protocol "Escherichia coli Gyrase Supercoiling Inhibition Assay" from Inspiralis (https://www.inspiralis.com/assets/TechnicalDocuments/E.coli-Gyrase-Supercoiling-Assay-Protocol.pdf).

The protocol for the traditional cleavage assay was adapted from the "Escherichia coli Gyrase Cleavage Assay" from Inspiralis. Broadly, 500 ng of supercoiled or relaxed pBR322 plasmid was incubated for 30 min at 37°C with gyrase, 10 µg/mL ciprofloxacin, and 10 mM $MgCl_2$ in a final reaction of 30 µL. The reaction mix was then incubated 30 more min at 37°C with 3 µL of 2% SDS and 1.5 µL of 10 mg/mL Proteinase K. In the experiments with cell lysates, the last step was performed with 5 µL of lysate.

To stop the supercoiling and cleavage reactions, I added 20 µL of STEB and 30 µL of chloroform/isoamyl alcohol. 15 µL of the samples were then loaded on a 1% agarose gel and run at 80 V for 2 h. The gel was then stained and visualised as in 2.2.2.4.

2.2.5 Lon protease assays

2.2.5.1 Lon degradation of α-casein

A range of 0.3-10 µg Lon were incubated with 20 µg of α-casein (Sigma) in the absence or presence of 4 mM ATP for 0, 30, 60 and 120 minutes at 37°C (the buffer contained 20 mM Tris.HCl pH 8.0, 200 mM NaCl, 1 mM 2-Mercaptoethanol, 10% glycerol and 10 mM $MgCl_2$). At every time point, a 30 µL sample was taken, added 10 µL of 4x loading buffer, boiled for 5 min, and loaded on a 12% SDS-PAGE gel. The gel was run and visualised as in 2.2.3.2.

2.2.5.2 Lon degradation of gyrase

An amount of 2 µg of GyrA, GyrB or gyrase were incubated in a buffer with 20 mM Tris.HCl pH 8.0, 200 mM NaCl, 1 mM 2-Mercaptoethanol, 10% glycerol, 10 mM $MgCl_2$, 4 mM ATP, 30 µM ciprofloxacin and 500 ng of supercoiled pBR322 for 30 min at 37°C. 2 µg of Lon, and/or 5 µL of a cell lysate were then added and incubated for 0, 30, 60 and 120 minutes at 37°C in a final volume of 30 µL. The reaction was stopped by adding 10 µL of sample buffer and boiling the samples for 5 min. The samples were loaded on a 12% SDS-PAGE gel as in 2.2.3.2.

2.2.6 Tyrosyl phosphodiesterase activity assay

A range of 100-1000 ng of MBP-TDP2, 10-10,000 ng of His-Exo III, 1-10,000 of MBP-YafD or 1-1000 ng of His-YbhP were incubated with 0.5 µL of 1 mM of Y-18-F or Y-19-F oligo and 10 mM $MgCl_2$ for 30 min at 37°C in a final volume of 10 µL. The buffer contained 50 mM Tris pH 8.0, 100 mM NaCl, 0.2 mM 2-Mercaptoethanol, 10% glycerol. The reaction was stopped with the addition of 2 µL of loading dye (TBE-Urea Sample Buffer, Invitrogen) and then loaded on a 20% acrylamide gel (Novex™ TBE Gels 20%, Invitrogen) that was

run for 3-4 h at 60-80 V using 0.5x TBE running buffer (Invitrogen). The gel was imaged via Gel doc imager (Syngene) using the FAM filter.

2.2.7 Growth curve assay

To measure the growth curves, an overnight culture was inoculated in a 96-well plate and diluted in LB and/or supplemented with antibiotics (when appropriate) to make a final volume of 150 µL. Wells at the ends of the plate were used to measure the blank (LB only) and each sample was assayed in triplicate. OD_{600} measurements were taken every 15 minutes for 15-24 h using a CLARIOstar® plate reader, and cells were incubated at 37°C with agitation (200 g orbital shake).

2.2.8 Minimum inhibitory concentration (MIC) assay

To determine the MIC broth values, the OD_{600} of an *E. coli* overnight culture was measured and diluted to 5×10^5 cells/mL ($OD_{600} = 0.003$) as stated by Andrews [118]. 75 µL of the dilution was added into the wells of a 96-well plate containing 2-fold dilutions of an antibiotic. The first and last well of each row were used as only-LB controls (blank). Each well was performed in triplicate. The plate was incubated for 20-22 h at 37°C and OD_{600} measurements of the wells were performed using a CLARIOstar® plate reader (BMG LABTECH). The blank-corrected mean value of each replicate was used to calculate the MIC value. The MIC value was designated as the lowest antibiotic concentration that gave an $OD_{600} \leq 0.1$.

MIC solid-agar values were calculated from an overnight culture adjusted to 10^4 cells/ 2 µL ($OD_{600} = 0.03$) as shown in Andrews [118]. 2 µL of the diluted overnight culture were spotted on LB-agar Petri dishes supplemented with 2-fold dilutions of an antibiotic (e.g., 0, 1, 2, 4, 8, 16 µg/mL of antibiotic). Plates were incubated 20-22 h at 37°C. The MIC value was defined as the lowest antibiotic concentration in which there was no visible growth.

Alternatively, 4 µL of 1/10 serial dilutions of an $OD_{600} = 1$ culture were spotted on LB-agar Petri dishes supplemented with 2-fold dilutions of an antibiotic. Plates were incubated 20-22 h at 37°C. The MIC value was defined as the lowest antibiotic concentration in which there was no visible growth in the $OD_{600} = 0.01$ spot (~10,000 cells).

2.2.9 Survival assay

Cells were grown until logarithmic phase and then treated or not with 2x MIC of ciprofloxacin or 10x MIC of ciprofloxacin (0.054 or 0.27 µg/mL, respectively) and/or 5x

MIC of chloramphenicol (20 μg/mL). 0, 30, 60 and 90 min after the addition of the drug, a sample from each culture was taken and plated on LB, or LB with 5% DMSO to count the number of colony forming units (CFU) per mL.

2.2.10 Quinolone-induced antimicrobial resistance (QIAR) assay

To measure the frequency of antibiotic-resistant bacteria in a population, I used a protocol designed by Natassja Bush during her PhD [55] (**Figure 2.3**). 50 μL of an overnight culture was added into a 250 mL Erlenmeyer containing 50 mL of LB with 0x, 0.25x, 0.5x or 1x the MIC of an antibiotic. Cells were incubated for 24 h at 37°C with agitation and 12.5 mL of the culture was centrifuged 30 minutes at 3000 g. The pellet was resuspended in 2.5 mL LB and 400 μL of the resuspended culture (with ~ 10^{10} cells) was plated on 15-cm LB agar plates supplemented with a high concentration of an antibiotic (e.g., 32 μg/mL chloramphenicol). Glass beads were used to spread the bacteria. Serial dilutions of the resuspended culture were plated on LB agar for colony counting. Plates were incubated for 24 h at 37°C and left on the bench for another 24 h. After the 48-h incubation, the resistant colonies were re-streaked on plates supplemented with the same concentration of antibiotic in which they were first selected (e.g., 32 μg/mL chloramphenicol).

2.2.11 Mutation frequency assay (MFA)

To be able to measure the frequency of chloramphenicol-resistant colonies that appeared after the exposure to low levels of ciprofloxacin or mitomycin C, I designed a mutation frequency assay (MFA) (**Figure 2.3**). Ten independent colonies were grown overnight in 5 mL LB at 37°C. 50 μL of a 1/1,000 dilution of the overnight culture was poured in tubes with 5 mL LB. Each overnight culture was split into two tubes: one that was not treated with ciprofloxacin or mitomycin C, and another that was treated with 0.25x MIC of ciprofloxacin or mitomycin C after growing for 2 h in LB. The cultures were incubated 24 h. After the incubation 1.5 mL of each culture was centrifuged 10 min at 3,000 g. The pellet was resuspended in 400 μL of LB. 10^{-6} and 10^{-7} dilutions of each culture were plated on LB plates to count the CFU. 400 μL of the culture was plated on plates with 8x MIC chloramphenicol and incubated at 37°C for 24 h and on the bench for 24 h. The colonies that appeared were re-streaked on plates with 8x MIC chloramphenicol. The re-streaked colonies that grew were considered chloramphenicol-resistant mutants. To calculate the frequency of chloramphenicol-resistant mutants, I divided the number of chloramphenicol-resistant colonies by the number of CFU.
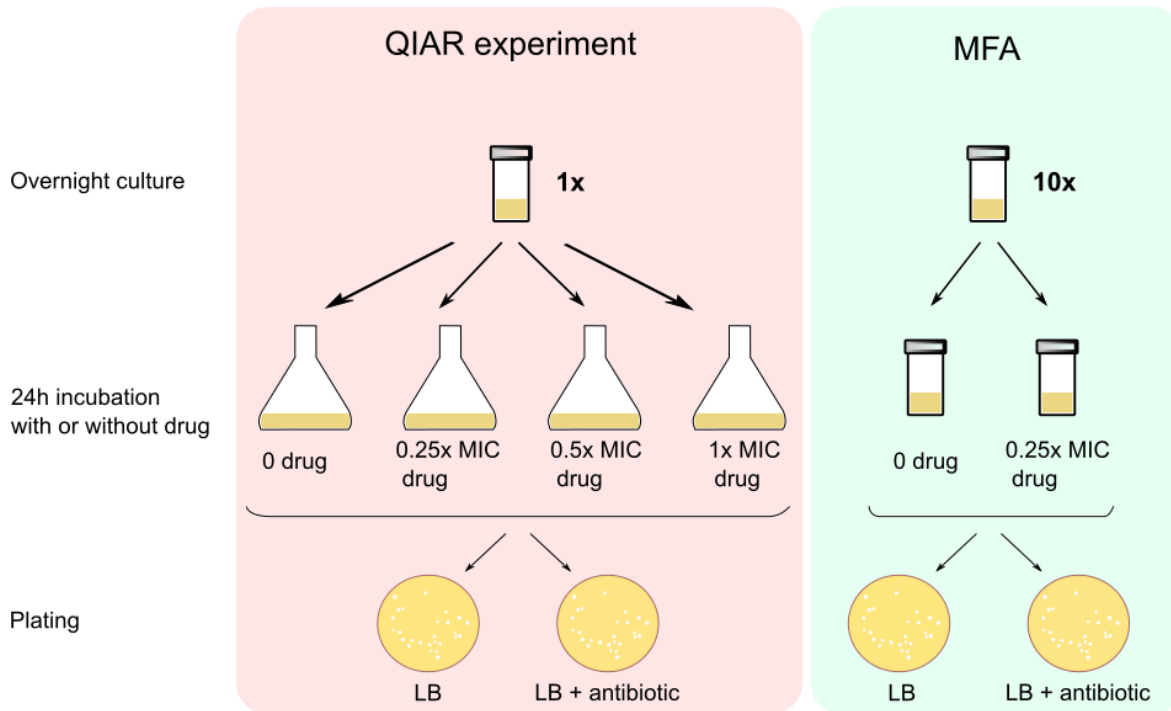
Figure 2.3. Comparison between the QIAR and MFA experiments. Overnight cultures from one colony (in the case of the QIAR experiment) or from 10 colonies (in the case of MFA) are split into four tubes with four different treatments (in the case of the QIAR experiment) or two tubes with two different treatments (in the case of MFA). The cultures were incubated at 37°C for 24 h and then plated on LB plates supplemented with antibiotics to select for antibiotic resistance. Dilutions of the cultures were plated on LB-only plates to count the number of colonies plated. The frequency of resistant colonies was then calculated by dividing the number of resistant colonies by the total number of colonies plated.

2.2.12 Fluorescence microscopy

2.2.12.1 Preparation of the slides

An overnight culture of *E. coli* Gam-GFP was diluted 1:4,000 (6.25 µL in 25 mL LB in a 250 mL flask) and incubated at 37°C for 3 h. 1/3 of the culture was diluted (1 mL in 2 mL LB in a 10 mL tube) and added ciprofloxacin. The culture was incubated for further 90 min. After the incubation, 40 ng/mL of doxycycline was added in 1.5 mL culture. The culture was incubated for 2 h. 1 mL of culture was centrifuged at 3,000 g for 4 min and resuspended in 1 mL H_2O two times. 50 µL of the resuspended culture and of a 1/10 dilution were centrifuged using a cytocentrifuge (Shandon CytoSpin II Cytocentrifuge, GMI) for 3 min at 50 rpm to set down a monolayer of cells on a glass slide (VWR). 12 µL

of Vectashield (Vector Laboratories) were added on the cells. The slide was covered, sealed with nail polish and stored at 4°C.

2.2.12.2 Microscopy

Images were captured using a widefield and up-right Axio Imager Z2 microscope (Zeiss) with 100x/1.3 Oil Ph3 M27 objective lens (Zeiss) and a Hamamatsu Orca FLASH 4.0v3 camera. The images were taken with Z stacks (0.2 µm intervals) and using 50% LED light and 50-500 ms exposure. The Gam-GFP, and GFP-RecB imaging acquisition was recorded as a set of two acquisitions: phase contrast image and GFP fluorescence. The microscope was controlled with the ZEN Pro software.

2.2.12.3 Analysis of the images

The analysis of the images was done with ImageJ. First, phase contrast and fluorescent Z-stacks were combined in separate Z projects and converted to 8-bit with the following Macro script:

```
waitForUser("Select the image for cell counting");
run("Z Project...", "projection=[Sum Slices]");
setOption("ScaleConversions", true);
run("8-bit");
waitForUser("Select the initial image for cell counting");
close();
waitForUser("Select the image for foci counting");
run("Z Project...", "projection=[Max Intensity]");
setOption("ScaleConversions", true);
run("8-bit");
waitForUser("Select the initial image for foci counting");
close();
setOption("ScaleConversions", true);
run("8-bit");
```

Then the cells in the phase contrast Z project were sorted from the background using "Adjust>Threshold". I did this manually to ensure that the threshold was correct.

To measure the area of the cells in the phase contrast Z project, and to localise the fluorescent foci in the fluorescent Z-project, I linked individual bacteria to the number of maxima (or foci) in the cell using the following Macro script:

```
run("Analyze Particles...", "size=1-Infinity circularity=0.00-0.96
display clear summarize add");
waitForUser("Select the image for spot counting");
for(i=0; i<roiManager("count"); i++) {
     roiManager("select", i);
     run("Find Maxima...", "noise=10 output=[Count]");
     run("Find Maxima...", "noise=10 output=[Point Selection]");
```

```
run("Add Selection...");}
```

2.2.13 *Galleria mellonella* (*G. mellonella*)

2.2.13.1 Depletion of *G. mellonella*'s microbiota

G. mellonella was fed with food supplemented with 15 mg of streptomycin and oxytetracycline per 100 g of food, for 10 days.

2.2.13.2 Injection and extraction of bacteria from *G. mellonella*

50 µL of a 5 mL overnight culture of *E. coli*, *En. gallinarum* or *En. faecalis* was grown on 5 mL LB (in the case of *E. coli*) or BHI (in the case of Enterococci) until mid-log phase. The OD_{600} was measured and a H_2O dilution with 10^6-10^8 bacterial cells per 10 µL was prepared (OD_{600} = 1 indicates ~ 10^8 cells/mL). In the laminar hood, a 1 mL tip was taped on paper and a syringe (Hamilton syringe 701N needle size 26s) was sterilised with ethanol and UV-irradiated. Larvae on their 4th stage (~250 mg) were placed on ice. 10 µL of the bacterial suspension was injected in the last pro-leg of the larva by holding the larva on top of the 1 mL tip (**Figure 2.4**).

Figure 2.4. Injection of *G. mellonella*. The tip of the needle points a pro-leg.

To inject the larvae with 1/4x MIC ciprofloxacin (0.007 µg/mL of ciprofloxacin for *E. coli* and 0.125 µg/mL of ciprofloxacin for *En. gallinarum*), I inferred the liquid volume of the larvae from the weight on the larva based on the data from Andrea et al. [119]. In that study they showed that a larva that weights 250 mg has 150 µL of liquid.

Injected larvae were incubated at 37°C for 24 h, then homogenised using a mortar and a pestle adding 100 µL of H_2O per larva. The homogenate was filtered using Miracloth and

plated on LB (for *E. coli* cells) or BHI (for *En. gallinarum* cells) plates supplemented with 1-5x MIC of ciprofloxacin or chloramphenicol. 10-fold dilutions of the homogenate were plated on LB or BHI only plates to count the total number of bacteria plated. The MIC (in µg/mL) of ciprofloxacin for *E. coli* MG1655 was 0.027, for *E. coli* 29-1 was 0.032, and for *En. gallinarum* was 0.5. The MIC of chloramphenicol was 4 µg/mL for all bacterial strains. Plates were incubated at 37°C for 24 h, then at room temperature for further 24 h. The colonies that grew after the incubation were re-streaked in plates with the same concentration of antibiotic that was used in the selection (i.e., 1-5x MIC of ciprofloxacin or chloramphenicol). The re-streaked colonies that grew were also grown in selective media to check that they were *E. coli* (*E. coli* cells but not Enterococci can grow on MacConkey agar) or *En. gallinarum* (only Enterococci cells can grow on Enterococcus selective media).

Chapter 3:

3   Repair of quinolone-induced damage: role of putative tyrosyl-DNA phosphodiesterases (TDPs)

3.1   Introduction

Quinolones can kill bacteria, but how they do it is not completely understood. We know that quinolones trap bacterial topoisomerases on the DNA which leads to the inhibition of DNA synthesis, the accumulation of reactive oxygen species (ROS) and DNA damage - the latter of which is likely to be the real cause of bacterial death [12]. However, to fully understand quinolone lethality, it is important to consider that the quinolone-induced DNA damage can be repaired, as several experiments have shown that the bacterial chromosome has less breaks over time when the quinolones are removed [79, 94]. Thus, quinolone lethality also depends on the ability of bacteria to repair quinolone-induced DNA damage. However, not much is known about how bacteria repair quinolone-induced DNA damage, other than that DNA repair proteins and the nucleases Exo VII and maybe SbcCD are involved [93, 120, 121]. This knowledge gap in the understanding of the repair of quinolone-induced damage caught our attention and we decided to investigate it further, not only because it could help us understand how quinolones kill bacteria, but also because it might explain how quinolones lead to mutations (which will be discussed in Chapter 5 and Chapter 7).

In this chapter and in Chapter 4, I present my results on the research into quinolone-induced damage repair. I based my hypothesis on how eukaryotes repair their trapped topoisomerase-associated damage and on information found in the literature. Eukaryotes have topoisomerases that can be trapped on the DNA in a similar manner to how quinolones trap gyrase and topo IV [122]. Once the eukaryotic topoisomerase is trapped on the DNA, the cell needs to remove it from the DNA. If it does not do so, it would cause DNA breaks when the replication fork collides with the topoisomerase-DNA complex (note that, by contrast, DNA breaks do not happen in bacterial topoisomerase-DNA-quinolone complexes when the replication fork collides, and it seems that the source of DNA breaks might come from downstream events like the accumulation of ROS, see Introduction 1.2.4). To remove the trapped topoisomerase from the DNA, eukaryotic cells first digest part of the trapped topoisomerase using a protease. Then they release the partially digested topoisomerase from the DNA using a nuclease or a tyrosyl-DNA phosphodiesterase (TDP) [123].

Repair of quinolone-induced damage: role of putative tyrosyl-DNA phosphodiesterases (TDPs)

TDPs, which are the main subject of this chapter, are proteins involved in the repair of DNA breaks caused by poisoned topoisomerases [124, 125]. TDPs specifically hydrolyse the bond between a tyrosine residue from a topoisomerase and a phosphate from a nucleotide (**Figure 3.1**). This reaction releases a trapped topoisomerase from the DNA, allowing the cell to repair the DNA break made by the topoisomerase. If trapped topoisomerases stay on the DNA, replication and transcription are blocked, the DNA break is not repaired, and the cell eventually dies. Hence, TDPs are essential in the repair of trapped topoisomerase damage [126]. TDPs have only been found in eukaryotes, and they can be divided in two types: TDP1 that acts on type I topoisomerases (that make a single-strand break on the 3' end of a DNA strand) and TDP2 that acts predominately on type II topoisomerases (that make a double-strand break on the 5' end of two DNA strands). Because quinolones poison type II topoisomerases like gyrase, in this project I have focused on TDP2.

Bacteria do not have any protein that resembles the sequence of TDP2 (nor TDP1) and, so far, none of their proteins has shown tyrosyl-DNA phosphodiesterase activity [127]. However, it is possible that bacteria have a TDP2 protein because, as I mentioned, quinolones cause DNA damage that can be repaired. DNA repair proteins fix this damage [94, 128], but to do so they need free DNA as a substrate [129], and therefore they cannot repair the DNA if the topoisomerase is trapped on the DNA. Also, bacterial and eukaryotic type II topoisomerases are relatively similar and can be inhibited causing the death of the cell [122, 130], hence, bacteria could have similar proteins to eukaryotes that can remove poisoned topoisomerases. This led me to hypothesise that there was a TDP2-like protein in the model bacterium *Escherichia coli* (*E. coli*).

In the following sections I show my attempts to find a TDP2-like protein in *E. coli* using lysates in an *in vitro* assay (the cleavage assay) that allows us to visualise the removal of gyrase from the DNA. I also investigated three putative structural homologs of TDP2 in *E. coli* (Exonuclease III, YafD and YbhP) to determine if any of these proteins was involved in the repair of quinolone-induced damage and if they had tyrosyl-DNA phosphodiesterase activity.

Repair of quinolone-induced damage: role of putative tyrosyl-DNA phosphodiesterases (TDPs)
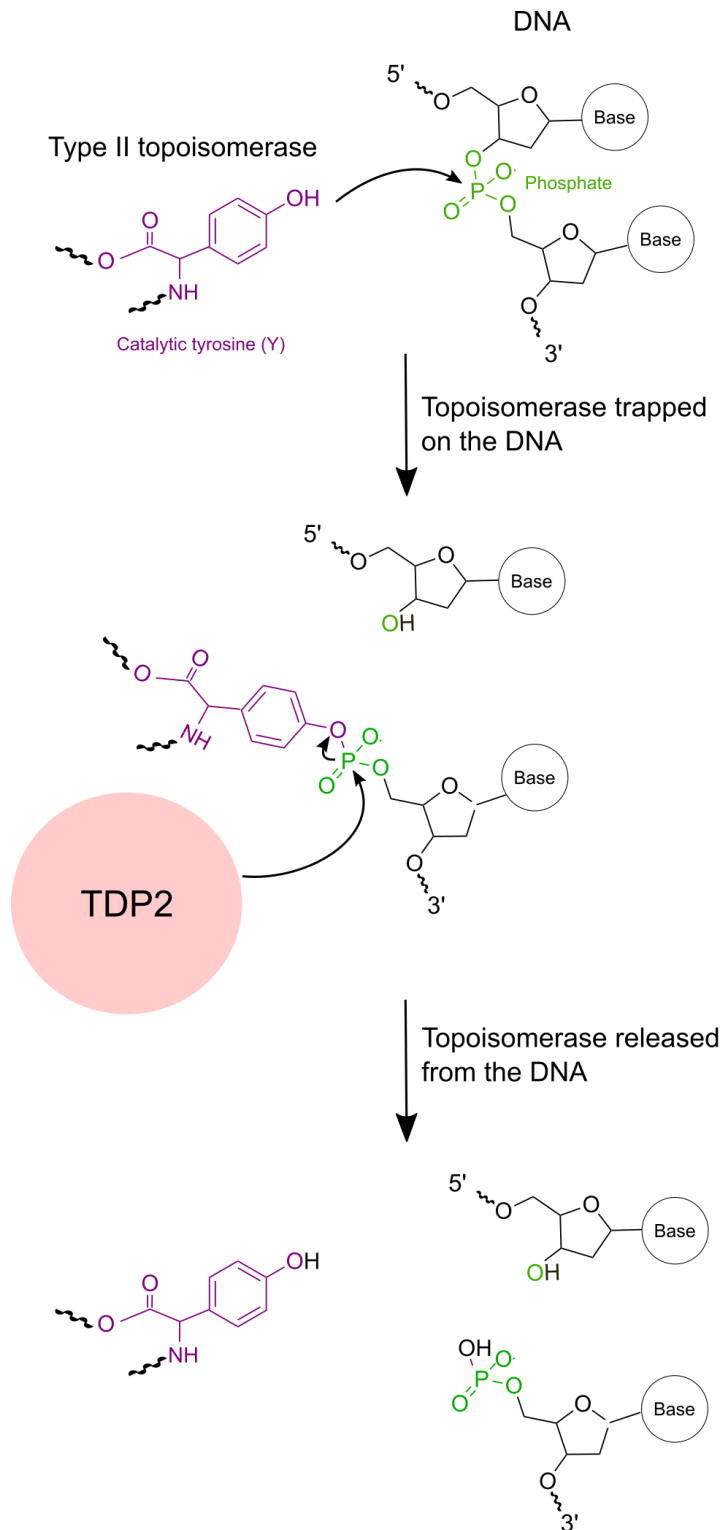
Figure 3.1. Mechanism of action of TDP2. Type II topoisomerases bind to the DNA and generate a double-strand break (DSB) when two catalytic tyrosine residues from the topoisomerase attack two phosphate groups from two complementary DNA strands. If the topoisomerase is inhibited by a poison (e.g., doxorubicin), the topoisomerase remains bound to the DNA, blocking DNA synthesis. TDP2 binds to the topoisomerase-DNA complex and hydrolyses the 5'-tyrosyl phosphodiester bond which releases the

topoisomerase from the DNA. This frees the DSB that can then be repaired. (Note that for simplicity I have just represented one catalytic tyrosine and the corresponding single-strand DNA break).

3.2   Results

3.2.1   Using the cleavage assay to find a TDP2-like protein in *E. coli* lysates

The first strategy to identify a TDP2-like protein in *E. coli* combined the cleavage assay and *E. coli* lysates. The cleavage assay is an *in vitro* technique used to visualise and to measure the stabilisation of a topoisomerase in the DNA under quinolone exposure on the DNA. Because my model bacterium was *E. coli*, I used the quinolone ciprofloxacin (as this is the main quinolone used to treat *E. coli* infections) and the topoisomerase gyrase (as this is the main target of ciprofloxacin in *E. coli*).

The cleavage assay makes use of ciprofloxacin's ability to stabilise the state in which gyrase is covalently bound to the DNA and has made a double-strand break (DSB). As I mentioned in the Introduction (section 1.2.3), during the mechanism of action of gyrase, there is a state in which gyrase covalently binds to the DNA through its two catalytic tyrosine residues making a DSB. This state is called "cleavage complex". In the cleavage assay, gyrase is incubated with ciprofloxacin and plasmid DNA. Ciprofloxacin traps gyrase on the plasmid DNA, but the addition of Proteinase K and SDS, that can denature and digest the gyrase, reveals the DSB of the cleavage complex. The exposure of the DSB linearises the plasmid DNA, which can be observed on an agarose gel (**Figure 3.2**).
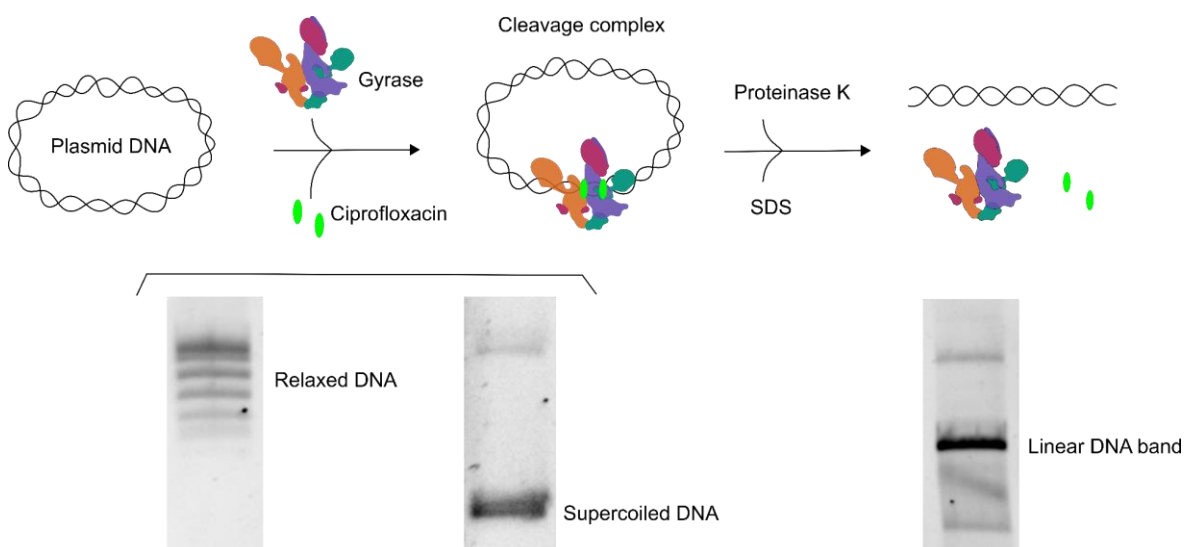
Figure 3.2. Rationale of the cleavage assay with gyrase. The substrate of gyrase is relaxed or supercoiled DNA. The supercoiling or relaxation of DNA by gyrase can be

observed in an agarose gel as supercoiled DNA travels faster than relaxed DNA. However, if gyrase is also incubated with the quinolone ciprofloxacin, the relaxation or supercoiling activity of gyrase is inhibited. Moreover, gyrase remains bound to the DNA forming a gyrase-DNA complex in which there is a DSB. Upon the addition of Proteinase K and SDS, gyrase is denatured and cut from the DNA. The removal of the gyrase exposes the DSB which linearises the plasmid. The linearisation of the plasmid can be observed in an agarose gel as a linear DNA band.

E. coli lysates contain all proteins present in the cytoplasm of *E. coli* cells. If there is a TDP2-like protein in *E. coli*, it should be present in its cytoplasm and, therefore, the lysate should also contain it. As I mentioned above, in the traditional cleavage assay we use a protease and a denaturing agent to remove a trapped gyrase from the DNA. In this project, I have modified the cleavage assay so that instead of adding a protease and a denaturing agent, I used *E. coli* lysates. The rationale behind this is that if there is a TDP2-like protein in the *E. coli* lysate, it should release the trapped gyrase from the DNA freeing the DSB and linearising the plasmid. The main limitation of this approach is that there are nucleases and proteases in the lysates that can cut the plasmid which can obscure the results. I will discuss this problem later.

3.2.1.1 Optimisation of the conditions for the cleavage assay

Before doing the cleavage assay, I checked if the gyrase was active and if it could be inhibited by the quinolone ciprofloxacin. Gyrase can relax negatively and positively supercoiled DNA as well as negatively supercoil relaxed DNA. But when ciprofloxacin binds to the gyrase-DNA complex, gyrase is inhibited and there is no relaxation or supercoiling. As an example, I show in **Figure 3.3** what happens when gyrase is incubated with supercoiled plasmid DNA in the presence or absence of ciprofloxacin. Supercoiled plasmid DNA travelled faster in an agarose gel than relaxed DNA, and I could see that gyrase was able to relax it, but the relaxation was inhibited in the presence of ciprofloxacin. This experiment confirmed that gyrase was active and that it could be inhibited by ciprofloxacin.

Once I knew that gyrase was active, I did the cleavage assay using different DNA substrates (**Figure 3.4**). As expected, I observed a linear DNA band after the addition of Proteinase K and SDS, indicating that the gyrase had been released from the DNA.
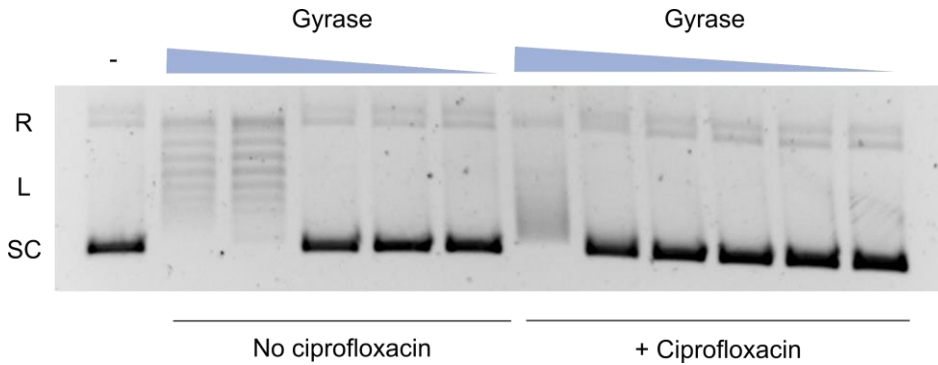
Figure 3.3. Relaxation assay with _E. coli_ gyrase. 1/3 dilutions of 2 U/µL gyrase were incubated for 30 min with 500 ng supercoiled DNA in the presence or absence of 10 µg/mL ciprofloxacin. Gyrase can relax negatively supercoiled DNA - which runs faster in an agarose gel than relaxed DNA - but cannot do this in the presence of ciprofloxacin. Negatively supercoiled pBR322 was used as the DNA substrate. R stands for relaxed DNA, L for linear DNA and SC for supercoiled DNA.
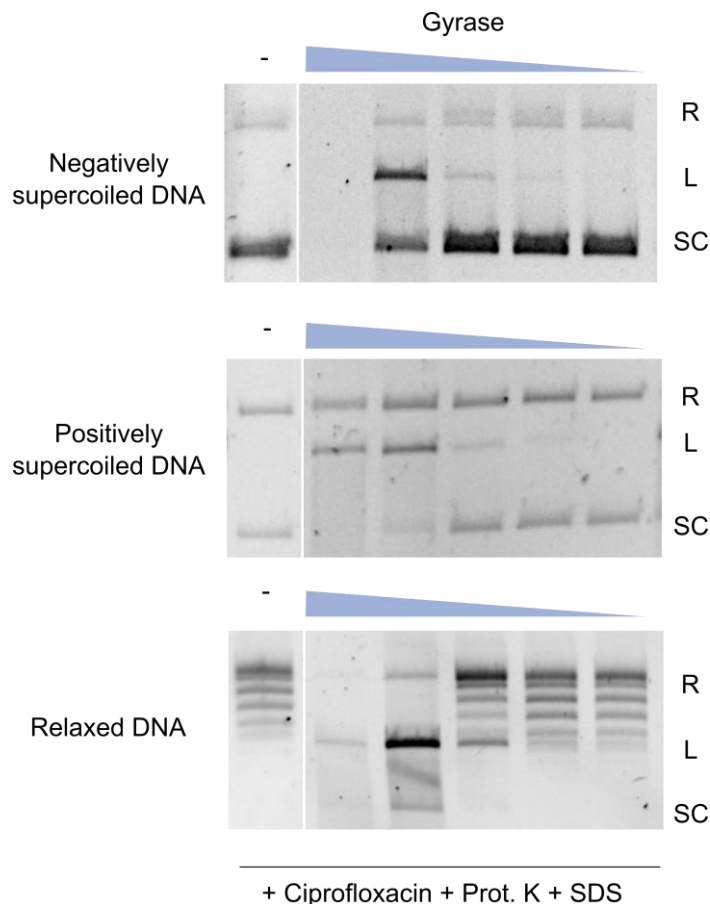
Figure 3.4. Traditional cleavage assay with _E. coli_ gyrase. Gyrase is stabilised in the DNA in the presence of 10 µg/mL ciprofloxacin, and the addition of 3 µL 2% (w/v) SDS and 1.5 µL of 10 mg/mL Proteinase K (Prot. K) releases the gyrase from the DNA causing the linearization of the DNA. 1/2 dilutions of 10 U/µL gyrase were added. The reaction

products were run on an 1% w/v agarose gel for 2 h at 80 V. 500 ng of negatively or positively supercoiled, or relaxed pBR322* was used as the DNA substrate. R stands for relaxed DNA, L for linear DNA and SC for supercoiled DNA.

3.2.1.2 *E. coli* lysates contain protein(s) that can cut the DNA and/or release gyrase from the DNA.

Once I optimised the conditions for the cleavage assay, I investigated whether proteins in *E. coli* lysates could also release a trapped gyrase. The rationale behind this was that, if such protein existed, when cell lysates were added in a cleavage assay instead of SDS and Proteinase K, a linear band would be observed (meaning that there was something in the lysate that could process the gyrase-DNA cleavage complex). The main limitation of this approach was the presence non-specific nucleases in the cell lysate. Those nucleases could cut the DNA and linearise the plasmid. Thus, it would be impossible to distinguish between their action and the processing of the gyrase by a TDP2-like protein.

Sylvain Mitelheiser, a previous PhD student, designed and performed the first experiment using *E. coli* lysates to find a protein involved in the release of trapped gyrase [131]. He reasoned that such protein should be induced by quinolones. Therefore, he used two types of lysates: one that had been treated with the quinolone oxolinic acid, and another that had not been treated. He also hypothesised that the protein should be acting only when the gyrase-DNA complex was stabilised with ciprofloxacin. Thus, for each experimental condition, ciprofloxacin was either present or absent. Finally, he used dilutions of the lysate to avoid the action of non-induced nucleases. Despite obtaining a linear DNA band when he did a cleavage assay with an induced lysate that was diluted and tested in the presence of ciprofloxacin, he was not able to reproduce the experiment and it was eventually abandoned (**Figure 3.5A**).

I tried to reproduce Sylvain's experiment using different DNA substrates (**Figure 3.5B**), but I could not see the linear DNA band he predicted, that is, a linear DNA band only in oxolinic acid-treated lysates that were diluted and tested in the presence of ciprofloxacin. What I could see was a faint linear DNA band regardless of the presence of ciprofloxacin, whether cells had been treated with oxolinic acid or not, or what DNA substrate I used. I also tried lysates from *E. coli* cells grown until log or stationary phase that had been induced with high or low levels of oxolinic acid. In all conditions I found linear DNA bands irrespective of the presence of ciprofloxacin or the treatment with oxolinic acid. These results indicated that there was something (probably a protein) in *E. coli* lysates that could linearise the plasmid but that it was not induced by oxolinic acid, nor acting specifically when ciprofloxacin stabilised the gyrase-DNA complex. Two types of proteins could be

Repair of quinolone-induced damage: role of putative tyrosyl-DNA phosphodiesterases (TDPs)

responsible for the linearisation of the plasmid: a TPD2-like protein or a nuclease. I tried to find out which type of protein it was in the following section.

A)
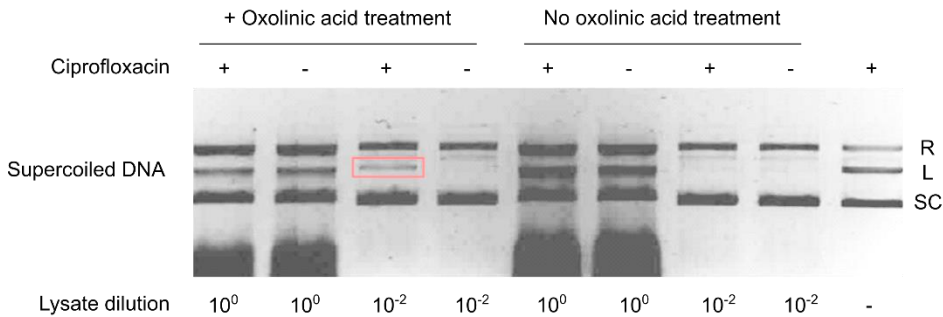
B)
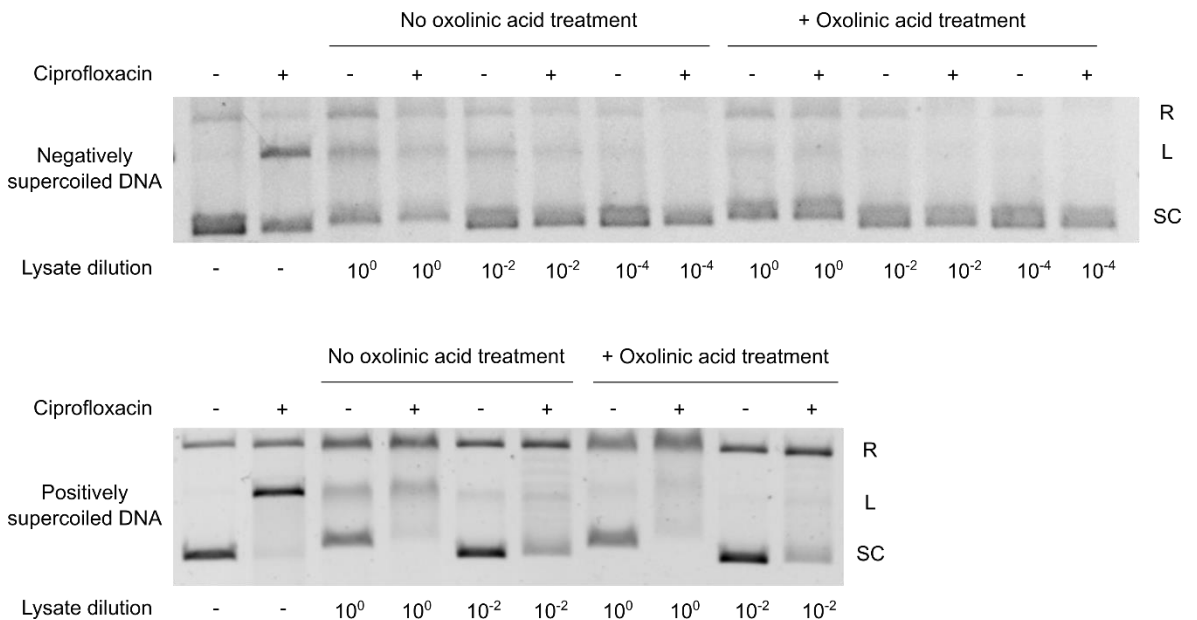
Figure 3.5. Cleavage assay with gyrase and *E. coli* lysates. A) Cleavage assay using *E. coli* cell extracts performed by Sylvain Mitelheiser during his PhD adapted from [131]. Gyrase was incubated with negatively supercoiled pBR322 and with or without 10 µg/mL of ciprofloxacin for 30 minutes. Cleaved DNA (linear DNA band, L) was revealed after the digestion of gyrase by the addition of Proteinase K and SDS (Control, lane 9), or by the addition of cell lysates that had been treated 30 min with 100 µg/mL of oxolinic acid (lanes 1-4) or had not been treated with oxolinic acid (lanes 5-8). The red square indicates the linear band that was thought to be caused by a protein induced by quinolone treatment that could release the gyrase from the DNA. B) Cleavage assay using *E. coli* lysates with negatively supercoiled (upper gel) or positively supercoiled DNA (lower gel). Gyrase was incubated with supercoiled pBR322 for 30 minutes and with or without 30 µM of ciprofloxacin. Cleaved DNA (linear DNA band, L) was revealed after the digestion of

gyrase by the addition of Proteinase K and SDS (lanes 1 & 2), or by the addition of cell lysates of different dilutions that had been treated 30 min with 100 µg/mL oxolinic acid (lanes 9-14 in the upper gel, lanes 7-10 in the lower gel) or had not been treated with oxolinic acid (lanes 3-8 in the upper gel, lanes 3-6 in the lower gel). Note that the MIC for oxolinic acid is 0.4 µg/mL.

3.2.1.3 EDTA inhibits the lysate protein(s) that cut the DNA and/or release gyrase from the DNA

To find out if nucleases or a TDP2-like protein caused the linearisation of the plasmid in the modified cleavage assay, I used ethylenediaminetetraacetic acid (EDTA), which is a chelator of metal ions that can affect the formation of the gyrase-DNA complex. At moderate concentrations (0.5-10 mM) EDTA can stimulate the resealing of DNA that was broken in gyrase-DNA complexes, but at high concentrations (20-75 mM) the DNA breaks are not reversed [132, 133].

The properties of EDTA on gyrase-DNA complexes can be used to design a cleavage assay with lysates that can distinguish between proteins that are affected by EDTA from the ones that are not. As EDTA is a chelator of metal ions, its presence inhibits the action of proteins dependent on metal ions, like nucleases and metalloproteins. Hence, if the TDP2-like protein that I am looking for is not dependent on metal ions, it will not be affected by EDTA, and I could differentiate it from nucleases. As increasing concentrations of EDTA reverse or maintain the gyrase-DNA complex, if there is a TDP2-like protein that is not affected by EDTA, at low concentrations of EDTA I should see a linear DNA band (as the TDP2-like protein has removed the gyrase from the DNA releasing the DSB), at high concentrations of EDTA I should not see a linear DNA band (as EDTA stimulated the resealing of the DSB by gyrase), and at very high concentrations of EDTA I should see again the linear DNA band (as EDTA does not stimulate the resealing of the DSB by the gyrase). In contrast, if there is a nuclease, at low concentrations of EDTA I should see a linear DNA band (as the nuclease cut the plasmid), but at very high concentrations of EDTA I should not see a DNA linear band (as gyrase cannot reseal the DNA break caused by the nuclease) (**Figure 3.6A**).

I first did a traditional cleavage assay using increasing concentrations of EDTA. As expected, I could observe the appearance, disappearance, and re-appearance of the linear DNA band as I increased the concentrations of EDTA (lanes 3-5) (**Figure 3.6B**). However, when I used cell lysates instead of Proteinase K and SDS (lanes 8-10 and 13-15), there was no linear DNA band at very high concentrations of EDTA. These results showed that EDTA inhibited the protein(s) in the lysate responsible for the linearisation of

the plasmid. As most nucleases are inhibited by EDTA, it is likely that the linearisation of the plasmid was caused by nucleases. Whether any of these nucleases was able to specifically remove the trapped gyrase from the DNA cannot be discerned with this experiment. It is also possible that the TDP2-like protein needs metal ions and therefore it would also be inhibited by high concentrations of EDTA. In this case, I would not be able to see the linearisation of the plasmid at high concentrations of EDTA, and I could not distinguish it from a nuclease. In conclusion, I have not found evidence of the presence of a TDP2-like protein in *E. coli* unless that TDP2-like protein needs metal ions, in which case this assay cannot be used to distinguish such protein from a nuclease.

A)

B)
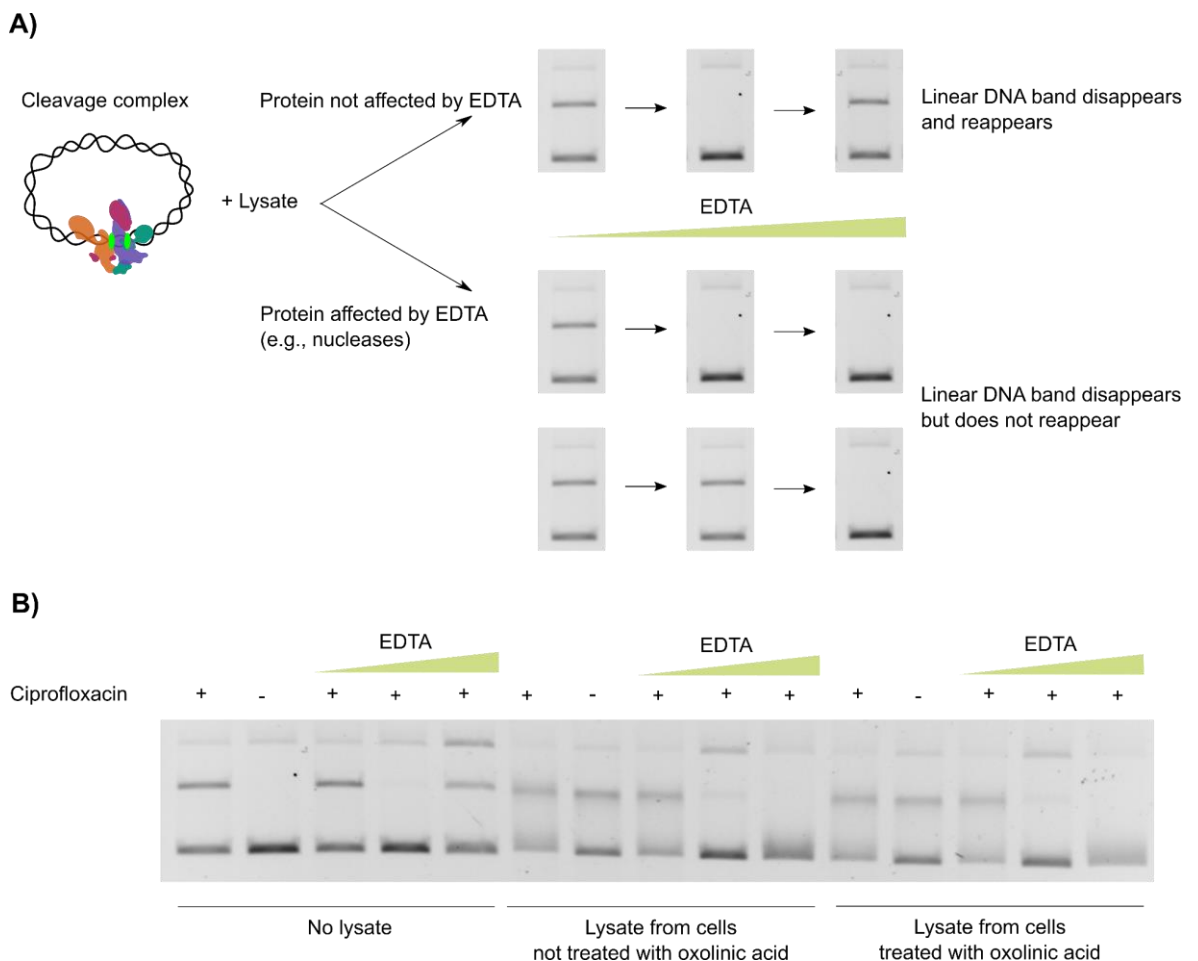
Figure 3.6. The cleavage assay with EDTA. A) Rationale of the experiment that combines the cleavage assay with an additional incubation with EDTA. The goal of the experiment was to distinguish between the action of nucleases that cut the DNA but do not dissociate gyrase from the DNA (protein affected by EDTA), and a protein that dissociates gyrase from the DNA and exposes DNA breaks (protein not affected by EDTA). Different concentrations of EDTA can reverse or maintain the complex of gyrase covalently bound to DNA (or cleavage complex). The effects of EDTA can be observed by looking at the presence of a linear DNA band. Such a band appears when the plasmid

that is used as a substrate in the assay is linearised. When the cleavage complex is stabilised by the addition of ciprofloxacin, SDS and Proteinase K can dissociate the gyrase from the cleavage complex, free the DNA that has a DSB and thus linearise the plasmid. If there is a protein in the *E. coli* lysate that can dissociate the gyrase from the DNA (like Proteinase K and SDS), the linear band would appear, disappear, and reappear at increasing concentrations of EDTA. However, if there is not such a protein but non-specific nucleases, the linear band cannot disappear and reappear, as the cut in the DNA could not be resealed. Because EDTA can inhibit nucleases, in the case of the non-specific nucleases it would be possible to see the disappearance of the linear band (meaning that the nuclease is inactive) as I increase the concentration of EDTA. B) Cleavage assay with lysates and EDTA. Gyrase was incubated for 30 min at 37°C with 0.3 µg of supercoiled DNA and 0.25 mM $MgCl_2$ in the presence or absence of 10 µg/mL of ciprofloxacin to a final volume of 30 µL. I then added 7.5 µL of 0, 0.1, 10 or 75 mM of EDTA and incubated for 20 min. Finally, I added 3 µL 2% (w/v) SDS and 1.5 µL of 10 mg/mL Proteinase K (lanes 1-5), 4.5 µL of lysate from *E. coli* cells (lanes 6-10), or 4.5 µL of lysate from *E. coli* cells treated with oxolinic acid (lanes 11-15), and incubated 30 min. The *E. coli* lysates were obtained from 50 mL cultures of *E. coli* treated or not with 0.2 µg/mL of oxolinic acid. The cultures were centrifuged, and the pellet was resuspended in 400 µL of water and 40 µL of 100 mg/mL lysozyme. I used a 1/100 dilution of the lysate.

3.2.2 TDP2 structural homologs in *E. coli*

As I could not find a TDP2-like protein in *E. coli* lysates using the cleavage assay, I tried another strategy: using bioinformatics to find TDP2 homologs. I reasoned that *E. coli* proteins that were similar to TDP2 in terms of their sequence or structure could also have a similar role. Hence, TDP2 homologs could participate in the repair of quinolone-induced DNA damage, so their absence would make cells more sensitive to quinolones whereas their overexpression would make cells more resistant to quinolones. Besides, they should have 5'-tyrosyl DNA phosphodiesterase activity. I tested all these hypotheses in the next sections.

3.2.2.1 *E. coli* has three putative structural homologs of TDP2

When looking for TPD2 homologs in *E. coli*, I first tried to find *E. coli* proteins that were similar to TDP2 in terms of their protein sequence by doing a protein BLAST. I got no results. However, when I used the software Backphyre [134] to compare the structural data of TDP2 with all proteins in *E. coli*, I found several putative structural homologs: Exonuclease III (Exo III), YbhP, YafD, SbcD, YaeI, YafV and RuvC (**Table 3.1**).

Repair of quinolone-induced damage: role of putative tyrosyl-DNA phosphodiesterases (TDPs)

Table 3.1. List of proteins in *E. coli* MG1655 that were structurally related to crystal structures of TDP2 from different organisms. Results were obtained from the Phyre2 web portal using Backphyre.

Query protein	PDB format	Structural homologs in *E. coli*
Crystal structure of m2hTDP2-CAT	5J3Z	None
Crystal structure of *Mus musculus* Tdp2 bound to dAMP and Mg^{2+}	4GYZ	exodeoxyribonuclease III Exo III endonuclease/exonuclease/phosphatase domain-containing protein YbhP endonuclease/exonuclease/phosphatase domain-containing protein YafD 2-oxoglutaramate amidase YafV
Crystal structure of TDP2 from *C. elegans*	4GEW	exodeoxyribonuclease III Exo III endonuclease/exonuclease/phosphatase domain-containing protein YbhP endonuclease/exonuclease/phosphatase domain-containing protein YafD nuclease - SbcD subunit endodeoxyribonuclease RuvC phosphodiesterase YaeI
Crystal structure of TDP2 from *Danio rerio* complexed with a single-stranded DNA	4F1H	exodeoxyribonuclease III Exo III endonuclease/exonuclease/phosphatase domain-containing protein YbhP endonuclease/exonuclease/phosphatase domain-containing protein YafD phosphodiesterase YaeI 2-oxoglutaramate amidase YafV
Crystal structure of the catalytic domain of human TDP2	5J3P	exodeoxyribonuclease III Exo III endonuclease/exonuclease/phosphatase domain-containing protein YbhP endonuclease/exonuclease/phosphatase domain-containing protein YafD

TDP2 has four putative catalytic residues within the catalytic domain extending from amino acids 113–362 (**Figure 3.7A**). I aligned all the *E. coli* putative homologs against TDP2 and found that only Exo III, YafD and YbhP shared the TDP2 catalytic residues (**Figure 3.7B**). Moreover, the location of the TDP2 catalytic residues in the 3D structures of TDP2, Exo III, YafD and YbhP was similar (**Figure 3.7C**).

Exo III is a well-known nuclease that has 3'-phosphatase, 3'-exonuclease and apurinic/apyrimidinic endonuclease activity [135]. YafD and YbhP are uncharacterised proteins that, by sequence homology, are predicted to belong to the endonuclease/exonuclease/phosphatase family. None of these proteins has ever been associated to the repair of quinolone-induced damage.

A)

TDP2

N120 E152   D262   H351

Catalytic domain

1   50   100   150   200   250   300   350 362 aa

B)

```
TDP2     1 MELGSCLEGGREAAEEEGEPEVKKRRLLCVEFASVASCDAAVAQCFLAENDWEMERALNSYFEPPVEESALERRPET  77
Exo_III  1 MKFV------------------------------------------------------------------------   4
YafD     1 MRKNTYA--MRYV---AGQP--AERILPPGSFASIGQ---AL--------------------PPGEPLSTE-----  41
YbhP     1 MPDQTQ-----------------------------------------------------------------Q-----   7

TDP2    78 ISEPKTYVDLTNEETTDSTTSKISPSEDTQQENGSMFSLITWNIDGLD-LNNLSERARGVCSYLALYS--PDVIFLQ 151
Exo_III  5 --------------------------------SFNINGL------RARPHQLEAIVEKHQ--PDVIGLQ  33
YafD    42 ERIRILVWNIYKQQRA-------EWLSVLKNYGKDAHLVLLQ  76
YbhP     8 FSFKVLTINIHKGFTAFNRRFILPELRDAVRTVS--ADIVCLQ  48

TDP2   152 EVIPPYYSYL-----KKRSSNYEI--------------ITGHEEGY-FTAIMLK--------------------KS 187
Exo_III 34 ETKVHDDMFPLEEVA-----------KLGYNV-----FYHGQKGHYGVALLTKETPIAV--RRGFPGD-----DEEA  87
YafD    77 EAQTTPELVQFATANYLAADQVP--------AFV---LP---QHPSGVMTLSAAHPVY-----CCPLREREPILRLA 134
YbhP    49 EVMGAHEVHPLHVENWPDTSHYEFLADTMWSDFAYGRNAVYPEGHHGNAVLSR-YPIEHYENRDVSVD-----GAEK 119

TDP2   188 RVKLKSQEIIPFPSTKMMRNLLCVHVNVSGNELCLMTSHLESTRGHAAER------MNQLKMVLKK-MQEAPESATV 257
Exo_III 88 QRRII-MAEIP-SLLGNV--------------TVINGYFPQGES-RDHPIKFPAKAQFYQNLQNYLETELKRDNPV 146
YafD   135 KSALV--TVYPLPDTRLLMV-----------VNIHAVNFSLG---VDVY------SKQLLPIG---DQIAHHSGPV 185
YbhP   120 RGVLY-CRIVP-PMTGKAI--------------HVMCVHLGLR---EAHR------QAQLAMLAEW-VNELPDGEPV 170

TDP2   258 IFAGDTNLRD----------------REVTRCGGLPNN---------I----------VDVWEFLGKPKHCQYTWDT 299
Exo_III 147 LIMGDMNISPTDLDIGIGEENRKRWLRTGKC-SFLPEEREWMDRLMSW--GL------VDTFRHANPQTADRFSWFD 214
YafD   186 IMAGDFNAWS-----------------RRRMN-ALYRFA---------REMSLRQVRFTDDQRRRAFGRP-------- 228
YbhP   171 LVAGDFNDWR----------------QKANH-PL-KVQ---------A--GL------DEIFTRAHGRPARTFP--- 209

TDP2   300 QMNSNLGITAACKLRFDRIFFRAA------AEEGHIIPRSLDLLGLEKLDCGRFPSDHWGLLCNLDIIL---     362
Exo_III 215 YRSKGFDDN--RGLRIDLLLASQPLAECCVETGIDYE----------IRSMEKPSDHAPVWATFRR-----     268
YafD   229 ---------------LDFVFYRGL----NVSEASV--------------LVTRASDHNPLLVEFSPGKPDK     266
YbhP   210 ---VQFP-----LLRLDRIYVKNA----SASAPTALP-----------LRTWRHLSDHAPLSAEIHL-----     253
```

C)

TDP2

Exo III

YafD

YbhP

Figure 3.7. Structural similarities between TDP2, Exo III, YafD and YbhP. A)
Schematic representation of human TDP2, highlighting the relative position of its catalytic

domain (residues 113 to 362) and its catalytic residues (N120, E152, D262 and H351). B) Structural alignment of human TDP2 (sp|095551|TYDP2), *E. coli* Exo III (NP_416263.1), *E. coli* YafD (NP_414745.1) and *E. coli* YbhP (NP_415311.1) using T-Coffee Expresso [136]. Highlighted in purple are the catalytic residues of TDP2 that are also present in Exo III, YafD and YbhP. C) TDP2 structure (PDB: 5INL), Exo III structure (PDB: 1AKO), YafD (PDB structure predicted by AlphaFold (Jumper, 2021 #318)) and YbhP (PDB structure predicted by AlphaFold) with the corresponding TDP2 catalytic amino acids coloured in purple.

3.2.2.2 The deletion of *xthA* (that encodes for Exo III) makes cells more sensitive to 1st generation quinolones

To find out whether the deletion of the three structural homologs of TDP2 in *E. coli*, Exo III (encoded by *xthA*), YafD (encoded by *yafD*) and YbhP (encoded by *ybhP*), affected the sensitivity of the cells to quinolone exposure, I deleted *xthA*, *yafD* and *ybhP* in *E. coli* MG1655, the WT strain. None of the genes or any combinations of them were essential, as they all could be deleted. The deletions did not affect growth in the absence of quinolones, as the growth curves were similar to the WT (data not shown). However, when I did a minimum inhibitory concentration (MIC) assay using first generation quinolones and fluoroquinolones, I found that the deletion of *xthA* made *E. coli* cells twice as sensitive to oxolinic acid and nalidixic acid (**Table 3.2**). Surprisingly, when cells were grown at room temperature (~20°C) instead of the normal assay conditions (37°C), such sensitivity was "reversed" and Δ*xthA* cells were more resistant to quinolones than the WT cells.

Because the MIC assay shows if the growth of the cells is affected by the drugs but not how well cells survive, I also did an assay to check if the deletion of *xthA*, *yafD* and *ybhP* affected the survival of bacteria when exposed to ciprofloxacin. In order to do this, I compared the number of colonies that could grow after 0, 30, 60 and 90 min of being exposed to ciprofloxacin (**Figure 3.8**). I found no differences between the survival of WT, Δ*xthA*, Δ*yafD* and Δ*ybhP* cells to ciprofloxacin. These results showed that the absence of *xthA* (Exo III) affected the lethality of 1st generation quinolones (as the MIC to oxolinic acid and to nalidixic acid was lower than for WT cells) but not of fluoroquinolones like ciprofloxacin (as the MIC and the survival to ciprofloxacin were the same as for WT cells).

Repair of quinolone-induced damage: role of putative tyrosyl-DNA phosphodiesterases (TDPs)

Table 3.2. Oxolinic acid, nalidixic acid, ciprofloxacin and norfloxacin MIC values for the *E. coli* MG1655 WT, *xthA*, *yafD* and *ybhP* mutants. The strains were grown at 37°C for 20 hours or at 20°C for 48 hours. Highlighted in green are the mutants that were more sensitive than WT cells and highlighted in yellow are the mutants that were more resistant than WT cells. Each MIC value is the mean of three replicates.

| | 1st generation quinolones | | | |
| | Oxolinic acid MIC (µg/mL) | | Nalidixic acid MIC (µg/mL) | |
Strain	37°C	20°C	37°C	20°C
MG1655 WT	0.4	0.2	6.4	3.2
Δ*xthA*	0.2	0.2	3.2	6.4
yafD::Cam^R	0.4	0.2	6.4	3.2
ybhP::Kan^R	0.4	0.2	6.4	3.2
Δ*xthA yafD*::Cam^R	0.2	0.2	3.2	6.4
Δ*xthA ybhP*::Kan^R	0.2	0.2	3.2	6.4
yafD::Cam^R *ybhP*::Kan^R	0.4	0.2	6.4	3.2
Δ*xthA yafD*::Cam^R *ybhP*::Kan^R	0.2	0.2	3.2	6.4

| | Fluoroquinolones | | | |
| | Ciprofloxacin MIC (µg/mL) | | Norfloxacin MIC (µg/mL) | |
Strain	37°C	20°C	37°C	20°C
WT MG1655	0.027	0.008	0.128	0.032
Δ*xthA*	0.027	0.012	0.128	0.032
yafD::Cam^R	0.027	0.008	0.128	0.032
ybhP::Kan^R	0.021	0.008	0.128	0.032
Δ*xthA yafD*::Cam^R	0.027	0.012	0.128	0.032
Δ*xthA ybhP*::Kan^R	0.027	0.012	0.128	0.032
yafD::Cam^R *ybhP*::Kan^R	0.027	0.008	0.128	0.032
Δ*xthA yafD*::Cam^R *ybhP*::Kan^R	0.027	0.012	0.128	0.032
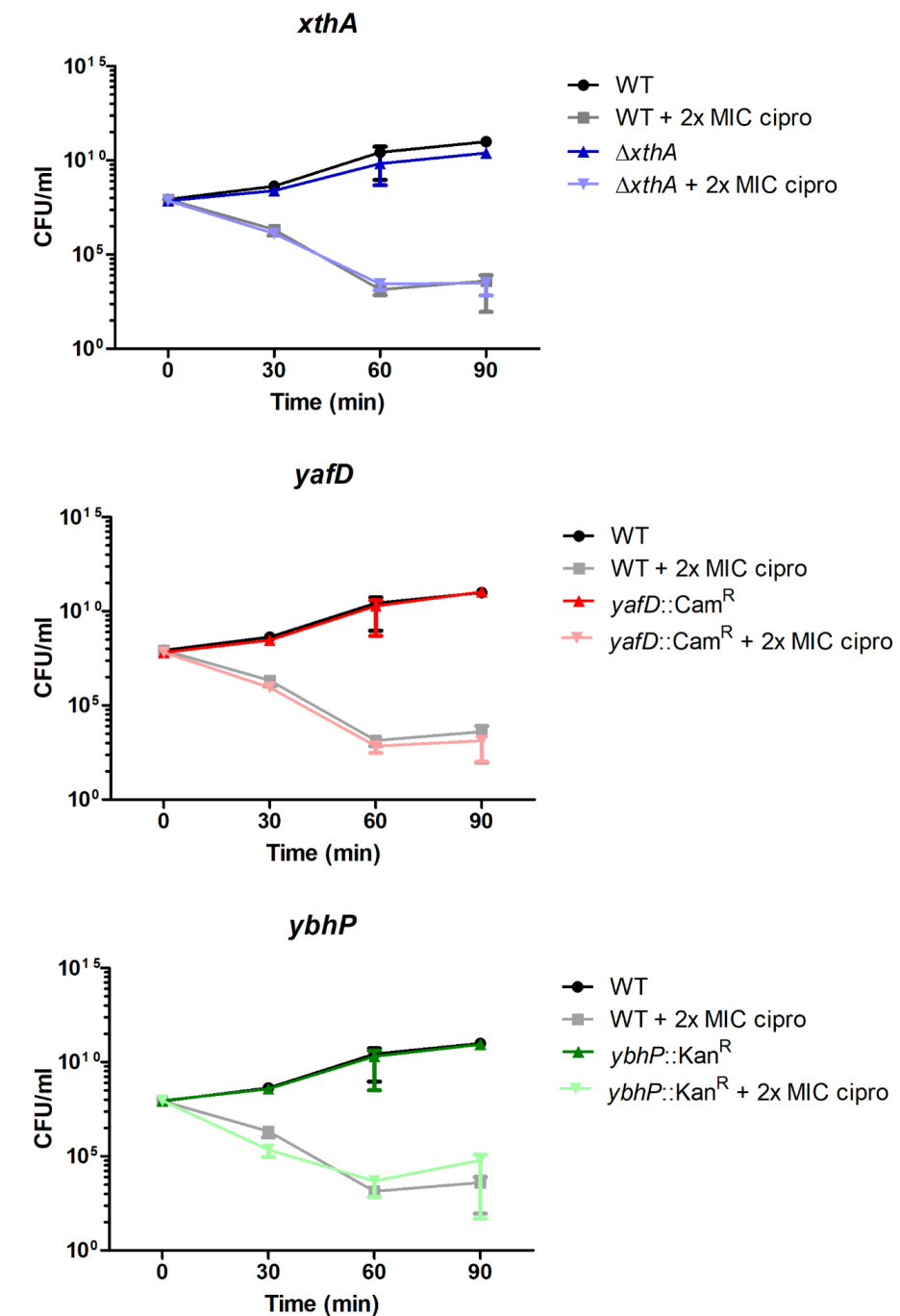
Figure 3.8. Survival assay of WT, *xthA*, *yafD* and *ybhP* mutants. Cells were grown until logarithmic phase and then split into two cultures: one was treated with 2x MIC of ciprofloxacin (0.054 µg/mL) and the other was left untreated. The drug was added after 0, 30, 60 and 90 min. At each of these time points, a sample from each culture was taken and plated on LB to count the number of colony forming units (CFU) per mL. Each point in the graph represents the average CFU/mL of two replicates. The error bars show the standard deviation.

3.2.2.3 *yafD* might participate in the repair of ciprofloxacin-induced damage independent of ROS accumulation

Quinolones lead to the formation of reactive oxygen species (ROS) which can cause DNA damage. It is believed that part of quinolone-induced DNA damage is due to the accumulation of ROS [137]. How important ROS are in the lethality of quinolones, depends on the type of quinolone. In the case of ciprofloxacin, the accumulation of ROS seems to be crucial to kill the cells [24]. Hong et al. [24] showed that when cells were treated with ciprofloxacin and chloramphenicol, and then grown in the presence of dimethyl sulfoxide (DMSO), there was almost no cell death. They claimed that the inability of ciprofloxacin to kill the bacteria was due to the inhibition of ROS accumulation caused by chloramphenicol and DMSO. Chloramphenicol is thought to inhibit the synthesis of proteins lowering the activity of the cells and thus the formation of ROS [19, 138] and DMSO is an inhibitor of ROS [24].

Based on the Hong et al. [24] experiment, I hypothesised that if any of my TDP2-like candidates was involved in the repair of ciprofloxacin-induced damage caused by ROS, in the absence of those proteins, the attenuation of ROS would not affect the survival of the cells to ciprofloxacin. Conversely, the absence of a protein involved in the repair of ciprofloxacin-induced damage independent of ROS, would make cells susceptible to ciprofloxacin even if there is no ROS accumulation.

To test if Exo III, YafD or YbhP were involved in the repair of ciprofloxacin-induced ROS damage, I exposed the *xthA*, *yafD* and *ybhP* mutants to ciprofloxacin and chloramphenicol and plated the cells in the presence or absence of DMSO (**Figure 3.9**). I found that the treatment with high concentrations of ciprofloxacin killed most of the cells after 30 min (only ~1 in 100,000 cells survived), although in the presence of DMSO the killing was diminished. However, when WT cells (as well as Δx*thA* cells) were co-treated with ciprofloxacin and chloramphenicol, most of the cells survived, regardless of the presence or absence of DMSO, presumably because the cells were not killed by the accumulation of ROS. The same happened with *ybhP*::Kan^R cells (results not shown). These results were consistent with Hong et al. [24] experiments in which they showed that ciprofloxacin lethality greatly relied on ROS accumulation.

Interestingly, the absence of *yafD* made cells sensitive to the co-treatment of ciprofloxacin and chloramphenicol in the absence of DMSO (again only 1~ in 100,000 cells survived), and in the presence of DMSO the cell death was lower. These results indicated that ROS are important contributors to ciprofloxacin death and that *yafD* might participate in the repair of ciprofloxacin-induced damage independent of the accumulation of ROS.

Repair of quinolone-induced damage: role of putative tyrosyl-DNA phosphodiesterases (TDPs)
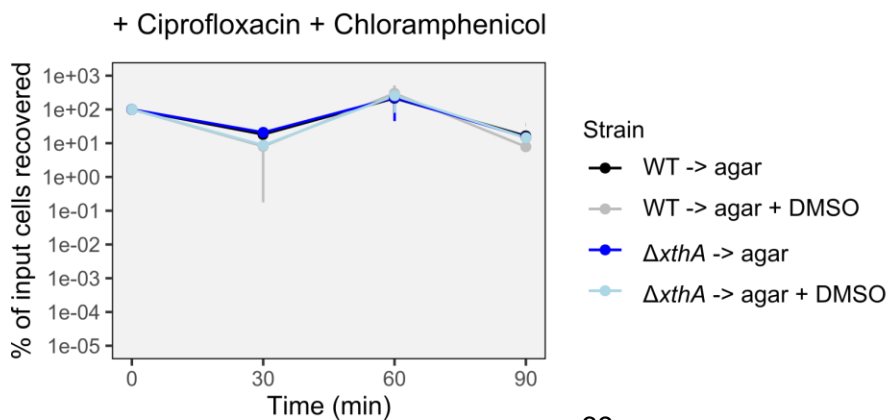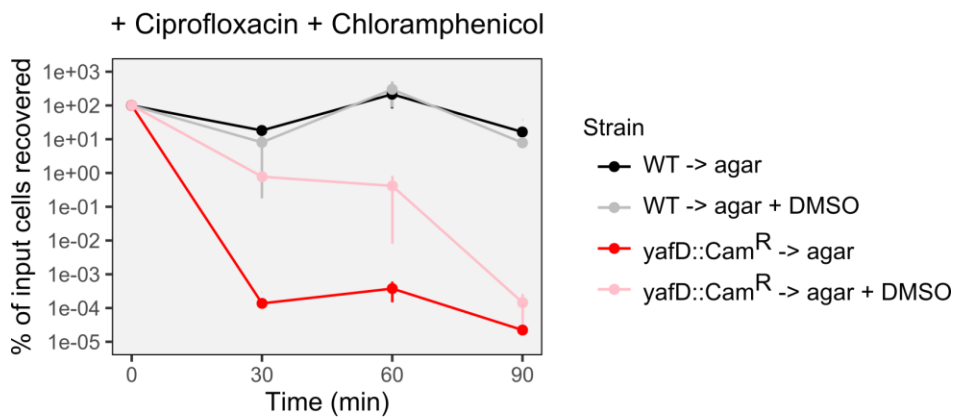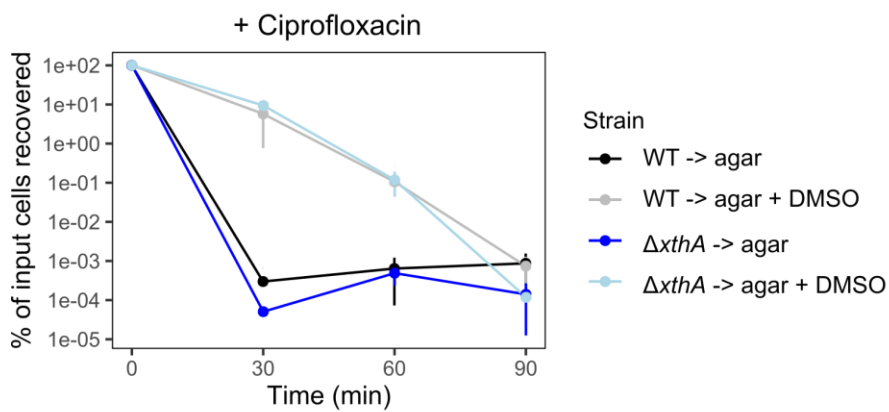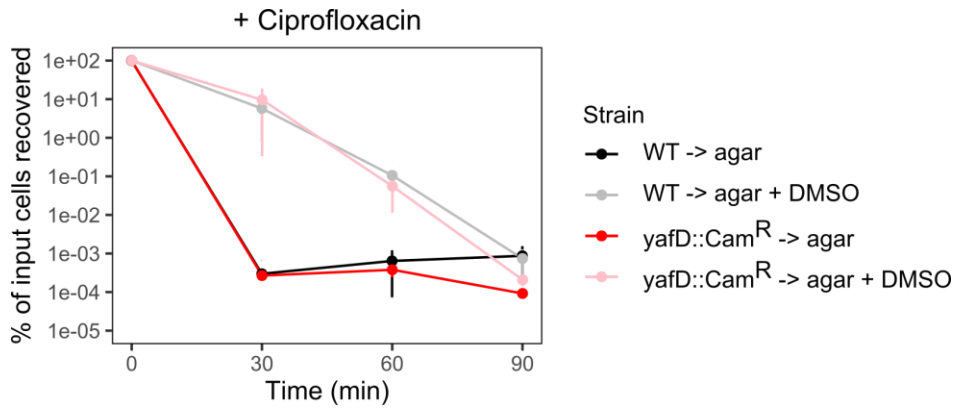
Figure 3.9. Survival of WT, *yafD* and *xthA* mutants after exposure to ciprofloxacin and/or chloramphenicol. Cells were grown until log phase and treated or not with 10x MIC to ciprofloxacin (0.27 µg/mL) and/or 5x MIC to chloramphenicol (20 µg/mL). was treated with 2x MIC of ciprofloxacin (0.054 µg/mL) and the other was left untreated. The drug(s) was added after 0, 30, 60 and 90 min. At each of these time points, a sample from each culture was taken and plated on LB or LB with 5% DMSO for the determination of colony forming units. Points represent the average of 3 replicates and the error bars represent the standard deviation.

3.2.2.4 The overexpression of Exo III, YafD or YbhP does not significantly affect the sensitivity to quinolones

Another way of testing if Exo III, YafD or YbhP participated in the repair of quinolone-induced damage, was to check if their overexpression affected the resistance to quinolones. The rationale behind this was that, if Exo III, YafD or YbhP help bacteria against quinolones, having more Exo III, YafD, or YbhP might make cells more resistant to quinolones. To overexpress these proteins in *E. coli* I used two systems: an overexpression system in *E. coli* MG1655 background and another in *E. coli* BL21. The reason why I used two *E. coli* strains was because it was difficult to overexpress proteins in MG1655 cells, whereas BL21 cells that had several mutations compared to MG1655 (e.g., deficiency in Lon and Opt proteases), were better at overexpressing proteins.

Both MG1655 and BL21 cells were transformed with pET28 plasmids containing *xthA*, *yafD*, or *ybhP* under a T7-LacO promoter (those plasmids were then used to purify Exo III and YbhP). Because MG1655 cells did not express the T7 polymerase they were also transformed with another plasmid (a pCS6 plasmid) that expressed T7 polymerase in the presence of arabinose. When 0.2% w/v of arabinose is present, T7 RNA polymerase is expressed, and when 1mM IPTG is added, it causes lac repressor dissociation, and it allows T7 RNA polymerase to start the transcription of *xthA*, *yafD* or *ybhP*.

I then tested the growth of the strains overexpressing Exo III, YafD and YbhP in the presence of ciprofloxacin and oxolinic acid (**Figure 3.10**). I found no differences in the growth under oxolinic acid or ciprofloxacin exposure between the control strain and the MG1655 strains overexpressing Exo III. The overexpression of Exo III and YbhP in BL21 cells was toxic for the cells and therefore it was not possible to look at the effect of quinolones. The overexpression of YafD in BL21 cells caused a slight increase in the resistance to quinolones. Overall, these results indicate that overexpressing Exo III, YafD or YbhP did not make cells more resistant to quinolones.

A)

B)
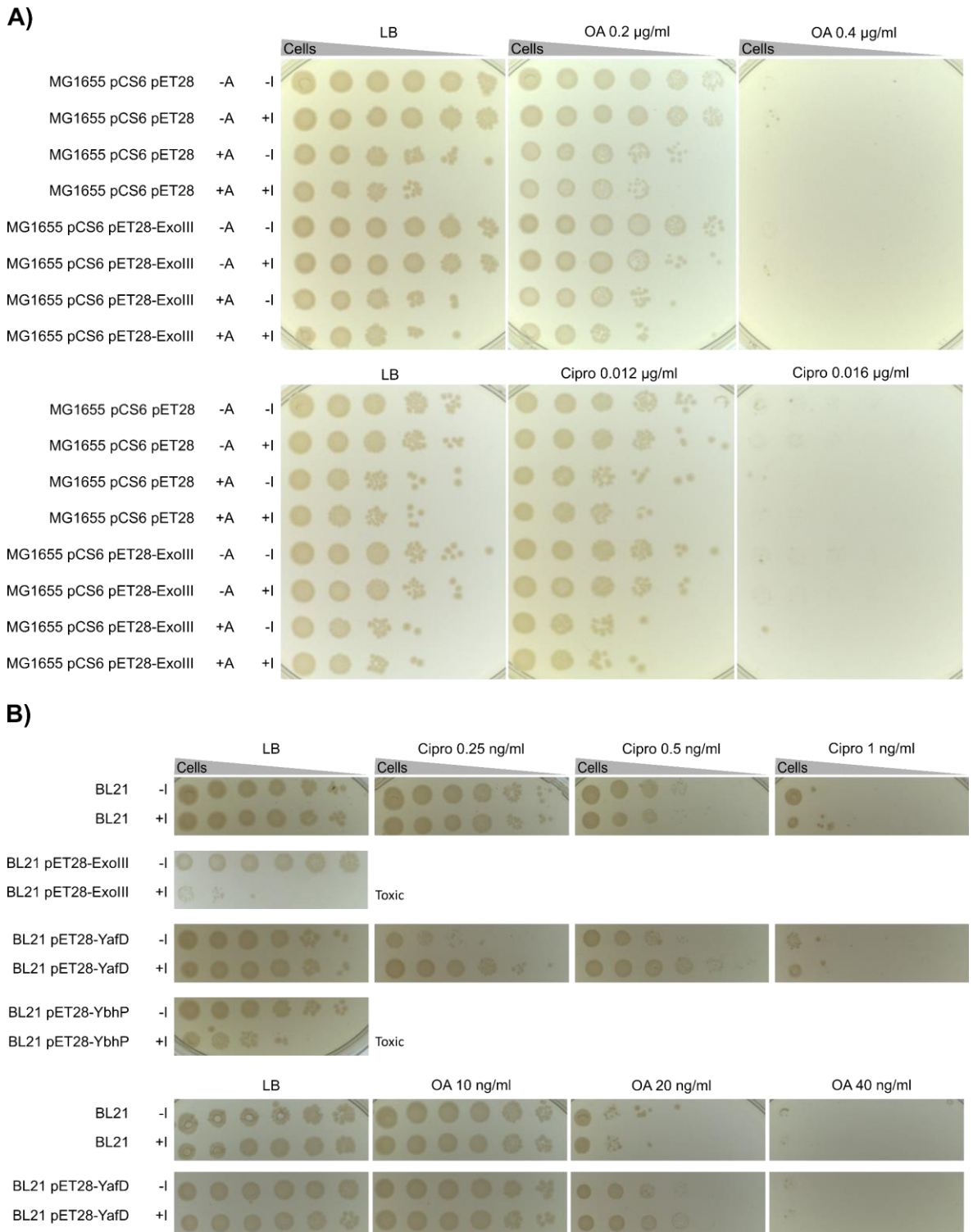
Figure 3.10. Ciprofloxacin and oxolinic acid minimum inhibitory concentration assay with cells overexpressing Exo III, YafD and YbhP. A) *E. coli* MG1655 pCS6 pET28-MHL and *E. coli* MG1655 pCS6 pET28-ExoIII were grown in the presence and/or absence of 0.2% Arabinose (A) and/or 1 mM IPTG (I). In the presence or arabinose, pCS6 expresses T7 RNA polymerase. In the presence of arabinose and IPTG, pET28-ExoIII expresses Exo III. B) *E. coli* BL21, *E. coli* BL21 pET28-ExoIII, *E. coli* BL21 pET28-YafD

and *E. coli* BL21 pET28-YbhP cells were grown in the presence and/or absence of 1 mM IPTG (I). In the presence of IPTG, Exo III, YafD or YbhP are expressed.

3.2.2.5 Purified TDP2 had 5'-tyrosyl phosphodiesterase activity whereas purified Exo III, YafD or YbhP did not

To test whether Exo III, YafD and/or YbhP had TDP2-like activity (that is, 5'-tyrosyl phosphodiestarase activity) I first purified Exo III, YafD and YbhP, as well as human TDP2 that I used as a positive control.

For the expression and purification of Exo III, I introduced *xthA* (the gene that encodes Exo III) in the pET28-MHL expression system (GenBank accession EF456735) and I transformed *E. coli* BL21(DE3) with that construct (note that *xthA* was introduced under an IPTG-inducible T7 promoter and that BL21 cells expressed the T7 RNA polymerase necessary to transcribe *xthA*). A 1L culture of *E. coli* BL21 pET28-Exo III cells induced with 1mM IPTG during 2 h at 37°C was lysed and centrifuged. The supernatant was subjected to metal affinity chromatography, anion exchange chromatography and finally gel filtration to obtain ~ 6 mg of Histidine (His)-tagged Exo III at a ~ 96% purity (**Figure 3.11**). The purified and mass of His-Exo III was confirmed by mass spectrometry analysis.

His-Exo III expected size: ~33 kDa
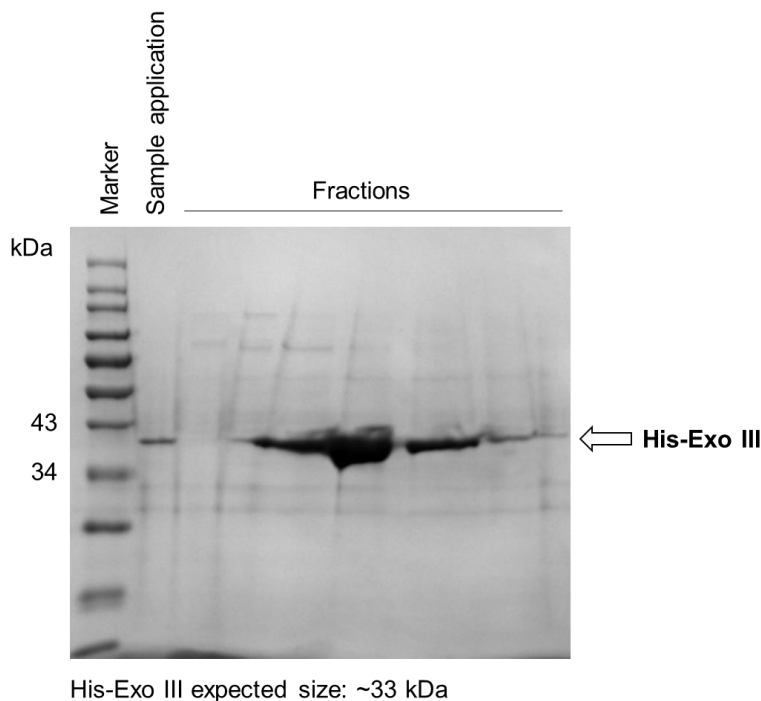
Figure 3.11. SDS-PAGE gel with fractions from gel filtration chromatography from the purification of Exo III. 1L *E. coli* BL21 pET28-Exo III was grown until $OD_{600} = 0.5$. The expression of Exo III was then induced with 1 mM IPTG for 2 hours at 28°C. The

pellet was homogenised, and the supernatant was run through a nickel column. The best fractions were dialysed and then ran through a MonoQ column. The best fractions from anion exchange chromatography were run through a gel filtration column. The ~40 kDa bands correspond to the UV peak around 11.2 mL and showed the presence of purified His-tagged Exo III.

The expression and purification of YafD was more challenging. I tried many expression conditions (different media, IPTG concentrations, temperatures, vectors, and purification procedures) until I found the best conditions (**Table 3.3**). Briefly, I found that YafD was insoluble and its overexpression with a His tag was poor. The co-expression with a SUMO tag increased its expression, so *E. coli* BL21 cells with a His-SUMO-YafD construct were lysed and run through a metal-binding column. The best fraction was run through a Q-column and the YafD band, as well as the most intense band were analysed by mass spectrometry. The analysis of both bands showed that YafD had a mass and a sequence consistent with His-SUMO-YafD that it co-purified with a 60 KDa chaperonin. To increase YafD expression and solubility I tried two other protein tags: GST and MBP. The co-expression with MBP improved the expression and solubility of YafD, but when a lysate of *E. coli* BL21 cells with an His-MBP-YafD construct was run through a metal-binding column, YafD co-purified with another protein that had the same size as the 60 KDa chaperonin found during the purification of His-SUMO-YafD. I tried to remove the chaperonin by doing ATP washes. However, this strategy did not work. I then tried running a lysate of *E. coli* BL21 cells with an His-MBP-YafD construct through an MBP column, instead of a metal-binding column, which resulted in a better separation of YafD from the rest of the proteins (**Figure 3.12**). With this last strategy I was able to obtain ~ 0.8 mg of His-MBP-YafD at a ~ 80% purity from a 1 L culture.

Table 3.3. Conditions tested for the expression and purification of YafD.

Medium	T°	Time of induction (h)	*E. coli* strain	Vector	Expression	Solubility	Purification quality
LB + 0.5 mM IPTG	30	2	BL21(DE3)Star	pET28	Y	Bad	-
LB + 0.5 mM IPTG	28	4	BL21(DE3)Star	pET28	Not clear	-	Bad
LB + 0.5 mM IPTG	28	O/N	BL21(DE3)Star	pET28	Not clear	-	Bad

LB + 1mM IPTG	28	2, 4, O/N	BL21(DE3)pLysS	pET28	Y	Bad	-
LB + 1mM IPTG	18	O/N	BL21(DE3)pLysS	pET28	Y	Bad	-
AIM	18	O/N	BL21(DE3)pLysS	pET28	Y	Bad	-
LB + 1mM IPTG	28	2, 4, O/N	BL21(DE3)pLysS	pOPIN-SUMO	Y	OK	Bad
LB + 1mM IPTG	28	2, 4, O/N	BL21(DE3)pLysS	pOPIN-GST	Y	Good	Bad
LB + 1mM IPTG	28	2, 4, O/N	BL21(DE3)pLysS	pOPIN-MBP	Y	Good	Good with MBP column
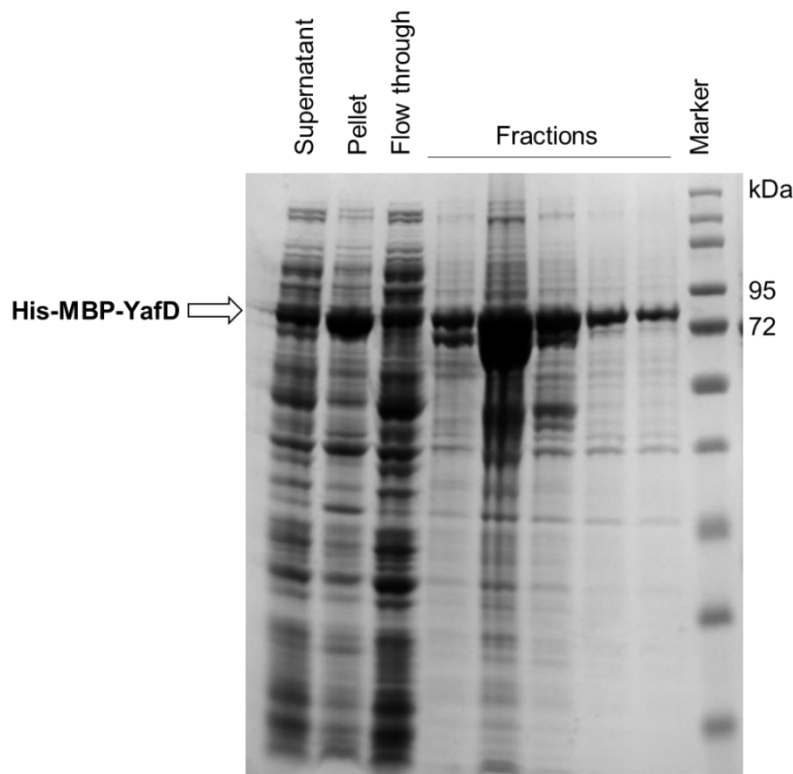
His-MBP-YafD expected size: ~75 kDa

Figure 3.12. SDS-PAGE gel with fractions of affinity chromatography from the purification of YafD. 1 L *E. coli* BL21 pOPINM-YafD was grown until OD_{600} = 0.5 and then the expression of His-MBP-YafD was induced with 1 mM IPTG for 2 hours at 28°C. The pellet was homogenised, and the supernatant was run through a nickel column. The ~75 kDa bands correspond to His-MBP-tagged YafD.

For the expression and purification of YbhP, I also introduced *ybhP* into the pET28-MHL vector and transformed *E. coli* BL21 cells with that construct. The expression and solubility were fine, and a 1 L culture of induced cells were lysed and run through a metal affinity column. The best fractions were then run through an ion exchange column and from the best fractions I obtained ~ 0.1 mg of His-YbhP at a ~ 40% purity (**Figure 3.13**). The purity of YbhP was not good, as it co-purified with another protein of ~ 70 kDa, but due to time constraints I could not re-do this purification.

His-YbhP expected size: ~31 kDa
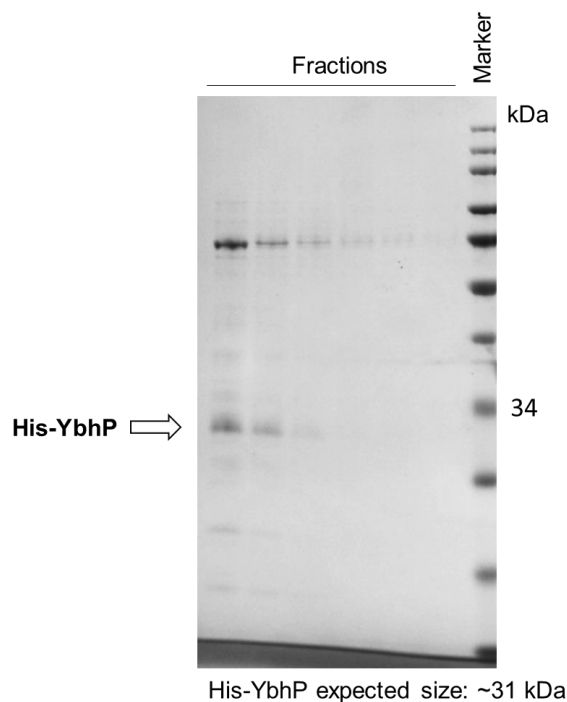
Figure 3.13. SDS-PAGE gel with fractions from anion exchange chromatography from the purification of YbhP. 1 L *E. coli* BL21 pET28-YbhP was grown until OD_{600} = 0.5. The expression of YbhP was then induced with 1 mM IPTG for 2 hours at 28°C. The pellet was homogenised, and the supernatant was run through a nickel column. The best fractions were dialysed and then run through a MonoQ column. The ~31 kDa bands corresponded to purified His-tagged YbhP.

TDP2 expression and purification was challenging in a similar way as the purification of YafD. Despite having been purified many times [125, 139], I found that it was difficult to purify as it was an insoluble protein that did not express well. I tried several conditions until I found one that gave us a reasonably pure TDP2 (**Table 3.4**). The co-expression with a SUMO tag increased its expression. Therefore, I ran a lysate of BL21 cells with a His-SUMO-TDP2 construct on a metal affinity column and then on an ion-exchange column. I found a band of the expected size that corresponded with TDP2 (I sent that

band for mass spectrometry to confirm that result), however, like what happened when I tried to purify His-SUMO-YafD, there was another thick band of the size of the 60 kDa chaperonin. I tried with two other tags: GST and MBP. These tags improved the expression and solubility of TDP2, but again TDP2 copurified with the 60 kDa chaperonin. To remove the chaperonin from TDP2, I attached His-MBP-TDP2 to a metal affinity column and washed it several times with a buffer containing ATP. As the presence of ATP helps the chaperonin to release its substrates (in this case, His-MBP-TDP2) I reasoned that the ATP washes would help us to separate His-MBP-TDP2 from the chaperonin. This strategy worked although there was still some chaperonin, and from a 4 L culture induced with 1mM IPTG at 18°C for 18 hours I obtained ~ 1 mg of His-MBP-TDP2 at a ~94% purity (**Figure 3.14**).

Table 3.4. Conditions tested for the expression and purification of TDP2.

Medium	T°	Time of induction (h)	*E. coli* strain	Vector	Expression	Solubility	Purification quality
LB + 1 mM IPTG	28	2, 4	BL21(DE3)pLysS	pET28	Y	Bad	Bad
LB + 1 mM IPTG	28	2	BL21(DE3)pLysS	pOPIN-SUMO	Y	OK	OK
LB + 1 mM IPTG	28	2	BL21(DE3)pLysS	pOPIN-GST	Y	OK	OK
LB + 1 mM IPTG	28	2	BL21(DE3)pLysS	pOPIN-MBP	Y	Good	OK
LB + 1 mM IPTG	18	16	BL21(DE3)pLysS	pOPIN-MBP	Y	Good	Good after ATP washes

His-MBP-TDP2 expected size: ~84 kDa
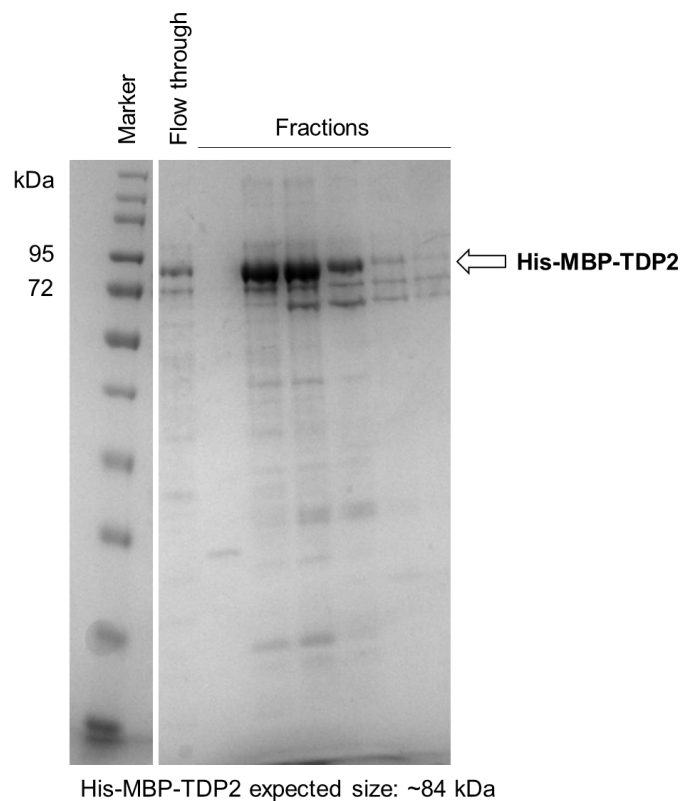
Figure 3.14. SDS-PAGE gel with fractions from anion exchange chromatography from the purification of TDP2. 1 L *E. coli* BL21 pOPINM-TDP2 was grown until OD_{600} = 0.5. The expression of TDP2 was then induced with 1 mM IPTG for 2 hours at 28°C. The pellet was homogenised, and the supernatant was run through a nickel column. Before the elution, the column was washed several times with a buffer containing ATP. The best fractions were dialysed and then run through a MonoQ column. The ~84 kDa bands correspond to His-MBP-tagged TDP2.

Once I purified Exo III, YafD, YbhP and TDP2, I checked if any of these proteins had nuclease activity. As my final goal was to find out if any of these proteins had tyrosyl-phosphodiesterase activity, and to do that I used short single-stranded (ssDNA) or double-stranded DNA (dsDNA) oligos, I needed to know if any of these proteins had nuclease activity. As I mentioned before, Exo III is a well-known nuclease, TDP2 is a tyrosyl-phosphodiesterase that presumably does not have nuclease activity [140], and YafD and YbhP have never been tested although they are predicted to belong to a family of nucleases. I found no significant endonuclease or exonuclease activity for YafD, however, YbhP and TDP2 had endonuclease activity (**Figure 3.15**). These results were useful when I designed the oligos I used for the tyrosyl-phosphodiesterase activity, as I found out that I needed to use linear DNA.
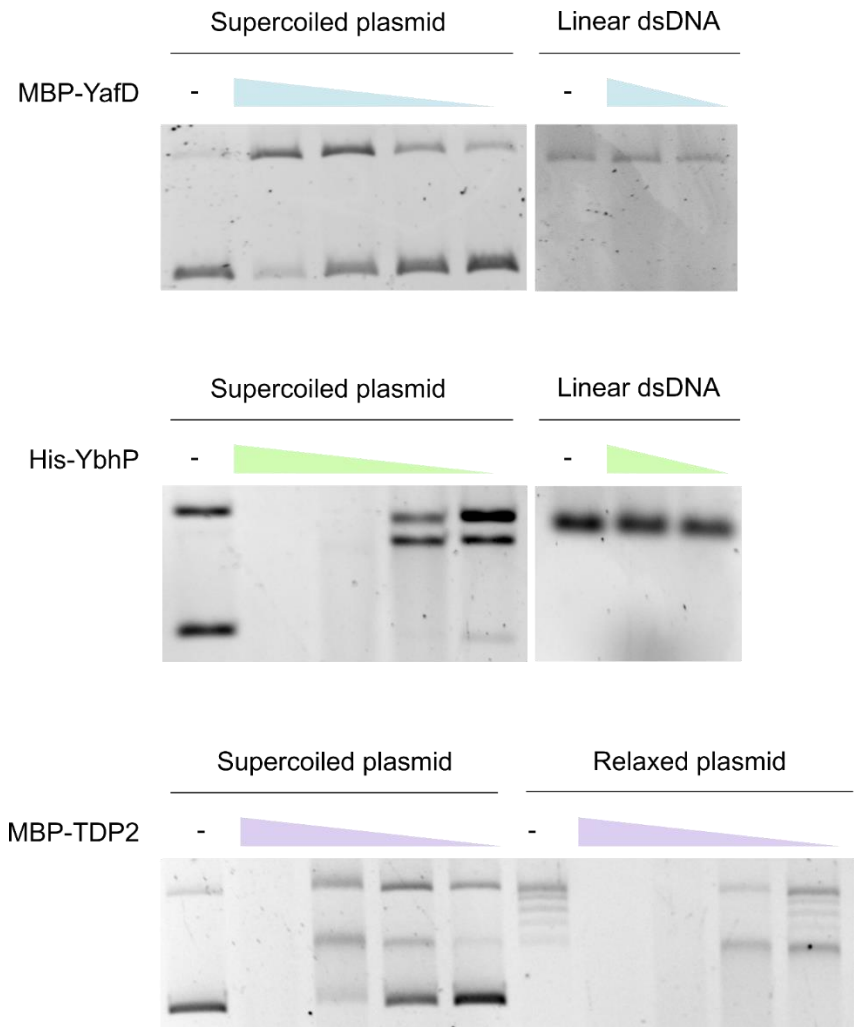
Figure 3.15. Nuclease activity of MBP-YafD, His-YbhP and MBP-TDP2. A range of 0.2-40 μg of MBP-YafD, 0.02-3 μg of His-YbhP and 0.32-40 μg of MBP-TDP2 were incubated with 10 mM MgCl$_2$ and 500 ng supercoiled plasmid pBR322 or 100 ng linear double-stranded DNA (dsDNA) for 30 min at 37°C. The reaction was stopped with 20 μL STEB and 30 μL ChCl$_3$/ISO and run on a 1% w/v agarose gel for 2 h at 80V.

Although YbhP did not look like it was able to degrade linear DNA, when I incubated YbhP with linear ssDNA or dsDNA with a fluorescein residue at the 3' end (18-F oligo), I found out that it had 3' exonuclease activity and/or was able to cut the 3' fluorescein. The same happened with Exo III. To avoid this 3' exonuclease activity on the DNA and/or on the fluorescein, I designed a new oligo that had a fluorescein in-between two nucleotides of the 3' end, and that a had phosphorothioate bond instead of a phosphodiester bond between the last 5 nucleotides on the 3' end (19-F oligo). The phosphorothioate bonds cannot be processed by nucleases. To the 18-F and the 19-F oligo, a tyrosine residue was added to the 5' end (Y-18-F and Y-19-F oligo). I then incubated the Y-18-F oligo with MBP-TDP2 and MBP-YafD, and the Y-19-F oligo with His-Exo III and His-YbhP (**Figure**

3.16). I ran the products on an acrylamide gel with the highest percentage of acrylamide I could add (20%) so that I could see a difference of a nucleotide and checked if any of these proteins were able to cut the tyrosine residue from the nucleotides of the oligo. I found that only TDP2 was able to do this, indicating that Exo III, YafD and YbhP did not have tyrosyl-phosphodiesterase activity.
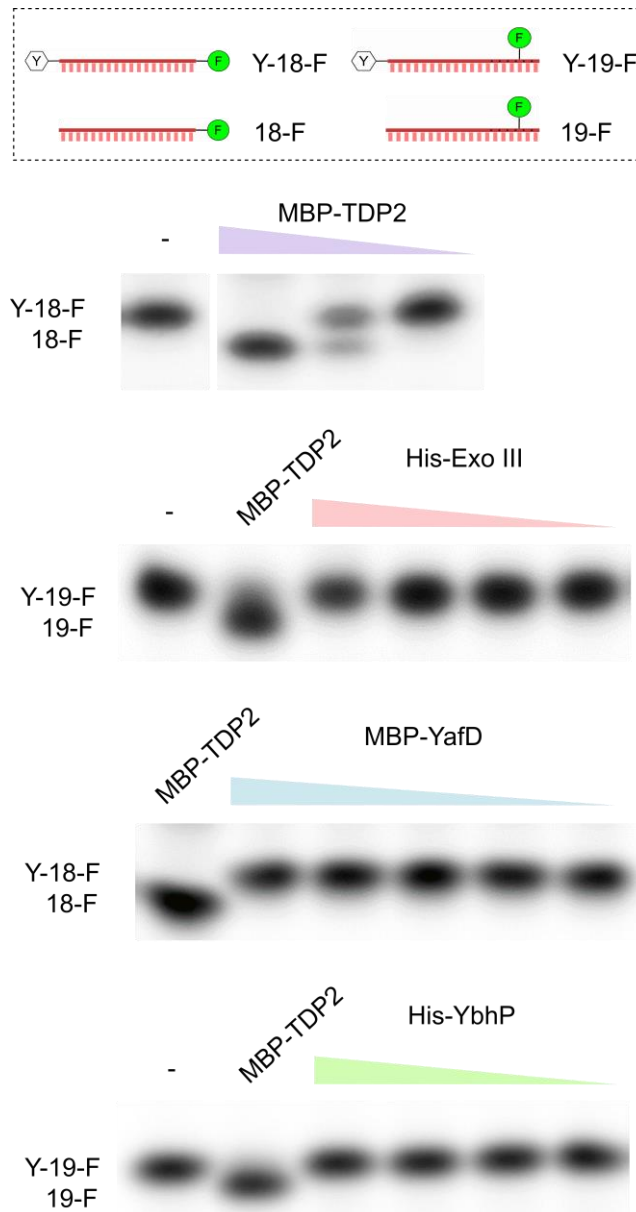
Figure 3.16. Tyrosyl-DNA phosphodiesterase activity assay with TDP2, Exo III, YafD and YbhP. A range of 100-1000 ng of MBP-TDP2, 10-10,000 ng of His-Exo III, 1-10,000 of MBP-YafD or 1-1000 ng of His-YbhP were incubated with 0.5 µL of 1 mM of Y-18-F or Y-19-F oligo and 10 mM MgCl$_2$ for 30 min at 37°C in a final volume of 10 µL. The reaction was stopped with the addition of 2 µL of loading dye and then loaded on a 20% acrylamide gel that was run for 3-4 hours at 60-80 V.

3.3 Discussion

In this chapter I looked for a TDP2-like protein in *E. coli* that was responsible for the repair of quinolone-induced DNA damage. Despite the efforts with the cleavage assay and the characterisation of the TDP2 homologs, I could not find such protein in *E. coli*. This could be due to the limitations of the methods I used. For example, the cleavage assay could not be used with proteins that were affected by EDTA, and the conditions for the tyrosyl phosphodiesterase activity assay with the TDP2 homologs might not have been the right ones. Nevertheless, I have found two new proteins that might participate in the repair of quinolone-induced damage: Exo III and YafD.

The evidence in favour of Exo III is genetic. In the absence of Exo III cells were more sensitive to 1st generation quinolones such as oxolinic acid and nalidixic acid, but not to fluoroquinolones. First generation quinolones kill cells in a different way than fluoroquinolones (see section 1.2.4) and it is likely that the damage they caused is also repaired differently. Hence, it is not surprising that a protein might be involved in the repair of damage caused by 1st generation quinolones but not so importantly for fluoroquinolones. Also, Exo III is a homolog of the eukaryotic proteins APE1 and APE2 which have been associated to the repair of DNA breaks caused by oxidative damage [141] and with the removal of trapped topoisomerase 1 [142]. Thus, it is possible that Exo III might be involved in the repair of ROS damage (this would be consistent with the experiment in 3.2.2.3 in which I showed that *xthA*- cells were not killed by a co-treatment of ciprofloxacin and chloramphenicol).

One intriguing aspect of Exo III is that its effect on quinolone lethality varies with the temperature. At a normal growing temperature (37°C) the absence of Exo III makes cells more sensitive to 1st generation quinolones, but at lower temperatures (20°C) the cells without Exo III are more resistant to those quinolones (**Table 3.2**). It is hard to know whether this effect depends on the activity of topoisomerases at different temperatures (at lower temperatures cells grow slower, and there is a lower need of topoisomerases) or any other factors. To the best of my knowledge, there is no other protein reported whose absence affects quinolone lethality differently depending on the temperature.

Regarding YafD, I found that cells without *yafD* died after a co-treatment with ciprofloxacin and chloramphenicol, whereas WT cells did not die. Presumably, the presence of chloramphenicol slows the metabolism of the cell, diminishing the formation of ROS. The fact that the absence of *yafD* made cells sensitive to the co-treatment with ciprofloxacin and chloramphenicol, suggests that *yafD* participates in the repair of ciprofloxacin-induced damage independent of the formation of ROS. Maybe, YafD is a nuclease that repairs the

DNA breaks caused by topoisomerases. However, the only information we have about YafD, is that it is a homolog of known nucleases and that YafD from *Salmonella* participated in the repair of DNA damage caused by egg albumen [143].

Perhaps there is not one TDP2-like protein in *E. coli* but multiple proteins with TDP2 activity. It is also possible that bacteria do not have a TDP2-like protein. This will be discussed further in Chapter 7.

3.4   Conclusions

In this chapter, I have investigated whether *E. coli* had a tyrosyl phosphodiesterase that could remove a trapped topoisomerase from the DNA. To find this protein, I used two strategies: first I used cell lysates in a biochemical assay, and secondly, I used a bioinformatics analysis. In the cell lysates experiments, I could not find a protein that specifically removed topoisomerases from the DNA, but the results suggested that, if that protein existed, it might be a metal-ion dependent protein. With the bioinformatics analysis I found three proteins (Exo III, YbhP or YafD) that were structural homologs of the 5'-tyrosyl phosphodiesterase TDP2, a eukaryotic enzyme that can remove trapped topoisomerase from the DNA. The deletion of *xthA* (Exo III) made cells twice more sensitive to oxolinic acid and nalidixic acid but it did not change the susceptibility or survival to ciprofloxacin nor norfloxacin. The overexpression of Exo III or YafD did not change the susceptibility to quinolones, and purified Exo III, YafD and YbhP did not show TDP2-like activity *in vitro* suggesting that none of these proteins is a tyrosyl phosphodiesterase.

3.5   Future work

Several aspects of the data presented in this chapters require further study. For example, it would be interesting to study the specific role of Exo III during the repair of quinolone-induced DNA damage. If Exo III participates in the repair of ROS damage, the Δ*xthA* (without Exo III) mutant should be more sensitive to ROS (e.g., H_2O_2) than WT cells, and the deletion of ROS related genes in this mutant (e.g., *kat* or *sod*) should also affect the survival to quinolones. The amount of DNA damage in Δ*xthA vs* WT cells in the presence of quinolones with/without ROS inhibitors could also be measured (maybe using the microscopy assay in Chapter 4). Also, it would be interesting to investigate how the temperature affects the lethality of quinolones in Δ*xthA* cells. Growth curves at different temperatures could be done with WT, Δ*xthA* and Δ*xthA* complemented with *xthA+*, in the

presence and absence of 1st generation quinolones to fully confirm whether Exo III is involved in the processing of DNA-topoisomerase adducts.

Another interesting aspect to study is the potential role of YafD in the repair of quinolone-induced DNA damage. If YafD participates in the release of trapped topoisomerase from the DNA, the absence of YafD would cause an increase in the amount of trapped topoisomerase. This could be measured *in vivo* using the RADAR assay [144].

Chapter 4:

4   Repair of quinolone-induced damage: role of proteases, nucleases and enzymes involved in DNA repair

4.1   Introduction

In the previous chapter I looked for proteins in *E. coli* involved in the very first step of the repair of quinolone-induced damage: the removal of a type II topoisomerase trapped on the DNA by quinolones. I focused on finding a tyrosyl-DNA phosphodiesterase (TDP), but I could not find any. In this chapter, I have focused on *E. coli* proteases, nucleases, and DNA repair proteins, that might be involved in quinolone-induced damage repair. The rationale behind choosing these types of proteins is based on how eukaryotes remove trapped type II topoisomerases from the DNA.

The first step in the removal of trapped type II topoisomerases in eukaryotes, is the degradation of the topoisomerases into peptides. This is done by the proteasome (a group of proteins that degrade other proteins) and the metalloprotease SPRTN [145-147]. This proteolytic digestion does not affect the covalent bond between the topoisomerase and the DNA, and thus the topoisomerase is not completely removed from the DNA. But the debulking of the topoisomerase is necessary for other proteins (nucleases and TDPs) to fully remove the topoisomerase from the DNA. After the trapped topoisomerase is partially digested by proteases, several nucleases can cleave the DNA strand to which the type II topoisomerase is linked covalently. These nucleases are the MRE11/RAD50/NBS1 complex, and the endonucleases XPG and FEN1 [148, 149]. Following the excision of the topoisomerase, the double-strand break (DSB) is repaired by non-homologous end-joining (NHEJ) or by homologous recombination (HR) [98]. Some major proteins in these pathways are the ligase LIG4 in the case of NHEJ [150] and the recombinase RAD51 in the case of HR [151].

E. coli has several proteases, nucleases and proteins involved in the repair of DNA [100, 135, 152]. Regarding the proteases, most of the intracellular proteolysis is carried out by ATP-dependent proteases like Lon protease, ClpXP, HflB and HslVU. ClpP and HslVU are putative homologs of the proteasome as they share homology in structural organization, and sequence and structure, respectively [153, 154]. Lon protease is necessary to survive high concentrations of quinolones [155] and its deletion makes cells

more susceptible to quinolones [156]. The deletion of other ATP-dependent proteases, such as *clpP*, *clpX*, or *hslVU*, does not make cells more susceptible to quinolones [157, 158]. Thus, out of all these proteases, Lon, ClpP and HslVU are the most promising candidates either because they participate somehow in the lethality of quinolones (Lon protease) or because they are homologs of the proteasome (ClpP and HslVU). In terms of the nucleases, only one *E. coli* nuclease has been shown to remove trapped topoisomerase from the DNA. This nuclease is Exonuclease VII (Exo VII), an enzyme that apart from having 5' exonuclease activity, has tyrosyl-nuclease activity [120]. Other nucleases have been proposed to have a similar activity. These are SbcCD and RuvC [84]. The deletion of SbcCD caused a slight decrease in the survival to 1st generation quinolones and an increase in trapped gyrase complexes under quinolone exposure *in vivo* [121]. The deletion of RuvC also affects the survival to quinolones [159], and other proteins that function alongside RuvC, RuvA and RuvB, can displace trapped topo IV from the DNA [83]. Hence, Exo VII and maybe SbcCD and RuvC are the nucleases in *E. coli* that remove topoisomerases from the DNA. In relation to proteins responsible for the repair of DNA damage, *E. coli* uses different proteins depending on the type of DNA damage. Since quinolones are thought to induce DSBs [75], I have focused on this type of damage. If there are DSBs, *E. coli* follows an HR pathway that starts when RecBCD binds to DSBs and forms 3' single-stranded overhangs onto which it loads RecA [129]. *E. coli* can also use a modified version of the eukaryotic NHEJ pathway for the repair of DSBs, which is initiated by RecBCD and followed by the ligase LigA [160]. The absence of RecBCD and RecA makes cells very sensitive to quinolones [96, 159] and therefore it is likely that these are the proteins that ultimately repair the DNA damage caused by quinolones.

Based on this information, I hypothesised that *E. coli* has protease(s), nuclease(s) and proteins involved in DNA repair that are able to, first, degrade the trapped topoisomerase, then, cleave the DNA close to the tyrosine residues of the topoisomerase bound to the DNA, and finally, repair the DSB. *E. coli* has many proteins that could do this, however, based on homology to eukaryotic proteins or based on information from the literature, I have chosen a couple of candidates for each step. These are: the proteases Lon and ClpP, the nucleases SbcCD and Exo VII and the proteins involved in DNA repair RecBCD and RecA (**Figure 4.1**).

Here I show my attempts to test if any of these proteins are involved in the repair of quinolone-induced DNA damage. I investigated the effect of their deletions by doing *in vitro* assays with trapped gyrase, and measuring DNA damage under the microscope.
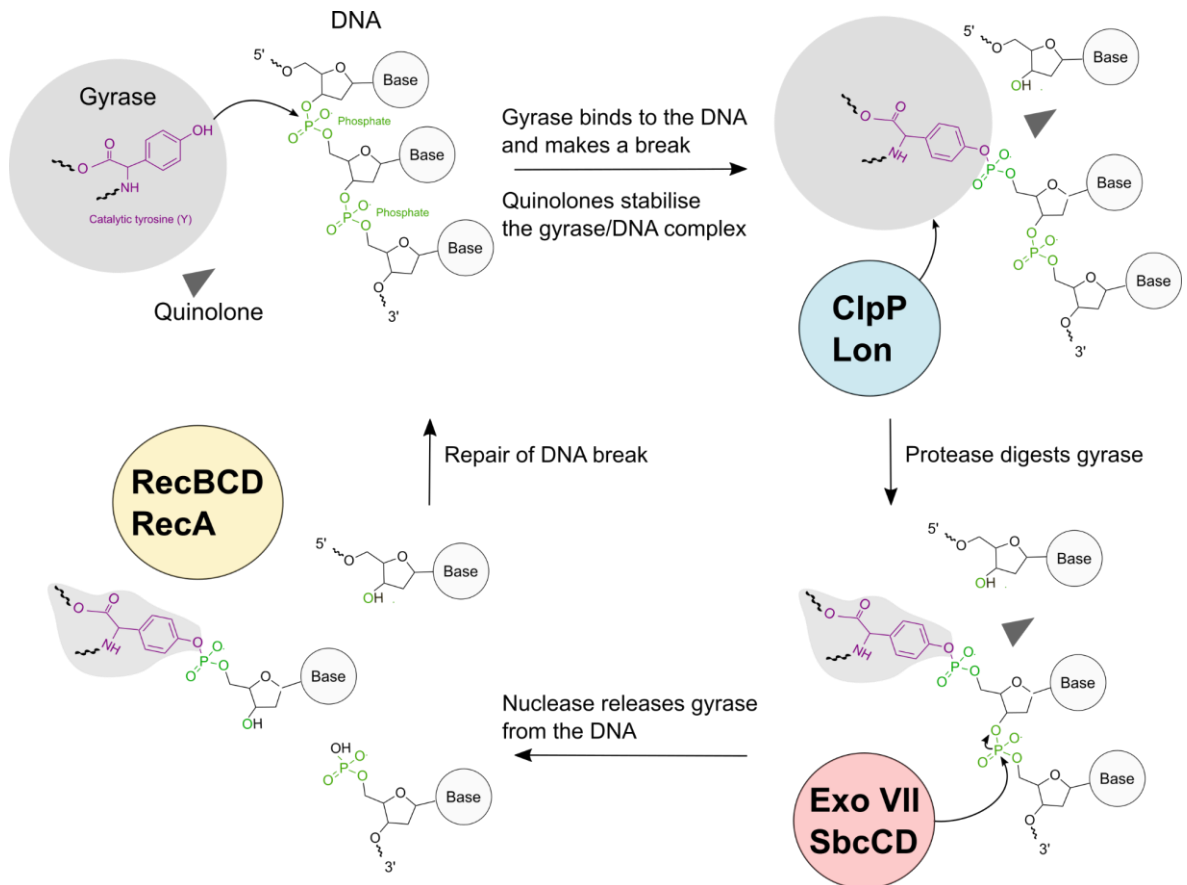
Figure 4.1. Proposed pathway of quinolone-induced damage repair. Quinolones trap gyrase on the DNA stabilising the gyrase-DNA complex in which gyrase is covalently bound to the DNA through its two catalytic tyrosine residues and has made a double-strand break (note that in the figure only one catalytic residue and a single-strand break are shown). A protease (e.g., Lon or ClpP) partially degrades the trapped gyrase, which allows a nuclease (e.g., Exo VII or SbcCD) to cleave the DNA close to the gyrase. This releases the partially digested gyrase from the DNA freeing the DSB. Proteins involved in repair of DNA damage (e.g., RecBCD and RecA) can then repair the DSB.

4.2   Results

4.2.1   Effect of the deletion of proteases, nucleases and enzymes that might be involved in DNA repair during quinolone lethality

To test if the deletion of any of the candidates in quinolone-induced damage repair (*lon*, *clpP*, *sbcCD*, *xseA* (encoding for the biggest subunit of Exonuclease VII), *recB* or *recA*) made cells more sensitive to quinolones, I began by making single mutants without those genes (**Table 4.1**). The rationale behind this was that if any of these genes were involved

in the repair of quinolone-induced DNA damage, its absence would make cells more sensitive to quinolones. I was able to delete all single genes except for *recB*, *recC* and *recA*. Luckily, I could obtain those strains from other sources (Chapter 2, **Table 2.1**). I could also construct several double mutants but failed to introduce the *xthA*- or *yafD*-mutation in the single deletion mutants. (*xthA* and *yafD* encode for Exonuclease III and YafD, respectively, which I found to be involved in quinolone-induced damage repair in Chapter 3).

Table 4.1. List of mutations made in *E. coli* MG1655. The 1st column indicates the WT (second cell) and single mutants (third to last cell). The 1st row indicates additional mutations. For example, the interception of the WT row with the *clpP*- column represents a *clpP*- mutation in the WT strain that was successful (Y); whereas the interception of the WT row with the *recB*- column represents an unsuccessful attempt (N) to introduce the *recB*- mutation in the WT strain. Highlighted in grey are the successful attempts to make single and double mutants.

	clpP⁻	*lon*⁻	*sbcCD*⁻	*xseA*⁻	*xthA*⁻	*yafD*⁻	*recB*⁻	*recC*⁻	*recA*⁻
WT	Y	Y	Y	Y	Y	Y	N	N	N
***clpP*⁻**	-	N	Y	Y	N	NT	NT	NT	NT
***lon*⁻**	N	-	N	Y	N	NT	NT	NT	NT
***sbcCD*⁻**	Y	N	-	Y	N	NT	NT	NT	NT
***xseA*⁻**	Y	Y	Y	-	N	N	Y	NT	NT
***xthA*⁻**	N	N	N	N	-	Y	NT	NT	NT
***yafD*⁻**	NT	NT	NT	N	Y	-	NT	NT	NT
***recB*⁻**	NT	NT	NT	Y	NT	NT	-	NT	NT

N: No, Y: Yes, NT: Not tried

4.2.1.1 The deletion of *lon*, *xseA*, *recB* or *recA* makes cells more sensitive to quinolones

To investigate if the absence of *lon*, *clpP*, *sbcCD*, *xseA*, *recB* or *recA* made cells more sensitive to quinolones, I grew mutants without those genes in the presence of ciprofloxacin or oxolinic acid (**Table 4.2**). I found that the deletion of *lon*, *xseA*, *recB* or *recA* made cells more sensitive to quinolones. Conversely, the deletion of *clpP* and/or *sbcCD* did not affect the growth under quinolone exposure. To further examine whether the deletion of *sbcCD* and/or *clpP* did not affect the survival to quinolones, I measured the number of cells that grew in the presence or absence of quinolones. I found no difference in the survival to ciprofloxacin (as well as oxolinic acid or nalidixic acid) between WT cells and *sbcCD*- and *clpP*- mutants (Appendix II, **Figure I**). These results indicated that *sbcCD* and *clpP* were likely not involved in the repair of quinolone-induced damage.

Repair of quinolone-induced damage: role of proteases, nucleases and enzymes involved in DNA repair

Table 4.2. Minimum inhibitory concentration (MIC) of different strains to ciprofloxacin and oxolinic acid. MICs were calculated as the average of three replicates using the solid MIC method. Highlighted in grey are the MICs that are below the WT MICs.

Strain	Ciprofloxacin MIC (µg/mL)	Oxolinic acid MIC (µg/mL)
MG1655 WT	0.027	0.4
BW25113 WT	0.024	0.4
MG1655 Δ*clpP*	0.027	0.4
MG1655 Δ*lon*	0.008	0.2
MG1655 Δ*sbcCD*	0.027	0.4
MG1655 Δ*xseA*	0.008	0.2
MG1655 *recA*::Kan^R	0.006	-
BW25113 *recB*::Kan^R	0.004	0.1
MG1655 Δ*sbcCD* Δ*clpP*	0.027	0.4
MG1655 Δ*xseA* Δ*clpP*	0.016	0.2
MG1655 Δ*xseA* Δ*lon*	0.002	0.1
MG1655 Δ*xseA* *recB*::Kan^R	0.008	0.17
MG1655 Δ*xseA* Δ*sbcCD*	0.008	0.2

4.2.1.2 The role of Exo VII, Lon and RecB in the repair of quinolone-induced damage might be epistatic

As the deletion of *xseA*, *lon* and *recB* made cells more sensitive to quinolones, I wondered whether all those genes participated in the same pathway of quinolone-induced damage repair. If this was true, the double or triple mutants should be as sensitive to quinolones as the single mutants. In other words, the effect of the deletions would be epistatic. I found that the *xseA⁻ recB⁻* double mutant was as sensitive to quinolones as the single mutants, indicating that their deletions might be epistatic, and that the *xseA⁻ lon⁻* double mutant was more sensitive to quinolones than the single mutants (**Table 4.2**). As I was unable to build the triple mutant (*xseA⁻ lon⁻ recB⁻*), I used an alternative strategy: a plasmid containing an isoform of λGam (GamS or GamL), a protein from λ phage that inhibits RecBCD [161]. First, I transformed MG1655 WT cells with the GamS or GamL plasmid to check if it made cells as sensitive to ciprofloxacin as it happened with BW25113 *recB*::Kan^R cells. I observed that MG1655 WT cells expressing Gam had a ciprofloxacin MIC of 0.004-0.008 µg/mL which was very similar to the one of BW25113 *recB*::Kan^R cells (0.004 µg/mL). Also, MG1655 Δ*xseA* cells expressing Gam had a ciprofloxacin MIC of 0.004-0.008 µg/mL, which again was very similar to the one of MG1655 Δ*xseA* *recB*::Kan^R cells (0.008 µg/mL). These results suggested that the expression of Gam was inhibiting RecBCD (**Figure 4.2**).
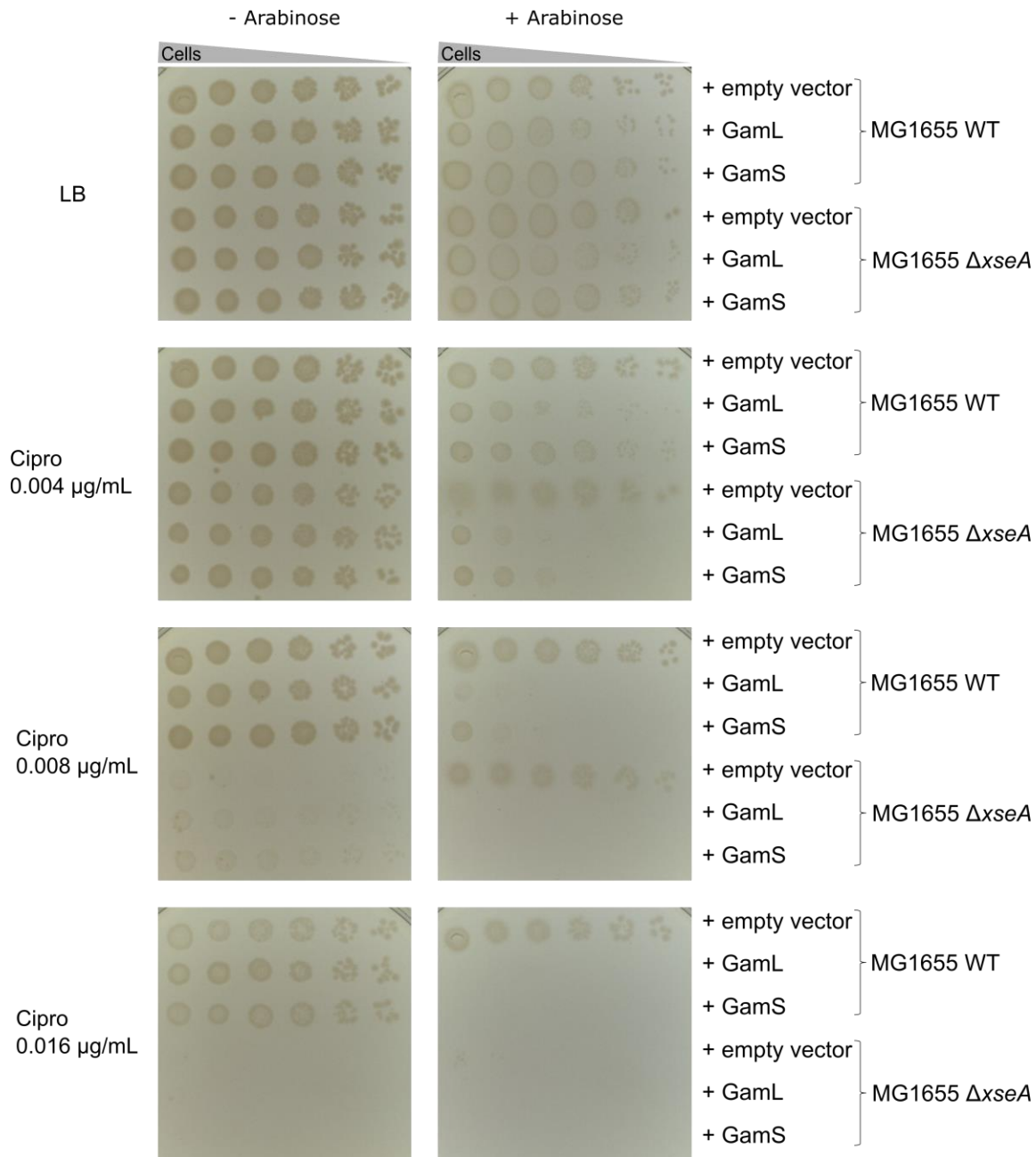
Figure 4.2. Minimum inhibitory concentration (MIC) of ciprofloxacin (Cipro) of MG1655 WT and Δ*xseA* cells expressing λGamL or λGamS. Cells were transformed with pBAD322-K (empty vector), pBAD322-GamL (GamL) or pBAD322-GamS (GamS) and plated on LB plates with 50 µg/mL kanamycin, with or without ciprofloxacin, and with or without 1% (w/v) of arabinose.

I then transformed my *xseA⁻ lon⁻* strain with the Gam plasmid and tested whether the inhibition of RecBCD influenced the sensitivity to ciprofloxacin (**Figure 4.3**). I saw that when GamS was expressed in the presence of arabinose, the cells were as sensitive to ciprofloxacin as the *xseA⁻ lon⁻* mutant. This result indicated that *xseA*, *lon* and *recB* might

be part of the same pathway in the repair of quinolone-induced damage. Still, as the inhibition of RecBCD in *xseA⁻ lon⁻* cells affected their growth on drug-free medium, this phenomenon should be studied more exhaustively to be confirmed.
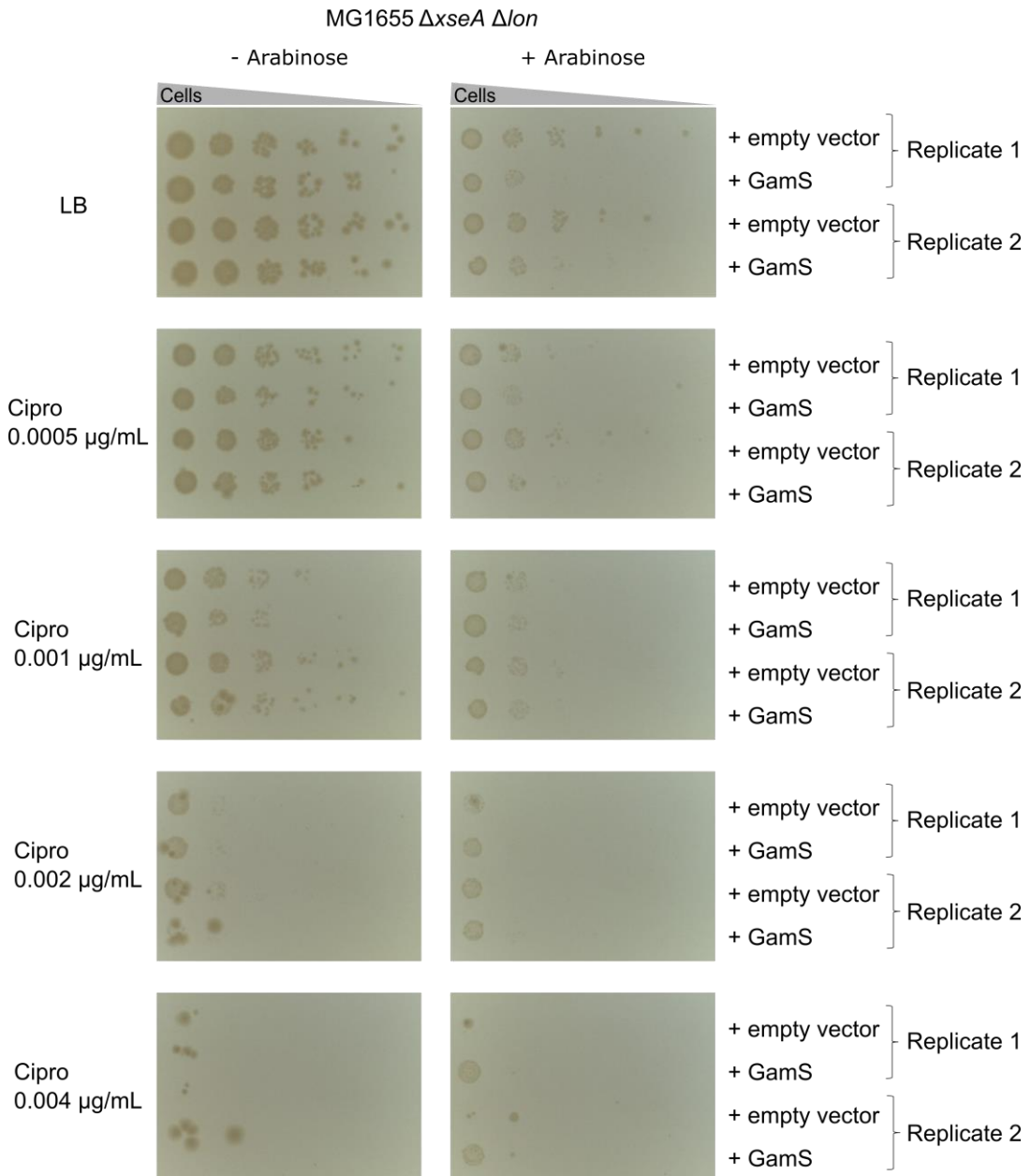
Figure 4.3. Minimum inhibitory concentration (MIC) of ciprofloxacin (Cipro) of MG1655 Δ*xseA* Δ*lon* cells expressing λGamS. Cells were transformed with pBAD322-K (empty vector) or pBAD322-GamS (GamS) and plated on LB plates with 50 µg/mL kanamycin, with or without ciprofloxacin, and with or without 1% (w/v) of arabinose.

4.2.2 *In vitro* assay with Lon protease and trapped gyrase

Lon is a protease that degrades mis-folded proteins and specific folded proteins such as SulA, UmuD and SoxS [162]. It does not recognise a single specific motive by multiple signals like an exposed cluster of aromatic side chains. As the deletion of *lon* made cells more sensitive to quinolones, and there is evidence that Lon protects bacteria at high levels of quinolones, I wondered whether Lon was the protease responsible for partially digesting trapped gyrase. To test if Lon was able to degrade trapped gyrase, I first purified Lon protease, then checked its activity and performed an *in vitro* experiment with trapped gyrase.

4.2.2.1 Purification of Lon

Several groups have purified Lon, either by using a Histidine (His) or a Maltose Binding Protein (MBP) tag [163, 164]. In this work, I followed the conditions from Sonezaki et al. [164] but with some modifications.

I used a pOPINM vector that had a His tag at the N-terminus of MBP, followed by a 3C protease site and a restriction site where I cloned my gene of interest (*lon*). I called this vector pOPINM-Lon. The fused His-MBP-3C-Lon protein was under a T7 promoter-lac operator, therefore, to induce the expression of the recombinant protein, I needed to have a T7 RNA polymerase and IPTG. *E. coli* BL21 (DE3) pLysS cells express T7 RNA polymerase, so I introduced the pOPINM-Lon vector in these cells and checked whether there was expression of His-MBP-3C-Lon in the presence of IPTG (**Figure 4.4**). As expected, only in the presence of IPTG I could see a band of a similar size to the one of His-MBP-3C-Lon. Luckily, His-MBP-3C-Lon was present in the supernatant, suggesting that it was a soluble protein.

To purify Lon, I induced the expression of His-MBP-3C-Lon in a 3L of *E. coli* BL21 (DE3) pLysS cells, lysed the cells, and ran the supernatant through a MBP column. This column separated most of His-MBP-3C-Lon from the other proteins present in the supernatant. I then cleaved the His-MBP tag by incubating the best fractions with 3C protease. I did this twice, since the first digestion was not very efficient. After the second digestion I ran the protein through a nickel column to separate the His-MBP tag from Lon. Some of the His-MBP tag and part of the non-digested His-MBP-3C-Lon remained, but most of the flow through was Lon (**Figure 4.5**).

To further polish the purification of Lon, I ran the best fractions from the affinity chromatography through a Q column that separated proteins based on their charge

(**Figure 4.6**). The best fractions contained Lon protease at a ~92% purity and His-MBP-3C-Lon at a ~7% purity. The bands of Lon and His-MBP-3C-Lon were sent to mass spectrophotometry to confirm that they were indeed Lon. At the end from the initial 3L culture I obtained ~ 0.5 mg of Lon.

BL21(DE3)pLysS + pOPINM-Lon
His-MBP-Lon expected size: ~130 kDa
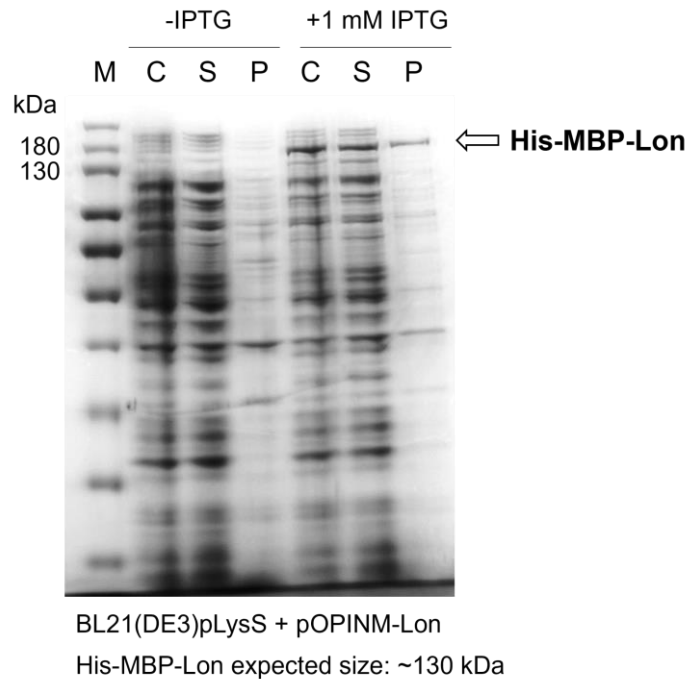
Figure 4.4. Small scale expression of His-MBP-Lon. *E. coli* BL21(DE3)pLysS cultures with pOPINM-Lon were grown with or without 1 mM IPTG at 28°C for 2 hours. The cells were lysed by freeze-thawing to obtain the crude extract (C). The crude extract was then spun to obtain the supernatant (S) and the pellet (P). The crude extracts, supernatants and pellets were run on a 12% SDS-PAGE gel.

His-MBP-Lon expected size: ~130 kDa
Lon expected size: ~90 kDa
His-MBP expected size: ~40 kDa
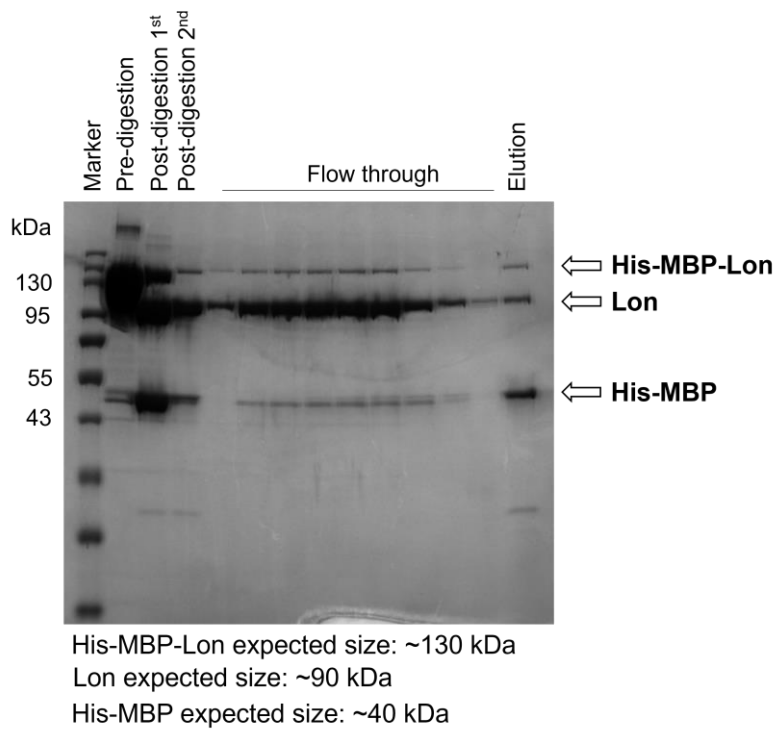
Figure 4.5. SDS-PAGE gel with fractions from affinity chromatography from the purification of His-MBP-Lon. A culture of 1 L *E. coli* BL21(DE3)pLysS cells with pOPINM-Lon was grown with 1 mM IPTG at 28°C for 2 hours. The pellet was homogenised, and the supernatant was run through an MBP column. The best fractions (Pre-digestion) were dialysed and incubated with 3C protease to cleave the His-MBP tag from the protein. The digestion was done twice (Post 1st digestion, Post 2nd digestion). After the second digestion the sample was run through a nickel column. The flow through fractions contained Lon without the His-MBP tag.

His-MBP-Lon expected size: ~130 kDa
Lon expected size: ~90 kDa
His-MBP expected size: ~40 kDa
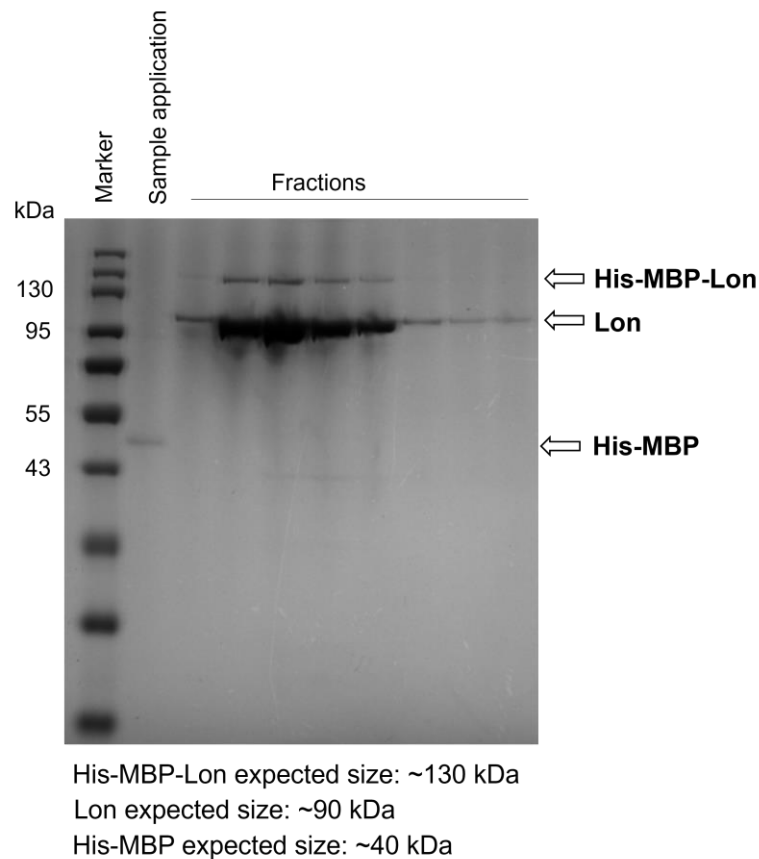
Figure 4.6. SDS-PAGE gel with fractions from anion exchange chromatography from the purification of Lon. Best flow through fractions from **Figure 4.5** were run through a MonoQ column.

4.2.2.2   Lon can degrade α-casein

Once I purified Lon, I checked whether it was active. One way of doing this is by incubating Lon with α-casein, a disordered protein present in milk that is a well-known target of Lon [164]. As Lon is an ATP-dependent protein, I incubated Lon with α-casein in the presence and absence of ATP. I expected to see the degradation of α-casein when ATP was present. As shown in **Figure 4.7**, only in the presence of ATP Lon was able to degrade α-casein, and this happened in a time- and dose-dependent manner, indicating that Lon was active.
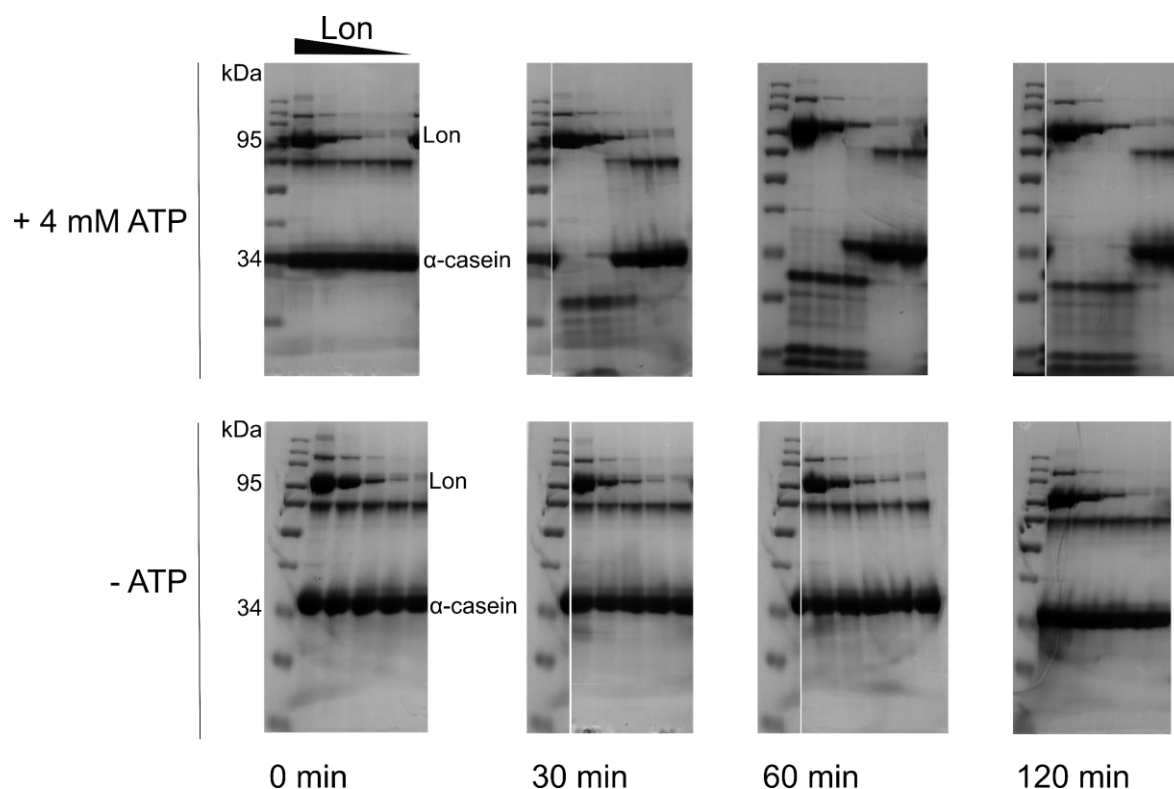
Figure 4.7. SDS-PAGE analysis of the degradation of α-casein by Lon. Different concentrations of Lon (10 µg, 2.5 µg, 0.6 µg, 0.3 and 0 µg) were incubated for 0, 30, 60 and 120 minutes at 37°C with 20 µg of α-casein in a final volume of 30 µL in the absence or presence of 4 mM ATP in a buffer with 20 mM Tris.HCl pH 8.0, 200 mM NaCl, 1 mM 2-Mercaptoethanol, 10% glycerol and 10 mM $MgCl_2$.

4.2.2.3   Lon binds to DNA

An interesting characteristic of Lon is that it binds to double-stranded DNA (dsDNA). Some groups have suggested that this interaction with dsDNA may happen in order to degrade transcriptional regulators [165]. To investigate if the purified Lon was able to bind to DNA, and, to confirm that there was not a nuclease contamination, I incubated Lon with dsDNA and ran it on a DNA agarose gel (**Figure 4.8**). I found that at high concentrations Lon retained the DNA in the gel, indicating that Lon was interacting with the DNA. I did not find any unusual nuclease activity, suggesting that the purified Lon was free from nucleases.

Relaxed plasmid

Linear dsDNA
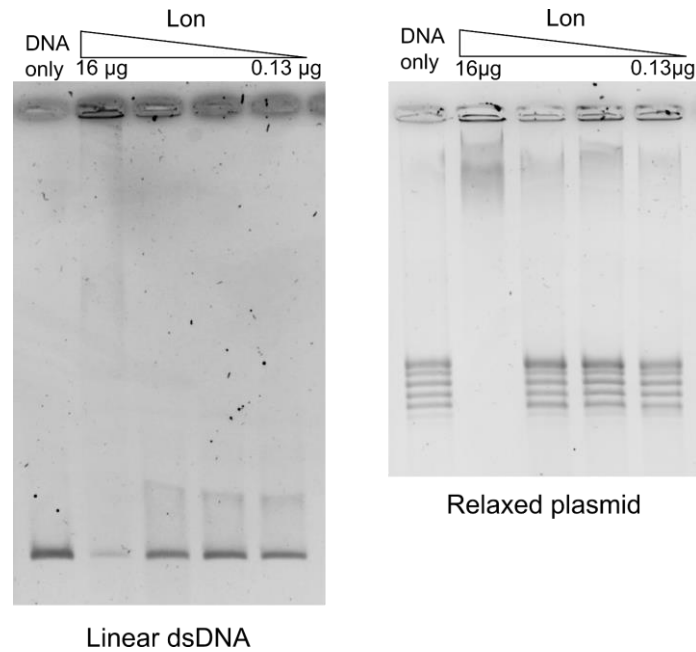
Figure 4.8. Interaction of Lon with DNA. A range of 16-0.13 µg Lon was incubated with 500 ng of linear DNA (~2 kbp) or relaxed pBR322 plasmid in a final volume of 30 µL in a buffer containing 20 mM Tris.HCl pH 8.0, 200 mM NaCl, 1 mM 2-Mercaptoethanol, 10% glycerol, 10 mM MgCl$_2$ and 20 mM ATP. The sample was incubated for 2 hours at 37°C, then added 20 µL of STEB and 30 µL chloroform/isoamyl alcohol. 15 µL of each sample were loaded on a 1% agarose gel and run for 2 hours at 80 V.

4.2.2.4 Lon does not degrade gyrase *in vitro*

Once I had purified active and nuclease-free Lon, I designed a simple experiment to test if it was able to degrade gyrase. For this I needed gyrase, which was purified by Natassja Bush and Lionel Costenaro (JIC). Gyrase is a heterotetrametric enzyme composed of two GyrA and two GyrB subunits. To test if gyrase was active, I mixed GyrA and GyrB in a 1:1 molar ration, and I checked if it was able to supercoil relaxed DNA. As shown in **Figure 4.9**, gyrase (formed of GyrA and GyrB) was able to supercoil relaxed plasmid DNA, which travels faster on an agarose gel than relaxed DNA. I checked gyrase activity under optimal and experimental conditions with Lon. In both situations gyrase was able to supercoil relaxed DNA, although gyrase was less active under the Lon assay conditions.
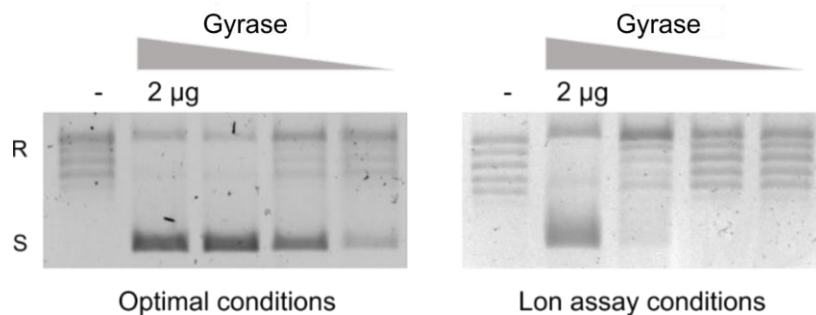
Figure 4.9. Supercoiling assay with gyrase used in Lon experiments. 1/10 dilutions of 2 mg/mL gyrase (GyrA and GyrB in 1:1 molar ratio) were incubated with 500 ng of relaxed pBR322 (R) under optimal conditions or the conditions used in the Lon assay (see 2.2.5.2). R stands for relaxed DNA and S for supercoiled DNA.

After confirming the activity of Lon and gyrase, I investigated if Lon degraded gyrase. To do this, I incubated gyrase, GyrB or GyrA with ciprofloxacin, and then added Lon protease. After 0, 30, 60, 120 minutes I took samples and ran them on an SDS-PAGE gel (**Figure 4.10**). I did not observe any extra bands in any of these conditions, suggesting that neither gyrase, nor GyrA, nor GyrB had been degraded by Lon.
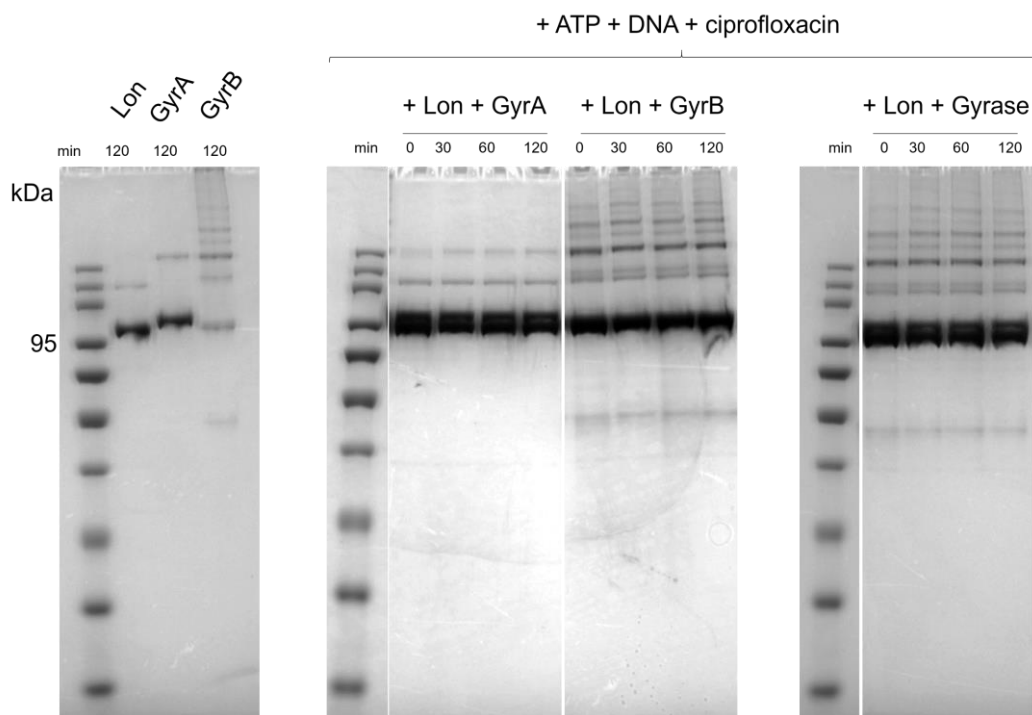
Figure 4.10. SDS-PAGE analysis of the degradation of GyrA, GyrB and gyrase by Lon. An amount of 2 µg of GyrA, GyrB or gyrase was incubated in a buffer with 20 mM Tris.HCl pH 8.0, 200 mM NaCl, 1 mM 2-Mercaptoethanol, 10% glycerol, 10 mM $MgCl_2$, 4 mM ATP, 30 µM ciprofloxacin and 500 ng of supercoiled pBR322 for 30 min at 37°C. 2 µg

of Lon were then added and incubated for 0, 30, 60 and 120 minutes at 37°C in a final volume of 30 µL. The reaction was stopped by adding 10 µL of sample buffer and boiling the samples for 5 min. 15 µL were loaded on a 12% SDS-PAGE gel and run for 45 min at 180V.

As Lon did not degrade trapped gyrase, I wondered whether Lon needed an extra component to fulfil such activity. To test this, I incubated trapped gyrase with Lon and/or the lysate of *E. coli* MG1655 Δ*lon* cells (**Figure 4.11**). Again, I could not observe any gyrase degradation. In case I was not seeing degradation because I did not use a concentrated lysate, I performed the experiment with a more concentrated lysate and checked the presence of GyrA by Western blot (**Figure 4.12**). I did not find degraded GyrA in the Western blot, suggesting that Lon did not degrade GyrA in the presence of the lysate.
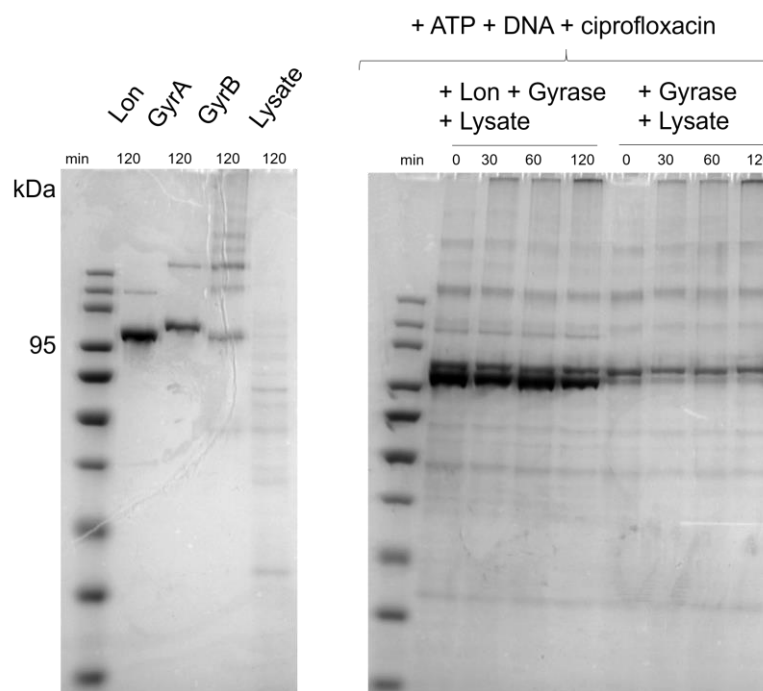
Figure 4.11. SDS-PAGE analysis of the degradation of gyrase by Lon. An amount of 2 µg of gyrase was incubated in a buffer with 20 mM Tris.HCl pH 8.0, 200 mM NaCl, 1 mM 2-Mercaptoethanol, 10% glycerol, 10 mM $MgCl_2$, 4 mM ATP, 30 µM ciprofloxacin and 500 ng of supercoiled pBR322 for 30 min at 37°C. 2 µg of Lon, and/or 5 µL of a cell lysate were then added and incubated for 0, 30, 60 and 120 minutes at 37°C in a final volume of 30 µL. The reaction was stopped by adding 10 µL of sample buffer and boiling the samples for 5 min. 15 µL were loaded on a 12% SDS-PAGE gel and run for 45 min at 180V. The cell lysate was obtained from 1 mL of *E. coli* MG1655 Δ*lon* cells grown until OD_{600} ~0.5 and then grown for 2 hours with 100 µg/mL of oxolinic acid.
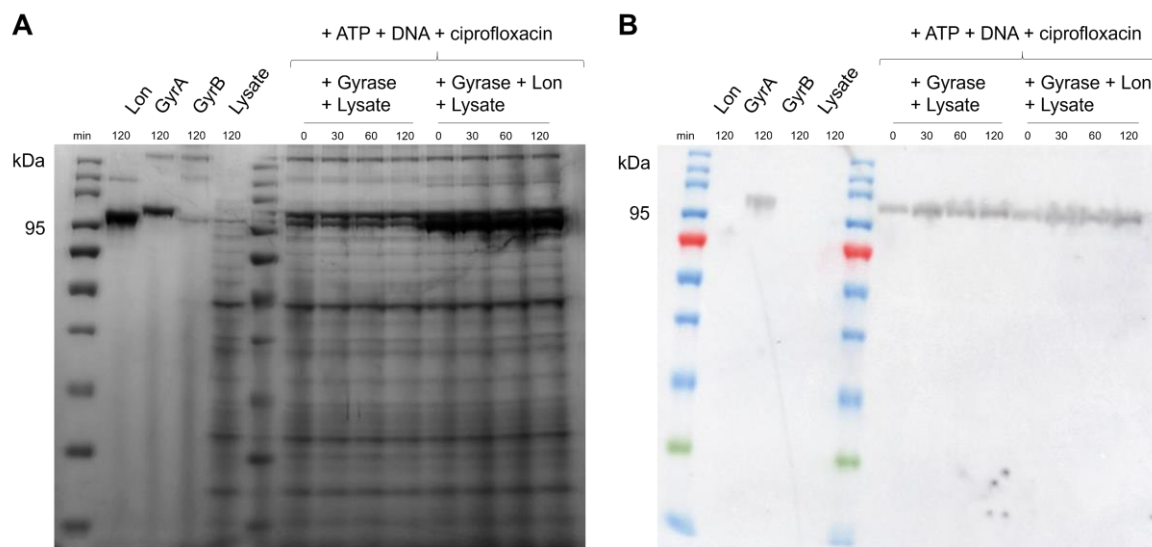
Figure 4.12. SDS-PAGE and western blot analysis of the degradation of gyrase by Lon. A) An amount of 2 μg of gyrase was incubated in a buffer with 20 mM Tris.HCl pH 8.0, 200 mM NaCl, 1 mM 2-Mercaptoethanol, 10% glycerol, 10 mM MgCl$_2$, 4 mM ATP, 30 μM ciprofloxacin and 500 ng of supercoiled pBR322 for 30 min at 37°C. 2 μg of Lon, and/or 5 μL of a cell lysate were then added and incubated for 0, 30, 60 and 120 minutes at 37°C in a final volume of 30 μL. The reaction was stopped by adding 10 μL of sample buffer and boiling the samples for 5 min. 15 μL were loaded on a 12% SDS-PAGE gel and run for 45 min at 180V. The cell lysate was obtained from 50 mL of *E. coli* MG1655 Δ*lon* cells grown until OD$_{600}$ ~0.5 and then grown for 2 hours with 100 μg/mL of oxolinic acid. B) Western blot analysis of the presence of GyrA in an SDS-PAGE run as in A). Proteins were immunoblotted with anti-GyrA-CTD antibody and then visualized with rabbit polyclonal antimouse-HRP conjugated antibody.

4.2.3 Measuring ciprofloxacin-induced DNA damage in *xseA⁻* cells

Because Exo VII participates in the repair of quinolone-induced DNA damage, I aimed to test if the deletion of *xseA* (the major subunit of nuclease Exo VII) had an effect in the amount of DNA breaks happening under ciprofloxacin exposure. My hypothesis was that the absence of *xseA* would cause an increase in the amount of DSBs under ciprofloxacin exposure. An increase in DNA damage in *xseA-* cells has already been shown by Sharma et al. [166]; however, in that study they showed DNA breaks by running the DNA of a population of *E. coli* cells on a gel, meaning that they could not measure the amount of DSBs per cell. To measure the quantity of DSBs in individual *E. coli* cells, I used fluorescently labelled proteins that bind or are associated to DSBs. Some examples of proteins that have been fluorescently labelled are RecA [167], RecN [23, 168] and

MuGam foci [77, 78]. MuGam is the protein Gam from Mu phage (not to be confused with Gam from λ phage which can inhibit RecBCD [161]). MuGam binds to DSBs and does not interact with other proteins. The main caveat of MuGam is that once it binds a DSB, that break cannot be repaired [169], thus it is not a good system to measure the formation of DSBs over time. RecA is a DNA strand exchange protein with multiple roles including the regulation of the SOS response and HR repair. It is activated in the presence of DNA damage, and it assembles on single-stranded DNA (ssDNA) tracts after RecBCD processes both ends of a DSB. However, because it does not only participate in the repair of DSB, measuring RecA foci as a proxy of DSBs can be misleading. RecN is a cohesin-like protein that participates in the repair of DSBs after RecA has bound the DNA [170]. It is, therefore, functioning several steps after the DSB has been processed. As I wanted to measure DSBs directly, I designed an alternative system using fluorescently labelled RecB (that directly binds DSBs) and I also used the MuGam system designed by Shee et al. [169].

4.2.3.1 Measuring RecB foci as a proxy for DNA damage

RecB is a recombinase that forms a complex with the helicases RecC and RecD (RecBCD) to process DNA damage. The complex RecBCD binds to DSBs and is responsible for the initiation of the repair of DSBs [129]. As far as I am aware, RecB fluorescent foci have never been used as an indicator of DNA damage. However, because of its specificity towards DSBs, I investigated if it could be used as an indicator of DNA damage.

To test whether RecB formed foci during the repair of DSBs, I created a N-terminal enhanced green fluorescent protein (eGFP) and DsRed2 fusions of RecB by introducing *recB* in eGFP-pBAD and DsRed2-pBAD plasmids, respectively. Those constructs were introduced in *recB*⁻ cells, so that all the RecB protein expressed would have a fluorescent tag. To check if eGFP-RecB and DsRed2-RecB were active, I measured the growth of the *recB*⁻ mutants with and without these plasmids in the presence or absence of ciprofloxacin. As ciprofloxacin affects *recB*⁻ cells more than WT cells, if eGFP-RecB and DsRed2-RecB were active, I expected to see an increase in growth when eGFP-RecB or DsRed2-RecB was expressed in *recB*⁻ cells. I observed an increase of growth when eGFP-RecB or DsRed2-RecB was expressed, which indicated that eGFP-RecB and DsRed2-RecB were active. I also checked the amount of GFP and DsRed fluorescence when eGFP-RecB and DsRed2-RecB were expressed. I found that eGFP-RecB fluorescence was more intense and happened quicker than DsRed2-RecB fluorescence, suggesting that eGFP-RecB was a better fluorescence system (**Figure 4.13**).

Repair of quinolone-induced damage: role of proteases, nucleases and enzymes involved in DNA repair
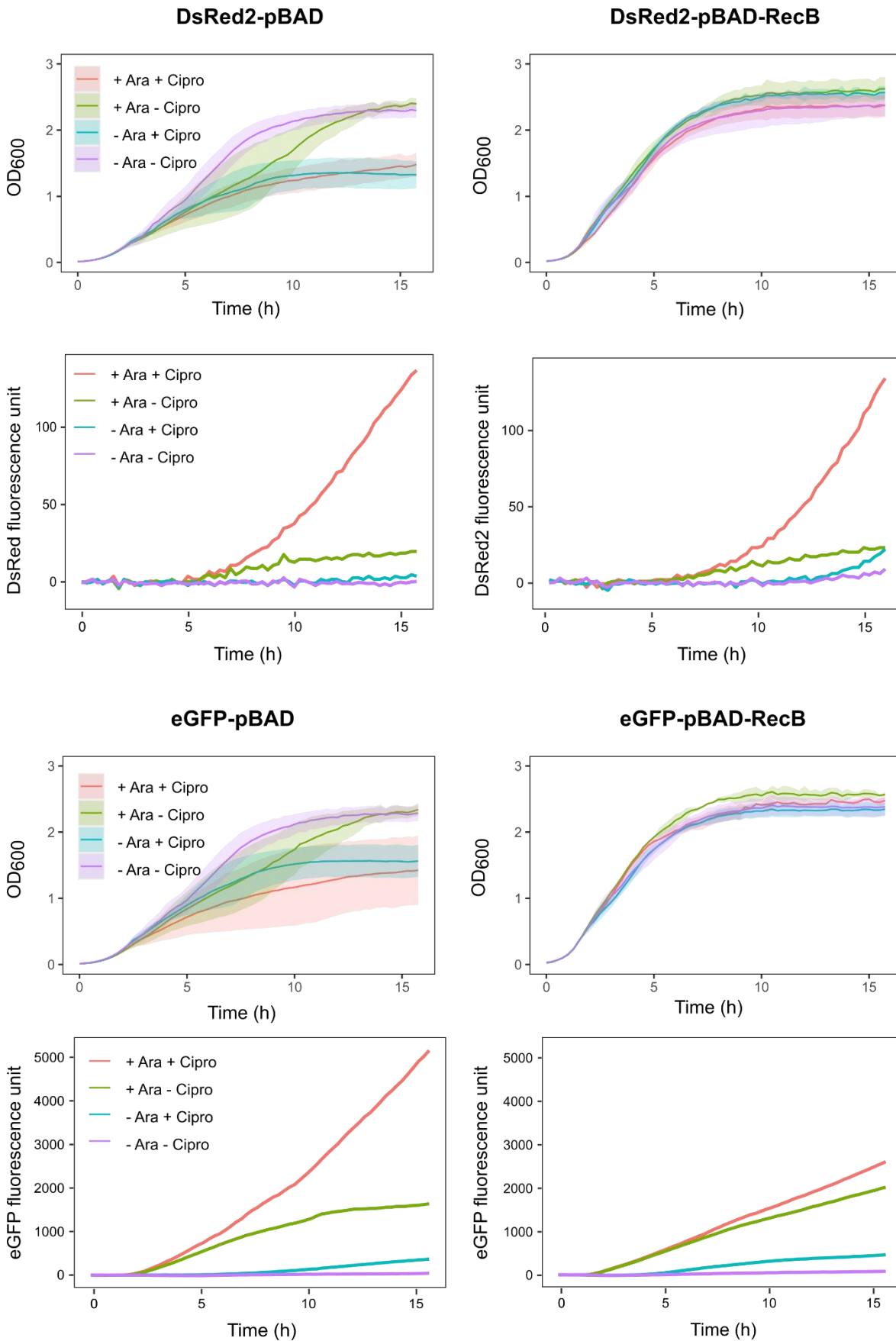
Figure 4.13. Growth curves and fluorescence intensity of BW25113 *recB*::Kan^R with eGFP-pBAD, eGFP-pBAD-RecB, DsRed2-pBAD or DsRed2-pBAD-RecB. Cells were grown in LB in the presence or absence of 0.2% (w/v) of L-Arabinose (Ara), and 0.004 µg/mL of ciprofloxacin (Cipro) in a 96-well plate. OD_{600}, GFP ($\lambda_{excitation}$ = 488 nm, $\lambda_{emission}$ = 509 nm) and DsRed2 ($\lambda_{excitation}$ = 561 nm, $\lambda_{emission}$ = 587 nm) measurements were taken every 15 minutes for 15.5 hours using a CLARIOstar® plate reader, and cells were incubated at 37°C with agitation. Each sample was assayed in triplicate (technical replicate). For the OD_{600} measurements, each of the strongest lines represents the average of three replicates for a particular condition, and shading represents the standard deviation for each condition. The GFP and DsRed measurements were done only once.

As the constructs were expressing active RecB, I checked how the cells looked when they were grown in the presence or absence of ciprofloxacin. When I imaged cells transformed with eGFP-RecB, I observed GFP fluorescence in the whole cells in the presence and absence of ciprofloxacin (**Figure 4.14**). Some of those cells had foci. The cells that had DsRed2-RecB did not emit any fluorescence, and I did not use them in further experiments. In terms of the size, ciprofloxacin caused an increase in the size of the cell. This is expected as quinolones induce the filamentation of the cells.
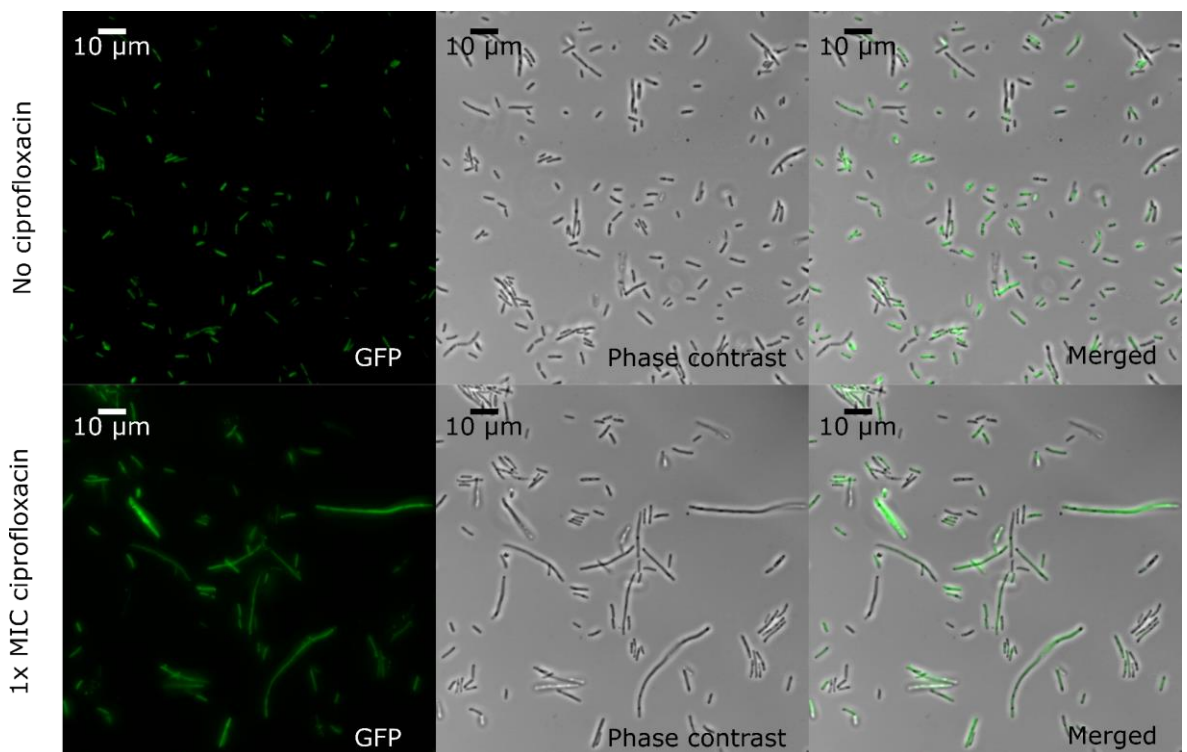
Figure 4.14. GFP fluorescence, phase contrast and merged GFP and phase contrast images of eGFP-pBAD-RecB. Cells were grown in LB supplemented with 100 µg/mL of

ampicillin until $OD_{600} = 0.5$, then they were treated or not with 0.027 µg/mL of ciprofloxacin (1x MIC cipro) for 2 hours.

To test if *recB* cells expressing eGFP-RecB could be used to measure DNA breaks, I counted the number of fluorescent foci per cell as well as size in the absence or presence of quinolones. Because quinolones cause DNA breaks, I expected to see an increase in fluorescent foci in the presence of ciprofloxacin. Also, as quinolones cause the filamentation of the cells, I expected to see an increase in cell size over time in the presence of ciprofloxacin. When I compared the number of foci in *recB* cells expressing eGFP-RecB in the presence or absence of ciprofloxacin, I did not see a higher number of foci per cell in cells exposed to ciprofloxacin compared to cells not exposed, and neither did I see an increase in the number of foci over time when cells were treated with ciprofloxacin (**Figure 4.15**). In fact, I saw the opposite (non-treated cells having more foci than ciprofloxacin-treated cells). These results suggested that the RecB system I designed could not be used to measure DSBs in *E. coli* cells.
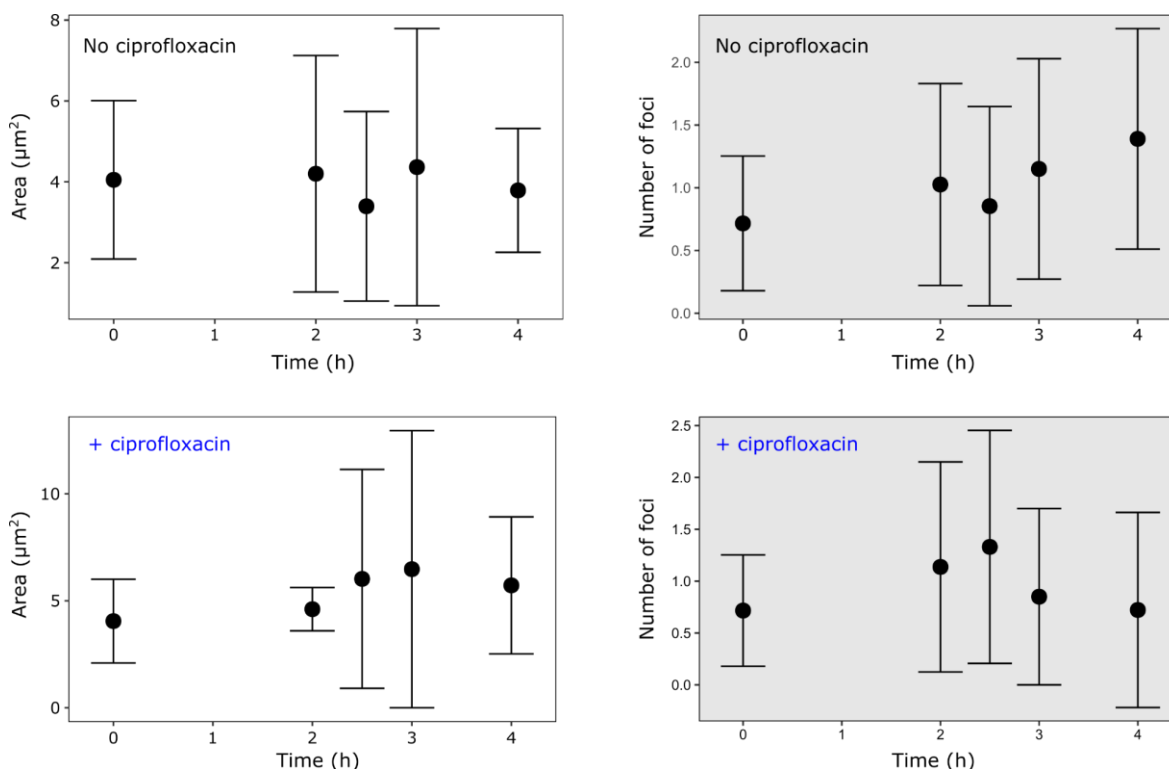
Figure 4.15. Area and number of foci over time of eGFP-pBAD-RecB cells grown in the absence or presence of 0.027 µg/mL of ciprofloxacin. The area and number of fluorescent foci were measured using an ImageJ macro. Each point represents the average of ≥ 150 cells, and the bars show the standard deviation.

4.2.3.2   Measuring Gam foci as a proxy for DNA damage

Another way of measuring DSBs in single cells is by counting Gam-GFP foci using the MuGam-GFP system [169]. In this system, *E. coli* MG1655 cells have an inducible MuGam-GFP cassette inserted in the chromosome. As Gam-GFP binds to DSBs, the number of Gam-GFP foci correlates with the amount of DSBs.

To confirm that the *E. coli* MG1655 Gam-GFP strain could be used to measure DSBs, I imaged the WT Gam-GFP strain under different concentrations of ciprofloxacin. I observed fluorescent foci in the cells, as well as an increase in foci number and cell size as the concentration of ciprofloxacin was higher (**Figure 4.16**). These results were consistent with previous work [77, 78] and suggested that the Gam-GFP system could be used to measure DSBs.

I then introduced the *xseA*- mutation in the Gam-GFP strain and used it to compare the number of foci in the presence and absence of ciprofloxacin with the Gam-GFP strain. I found that in the absence of ciprofloxacin, both strains had a similar average number of foci per cell, as well as a similar size (**Figure 4.17**). However, in the presence of ciprofloxacin, *xseA*- cells had on average twice as many foci per cell and were twice as big as the *xseA*+ cells. Interestingly, the distribution of the data showed that most of the *xseA*- cells did not have foci, but some of them had up to 9 foci per cell. This result suggested that the deletion of *xseA* caused an increase in the number of DSBs in some of the cells that were exposed to ciprofloxacin.
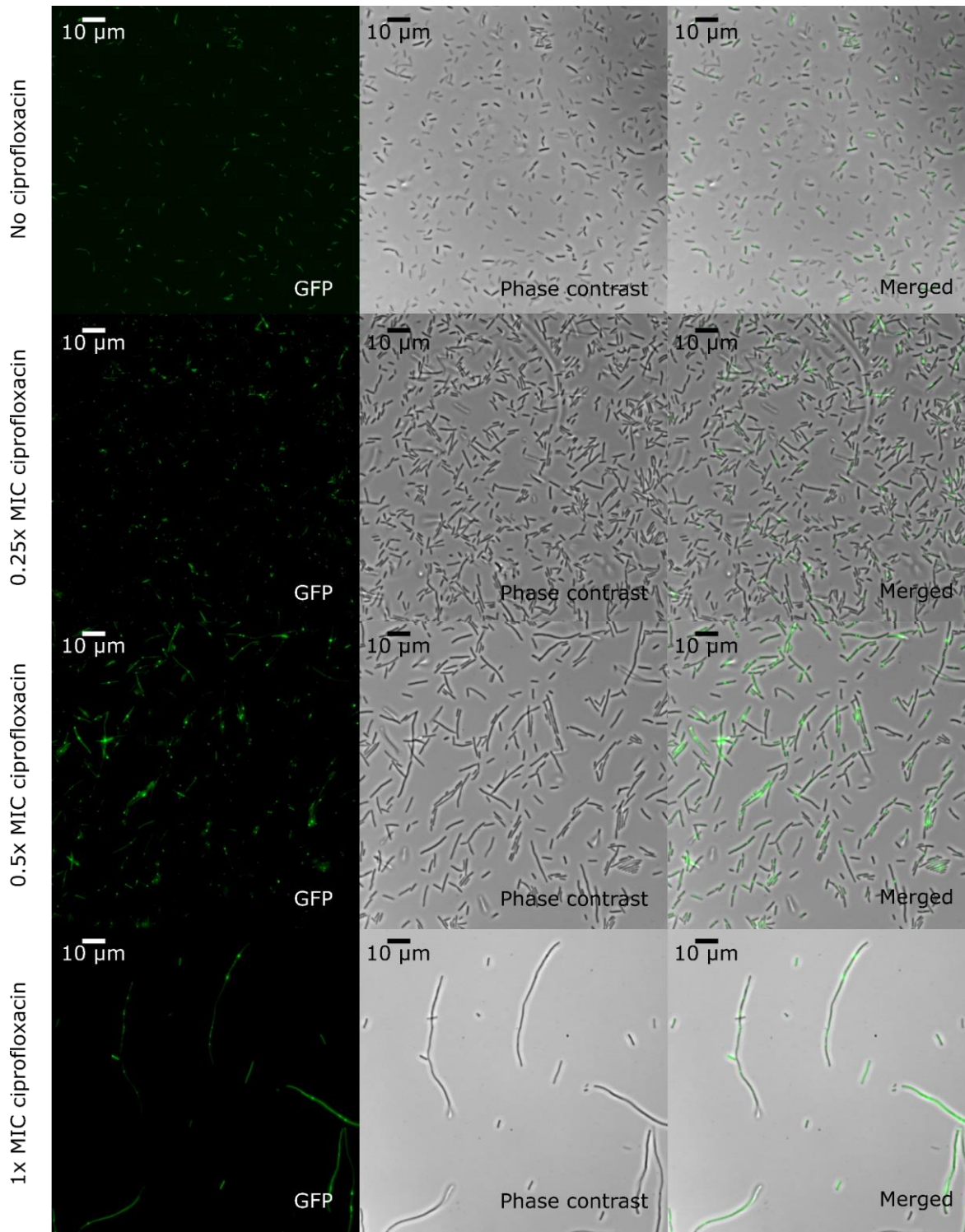
Figure 4.16. GFP fluorescence, phase contrast and merged GFP and phase contrast images of *E. coli* MG1655 Gam-GFP. Cells were grown in LB until $OD_{600} = 0.5$, then the expression of Gam-GFP was induced with doxycycline for 1.5 h, and cells were treated or not with 0.027 µg/mL of ciprofloxacin (1x MIC cipro) for 2 h.
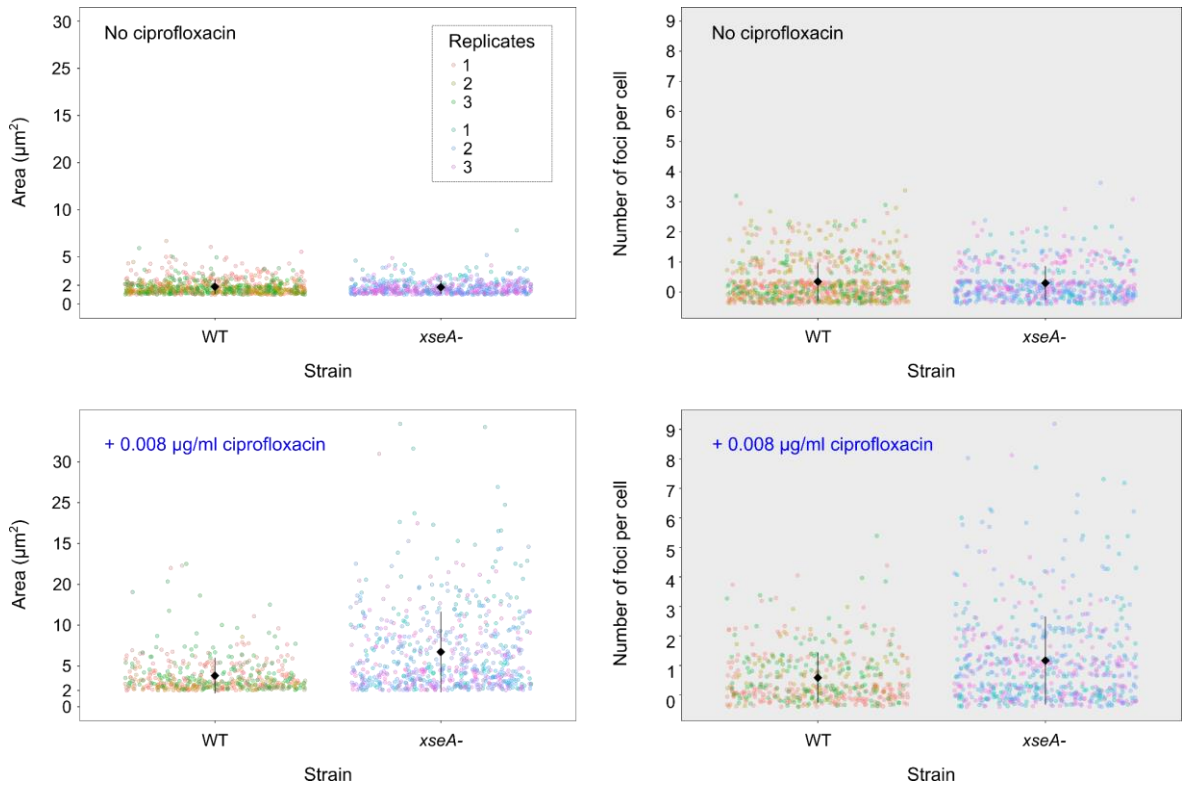
Figure 4.17. Area and number of foci of Gam-GFP or Gam-GFP ΔxseA cells grown in the absence or presence of 0.008 μg/mL of ciprofloxacin. Each coloured point represents a single cell. For each experiment three replicates were done, and for each of them the area and number of foci of ≥ 150 cells were measured using an ImageJ macro. The diamonds indicate the average number of foci or area per cell of all cells from the three replicates, and the bars show the standard deviation.

4.3   Discussion

In this chapter I have tested whether certain proteases, nucleases and recombinases participated in the repair of quinolone-induced damage. Out of all proteins tested in the genetic screen, the most promising candidates are the protease Lon, the nuclease Exo VII, and the recombinases RecB and RecA. This is because the mutants deficient in those proteins are more sensitive to quinolones. I must mention here that I could not reproduce previous results by Aedo et al. [121] in which they showed that the nuclease SbcCD affected the survival to quinolones (in my case I saw no difference in the survival to quinolones between WT and *sbcCD*⁻ cells), and, therefore, I do not think that this protein has a major role in the repair of quinolone-induced damage. By contrast, the nuclease Exo VII, is likely to be involved in the repair of quinolone-induced damage. This is because its deletion not only makes cells more sensitive to quinolones, but it causes an increase in DSBs.

In the introduction (section 4.1), I hypothesised that the pathway for the removal of trapped topoisomerases from the DNA (a step necessary for the repair of quinolone-induced damage) starts with a protease that degrades the trapped topoisomerase. Of all *E. coli* proteases, only the deletion of *lon* has been shown to make cells more sensitive to quinolones. This suggests that Lon is involved in the repair of quinolone-induced DNA damage. Also, as Lon binds to DNA, it might be possible that it is able to recognise gyrases that are trapped on the DNA. However, when I incubated Lon with trapped gyrase, I did not see any gyrase degradation. Perhaps, this was because Lon needed other factors to degrade the trapped gyrase. For example, in eukaryotes, trapped topoisomerases need to be ubiquitinated in order to be degraded by the proteasome [122]. To date, Lon has not been associated with any additional factor in order to degrade a protein. Nevertheless, I tested if Lon in combination with other proteins were able to degrade trapped gyrase. To do this, I incubated Lon with trapped gyrase and cell lysate. Again, I did not see any gyrase degradation. Maybe, I did not use the right *in vitro* conditions for the experiment, or the additional factor(s) were not present in the cell lysate. It is also possible that Lon is not the protease involved in the degradation of the gyrase. Further experiments to test these ideas are mentioned below.

4.4   Conclusions

The aim of this chapter was to find proteases, nucleases and DNA repair proteins involved in the repair of quinolone-induced DNA damage. An initial genetic screen showed that the protease Lon, the nuclease Exo VII, and the recombinases RecB and RecA were involved in quinolone-induced DNA damage repair, as their absence made cells more sensitive to quinolones. Interestingly, mutants lacking Exo VII, Lon and RecB were as sensitive to quinolones as the single mutants, suggesting that those three proteins might be part of the same pathway. However, Lon was not able to degrade trapped gyrase which would be the first step of the quinolone-induced repair pathway. I also found that the absence of Exo VII caused an increase of DSBs in the presence of quinolones, suggesting that this protein is indeed involved in the repair of quinolone-induced DNA damage.

4.5   Future work

This chapter has raised several unsolved questions. First, is the effect on quinolone sensitivity of the deletion of *xseA*, *lon* and *recB* epistatic? To confirm this, the sensitivity to quinolones of *xseA⁻ lon⁻* Gam⁺ cells should be tested in conditions that prevent the formation of DSBs that are not induced by quinolones (e.g., using minimal media and

avoiding sunlight). Secondly, does Lon or other proteases degrade trapped gyrase? I have already tried incubating Lon with cell lysates and trapped gyrase; however, the cell lysates were not very concentrated. Further experiments could use a more concentrated lysate. Also, it would be interesting to perform biochemical assays such as pull-down assays with trapped gyrase to investigate which proteases interact with gyrase. Third, does the deletion of other genes apart from *xseA* (e.g., *clpP*, *sbcCD*, *lon*, *recB*) cause an increase of DSBs under quinolone exposure? To examine this, Gam-GFP foci in Gam-GFP *clpP*, *sbcCD* or *lon* cells could be counted and compared to the ones of Gam-GFP WT cells.

Chapter 5:

5 Quinolone-induced antimicrobial resistance (QIAR)

5.1 Introduction

Quinolones can induce resistance to unrelated antibiotics (i.e., antibiotics that do not target topoisomerases like rifampin or ampicillin) [47, 77, 107]. This induced resistance is due to chromosomal mutations; however, it is not clear how those quinolone-induced mutations arise. Several groups have linked the SOS response to the formation of such mutations [47, 56, 77, 78, 108]. The SOS response is the bacterial response to DNA damage, and it is controlled by RecA and LexA. When the SOS response is activated (for example, when quinolones induce DNA damage), several genes like the ones that encode the error-prone polymerases, Pol IV (*dinB*) and Pol V (*umuCD*), and the high-fidelity polymerase Pol II (*polB*) are upregulated. SOS-upregulated polymerases can make point mutations that lead to quinolone-induced resistance to rifampin [47, 77] and ampicillin [77]. However, other mutations induced by quinolones can be independent of the SOS-upregulated polymerases [111]. Hence, it is not clear what molecular pathways are involved in the acquisition of quinolone-induced antibiotic resistance.

In our lab we have observed that different quinolones induce resistance to non-quinolone antibiotics. Natassja Bush, who first investigated this phenomenon during her PhD, named it quinolone-induced antimicrobial resistance (QIAR) [55]. She found ampicillin-, chloramphenicol-, kanamycin-, tetracycline-, triclosan- and ciprofloxacin-resistant colonies after treating *E. coli* with low levels of ciprofloxacin, other quinolones (oxolinic acid or norfloxacin) or RedX05931 (a compound that stabilises the topoisomerase-DNA complex but that it is not a quinolone) but not when she used coumermycin A1 (a topoisomerase inhibitor that does not stabilise the topoisomerase-DNA complex). These results indicated that only quinolones or other drugs that could stabilise the topoisomerase-DNA complex, could induce the acquisition of AR under sublethal concentrations of the drugs.

In this chapter, I continued Natassja's work on QIAR. After confirming the QIAR phenomenon, I focused on understanding one type of QIAR: ciprofloxacin-induced chloramphenicol resistance. I investigated when and how ciprofloxacin induced chloramphenicol resistance happened and if it depended on the SOS response or on the nucleases Exo VII and SbcCD (which might participate in the repair of quinolone-induced

DNA damage). Finally, I analysed the mutations that appeared after the exposure to ciprofloxacin.

5.2 Results

5.2.1 Low levels of ciprofloxacin increase the frequency of appearance of bacteria resistant to high levels of ampicillin, chloramphenicol, ciprofloxacin, and trimethoprim

Several studies have shown that quinolones induce resistance to several antibiotics [40, 77]. Based on these results, I hypothesised that *E. coli* cells exposed to low levels of ciprofloxacin would acquire antibiotic resistance to different types of antibiotics. To test this hypothesis, I exposed *E. coli* to low levels of the quinolone ciprofloxacin (or other drugs) and recorded the frequency of appearance of cells resistant to high levels of different types of antibiotics using the QIAR assay.

5.2.1.1 The QIAR assay

The QIAR assay was developed by Natassja Bush with the aim of testing if a drug could induce resistance to other drugs [55]. In this assay one colony of *E. coli* is grown in the presence or absence of low levels of drugs (treatment) and then plated on plates with high levels of different antibiotics (selection) (**Figure 5.1**). The frequency of antibiotic resistant mutants is then calculated by dividing the number of resistant colonies by the total number of colonies plated.
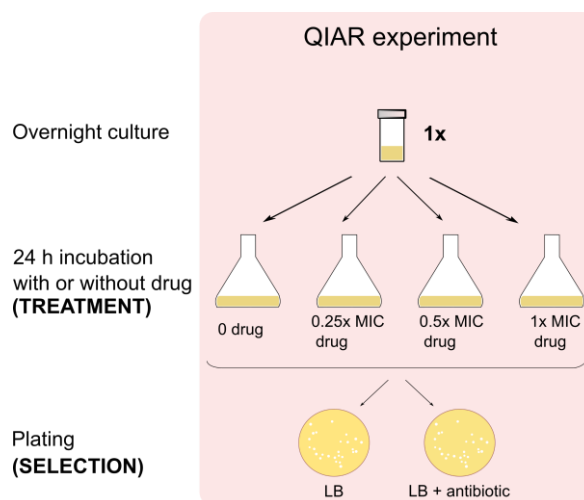
Figure 5.1. Schematic representation of the quinolone-induced antimicrobial resistance (QIAR) experiment. An overnight culture from a single colony is split into four

tubes: in one tube it is grown without a drug, in a second tube it is grown with 0.25x MIC of a drug, in a third tube it is grown with 0.5x MIC of a drug, and in a fourth tube it is grown with 1x MIC of a drug. The cultures are incubated at 37°C for 24 hours and then plated on LB plates supplemented with antibiotics to select for antibiotic resistance. Dilutions of the cultures are plated on LB-only plates to count the number of colonies plated. The frequency of resistant colonies is then calculated by dividing the number of resistant colonies by the total number of colonies plated.

There are four variables in the QIAR assay: a) the *E. coli* strain, b) the antibiotics used in the treatment, c) the antibiotics used in the selection, and d) the concentrations of antibiotics used.

a) The *E. coli* strain

In the QIAR experiments I used *E. coli* MG1655 and *E. coli* BW25113 strains. They are derivatives of the *E. coli* K-12 strain [171] that differ in the inability of BW25113 cells to degrade arabinose [172]. I chose MG1655 because the reference *E. coli* genome belongs to this strain and, therefore, if I were to analyse the genome of an *E. coli* MG1655 strain (as I did in section 5.2.5), I could compare it to a well-annotated and curated genome. I also worked with *E. coli* BW25113 because it is the parental strain of a collection comprising all non-essential single-gene deletion mutants [173]. This collection is called the Keio collection, and it is extremely useful because it contains all mutants with any non-essential gene deleted (for example, the *recB*⁻ mutant that I used in Chapter 4). Because I wanted to try the QIAR assay with different mutants, and I was not sure if I could make them in the MG1655 background, I tested if QIAR happened in MG1655 and BW25113 cells.

b) The antibiotics used in the treatment

E. coli cells were treated with low levels of ciprofloxacin or a non-quinolone antibiotic: either mitomycin C (a DNA intercalator that activates the SOS response), or chloramphenicol (a protein synthesis inhibitor). I chose ciprofloxacin because it is one of the most used quinolones worldwide, and it is also used to treat *E. coli* infections. Mitomycin C was used to test if a non-quinolone antibiotic that caused DNA damage would also induce antibiotic resistance. Similarly, chloramphenicol was used to test if a non-quinolone antibiotic that did not cause DNA damage would induce antibiotic resistance.

c) The antibiotics used in the selection

For the selection I used several antibiotics: ampicillin, chloramphenicol, ciprofloxacin, kanamycin, streptomycin, tetracycline, mitomycin C and/or trimethoprim. I used these antibiotics because they have different targets in bacteria, and bacteria have different mechanisms to cope with them. In short, ampicillin targets the bacterial cell wall, trimethoprim targets the metabolism of folic acid, mitomycin C targets the DNA, chloramphenicol targets the 50S subunit of the bacterial ribosome, and kanamycin, streptomycin and tetracycline inhibit the 30S subunit of the bacterial ribosome. These mechanisms of action differ greatly from that of the quinolones, which is to inhibit topoisomerases. In terms of mechanisms of resistance, bacteria can become resistant to these antibiotics by upregulating efflux pumps, or by having mutations in specific genes (e.g., *thyA* in the case of trimethoprim or *gyrA* in the case of ciprofloxacin).

d) The concentration of the antibiotics

In the QIAR assay I treated cells with low levels of antibiotics and then selected with high levels of antibiotics. To determine which were low or high levels of an antibiotic, I used the minimum inhibitory concentration (MIC). The MIC indicates the minimum amount of an antibiotic that is necessary to inhibit the growth of bacteria. Traditionally, concentrations of an antibiotic that are below the MIC value are considered low levels, whereas values over the MIC indicated are high levels. As I used two *E. coli* strains in the experiments (MG1655 and BW25113) I measured the MICs of the antibiotics for those strains. I also measured the MICs in two different ways: the solid method, in which bacteria are grown on solid media; and the broth method, in which bacteria are grown in liquid media. The MICs obtained with those methods were the same or very similar and were consistent with the MICs from the literature (**Table 5.1**). Because in the QIAR assays cells are grown in liquid medium (during the treatment) and on solid medium (during the selection), I used the broth MIC when cells were grown on liquid media and the solid MIC when cells were grown on solid media (**Table 5.2**). The specific concentrations of antibiotics were based on the concentrations from Natassja Bush's thesis [55]. For the treatment I used low levels of an antibiotic (0.25x, 0.5x or 1x MIC), whereas for the selection I used concentrations arranging from 8-27x MIC (**Table 5.2**). For the selection of mitomycin C, streptomycin, and trimethoprim (antibiotics that were not tested by Natassja) I used 20-25x MIC.

Table 5.1. Minimum inhibitory concentrations (MICs) of different antibiotics. The MICs were calculated as the average of three replicates using the solid or the broth method and compared to the MICs found in the literature.

Antibiotic	*E. coli* strain	MIC (µg/mL)		Literature MIC (µg/mL)	
		Solid MIC	Broth MIC	Solid MIC	Broth MIC
Ampicillin	BW25113	4	6	6 [159]	8 [174]
	MG1655	4	6	8 [89]	2 [20]
Chloramphenicol	BW25113	4	4	-	-
	MG1655	4	4	8 [175]	6 [20]
Ciprofloxacin	BW25113	0.024	0.027	0.016-0.020 [159]	0.024 [174]
	MG1655	0.024	0.027	-	0.023 [40], 0.016 [176]
Kanamycin	BW25113	6	-	-	13 [177]
	MG1655	6	-		8-16 [178]
Mitomycin C	MG1655	2	1.5	-	1.5 [179]
Streptomycin	BW25113	12	20		14 [177]
	MG1655	14	24	16 [175]	-
Tetracycline	BW25113	1.25	2.13	-	4 [177]
	MG1655	1.16	1.4	2 [175]	2 [20]
Trimethoprim	BW25113	0.4	0.4	-	0.6 [180]
	MG1655	0.4	0.4	-	1-2 [178]

Table 5.2. MIC doses of different antibiotics that were used in the quinolone-induced antimicrobial resistance (QIAR) assays.

Antibiotic used in treatment	Broth MIC (µg/mL)	MIC dose
Ciprofloxacin	0.027	0, 0.25x, 0.5x, 1x
Mitomycin C	1.5	0, 0.25x, 0.5x, 1x
Chloramphenicol	4	0, 0.25x, 0.5x, 1x
Antibiotic used in selection	**Solid MIC (µg/mL)**	**MIC dose**
Ampicillin	6	8.3x
Chloramphenicol	4	8x
Ciprofloxacin	0.024	14.6x
Kanamycin	6	8.3x
Mitomycin C	2	20x
Streptomycin	12 (BW25113), 14 (MG1655)	26.6x (BW25113), 23x (MG1655)
Tetracycline	1.25 (BW25113), 1.16 (MG1655)	8x (BW25113), 8.6x (MG1655)
Trimethoprim	0.4	25x

5.2.1.2 Results of the QIAR experiments

To test if *E. coli* MG1655 cells acquired antibiotic resistance after being exposed to low levels of ciprofloxacin, I did the QIAR experiment with *E. coli* MG1655 cells selecting for ampicillin, chloramphenicol, ciprofloxacin, kanamycin, streptomycin, and tetracycline resistance. I found ampicillin-, chloramphenicol-, and ciprofloxacin-resistant colonies when the cells had been exposed to ciprofloxacin, but not when the cells had not been treated with ciprofloxacin (**Figure 5.2**). Conversely, streptomycin- and kanamycin-resistant colonies appeared even when there was no ciprofloxacin treatment. This suggests that those resistances were caused by the appearance of spontaneous mutations rather than ciprofloxacin exposure. Also, no tetracycline-resistant colonies appeared after any ciprofloxacin treatment, indicating that ciprofloxacin did not induce tetracycline resistance. These results confirmed previous results on QIAR, as Natassja Bush also observed ciprofloxacin-, ampicillin- and chloramphenicol-resistant colonies only when they had been exposed low levels of ciprofloxacin [55]. The fact that I did not obtain any ciprofloxacin-induced tetracycline-resistant colonies as Natassja did, might be due to the fact that I only did three replicates of the QIAR experiment for that antibiotic selection.

The data hinted at an increase in the frequency of resistant colonies at higher concentrations of ciprofloxacin. However, this could only be confirmed in the case of chloramphenicol resistance, for which I did enough replicates to show a dose-dependent effect (**Figure 5.2**).

E. coli BW25113 cells showed a similar pattern of QIAR as *E. coli* MG1655 cells (**Figure 5.3**). Ampicillin-, chloramphenicol-, and ciprofloxacin-resistant colonies only appeared when cells had been exposed to ciprofloxacin, and streptomycin-resistant cells appeared regardless of the ciprofloxacin treatment. Interestingly, I checked if cells could become resistant to trimethoprim (I did not check that antibiotic with MG1655 cells) and in two out of three QIAR experiments cells became resistant to trimethoprim only after being exposed to ciprofloxacin. This result indicated that ciprofloxacin could also induce trimethoprim resistance in *E. coli* cells.
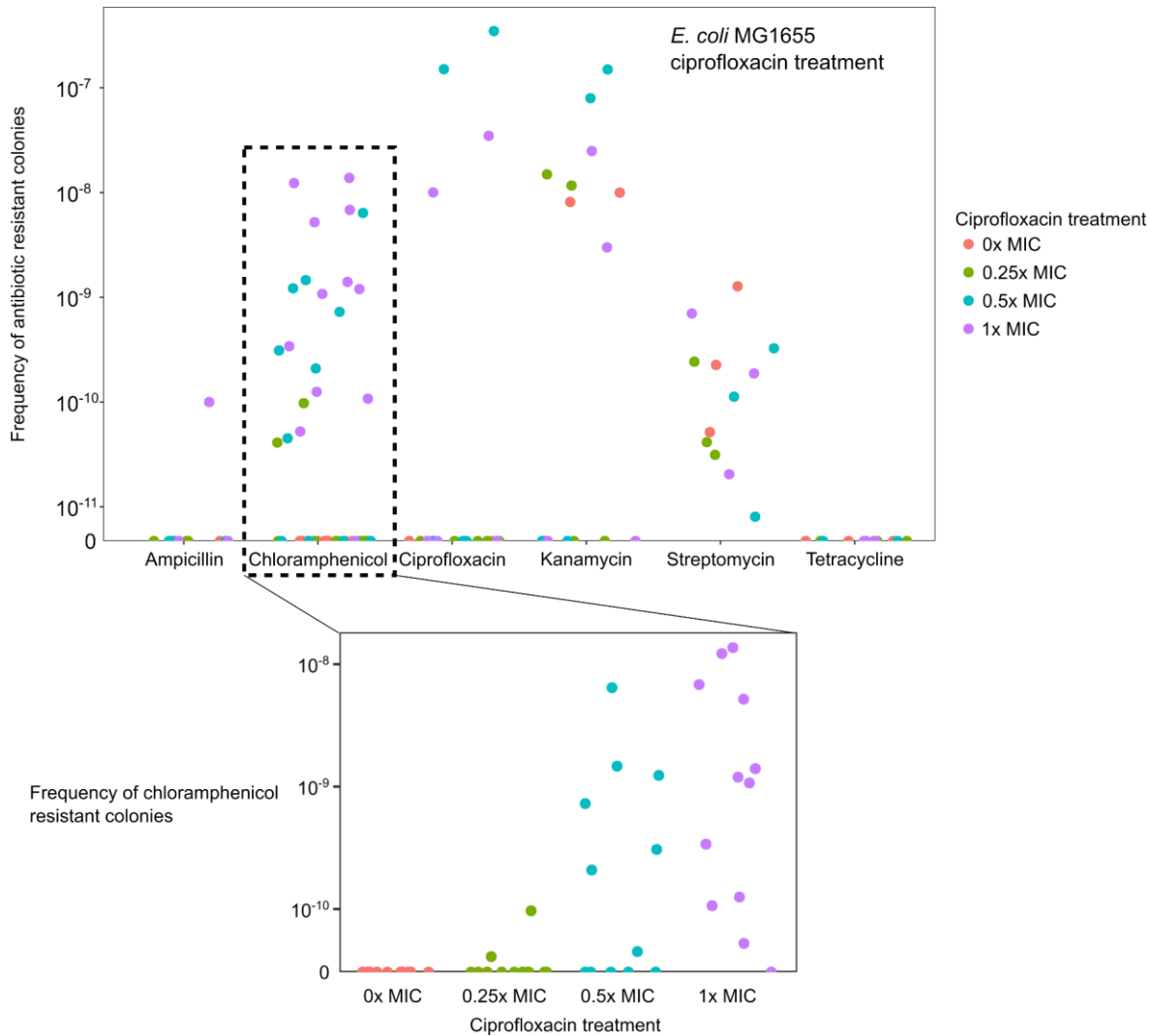
Figure 5.2. Frequency of antibiotic-resistant colonies after exposure of *E. coli* MG1655 cells to different doses of ciprofloxacin. *E. coli* MG1655 independent colonies were grown without or with 0.25x, 0.5x or 1x MIC of ciprofloxacin (broth MIC = 0.027 µg/mL) for 24 h at 37°C, then plated on plates supplemented with 8.3x MIC ampicillin (solid MIC = 6 µg/mL), 8x MIC chloramphenicol (solid MIC = 4 µg/mL), 14.6x MIC ciprofloxacin (solid MIC = 0.024 µg/mL), 8.3x MIC kanamycin (solid MIC = 6 µg/mL), 23x MIC streptomycin (solid MIC = 14 µg/mL), and 8.6x MIC tetracycline (solid MIC = 1.16 µg/mL). The bottom plot shows the frequency of chloramphenicol-resistant colonies separated by ciprofloxacin treatment. Each point represents the frequency of antibiotic resistance of one QIAR experimental condition (0x, 0.25x MIC, 0.5x MIC or 1x MIC).
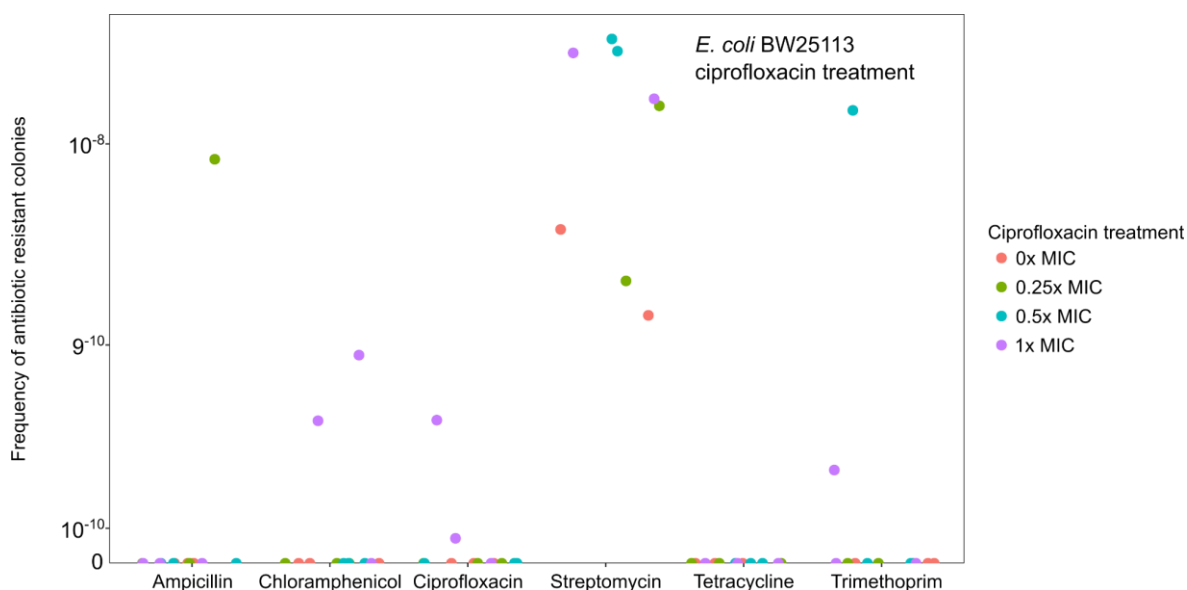
Figure 5.3. Frequency of antibiotic-resistant colonies after exposure of *E. coli* BW25113 cells to different doses of ciprofloxacin. *E. coli* BW25113 was grown without or with 0.25x, 0.5x or 1x MIC of ciprofloxacin (broth MIC = 0.027 µg/mL) for 24 h at 37°C, then plated on plates supplemented with 8.3x MIC ampicillin (solid MIC = 6 µg/mL), 8x MIC chloramphenicol (solid MIC = 4 µg/mL), 14.6x MIC ciprofloxacin (solid MIC = 0.024 µg/mL), 8.3x MIC kanamycin (solid MIC = 6 µg/mL), 26.6x MIC streptomycin (solid MIC = 12 µg/mL), and 8x MIC tetracycline (solid MIC = 1.25 µg/mL). Each point represents the frequency of antibiotic resistance of one QIAR experimental condition (0x, 0.25x MIC, 0.5x MIC or 1x MIC).

When I treated *E. coli* MG1655 cells with low levels of mitomycin C, I obtained resistant colonies to chloramphenicol, ciprofloxacin and mitomycin C (**Figure 5.4**). These resistances were only observed when cells had been exposed to mitomycin C. The selection with streptomycin again showed resistant colonies regardless of the mitomycin C treatment. As mitomycin C and ciprofloxacin activate the SOS response, it is possible that the chloramphenicol-induced resistance might depend on the SOS response. I further investigated the contribution of the SOS response in the induction of chloramphenicol resistance in section 5.2.4.
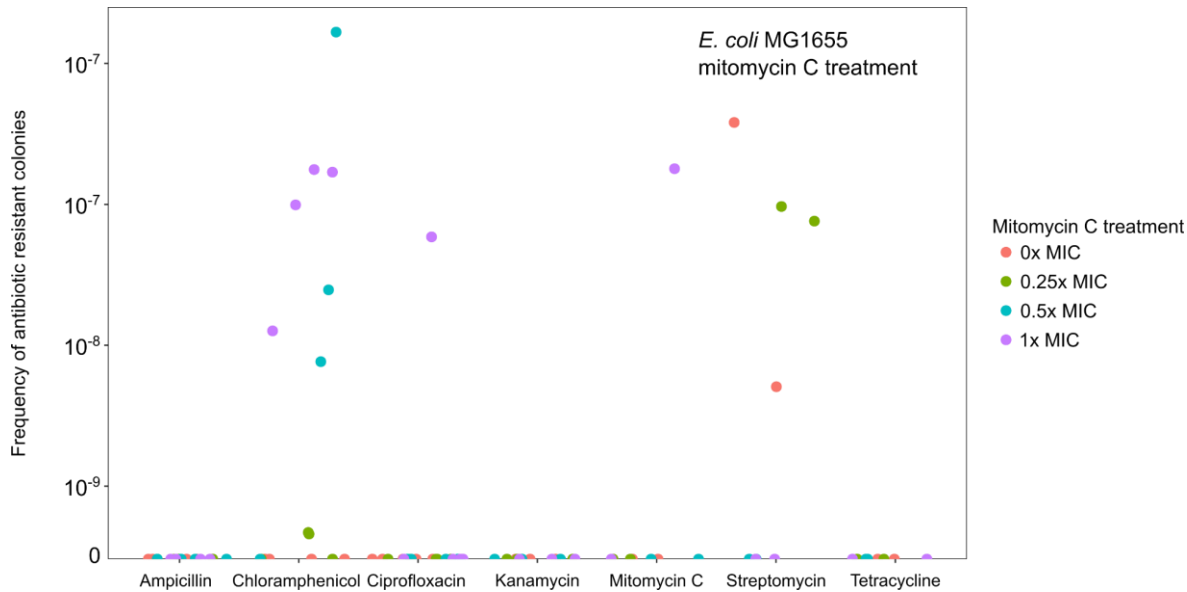
Figure 5.4. Frequency of antibiotic resistant colonies after exposure of *E. coli* MG1655 cells to different doses of mitomycin C. *E. coli* MG1655 was grown without or with 0.25x, 0.5x or 1x MIC of mitomycin C (broth MIC = 1.5 µg/mL) for 24 h at 37°C, then plated on plates supplemented with 8.3x MIC ampicillin (solid MIC = 6 µg/mL), 8x MIC chloramphenicol (solid MIC = 4 µg/mL), 14.6x MIC ciprofloxacin (solid MIC = 0.024 µg/mL), 8.3x MIC kanamycin (solid MIC = 6 µg/mL), 20x MIC mitomycin C (solid = 2 µg/mL), 23x MIC streptomycin (solid MIC = 14 µg/mL), and 8.6x MIC tetracycline (solid MIC = 1.16 µg/mL). Each point represents the frequency of antibiotic resistance of one QIAR experimental condition (0x, 0.25x MIC, 0.5x MIC or 1x MIC).

E. coli MG1655 was also incubated with low levels of chloramphenicol to test if the cells acquired resistance to other antibiotics (i.e., not ribosome-targeting antibiotics). I obtained chloramphenicol-, kanamycin-, and tetracycline-resistant colonies, but not ciprofloxacin- or ampicillin-resistant colonies after the chloramphenicol treatment (**Figure 5.5**). As chloramphenicol, kanamycin and tetracycline have the same cellular target, the bacterial ribosome, these results suggested that chloramphenicol promoted resistance to similar antibiotics but not to antibiotics that had a different target. This is different from the effect of quinolones, as they promoted resistance to a wide range of antibiotics.
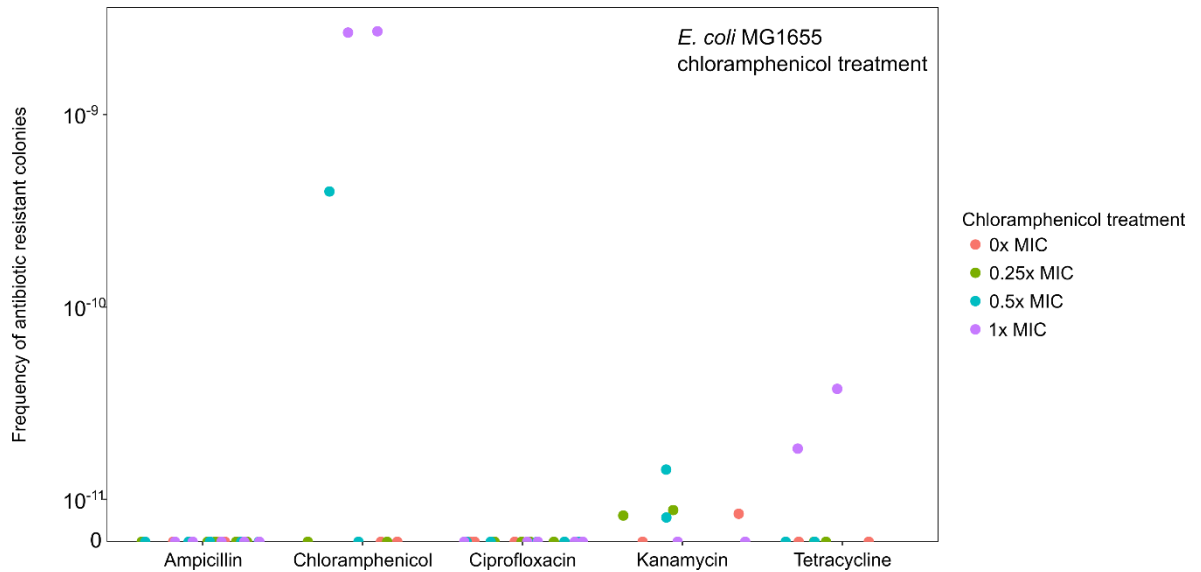
Figure 5.5. Frequency of antibiotic resistant colonies after exposure of *E. coli* MG1655 cells to different doses of chloramphenicol. *E. coli* MG1655 was grown without or with 0.25x, 0.5x or 1x MIC of chloramphenicol (broth MIC = 4 µg/mL) for 24 h at 37°C, then plated on plates supplemented with 8.3x MIC ampicillin (solid MIC = 6 µg/mL), 8x MIC chloramphenicol (solid MIC = 4 µg/mL), 14.6x MIC ciprofloxacin (solid MIC = 0.024 µg/mL), 8.3x MIC kanamycin (solid MIC = 6 µg/mL), and 8.6x MIC tetracycline (solid MIC = 1.16 µg/mL). Each point represents the frequency of antibiotic resistance of one QIAR experimental condition (0x, 0.25x MIC, 0.5x MIC or 1x MIC).

Taken together, the results from the QIAR assays indicated that quinolones (but not chloramphenicol) promoted resistance to unrelated antibiotics such as ampicillin, chloramphenicol, and trimethoprim in *E. coli* cells. Interestingly, mitomycin C, which is not a topoisomerase inhibitor, also promoted resistance to unrelated antibiotics like chloramphenicol and ciprofloxacin. From these results, I focused on studying ciprofloxacin-induced chloramphenicol resistance.

5.2.2 Ciprofloxacin-induced chloramphenicol-resistant colonies appear after 4 hours of being exposed to ciprofloxacin

In the previous section I found that low levels of ciprofloxacin induced resistance to several antibiotics such as chloramphenicol. To investigate the time *E. coli* cells take to acquire chloramphenicol resistance (Cam^R) while being exposed to low levels of ciprofloxacin, I performed a time course experiment in which I exposed cells to 0, 0.25x MIC, 0.5x MIC, 1X MIC of ciprofloxacin for 1, 3, 4, 5, 8 or 24 hours. I measured the frequency of chloramphenicol-resistant colonies under those conditions, and I found out

that most of the chloramphenicol-resistant colonies appeared after 4 hours (**Table 5.3**). These results indicated that most of the chloramphenicol-resistant colonies were not resistant to chloramphenicol before the incubation with ciprofloxacin, suggesting that this quinolone was able to induce them and not just to select for pre-existing resistant colonies.

Table 5.3. Frequency of chloramphenicol-resistant colonies exposed to low levels of ciprofloxacin over a time course. For each replicate, one *E. coli* MG1655 colony was grown in the presence or absence of ciprofloxacin (MIC = 0.027 µg/mL) for 1, 3, 4, 5, 8 and/or 24 h. The frequency of chloramphenicol-resistant colonies was calculated as the number of resistant colonies divided by the total number of colonies plated. Red squares indicate cultures with no chloramphenicol-resistant colonies, yellow and green squares show cultures with chloramphenicol-resistant colonies.

Replicate	Ciprofloxacin treatment	Frequency of chloramphenicol-resistant colonies					
		+ 1 h	+ 3 h	+ 4 h	+ 5 h	+ 8 h	+ 24 h
1	0	0E+00		0E+00			
	0.25x MIC	0E+00		7E-11			
	0.5x MIC	0E+00		9E-10			
	1x MIC	0E+00					
2	0	0E+00		0E+00		0E+00	
	0.25x MIC	0E+00		0E+00		0E+00	
	0.5x MIC	2E-09		0E+00		9E-10	
	1x MIC	8E-09		0E+00		6E-08	
3	0	0E+00		0E+00		0E+00	
	0.25x MIC	0E+00					
	0.5x MIC	0E+00					
	1x MIC	0E+00					
4	0	0E+00		0E+00		0E+00	
	0.25x MIC	0E+00					
	0.5x MIC	0E+00					
	1x MIC	0E+00					
5	0	0E+00	0E+00	0E+00	0E+00	0E+00	8E-12
	0.25x MIC	0E+00	0E+00	1E-10	0E+00	0E+00	6E-11
	0.5x MIC	0E+00	0E+00	0E+00			5E-09
6	0	0E+00	0E+00	0E+00	0E+00		0E+00
	0.25x MIC	0E+00	0E+00	0E+00	0E+00		0E+00
	0.5x MIC	0E+00	0E+00	0E+00	0E+00		0E+00
7	0	0E+00	0E+00	0E+00	0E+00	0E+00	0E+00
	0.25x	0E+00	0E+00	0E+00	4E-12	4E-12	5E-12
	0.5x	0E+00	0E+00	0E+00		ND	5E-10
8	0	0E+00	0E+00	0E+00		0E+00	0E+00
	0.25x	0E+00	0E+00	2E-11		0E+00	3E-12
	0.5x	0E+00	0E+00			8E-09	0E+00

9	0	0E+00	0E+00	0E+00	0E+00	0E+00	0E+00
	0.25x	0E+00	0E+00	0E+00	1E-11	5E-12	0E+00
	0.5x	0E+00	0E+00			2E-09	

5.2.3 Ciprofloxacin-induced chloramphenicol-resistant colonies remained resistant to chloramphenicol over generations and some of them were resistant to several drugs

To test if ciprofloxacin-induced Cam^R was inheritable and if they were resistant to other drugs, I randomly picked 27 chloramphenicol-resistant colonies obtained from the QIAR assays and incubated them without selection (in LB only) for 2 days. The cultures were then streaked onto a plate with the antibiotic the original colony was identified on (8x MIC of chloramphenicol), as well as on plates with ampicillin, ciprofloxacin, kanamycin, rifampin, streptomycin, triclosan and trimethoprim. As a control, I plated colonies from those QIAR experiments that had been exposed to ciprofloxacin but that had not acquired Cam^R. Out of the 27 chloramphenicol-resistant colonies, 25 remained resistant to chloramphenicol (13 had a chloramphenicol MIC < 16 µg/mL and 12 had a chloramphenicol MIC ≥ 16 µg/mL). This result indicated that in most of the cases the resistance was heritable and not due to tolerance or persistence to the drug and that the level of acquired Cam^R differed between colonies. In terms of multidrug resistance, 6/25 of chloramphenicol-resistant colonies were resistant to another drug apart from chloramphenicol, and 2/25 were resistant to 3 drugs apart from chloramphenicol. This result suggested that some colonies were likely to have mutations affecting multidrug resistance.

5.2.4 Cam^R mutations were dependent on the SOS response, and independent of the SOS-activated polymerases or nucleases involved in the repair of quinolone-induced DNA damage

So far, I have shown that low levels of ciprofloxacin induced Cam^R. However, I do not know how the cells acquire such resistance. One possibility is that the DNA damage caused by quinolones activates the SOS response which then stimulates the transcription of polymerases. The SOS-activated polymerases are Pol II (*polB*), Pol IV (*dinB*) and Pol V (*umuDC*) and are known to introduce mutations during the repair of the DNA. If these mutations affect genes involved in antibiotic resistance, they can be the ultimate cause of QIAR. Thus, I hypothesised that the SOS response and the SOS-activated polymerases

were responsible for the acquisition of ciprofloxacin-induced Cam^R. To test this hypothesis, I measured the frequency of chloramphenicol-resistant colonies in mutants that were not able to activate the SOS response or that they lacked the SOS-activated polymerases. To do this I used an experimental method called mutation frequency assay (MFA).

5.2.4.1   The mutation frequency assay (MFA)

The MFA is an assay to measure the frequency of several independent chloramphenicol-resistant colonies grown in the presence or absence of a drug. This experiment is very similar to the QIAR assay; however, it has the advantage that it tests 10 independent colonies per assay instead of testing one (**Figure 5.6**). Because the QIAR phenomenon happens at very low frequencies, it is important to study the phenomenon in as many independent colonies as possible.
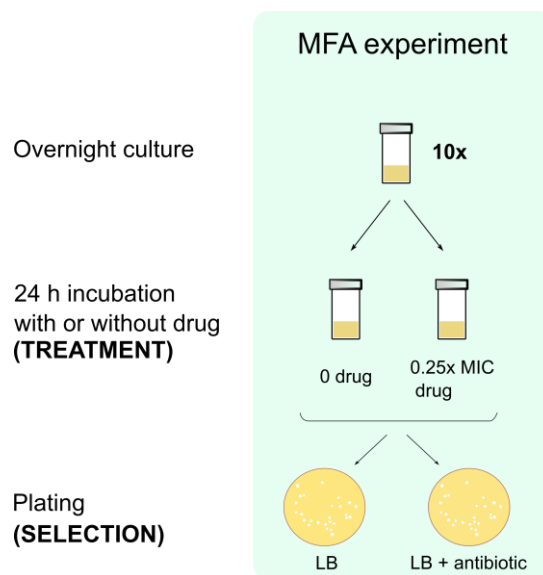
Figure 5.6. Scheme of the mutation frequency assay (MFA). Ten independent colonies are grown overnight and then split into two tubes with two different treatments: in one tube cells are grown without a drug, in a second tube cells are grown with 0.25x MIC of a drug. The cultures are incubated at 37°C for 24 hours and then plated on LB plates supplemented with antibiotics to select for antibiotic resistance. Dilutions of the cultures are plated on LB-only plates to count the number of colonies plated. The frequency of resistant colonies is then calculated by dividing the number of resistant colonies by the total number of colonies plated.

As with the QIAR assay, the MFA assay has four variables:

   a) The *E. coli* strain

I used the *E. coli* MG155 WT strain and several MG1655 mutants that were deficient in the SOS response or that lacked SOS-response activated polymerases or the nucleases Exo VII or SbcCD. In terms of the mutants of the SOS response, I used a mutant without *recA* (that could not activate the SOS response) and a mutant with a point mutation in *lexA* (*lexA*(S119A)) which also blocked the activation of the SOS response. The *recA⁻* strain was obtained from Susan Rosenberg (**Table 2.1**). I constructed the *lexA*(S119A) strain (see 2.2.2.10) and deleted the three SOS-activated polymerases (*dinB, polB* and *umuD*) and the nucleases *xseA* and *sbcCD* in MG1655 cells. To confirm that the deletions were correct and that they did not affect other parts of the genome, the whole genome of the *lexA*(S119A) and the *dinB*, *polB* and *umuD* mutants was sequenced.

Once I had all the strains, I measured their MICs for ciprofloxacin and chloramphenicol (**Table 5.4**). The deletion of the SOS-activated polymerases did not affect the sensitivity of the strains to ciprofloxacin, whereas the *recA* mutant was more sensitive than the WT strain. These results were consistent with the MICs from Cirz et al. [56]. However, my *lexA* mutant was more sensitive to quinolones than the WT strain and Cirz et al. [56] claimed that it had the same MIC as the WT strain. Cirz et al. [56] only checked that their *lexA* mutant had the S119A mutation in *lexA* and that *lexA* was followed by a Kan[R] cassette. As I analysed the whole genome sequence of my *lexA* mutant, and the only mutations I could find were the *lexA*(S119A) mutation and the Kan[R] cassette after *lexA*, I was confident that my *lexA*(S119A) mutant and, consequently, the ciprofloxacin MIC were correct.

Table 5.4. Ciprofloxacin and chloramphenicol MICs of SOS response and nuclease mutants. The MICs were calculated as the average of three replicates using the solid or the broth method and compared to the MICs found in Cirz et al. [56].

E. coli MG1655 strain	Broth MIC ciprofloxacin (µg/mL)	Solid MIC chloramphenicol (µg/mL)	Cirz et al. [56] MIC ciprofloxacin (µg/mL)
WT	0.027	4	0.035
recA::Kan[R]	0.006	4	0.005
lexA(S119A) Kan[R]	0.008	4	0.030
Δ*dinB*	0.032	4	0.035
Δ*polB*	0.032	4	0.030
Δ*umuD*	0.021	4	0.035
Δ*dinB* Δ*polB*	0.032	4	0.030
Δ*dinB* Δ*umuD*	0.021	4	0.030
Δ*polB* Δ*umuD*	0.032	4	0.035
Δ*dinB* Δ*polB* Δ*umuD*	0.032	4	0.030
Δ*xseA*	0.008	4	-
Δ*sbcCD*	0.027	4	-

b) The antibiotics used in the treatment

I used ciprofloxacin or mitomycin C. I chose ciprofloxacin because it is one of the most used quinolones and because I had used it in the QIAR assay. I chose mitomycin C because it is a potent inducer of the SOS response.

c) The antibiotics used in the selection

I selected on high levels of chloramphenicol as I wanted to study the acquisition of Cam^R.

d) The concentration of the antibiotics

For the treatment, I used no drugs or 0.25x MIC of ciprofloxacin or mitomycin C. For the selection I used 8x MIC of chloramphenicol (**Table 5.5**).

Table 5.5. MIC doses of the antibiotics used in the mutation frequency assay (MFA).

Antibiotic used in treatment	Broth MIC (µg/mL)	MIC dose
Ciprofloxacin	0.027	0, 0.25x
Mitomycin C	1.5	0, 0.25x
Antibiotic used in selection	**Solid MIC (µg/mL)**	**MIC dose**
Chloramphenicol	4	8x

5.2.4.2 Results of the MFA assay

To understand if the SOS response was involved in the acquisition of antibiotic resistance after exposure to quinolones, I measured the frequency of chloramphenicol-resistant colonies after ciprofloxacin exposure using different strains and conditions. I found that exposing WT cells to ciprofloxacin or the SOS-inducer mitomycin C led to the acquisition of Cam^R (**Figure 5.7**). However, when I exposed cells without the SOS response activator RecA (*recA*::Kan^R), or with a mutation in the SOS response repressor LexA (*lexA*(S119A) Kan^R) to ciprofloxacin, the frequency of chloramphenicol-resistant colonies was zero. These results indicated that the activation of the SOS response was responsible for the acquisition of Cam^R after ciprofloxacin exposure.

I also investigated if the error prone polymerases (*dinB*, *polB* and *umuDC*) were responsible for the acquisition of ciprofloxacin-induced Cam^R. I found no differences between the frequency of chloramphenicol-resistant colonies in WT cells and error-prone polymerase mutants, suggesting that the error-prone polymerases were not responsible for the acquisition of ciprofloxacin-induced Cam^R.
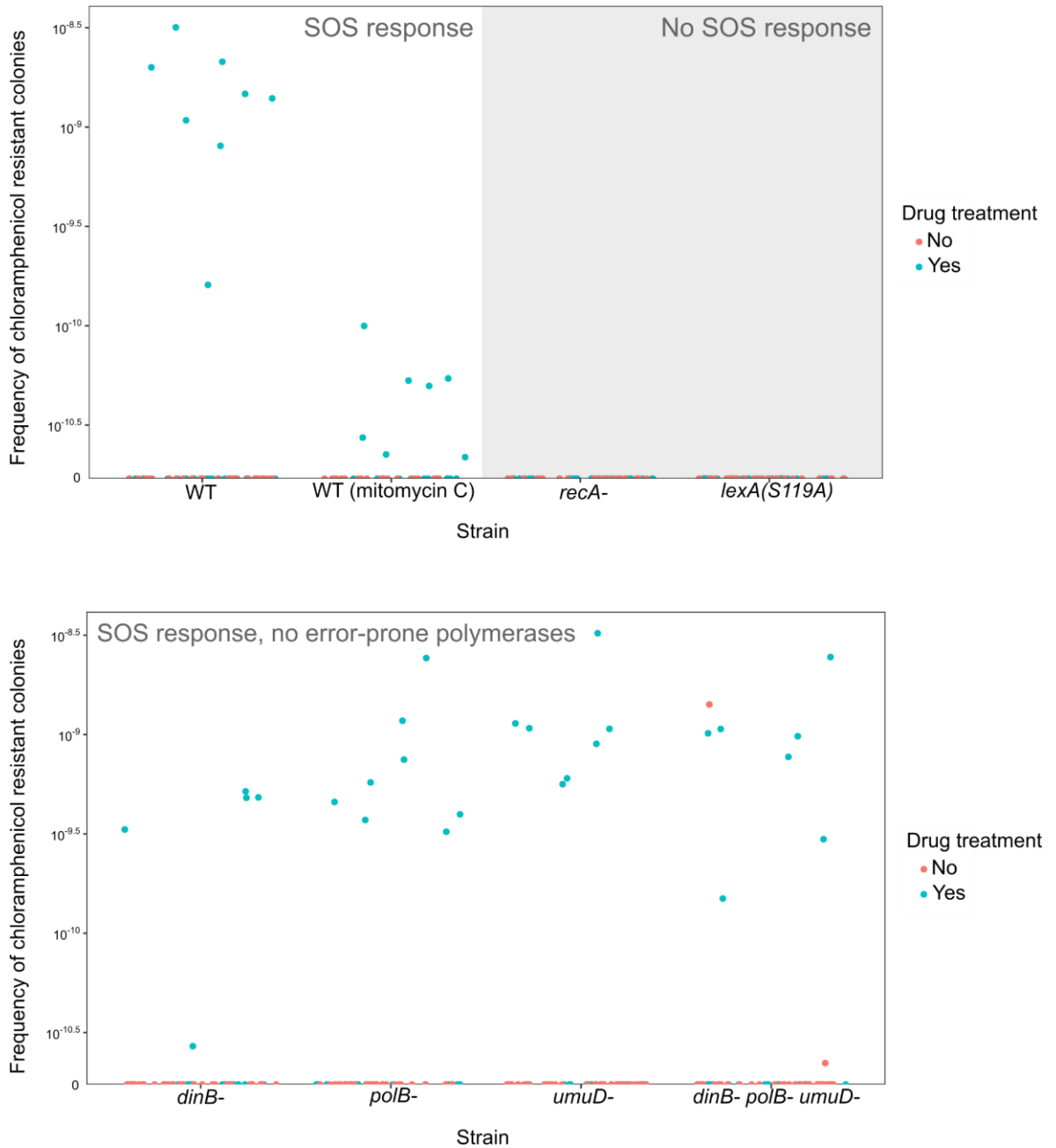
Figure 5.7. Frequency of chloramphenicol-resistant colonies of SOS response mutants that were incubated with and without low levels of ciprofloxacin. *E. coli* MG1655 WT, mutants that were not able to activate the SOS response (*recA*⁻ and *lexA*(S119A)) and mutants that did not have the SOS-activated polymerases (*dinB*⁻, *polB*⁻, *umuD*⁻, and *dinB*⁻ *polB*⁻ *umuD*⁻) were grown in the presence or absence of 0.25x MIC of ciprofloxacin (or 0.25x MIC mitomycin C if stated). For each strain, 3 MFAs were performed (30 independent colonies were tested in total).

The involvement of the SOS response in QIAR suggests that the quinolone-induced DNA damage might be the root of QIAR phenomenon. If this is the case, proteins that are

involved in the repair of quinolone-induced DNA damage might be able to modulate this. As shown in Chapter 4, the nucleases Exonuclease VII (Exo VII) and SbcCD have been proposed as the proteins that can remove trapped topoisomerase from the DNA. If the removal of the topoisomerase exposes the double-strand break (DSB), and this DSB activates the SOS response, then the absence of these proteins would cause a decrease in the DSBs and less DNA damage, and therefore, the SOS would not be activated, and colonies would not acquire Cam^R. Thus, I hypothesised that the absence of Exo VII or SbcCD would inhibit the acquisition of Cam^R. To test this, I measured the frequency of chloramphenicol-resistant colonies that appeared in *sbcCD*$^-$ or *xseA*$^-$ cells after exposure to low levels of ciprofloxacin (**Figure 5.8**). I found chloramphenicol-resistant colonies after the ciprofloxacin treatment in both strains although at much lower frequencies than the WT cells, suggesting that Exo VII and SbcCD were not essential for the acquisition of Cam^R but may be involved.
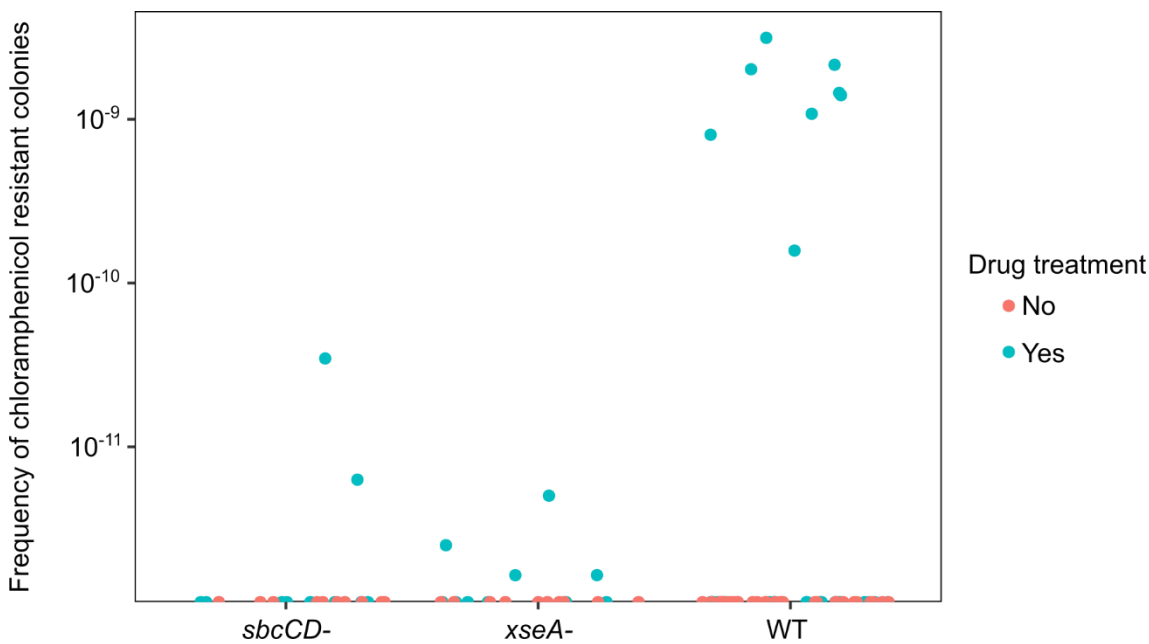
Figure 5.8. Frequency of chloramphenicol-resistant colonies of WT cells and *sbcCD* and *xseA* mutants that were incubated with and without low levels of ciprofloxacin. *E. coli* MG1655 WT, Δ*sbcCD* and Δ*xseA* cells were grown in the presence or absence of 0.25x MIC of ciprofloxacin. For the WT strain, 3 MFAs were performed (30 independent colonies were tested in total) whereas for the mutant strains, 1 MFA was performed (10 independent colonies were tested in total).

5.2.5 Ciprofloxacin-induced chloramphenicol-resistant colonies have few but diverse mutations

To better understand the QIAR phenomenon, I investigated the genomes of eight ciprofloxacin-induced chloramphenicol-resistant colonies. My hypothesis was that the chloramphenicol-resistant colonies acquired mutations while being exposed to ciprofloxacin and that those mutations caused the Cam^R phenotype. To test this, I analysed the whole genome of colonies that had been exposed to ciprofloxacin and that had or had not acquired Cam^R (I called them _CamR or _noCamR, respectively). Also, to test if there were any obvious differences between the mutations found in WT or SOS-activated polymerase mutants, I analysed the sequences of colonies from different backgrounds (WT, dinB or dpu cells). Finally, I studied the mutations in colonies that had been exposed to mitomycin C instead of ciprofloxacin. **Figure 5.9** shows a scheme of the source of the 14 samples that were sent for whole genome sequencing.

To analyse the genome of each sample, first I trimmed the reads of the samples that still had the adapters, and I then checked the quality of all the reads. Each sample had an average read length of 150-200 base pairs, a GC content of ~50% and 0.3-1 million of reads. The quality of the reads as shown by FastQC mean quality score was good for all the reads. Next, I looked for SNPs, indels, deletions or amplifications. To find SNPs and indels, I ran the software SNIPPY. To find deletions and amplifications, I first aligned the reads to the reference *E. coli* genome, and I then looked for regions with low or high coverage, to find potential deletions and amplifications, respectively. All the potential SNPs, indels, deletions and amplification were double-checked by visualising the alignments on IGV. This way, I was able to distinguish clear mutations from dubious ones. Once I had a list with all the mutations (Appendix III, **Table II**), I pinpointed the ones that were only present in the chloramphenicol-resistant colonies. Interestingly, there were only four loci with mutations in them: *marR*, e14, *icd* and *mdfA* (**Table 5.6**). *marR* encodes a repressor of the *marRAB* operon that controls genes involved in antibiotic resistance. e14 is a prophage that encodes genes with potential roles in stress responses. *icd* encodes an enzyme that plays an important role in energy metabolism. Finally, *mdfA* encodes a multidrug efflux pump.
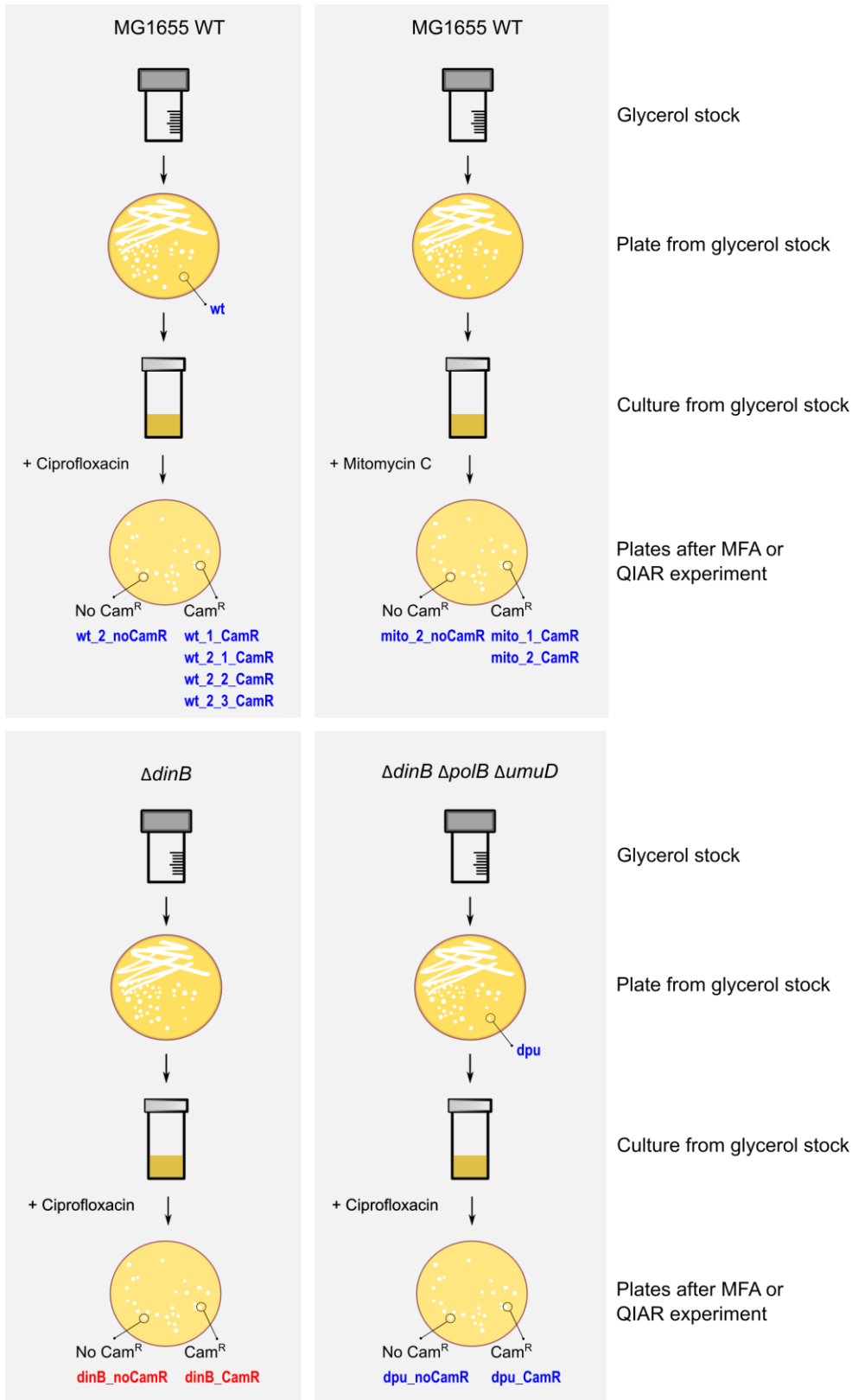
Figure 5.9. Scheme of strains sent for whole genome sequencing. In blue are all the 12 strains sent for Illumina sequencing. In red are the 2 strains that were sent for both Illumina and Nanopore sequencing. The samples belonged to different *E. coli* MG1655 backgrounds: WT, Δ*dinB* and Δ*dinB* Δ*polB* Δ*umuD*. From the WT background, I sent the

parental strain [110], strains that were exposed to low levels of ciprofloxacin or mitomycin C but did not acquire Cam[R] (e.g., wt_2_noCamR), and strains that were exposed to low levels of ciprofloxacin or mitomycin C and that acquired Cam[R] (e.g., wt_2_CamR). From the Δ*dinB* background I sent a strain that was exposed to low levels of ciprofloxacin but did not acquire Cam[R] (dinB_noCamR) and a strain that was exposed to low levels of ciprofloxacin and acquired Cam[R] (dinB_CamR). From the Δ*dinB* Δ*polB* Δ*umuD* background I sent the parental strain (dpu), a strain that was exposed to low levels of ciprofloxacin but did not acquire Cam[R] (dpu_noCamR) and a strain that was exposed to low levels of ciprofloxacin and acquired Cam[R] (dpu_CamR).

Table 5.6. Distinctive mutations of the chloramphenicol-resistant strains. The whole genomes of ciprofloxacin-induced chloramphenicol-resistant colonies were compared against the genomes of ciprofloxacin-treated not chloramphenicol-resistant colonies and parental strains to find SNPs, indels or amplifications that were specific for each chloramphenicol-resistant strain.

Samples	Mutations in *icd*	Mutations in e14	Mutations in *marR*	Mutations in *mdfA*
wt_1_CamR	-	-	Indel	-
wt_2_1_CamR	-	-	-	-
wt_2_2_CamR	SNPs	Deletion	-	-
wt_2_3_CamR	SNPs	Deletion	-	Amplification
mito_1_CamR	SNPs	Deletion	-	Amplification
mito_2_CamR	SNPs and indel	Deletion	Indel	Amplification
dinB_CamR	-	-	Deletion	Amplification
dpu_CamR	-	-	-	Amplification

The amplification of *mdfA* was found in several _CamR samples as well as in the dinB_noCamR sample. Despite being present in a non-Cam[R] sample, I have included the amplification of *mdfA* in the list of Cam[R] mutations because it is likely that *mdfA* was more amplified in the _CamR samples than in the dinB_noCamR sample. This is because I observed a 10x increase in the coverage of the *mdfA* region in the dinB_CamR strain compared to the dinB_noCamR strain (**Figure 5.10**).
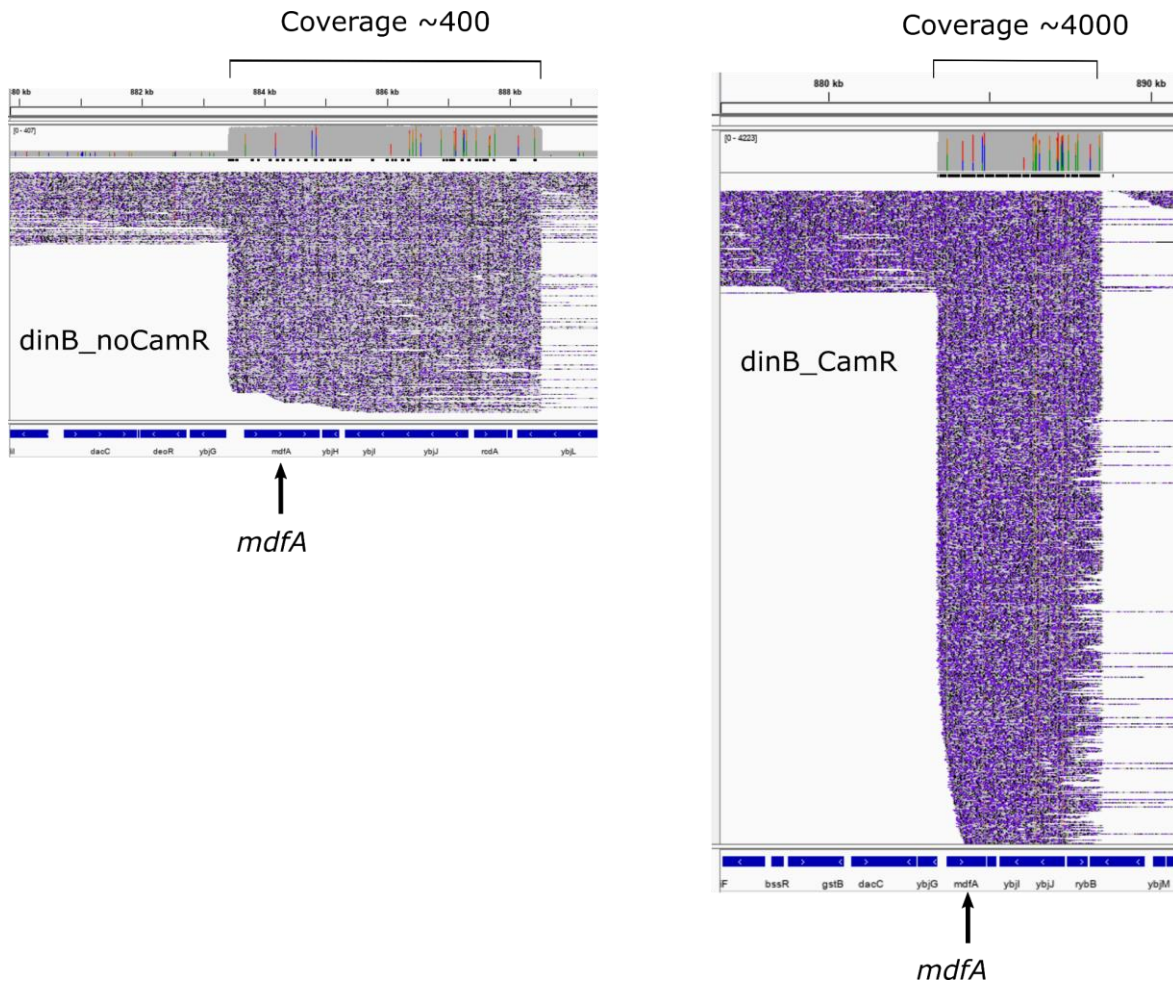
Figure 5.10. Visualisation of the *mdfA* amplification in dinB_noCamR and dinB_CamR samples. Nanopore reads from the dinB_noCamR or the dinB_CamR samples were aligned against the *E. coli* reference genome and visualised on IGV.

I also tested if the strains that I sent for sequencing were resistant to chloramphenicol and/other antibiotics. I found that all chloramphenicol-resistant strains remained resistant to chloramphenicol, although the level of resistance varied (**Table 5.7**). Interestingly, all the chloramphenicol-resistant strains that had mutations in *marR* were also resistant to at least 3 other antibiotics.

Collectively, the results from the analysis of the genomes and the antibiotic resistance profile of the ciprofloxacin-induced chloramphenicol-resistant strains, showed that chloramphenicol-resistant strains had few but diverse mutations compared to the no_CamR or the parental strains. Also, SNPs and indels occurred in the WT strains, but not in the strains lacking SOS-induced polymerases, and deletions and amplifications occurred in all backgrounds. There were no obvious differences between the mutations found after ciprofloxacin or mitomycin C treatment. Finally, some of the chloramphenicol-

resistant strains were multidrug resistant, as it happened with other chloramphenicol-resistant strains colonies from QIAR assays tested in section 5.2.3.

Table 5.7. Chloramphenicol (Cam) MIC, multidrug resistance, and presence of key mutations in the samples sent for whole genome sequencing.

Sample	Cam MIC (µg/mL)	Multidrug resistance (>3 drugs)	Mutations in *marR*	Excision of e14	Amplification of *mdfA*
wt_1_CamR	32	Y	Y	N	N
wt_2_1_CamR	16	N	N	N	N
wt_2_2_CamR	8-16	N	N	Y	N
wt_2_3_CamR	>32	N	N	Y	Y
mito_1_CamR	>32	N	N	Y	Y
mito_2_CamR	32	Y	Y	Y	Y
dinB_CamR	>32	Y	Y	N	Y
dpu_CamR	32	N	N	N	Y

5.2.5.1 A *marR* deletion causes Cam[R]

Following the analysis of the genomes of the ciprofloxacin-induced chloramphenicol-resistant strains, I tested if the mutations in *marR* caused Cam[R]. Because MarR represses a transcriptional regulator involved in antibiotic resistance and mutations in *marR* are known to cause an increase in Cam[R] [181], I expected to see an increase in Cam[R] in the absence of *marR*. Thus, I tested if the absence of *marR* or part of *marR* (as in the dinB_CamR sample) changed the MIC to chloramphenicol. To do this, I built two mutants in *E. coli* MG1655: a mutant without the whole open reading frame of *marR* (Δ*marR*) and another mutant that had a partial deletion of *marR* starting from the nucleotide 170 of *marR* (*marR170*) as it happened in the dinB_CamR sample (Appendix III, **Table II**).

I observed that the deletion of *marR* did not change the chloramphenicol MIC whereas the partial *marR* deletion mutant (*marR170*) had an 8 times higher chloramphenicol MIC (**Figure 5.11**). These results showed that mutations in *marR* could confer Cam[R].

A)

B)

C)
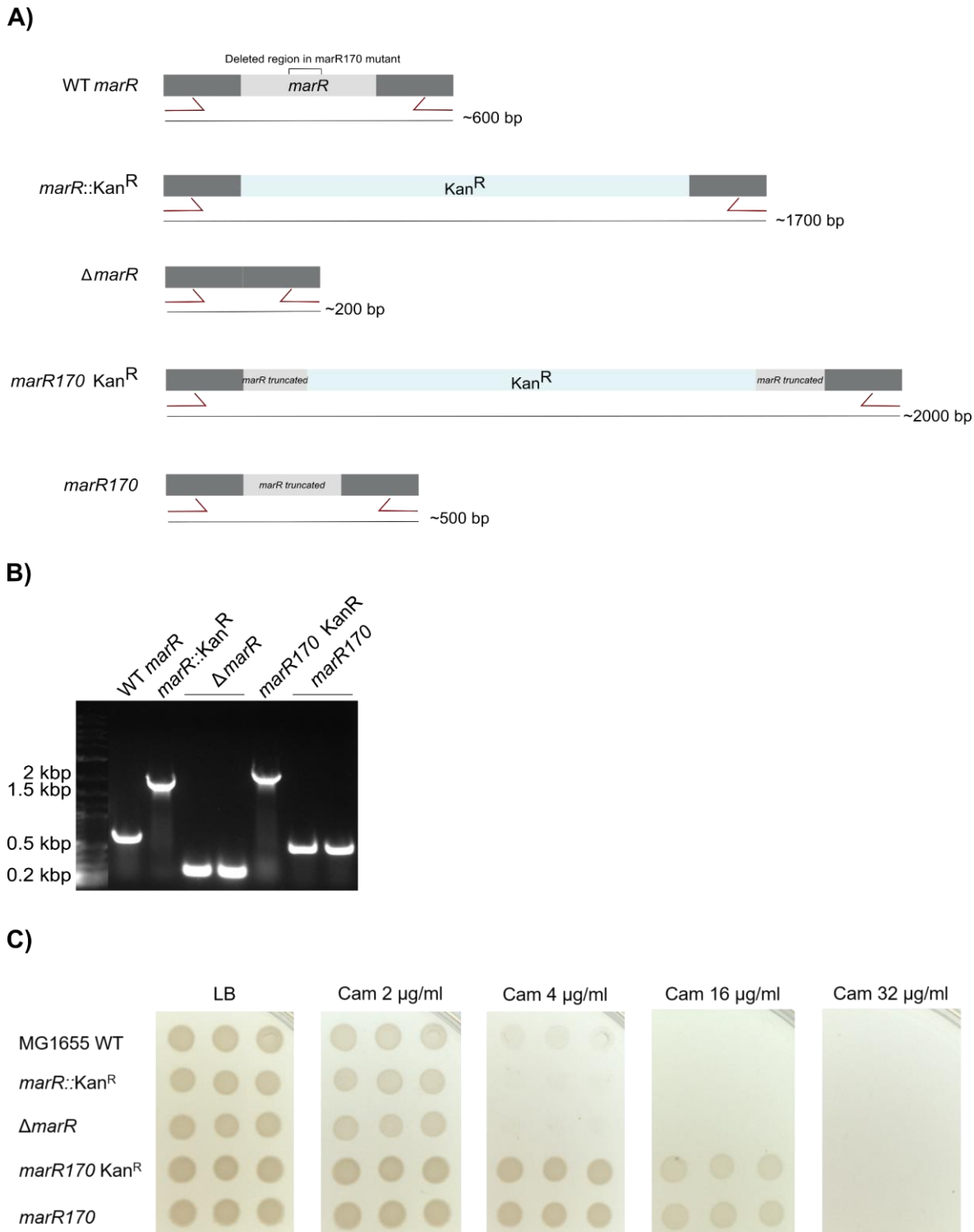
Figure 5.11. Scheme of a partial deletion in *marR* (*marR170*) and the chloramphenicol (Cam) MIC of *marR* mutants. A) Diagrams of the *marR* mutants. *marR* has 435 base pairs and it coordinates in *E. coli* MG1655 are 1,619,120-1,619,554. *mar170* is a truncated version of *marR* that has a 157 base pair deletion starting from the base pair 170. To delete *marR* or *marR170*, a kanamycin resistance (Kan^R) cassette was inserted to replace *marR* or the deleted region in *marR170*. The Kan^R cassette was then

removed to create the Δ*marR*, and *marR170* mutants. The arrows represent the position of the primers used to confirm the mutations. B) Agarose gel showing the PCR products to confirm the *marR* mutations. The PCR products were amplified using primers that were upstream and downstream *marR* (red arrows shown in A). C) Chloramphenicol (Cam) MIC of the *marR* mutants.

5.2.5.2 The deletion of e14 makes cells more sensitive to chloramphenicol

Another common mutation found in the ciprofloxacin-induced chloramphenicol-resistant strains was the deletion of e14. This is a cryptic prophage whose role in *E. coli* is unknown, although it is believed to participate in resistance to environmental stresses [182]. The prophage e14 contains 21 putative genes, some of which (e.g., cell division inhibitor genes *ymfL*/M or cell death peptidase Lit) might have a role in such stress resistance [182, 183].

Because I observed the loss of e14 in several ciprofloxacin-induced chloramphenicol-resistant mutants and e14 might be involved in resistance to stress, I hypothesised that the loss of e14 would cause an increase in Cam^R in *E. coli* MG1655. To test this, I tried to delete the whole e14 (~14 kbp) or smaller portions of it (3-4 kbp) using double-stranded DNA recombineering. But unfortunately I failed (probably because the regions to delete were too big). An alternative strategy was to delete individual genes within e14. Out of the 21 putative genes in e14, 3 of them (cell death peptidase *lit* and putative cell division inhibitor *ymfL/M*) seemed more likely to be involved in stress resistance. Hence, I deleted those genes in *E. coli* MG1655 to test whether they were involved in Cam^R. I also tested an *E. coli* BW25113 strain without e14 obtained from the National Collection of Type Cultures.

I found that the deletion of *lit* or *ymfL/M* did not affect the sensitivity to chloramphenicol, indicating that these genes might not have a role in antibiotic resistance (**Figure 5.12**). To my surprise, the deletion of e14 in BW25113 made cells more sensitive to chloramphenicol, which was the opposite of what I expected.

A)

B)
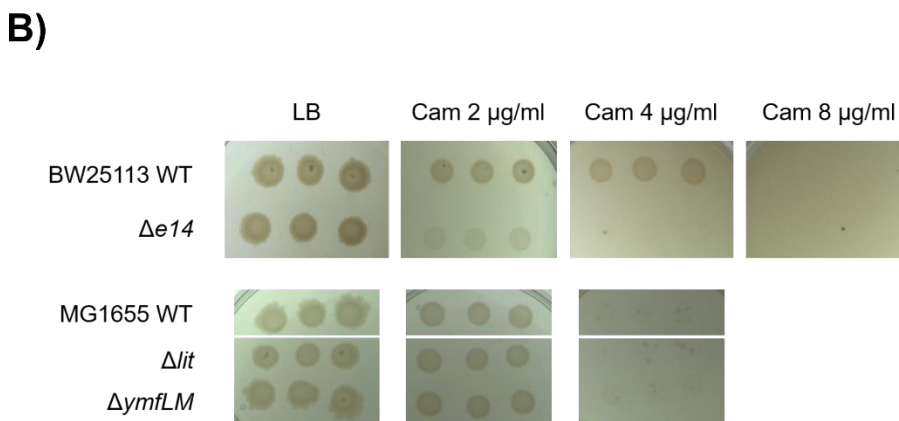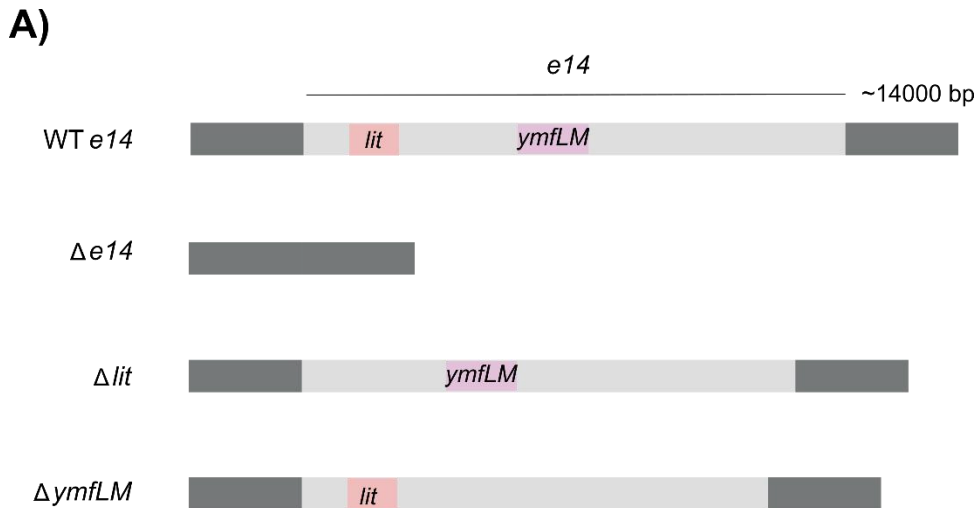
Figure 5.12. Effect of the deletion of e14 in chloramphenicol resistance. A) e14 constructs used in the MIC experiments. e14 has ~14 kbp and comprises several genes like *lit* or *ymfL/M*. B) Chloramphenicol (Cam) MIC of e14 mutants.

5.3   Discussion

5.3.1   Ciprofloxacin-induced antibiotic resistance

In this chapter I showed that ciprofloxacin was able to induce resistance to chloramphenicol, ampicillin, ciprofloxacin, and trimethoprim in *E. coli* cells. Other groups have observed ciprofloxacin-induced ampicillin [77] or ciprofloxacin resistance [184] but to the best of my knowledge, ciprofloxacin-induced chloramphenicol or trimethoprim resistance has only been shown here and in Natassja Bush's thesis [55]. I focused on understanding ciprofloxacin-induced Cam^R and found that the chloramphenicol-resistant mutants were likely induced and not selected by ciprofloxacin because i) they only

acquired resistance in the presence of ciprofloxacin, ii) chloramphenicol-resistant mutants appeared after being exposed to ciprofloxacin for 4 hours and iii) chloramphenicol does not seem to have a mutagenic effect [107] which suggests that the selection on chloramphenicol plates did not cause the mutations.

5.3.2 Is the SOS response involved in ciprofloxacin-induced Cam^R?

The SOS response is the bacterial response to DNA damage, and it is regulated by RecA and LexA [100]. During normal growth, the SOS genes are negatively regulated by the repressor LexA. Activation of the SOS genes occurs after DNA damage when RecA interacts with LexA to facilitate the self-cleavage of LexA. The autocatalytic proteolysis of LexA results in the derepression of the SOS regulon that controls the expression of genes including the ones that encode error-prone polymerases that can make mutations. I have tested the role of the SOS response in quinolone-induced antibiotic resistance by using two strategies. First, I have used a $\Delta recA$ and *lexA*(S199A) strain that are not able to activate the SOS response. Secondly, I have used mitomycin C treatment instead of ciprofloxacin with the WT strain. Mitomycin C is an intercalator of the DNA and a potent inducer of the SOS response. No $\Delta recA$ or *lexA*(S119A) cells became Cam^R, whereas the WT cells did become chloramphenicol-resistant after treatment with mitomycin C or ciprofloxacin. The main limitation of these experiments was that $\Delta recA$ and *lexA*(S119A) cells are ~4 times more sensitive to ciprofloxacin than the WT, and therefore I have used 1/4 of the amount of ciprofloxacin I used with the WT. Still, it is very likely that SOS response is responsible for the acquisition of Cam^R, as I have not seen any chloramphenicol-resistant strain after incubating 30 independent cultures with low levels of ciprofloxacin, and the mitomycin C treatment also led to the acquisition of Cam^R.

5.3.3 What mutations caused Cam^R?

The analysis of the genomes of ciprofloxacin-induced chloramphenicol-resistant mutants showed that cells had mutations in *marR*, *icd*, e14, and/or *mdfA*.

MarR is the transcriptional repressor of the *marRAB* operon and affects the transcription of antibiotic resistance genes like efflux pumps (**Figure 5.13**). I found that the deletion of the whole *marR* open reading frame did not change the MIC of chloramphenicol. This result was slightly different to the result of Ruiz et al. [185] and Suzuki et al. [186] who found that the deletion of *marR* caused an increase of 1.23 or 2 times the MIC for chloramphenicol (**Table 5.8**) and it might be due the fact that *marR* and *marA* share the

same operon, and by deleting the whole *marR,* it disturbed the way the operon works. I then checked the chloramphenicol MIC of a mutant that had a partial deletion of *marR* (*marR170*). This mutant had the same mutation in *marR* as the one found in a ciprofloxacin-induced chloramphenicol-resistant mutant (dinB_CamR). This time, the chloramphenicol MIC of the *marR170* mutant was 8x higher than the WT (similar results have been found in other strains with point mutations in *marR* (**Table 5.8**)). This result indicates that mutations in *marR* are likely to cause an increase in Cam^R.
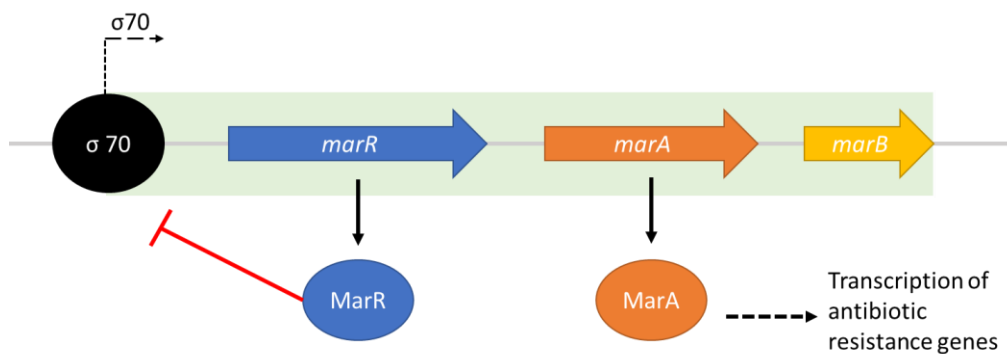
Figure 5.13. The *marRAB* operon in *E. coli*. MarR binds the *marRAB* promoter and negatively regulates the expression of the operon genes. In the presence of inducers such as salicylate and other phenolic compounds, MarR cannot bind DNA anymore, and thus MarA is expressed. MarA is a transcriptional regulator of genes that encode, for example, efflux pumps which are involved in antibiotic resistance.

Table 5.8. Comparison of the chloramphenicol (Cam) MIC of different *marR* mutants found in the literature with their WT.

Mutant	Strain	Cam MIC (µg/mL) mutant / WT	Source
Δ*marR*	BW25113	2.2	[185]
Δ*marR*	MDS42	1.23	[186]
Δ*A1821* (point mutation)	ATCC 25922	8	[181]
MarR1 (point mutation)	AG100	5.25	[187]
MarR1 (point mutation)	AG100	2	[188]
G to A in 3rd position of start codon GTG	MG1655	2	[105]

Another common mutation in the ciprofloxacin-induced chloramphenicol-resistant mutants was the deletion of the cryptic prophage e14. The role of e14 in antibiotic resistance is uncertain; however, Wang et al. [182] found that cells without e14 were more sensitive to nalidixic acid and I have seen that the same cells are more sensitive to chloramphenicol.

Thus, it seems that the excision of e14 does not help cells to cope with antibiotics. On the other hand, cells without e14 are more resistant to oxidative damage [182]. Since quinolones cause oxidative stress, the excision of e14 might help cells to cope with the ciprofloxacin treatment rather than having a role in the acquisition of Cam^R.

The ciprofloxacin-induced chloramphenicol-resistant colonies also had mutations in *icd* that encodes for the isocitrate dehydrogenase. Icd is an enzyme that participates in the tricarboxylic acid cycle. Mutations in *icd* have been associated with antibiotic resistance [189]. However, because the e14 prophage maps at the *icd* site and supplies the C-terminal sequence of the gene, the excision of e14 probably caused the SNPs that I found in the ciprofloxacin-induced chloramphenicol-resistant colonies, and the activity of *icd* might not have been affected [190]. Thus, the mutations in *icd* might not cause the Cam^R.

The last mutation found in the ciprofloxacin-induced chloramphenicol-resistant colonies was the amplification of *mdfA*. The MdfA protein is a multidrug efflux pump whose overexpression conferred resistance to many antibiotics like chloramphenicol or fluoroquinolones [191, 192]. Interestingly, the more MdfA is expressed, the more resistant *E. coli* is [193]. Thus, it is likely that the ciprofloxacin-induced chloramphenicol-resistant colonies had many copies of *mdfA* that could increase the resistance to chloramphenicol.

5.3.4 What was the ultimate cause of the ciprofloxacin-induced Cam^R?

Although I have found mutations that are likely to confer Cam^R (a deletion in *marR* or the amplification of *mdfA*), I have not found much evidence on what caused those mutations. My hypothesis was that quinolones activated the SOS response, which then induced the transcription of polymerases responsible for the resistance-conferring mutations. I found that the SOS response was indeed necessary for the acquisition of Cam^R; however, the SOS-inducible polymerases were not essential. SOS-inducible polymerases cause point mutations [194]. Therefore, I was expecting to see SNPs or indels in the WT strains but not in the samples deficient in the SOS-inducible polymerases. Consistent with this, I did not find any SNPs nor indels in the two samples that I sent for sequencing that were deficient in SOS-activated polymerases. Similar results were obtained by Pribis et al. [77] who investigated the mutations caused by ciprofloxacin treatment in ampicillin-resistant or rifampin-resistant colonies by looking at the *ampD* or *rpoB* gene, respectively. They analysed 24 isolates and found indels only when the isolate had been treated with ciprofloxacin but not in mutants without the SOS-activated polymerases. Song et al. [111] did a more exhaustive study (they used > 30 isolates per condition) looking at the mutations caused by norfloxacin in the *rpoB* or *thyA* gene. They found that norfloxacin

treatment increased point mutations and indels; however, in cells lacking *dinB* they only found deletions. Thus, it might be possible that the SNPs and indels I found in *marR* had been caused by the SOS-activated polymerases. Nevertheless, the strains deficient in SOS-induced polymerases had other mutations like an e14 deletion and/or an amplification of *mdfA*. e14 is excised from the chromosome when there is SOS response, thus, we can argue that this was the cause of that mutation. In fact, loss of e14 has been observed after norfloxacin treatment [105] and after the combination of enrofloxacin and tetracycline treatment [22]. The amplification of *mdfA* is more difficult to explain. Gene amplifications can happen randomly in a population of bacteria [195]; however, they have been found to modulate antibiotic resistance as they can cause an increase in gene dosage that can increase resistance [196]. The mechanism behind these stress-induced amplification is unknown.

5.4   Conclusions

In this chapter I have shown that ciprofloxacin induced resistance to chloramphenicol, ampicillin, trimethoprim, and ciprofloxacin, confirming the QIAR phenomenon. Some of the ciprofloxacin-induced chloramphenicol-resistant colonies had mutations in *marR* and *mdfA* that were likely to be responsible for the multidrug resistance phenotype. However, I have not found a genetic explanation for the Cam[R] in all the ciprofloxacin-induced chloramphenicol-resistant colonies, nor have I found the origin of those mutations. Nevertheless, I have found some clues on the origin of QIAR – that the SOS response is essential but the SOS-activated polymerases as well as Exo VII a SbcCD are not necessary. The implications of these findings will be discussed further in Chapter 7.

5.5   Future work

There are a few aspects related to this chapter that could be further investigated. In terms of the ciprofloxacin-induced Cam[R], it would be interesting to test whether other quinolones also induce Cam[R]. If that is the case, it would be worth analysing the whole genome of some chloramphenicol-resistant strains to compare the mutation profile from different quinolone treatments. Also, the phenomenon of ciprofloxacin-induced ampicillin or trimethoprim resistance could be investigated. For example, ciprofloxacin-induced ampicillin-resistant or trimethoprim-resistant colonies could have the *ampC* or *dfr* genes sequenced (mutations in those genes cause resistance to ampicillin or trimethoprim, respectively) to find SNPs or indels. These mutations could then be compared with the ones of ciprofloxacin-induced ampicillin-resistant or trimethoprim-resistant colonies lacking

the SOS-activated polymerases. Moreover, it would be interesting to study whether the amplification of *mdfA* is responsible for the acquisition of chloramphenicol resistance and whether this was caused by an increased plasmid copy-number or a duplicated locus within the chromosome.

Chapter 6:

6 *Galleria mellonella* as a model to study quinolone-induced antimicrobial resistance

6.1 Introduction

In the previous chapter, I studied the QIAR phenomenon *in vitro*. To understand if QIAR can develop *in vivo*, I investigated whether bacteria from the insect *Galleria mellonella* could develop antibiotic resistance after being exposed to quinolones. *Galleria mellonella* (*G. mellonella*, or greater wax moth) is a moth that parasites beehives. It is one of the few animals that can eat beeswax and plastic bags (as well as Petri dishes and Parafilm, based on personal observation) [197]. But for our purpose, its most interesting characteristic is that it can be used as an animal model to assess bacterial and fungal diseases.

G. mellonella has been used to measure the virulence of pathogenic bacteria such as *Mycobacterium tuberculosis* [110], *Acinetobacter baumannii* [198], *Pseudomonas aeruginosa* [199], *Staphylococcus aureus* [200] and fungi like *Candida albicans* [201]. In those studies, healthy larvae were injected with the pathogenic microorganism and the virulence of the microorganism was measured as the percentage of *G. mellonella* mortality. Interestingly, the virulence of some of those microorganisms was similar in *G. mellonella* and in mice, suggesting that *G. mellonella* might be a good animal system to study how bacteria and fungi infect mammals [199, 202, 203].

In comparison to mammal models *G. mellonella* has several advantages [204]. For example, it is cheap to maintain, easy to manipulate, requires no ethical approval and can grow at 37°C. Although it does not have an adaptive immune system like mammals do, it has an innate immune system comprised of both humoral and cellular immune responses mediated by antimicrobial peptides and phagocytic cells [205]. Also, because its defence mechanisms against microbes entails the deposition of melanin (which makes it look darker), it is easy to distinguish between infected (dark) and non-infected (clear) larvae.

G. mellonella has four developmental stages during its life cycle: egg, larva, pupa, and moth. Under laboratory conditions (37°C and artificial diet), the whole life cycle takes ~7 weeks of which it is in the phase of the larva ~3 weeks, which is the stage used for infection experiments (**Figure 6.1**). The larvae have a head, a thorax, and an abdomen. In

the abdomen there are eight prolegs or "false legs" through which the larvae are typically injected with the organism of interest without causing much damage to the larva.
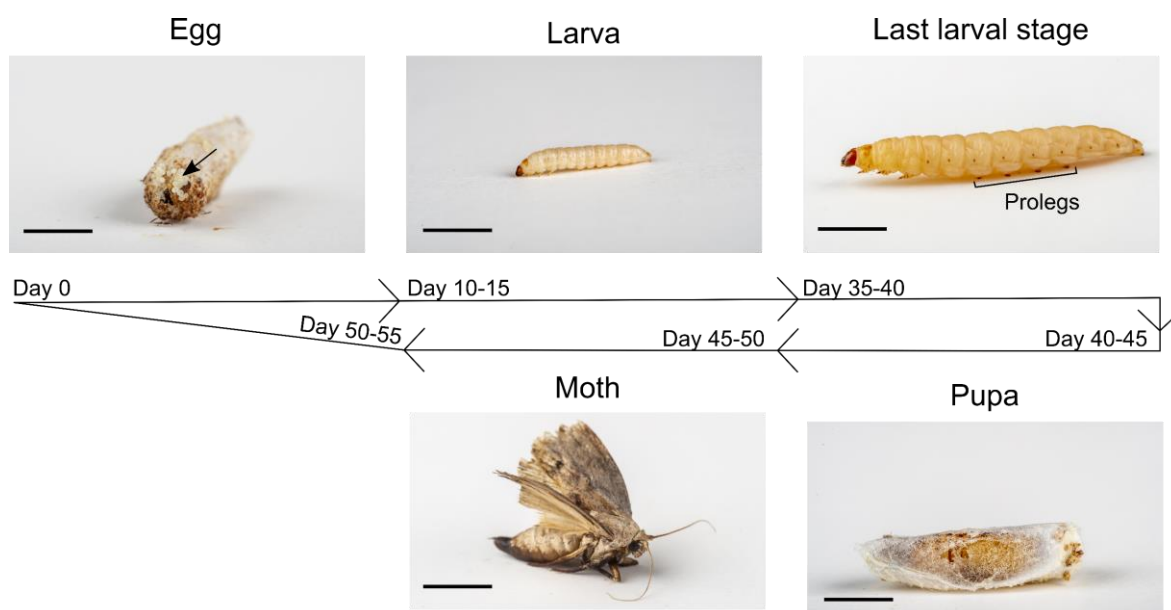
Figure 6.1. Life cycle of *Galleria mellonella*. There are four developmental stages in *Galleria mellona*'s life cycle: egg, larva, pupa, and adult. Under laboratory conditions (37°C and artificial diet) eggs hatch in 10-15 days, and the larvae grow for ~25 days until they pupate. Moths emerge from the pupa after ~5 days, mate, lay the eggs and the cycle starts again. Pictures were taken of *G. mellonella* grown in the laboratory. The bar represents 5 mm.

Like most animals, *G. mellonella* has a microbiome. This microbiome is sparse, and it is mainly composed of Enterococcal species [206]. Enterococci are Gram-positive gastrointestinal tract colonisers that are thought to block the invasion of other bacterial species in *G. mellonella* [207]. But the microbiome is not essential as *G. mellonella* can survive without it under laboratory conditions [208, 209].This was also shown by a previous PhD student in the lab, Katarzyna Ignasiak, who cleared the microbiota of adult larvae using antibiotics [210]. The fact that microbiome-free *G. mellonella* are healthy, made us wonder if it could be used as an animal model, not just to test bacterial infections, but to study what happens to the bacteria that colonise (but do not kill) the larvae. If we introduce a bacterium of our interest, say *E. coli*, we could study what happens with those bacteria; for example, if *E. coli* becomes antibiotic-resistant when the larvae are administered antibiotics.

Because of the potential of *G. mellonella* as an animal model, in this chapter I aimed to test if the quinolone-induced antimicrobial resistance (QIAR) phenomenon could be

studied using bacteria living inside *G. mellonella*. In Chapter 5, I observed that *E. coli* cells became resistant to different antibiotics after being exposed to low levels of quinolones in a tube. Here, I have tried to replicate the same experiment in *G. mellonella*. My hypothesis was that *E. coli* cells in *G. mellonella* larvae would acquire antibiotic resistance more frequently when they were exposed to low levels of ciprofloxacin. To test this, first I have studied whether I could colonise microbiome-depleted *G. mellonella* larvae with different *E. coli* strains and then if those *E. coli* cells became antibiotic-resistant after being exposed to low levels of quinolones inside the larvae.

6.2   Results

6.2.1   *G. mellonella* microbiota can be cleared with antibiotics

Adult *G. mellonella* larvae were grown on Petri dishes with sterile food supplemented with antibiotics. I used the antibiotics streptomycin and oxytetracycline to clear the microbiome as they had already been tried by previous PhD student Katarzyna Ignasiak and research assistant Marjorie Labédan (data not published). I started by adding 10 mg of each antibiotic per 100 g of food, but it was not enough to clear the microbiome of the larvae (**Table 6.1**). Thus, I increased the concentration of the antibiotics to 15 mg and found that after 10 days there was no bacterial growth. This amount of antibiotics did not cause any effect on the development of the larvae other than making them bigger (Katarzyna Ignasiak also observed the same phenomenon [210]). Hence, in further experiments I fed the larvae for 10 days with 15 mg of streptomycin and oxytetracycline per 100 g of food to deplete *G. mellonella*'s microbiota.

Table 6.1. Different antibiotic treatments and their effects on the microbiome of *G. mellonella* larvae.

Number of larvae tested	Antibiotic treatment (mg of streptomycin and oxytetracycline per 100 g of food)	Duration of treatment (days)	Microbiome cleared
3	10	5	No
3	10	7	No
5	10	15	No
3	15	5	Yes
4	15	5	No
10	15	5	Yes
3	15	5	Yes
5	15	6	Yes
8	15	7	No

5	15	7	No
10	15	8	Yes
9	15	8	No
4	15	9	Mostly
1	15	9	No
7	15	10	Yes
1	15	10	Yes
2	15	10	Yes
3	15	10	Yes
4	15	13	Yes
5	15	17	Yes

6.2.2 Microbiome-depleted *G. mellonella* larvae can be injected with *E. coli*, Enterococci cells and ciprofloxacin without increasing mortality

To study the phenomenon of QIAR in *G. mellonella*, I first tested if I could inject microbiome-depleted *G. mellonella* with the *E. coli* strain I used throughout this thesis: *E. coli* MG1655. Many groups have injected *E. coli* in *G. mellonella* to study their virulence [211-213], however, only one group has tested if *E. coli* can colonise (and not kill) *G. mellonella* [214]. In this colonisation study, *E. coli mpk* was forced-fed to *G. mellonella*'s larvae that had not lost their native microbiome. 24 hours after forced-feeding the bacteria, they could not find any *E. coli* colonies. This result suggested that it might not be easy to colonise *G. mellonella* with non-pathogenic *E. coli*. Hence, to maximise my chances of colonising *G. mellonella* with *E. coli*, apart from using the MG1655 strain, I also tried other non-pathogenic strains extracted from human samples: 29-1, H-21-4, H-21-1, and H-18-2. Besides the *E. coli* strains, I tried several Enterococcal species. As I mentioned before, Enterococci are the most abundant bacteria in *G. mellonella* with *Enterococcus gallinarum* (*En. gallinarum*) the most frequently species [206]. Other less common species are *En. faecalis*, *En. faecium* or *En. mundtii* [206, 210]. Because of the natural presence of Enterococci in *G. mellonella* I reasoned that they had high chances of colonising microbiome-depleted larvae.

Apart from injecting bacteria, I also injected ciprofloxacin. As my aim was to test the effect of low levels of ciprofloxacin in the bacteria living inside *G. mellonella*, I injected the drug instead of feeding the larvae with this drug, so that I could control the amount of drug administered to each larva. I used the same concentration of ciprofloxacin that I used in the mutation frequency assays in Chapter 5: 1/4 of the minimum inhibitory concentration (MIC) of ciprofloxacin. To inject 1/4 x MIC ciprofloxacin to the larvae, I first measured the MIC (**Table 6.2**) and then calculated how much ciprofloxacin I had to inject by inferring the

liquid volume of the larvae from the weight of the larva based on the data from [119] (see 2.2.13.2).

Table 6.2. MIC of ciprofloxacin of the *E. coli* and Enterococcal strains injected in *G. mellonella.*

Bacteria	MIC ciprofloxacin (µg/mL)
E. coli MG1655	0.027
E. coli 29-1	0.032
E. coli H-21-4	0.016
E. coli H-21-1	ND
E. coli H-18-2	ND
E. gallinarum	0.5
E. faecalis	0.25

ND: Not Determined

With this information in mind, I tested the effect of the injection of *E. coli* and Enterococcal strains in microbiota-depleted *G. mellonella* larvae (**Figure 6.2** & **Table 6.3**). I injected the 4 non-pathogenic commensal *E. coli* strains obtained from human samples (29-1, H-21-4, H-21-1, and H-18-2), the *E. coli* MG1655 strain, a strain of *En. gallinarum* that had been isolated from *G. mellonella* and a laboratory strain of *En. faecalis*. When the bacteria did not increase the normal mortality of larvae, I also checked if a co-injection of low levels of ciprofloxacin or water affected the mortality. I found that the injection of *E. coli* MG1655, *E. coli* 29-1 and *En. gallinarum* did not affect the mortality of the larvae, whereas *E. coli* H-21-1, *E. coli* H-21-4, *E. coli* H-18-2 and *En. faecalis* resulted in a higher mortality. These results showed that some *E. coli* strains and *En. faecalis* were pathogenic for *G. mellonella* whereas others were not. As I wanted non-pathogenic bacteria for the QIAR experiments, I focused on *E. coli* MG1655, *E. coli* 29-1 and *En. gallinarum*.

A)

B)

| No bacteria injected | Bacteria injected | Bacteria and ciprofloxacin injected |

Enterococcus gallinarum

Enterococcus faecalis

Figure 6.2. Microbiome-depleted larvae 24 h after being injected with bacteria. A) Unhealthy larvae are darker than healthy larvae because there is deposition of melanin as a defence mechanism. B) The injection of *Enterococcus gallinarum* with or without ciprofloxacin did not affect the survival of the larvae. The injection of *Enterococcus faecalis* without ciprofloxacin killed 6 out of 10 larvae after 24 h.

Table 6.3. Mortality of microbiome-depleted *G. mellonella* larvae injected with different bacterial species. The percentage of mortality (% mortality) was calculated as the number of larvae that died divided by the total of larvae injected in an experiment. For each experiment (or replicate) groups of 4-16 larvae were tested. The mean % mortality is the average percentage of all the replicates for each condition. In some cases, larvae were injected with bacteria and 10 μL of water or 10 μL of ciprofloxacin (1.12 μL of 1 μg/mL ciprofloxacin and 8.88 μL of water in the case of *E. coli*, or 2 μL of 10 μg/mL ciprofloxacin and 8 μL of water in the case of *En. gallinarum* and *En. faecalis*).

Bacteria injected	Mean % mortality	Standard deviation	Replicates
None	7	11	7
E. coli MG1655	5	4	2
+ ciprofloxacin	7	7	8
+ water	6	8	7
E. coli 29-1	10	14	2
+ ciprofloxacin	5	4	2
+ water	7	7	3
E. coli H-21-4	80	-	1
E. coli H-21-1	40	-	1
E. coli H-18-2	20	-	1
En. gallinarum	0	-	1
+ ciprofloxacin	4	8	4
+ water	3	5	6
En. faecalis	60	-	1

6.2.3 *G. mellonella* bacteria can be extracted by mechanical means

Once I knew which *E. coli* and Enterococcal species could be injected in *G. mellonella* larvae without killing them, I investigated how I could extract those bacteria from the larvae. To extract bacteria from *G. mellonella* researchers have tried different strategies: a) homogenisation of the gut [215], b) haemolymph extraction (the haemolymph is the analogous to the blood in vertebrates) [216], or c) homogenisation of the whole larva [217]. Haemolymph extraction and whole larva homogenisation might be the most successful strategies as researchers were able to obtain 10^6-10^8 bacteria per larva, whereas not more than 10^3 bacteria were obtained per gut. However, none of these studies aimed to extract all the bacteria; they plated dilutions of their homogenates to estimate the number of bacteria present. Also, in the haemolymph and whole larva studies they used pathogenic bacteria. In my case, I wanted to extract as many non-pathogenic bacteria as possible and to plate all of them, not just the dilutions. As the QIAR phenomenon happens at very low frequencies (10^{-7} - 10^{-11}), I needed to plate at least 10^7 bacteria to observe this phenomenon.

To find the best method to extract bacteria from *G. mellonella*, I tried the haemolymph method as well as different ways of homogenising the larvae, and of separating the bacteria from the larva homogenate (**Figure 6.3**). The haemolymph method was easy to perform but it was the least effective method that I tried (**Table 6.4**). I did not find much difference between homogenising frozen or alive larvae using a bead ruptor or a mortar

and a pestle (data not shown). Thus, as the mortar and pestle method was easier, I chose that method. After the homogenisation of the larvae, I tried to separate the bacteria from the larvae by centrifugating the homogenised larvae. The centrifugation led to the appearance of three phases, all of which contained bacteria. Because I could not find any phase containing most of the bacteria, I did not to centrifuge the homogenates. I found that it was useful to filtrate the homogenates before plating them, and the best way to do this without losing too much of the homogenates, was by filtrating the homogenates with 100 μL of water per larva through Miracloth material (pore size of 22-25 μm). Still, even following the most effective steps (homogenising the whole alive larvae with a mortar and a pestle, adding 100 μL of water per larva, and doing Miracloth filtration) I never got a high number of bacteria (**Table 6.4**).
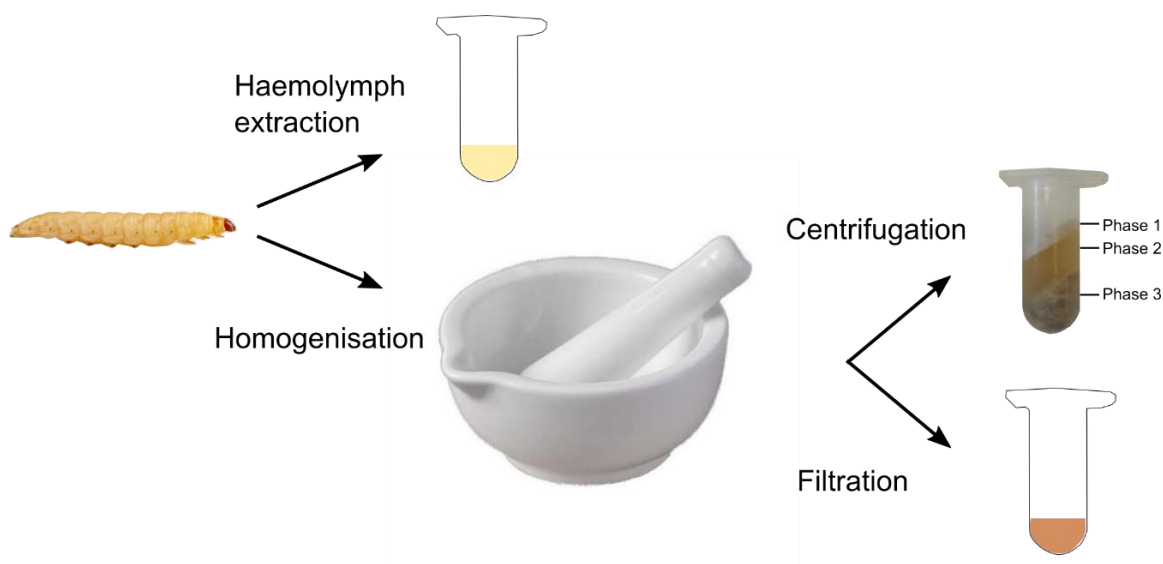
Figure 6.3. Extraction of bacteria from *G. mellonella* larvae. Adult larvae had their haemolymph extracted by making an incision at the end of their abdomen or were homogenised using a mortar and a pestle (100 μL of water was added for every larva). The homogenised larvae were either centrifuged or filtrated through Miracloth material.

Table 6.4. Comparison of the bacteria extracted from *G. mellonella larvae* after gut or whole larva homogenisation. For each experiment, three groups of 10 larvae were homogenised and then plated on LB to count the number of bacteria extracted using three different methods. One group of 10 larvae had their haemolymph extracted, another group of 10 larvae were homogenised using a mortar and a pestle and centrifuged (Phase 2 was plated), and a third group of 10 larvae were homogenised using a mortar and a pestle and filtered through Miracloth material.

Method	Bacteria extracted per larva	Experiment	Group
Haemolymph extraction	5	1	1
Whole larva homogenisation and centrifugation	10	1	2
Whole larva homogenisation and filtration	30	1	3
Haemolymph extraction	1,000	2	1
Whole larva homogenisation and centrifugation	3,140	2	2
Whole larva homogenisation and filtration	20,000	2	3

6.2.4 The number of bacteria extracted from *G. mellonella* varied greatly regardless of the bacterial specie, or the amount of bacterial injected

After finding the best conditions for the extraction of bacteria from *G. mellonella* larvae, I tested the number of different bacterial species I could extract after injecting different quantities of bacteria. I also checked if a co-injection with low levels of ciprofloxacin would influence the number of bacteria extracted.

I expected to extract more bacteria after injecting higher numbers of bacteria. But I found no correlation between the number of bacteria injected and the number of bacteria extracted (**Figure 6.4**). Also, I expected to extract a higher number of *En. gallinarum* cells compared to *E. coli* cells, as *En. gallinarum* is a natural coloniser of *G. mellonella*. However, I did not find a significant difference between the number of *En. gallinarum* and *E. coli* cells extracted. I also found that the co-injection with ciprofloxacin did not affect the number of bacteria extracted. These results indicate *E. coli* and *En. gallinarum* might not be good colonisers of microbiome-depleted larvae and/or that the method for the extraction of bacteria was not efficient.

The number of bacteria per larva I extracted ranged from 0 to 10^6 with an average of ~10^4. This result was not ideal since I was aiming to get at least 10^7 bacteria per larva, and it shows the difficulty of colonising and/or extracting bacteria from microbiome-depleted larvae.

A)

B)
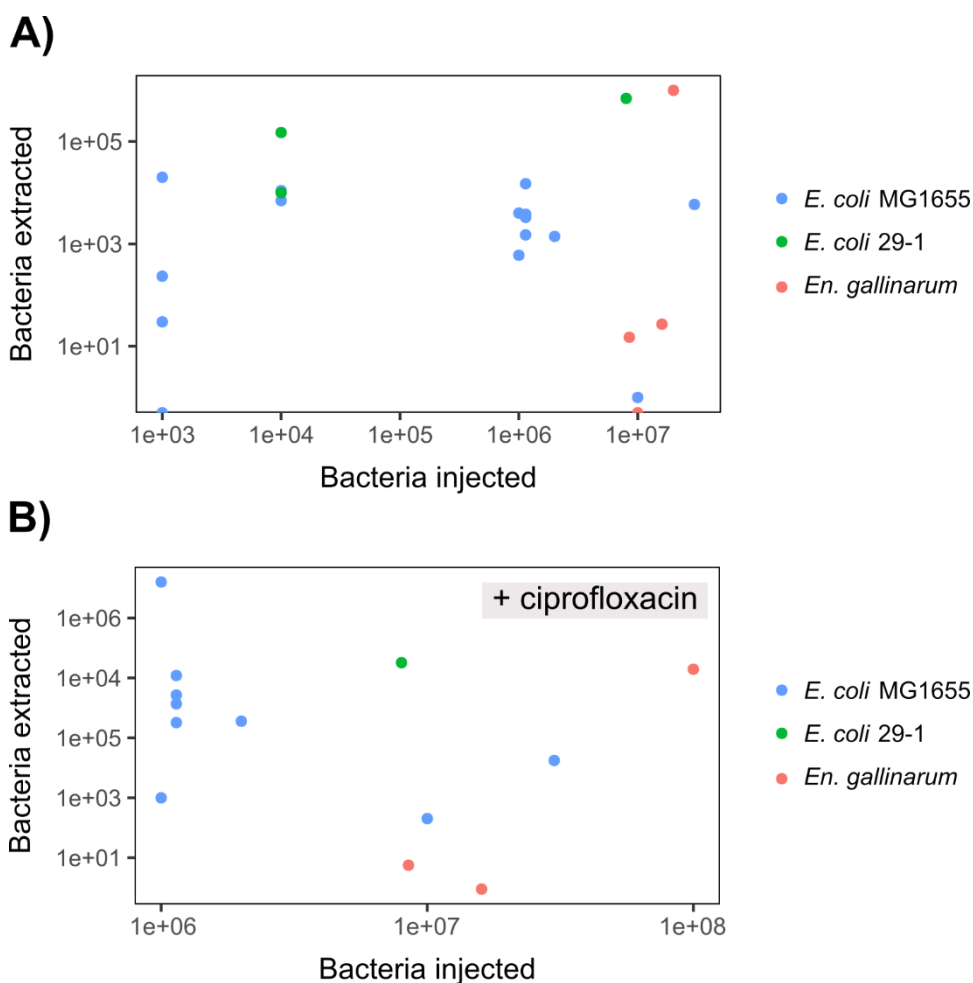
Figure 6.4. Number of bacteria extracted from microbiome-depleted *G. mellonella* larvae injected with *E. coli* MG1655, 29-1 or *En. gallinarum* cells and with low levels of ciprofloxacin. After 24 h the larvae were homogenised and filtered. Dilutions of the filtered homogenate were plated on LB plates to count the number of bacteria.

6.2.5 Bacteria extracted from microbiome-depleted *G. mellonella* did not seem to acquire antibiotic resistance

As I could only extract an average of 10^4 *E. coli* MG1655, *E. coli* 29-1 and *En. gallinarum* cells per larva, I looked for QIAR phenomena that happened at $>10^{-7}$ frequency.

From previous QIAR experiments, I found that the antibiotics that *E. coli* was more likely to acquire resistance to after being exposed to low levels of ciprofloxacin were ciprofloxacin itself and chloramphenicol. Thus, I focused on ciprofloxacin-induced ciprofloxacin or chloramphenicol resistance. To further increase the frequency of resistance, I selected on plates with moderate levels of ciprofloxacin or chloramphenicol (1x – 5x MIC) instead of using 23x or 8x MIC as I did in the QIAR assays for ciprofloxacin

and chloramphenicol, respectively (see 5.2.1.1). The objective was to inject *E. coli* or *En. gallinarum* cells into microbiome-depleted larvae, then to inject the larvae with low levels (1/4x MIC) of ciprofloxacin (or water as a control) and finally to extract the bacteria and to plate them on plates with 1x – 5x MIC of ciprofloxacin or chloramphenicol. In a similar manner as in the QIAR and MFA assay, those plates would be incubated at 37°C for one day and at room temperature for another day. The colonies that grew after those two days would be re-streaked on a plate with the same MIC of antibiotic. If it re-grew it would be considered as a ciprofloxacin-induced antibiotic-resistant colony. To avoid contamination, potential ciprofloxacin-induced antibiotic-resistant colonies were plated on selective media (*Enterococcus* selective media for *En. gallinarum* or MacConkey agar for *E. coli* strains) (**Figure 6.5**).
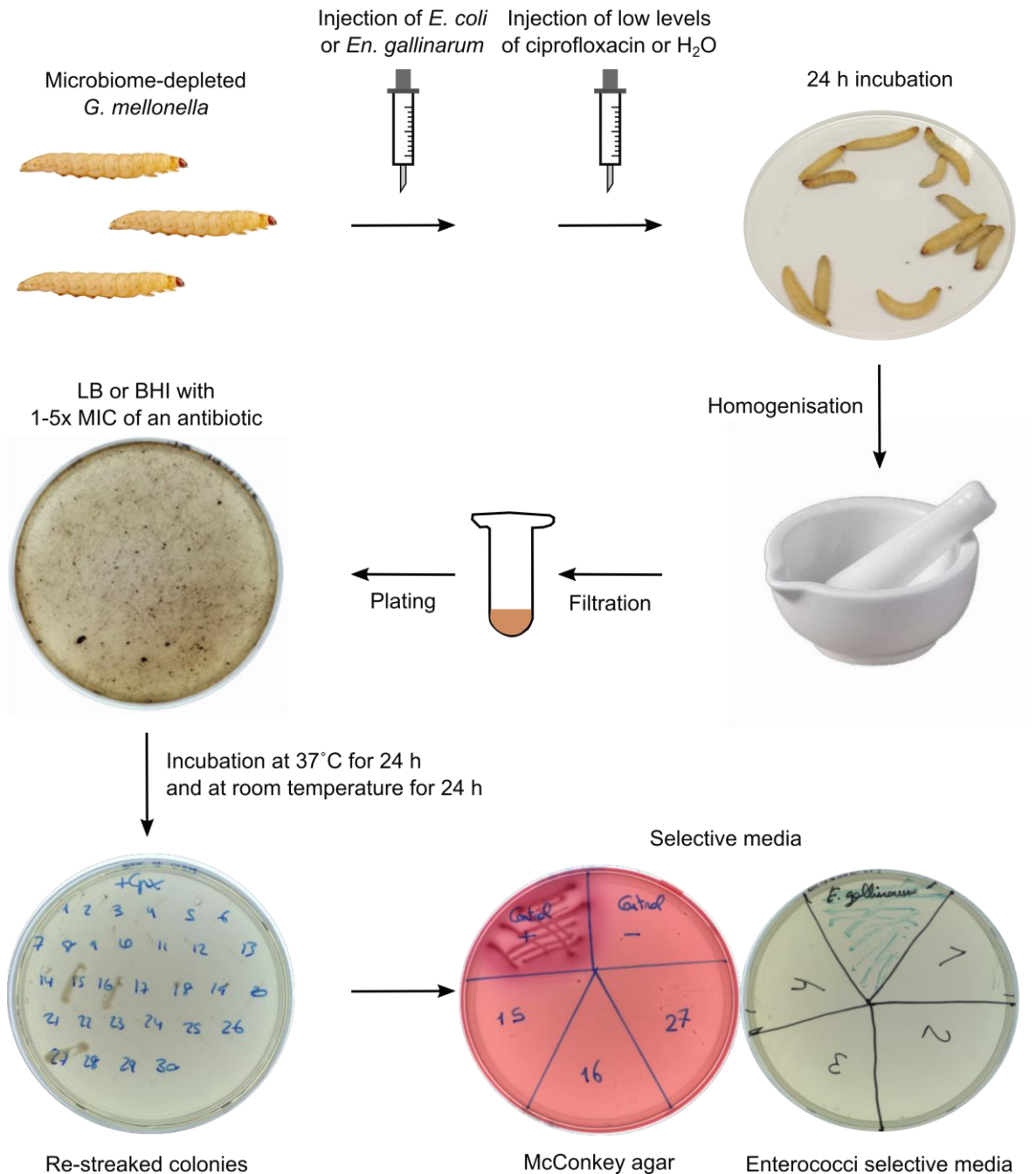
Figure 6.5. Workflow to test if low levels of ciprofloxacin induced resistance to antibiotics in *G. mellonella*. Groups of 4-16 adult larvae (~250 mg per larva) were fed for 10 days with artificial food supplemented with 15 mg of streptomycin and oxytetracycline per 100 mg of food at 37°C. Larvae were injected with 10^6-10^8 *E. coli* MG1655, *E coli* 29-1 or *En. gallinarum* cells, and 2 h later half of the larvae were injected with 1/4x MIC of ciprofloxacin (0.007 µg/mL of ciprofloxacin for *E. coli* and 0.125 µg/mL of ciprofloxacin for *En. gallinarum*). Larvae were incubated at 37°C for 24 h, then homogenised using a mortar and a pestle adding 100 µL of H_2O per larva. The homogenate was filtered using Miracloth and plated on LB (for *E. coli* cells) or BHI (for *En. gallinarum* cells) plates

supplemented with 1-5x MIC of ciprofloxacin or chloramphenicol. 10-fold dilutions of the homogenate were plated on LB or BHI only plates to count the total number of bacteria plated. The MIC (in µg/mL) of ciprofloxacin for *E. coli* MG1655 was 0.027, for *E. coli* 29-1 was 0.032, and for *En. gallinarum* was 0.5. The MIC of chloramphenicol was 4 µg/mL for all bacterial strains. Plates were incubated at 37°C for 24 h, then at room temperature for a further 24 h. The colonies that grew after the incubation were re-streaked in plates with the same concentration of antibiotic that was used in the selection (i.e., 1-5x MIC of ciprofloxacin or chloramphenicol). The re-streaked colonies that grew were also grown in selective media to check that they were *E. coli* (*E. coli* cells but not Enterococci can grow on MacConkey agar) or *En. gallinarum* (only Enterococci cells can grow on Enterococci selective media).

I started by investigating whether giving the larvae low doses of ciprofloxacin increased the frequency of ciprofloxacin- or chloramphenicol-resistant bacteria. I found that the bacteria extracted from microbiome-depleted larvae were either not resistant (frequency of resistance = 0) or all of them were resistant to ciprofloxacin or chloramphenicol (frequency of resistance = 1) (**Table 6.5**). Only in one experiment I was able to obtain a frequency of resistance between 0 and 1. These results suggested that the bacteria did not seem to acquire antibiotic resistance inside the larvae, as when I selected on >2x MIC I could not obtain any resistant bacteria, and when I selected on 1x MIC all the bacteria extracted were resistant (probably because those bacteria were already resistant before the injection). Thus, I have not been able to compare the frequencies of antibiotic resistant bacteria between the bacteria extracted from larvae treated with ciprofloxacin and the ones that were not treated. I will discuss these results in the next section.

Table 6.5. Frequency of antibiotic resistant bacteria extracted from microbiome-depleted larvae that had been exposed to low levels of ciprofloxacin or water. *E. coli* MG1655, *E. coli* 29-1 and *En. gallinarum* cells were injected in groups of 4-16 microbiome-depleted larvae. The larvae were also injected with low levels of ciprofloxacin (ciprofloxacin treatment) or water (no ciprofloxacin treatment). After 24 h incubation at 37°C, the larvae were homogenised and the bacteria were extracted and plated on plates with 1x-5x MIC of ciprofloxacin or chloramphenicol (MIC of ciprofloxacin (µg/mL) = 0.027 for *E. coli* MG1655, 0.032 for *E. coli* 29-1 and 0.5 for *En. gallinarum*; MIC of chloramphenicol (µg/mL) = 4 for all strains). Dilutions of the bacteria were also plated on LB or BHI plates (for *E. coli* or *En. gallinarum*, respectively). The frequency of ciprofloxacin or chloramphenicol resistant bacteria was calculated by dividing the number of resistant bacteria by the total number of bacteria extracted.

Bacteria injected	Ciprofloxacin treatment	Ciprofloxacin selection	Frequency of ciprofloxacin resistant bacteria
E. coli MG1655	No	1x MIC	10^{-4}
E. coli MG1655	Yes	1x MIC	0
E. coli MG1655	No	1x MIC	~1
E. coli MG1655	Yes	1x MIC	~1
E. coli MG1655	No	1x MIC	~1
E. coli MG1655	Yes	1x MIC	~1
E. coli MG1655	No	1x MIC	~1
E. coli MG1655	Yes	1x MIC	~1
E. coli MG1655	No	2x MIC	0
E. coli MG1655	Yes	2x MIC	0
E. coli MG1655	No	2x MIC	0
E. coli MG1655	Yes	2x MIC	0
E. coli MG1655	No	2x MIC	0
E. coli MG1655	Yes	2x MIC	0
E. coli MG1655	No	2x MIC	~1
E. coli MG1655	Yes	2x MIC	~1
E. coli 29-1	No	5x MIC	0
E. coli 29-1	Yes	5x MIC	0
En. gallinarum	Yes	1x MIC	0
En. gallinarum	No	1x MIC	~1
En. gallinarum	Yes	1x MIC	~1
En. gallinarum	No	2x MIC	0
En. gallinarum	Yes	2x MIC	0
En. gallinarum	No	3x MIC	0
Bacteria injected	**Ciprofloxacin treatment**	**Chloramphenicol selection**	**Frequency of chloramphenicol resistant bacteria**
E. coli MG1655	No	1x MIC	~1
E. coli MG1655	Yes	1x MIC	~1
E. coli MG1655	No	2x MIC	0
E. coli MG1655	Yes	2x MIC	0

6.3   Discussion

In this chapter I studied if *G. mellonella* could be used as a model to study QIAR. To the best of my knowledge, no group has ever investigated QIAR (that is the frequency of antibiotic-resistant bacteria in the presence or absence of quinolones) in an animal model. There are some examples, though, of groups that have tested the effect of quinolones in bacteria defective in the SOS response using a mouse model [56, 218, 219]. All those groups showed that only *E. coli* cells that could activate the SOS response could become resistant to antibiotics. However, none of those groups included a control group that was not administered ciprofloxacin. In my case, I have injected microbiome-depleted *G. mellonella* with five different *E. coli* strains as well as *En. gallinarum* and *E. faecalis* with the aim of testing if those bacteria became resistant to ciprofloxacin or chloramphenicol in the presence of low levels of ciprofloxacin. I found that some of those strains were pathogenic for the larvae, and that the ones that were not (*E. coli* 29-1, *E. coli* MG1655 and *En. gallinarum*) did not seem to replicate inside the larvae, as after 24 hours of being injected I extracted less bacteria than what I injected. The reasons why I got low numbers might be because of the method I used for the extraction and/or because those bacterial strains cannot colonise microbiome-depleted larvae.

There is not a standard method to extract bacteria from *G. mellonella*, and of all the known methods, none of them was designed to extract as many bacteria as possible in an acceptable volume that could then be plated (for example, in a 15-mm Petri dish the optimal volume for plating is 100 µL). I have tried different ways of homogenising the larvae, and of separating the bacteria from the larva homogenate. However, even with the most efficient one, I did not get enough bacteria.

Another reason why I did not get high numbers of *E. coli* or *En. gallinarum*, might be that *E. coli* cells cannot colonise the larvae. Other commensal bacteria have been introduced in *G. mellonella*. *E. coli mpk* and *Bacteroides vulgates* were introduced into *G. mellonella*'s larvae [214]. 24 hours after the injection there were no *E. coli* or *Bacteroides vulgates* colonies. Because genes coding antimicrobial peptides were upregulated after the administration of the bacteria, they suggested that the loss of the bacteria was caused by the larvae's immune response.

In any case, when I tested if *E. coli* or *En. gallinarum* injected in *G. mellonella* became resistant to ciprofloxacin or chloramphenicol, I could not show whether the QIAR phenomenon happened in bacteria living inside *G. mellonella*. I believe that the key problem in this experiment was the fact that I could not maintain a high number of bacteria inside the larvae. Because the QIAR phenomenon happens very rarely it is hard to study

QIAR when you do not have enough bacteria. In the next section I have suggested some experiments that could solve this issue.

6.4 Conclusions

The purpose of this chapter was to determine whether bacteria living inside the insect model *G. mellonella* became resistant to antibiotics after being exposed to low levels of ciprofloxacin. *G. mellonella* larvae had their microbiome depleted, were colonised with several *E. coli* and Enterococcal strains, and were injected with low levels of ciprofloxacin without causing significant mortality. However, the number of bacteria extracted from larvae that had had their microbiome cleared, had been injected with *E. coli* MG1655, *E. coli* 29-1 or *En. gallinarum*, and then had been treated with a low dose of ciprofloxacin, was not enough to test for the acquisition of antibiotic resistance.

6.5 Future work

G. mellonella has many advantages over other animal models (e.g., ethical considerations and facility of use) and thus, it is important to understand its full potential in the research of antibiotic resistance. Although I have not been able to establish *G. mellonella* as a model for QIAR, I believe there are a few experiments that could be done to further investigate this idea.

For example, we could study the efficacy of the protocol to extract bacteria from *G. mellonella*. To test how efficient this method is, we could extract the bacteria from microbiome-depleted larvae, just after being injected with the bacteria, and then compare the numbers of extracted *vs* injected larvae. If there is a significant difference between those numbers, this would suggest that the protocol should be further optimised before proceeding with any further research. On the other hand, if there is not much difference between the number of bacteria extracted and injected, this would indicate that the main problem is the lack of colonisation of the bacteria. To solve this issue, we could use pathogenic bacteria (like *E. coli* H-21-4 or *En. faecalis*) instead of non-pathogenic bacteria. Pathogenic bacteria replicate themselves inside the host, so we would be able to obtain higher numbers of bacteria. However, first, we should determine a dose that will not kill the larvae immediately, but over an appropriate time course (e.g., a few days) so that the bacteria can be exposed to low levels of quinolones for 1 day before the larvae are killed. This type of experiments has been done, for example, with pathogenic *En. faecalis* to test the efficacy of different antibiotics [220]. Another idea to improve the numbers of extracted bacteria, would be to overcome the immune response. Assuming that the bacteria that we inject cannot colonise *G. mellonella* because of the immune system of the

larvae, we could try knocking down the expression of genes involved in the immune response. For example, Johnson et al. [221] were able to knock down the expression of lysozyme using RNAi in *G. mellonella* which resulted in an increase in Enterococcal colonisers. Potentially, a *G. mellonella* lysozyme-knockdown could be colonised by *E. coli* MG1655 or *En. gallinarum*.

Chapter 7:

7 General discussion

7.1 Introduction

Quinolones have been used in medicine for more than 50 years and their mechanism of action has been studied exhaustively since then [222]. However, there are still many gaps in the understanding of how quinolones kill bacteria and how bacteria repair quinolone-induced DNA damage [12]. Even more puzzling is the fact that quinolones induce resistance to other antibiotics, a phenomenon called quinolone-induced antimicrobial resistance (QIAR) [223]. Previous studies have linked QIAR to errors in the repair of DNA damage, but this is yet to be confirmed. In this work I have investigated how bacteria repair quinolone-induced DNA damage and how this damage might lead to QIAR. I have not found the exact mechanism of quinolone-induced DNA repair, although I have confirmed that a particular QIAR phenomenon depended on the repair of quinolone-induced DNA damage. The discussion of these findings in a wider context is detailed below.

7.2 How do quinolones induce DNA damage?

Despite widespread agreement on the bactericidal action of quinolones (that is, the presence of DNA breaks that cause the loss of genetic integrity), the origin of the lethal DNA breaks remains a mystery. In the introduction (section 1.2.4) I mentioned three theories for the origin of quinolone-induced DNA damage: the removal of a trapped topoisomerase, the collision of the replication machinery with a trapped topoisomerase and the accumulation of reactive oxygen species (ROS). In this thesis I have investigated some aspects of the first and third theory.

There is direct evidence that one protein, Exonuclease VII (Exo VII), can remove trapped topoisomerases from the DNA [120]. Another protein, SbcCD, might also have a similar role [121], although as I showed in Chapter 4, I was not able to confirm this. Knowing that Exo VII can remove a trapped topoisomerase from the DNA, allows us to make some predictions about whether the removal of trapped topoisomerases causes lethal DNA breaks. For example, if the removal of the trapped topoisomerase causes lethal DSBs in the cell, and Exo VII is the protein responsible for the removal of the topoisomerase, the absence of Exo VII should cause less DSBs and therefore less death in the presence of

quinolones. However, the lack of Exo VII makes cells more sensitive to quinolones [97, 166], and these cells have more DNA breaks in the presence of quinolones [166]. In Chapter 4, I confirmed these results by showing that cells lacking Exo VII were more sensitive to quinolones, and that some of them had more DNA breaks than WT cells when exposed to quinolones. These findings suggest that the removal of the trapped topoisomerase helps bacteria to survive and not to kill them. Therefore, the origin of the lethal DNA breaks is likely to be a downstream event caused by the presence of trapped topoisomerases on the DNA rather than the release of the DSB from the cleavage complex.

Regarding the ROS theory, there is increasing evidence of the role of ROS in quinolone lethality. In Chapter 3, I reproduced Hong et al. [24] experiments in which they showed that cells treated with ciprofloxacin and chloramphenicol and grown in a medium with a ROS inhibitor did not die. This result supports the theory of ROS being key in the lethality of quinolones. However, I believe that this is an indirect way of testing this theory, as the addition of chloramphenicol and a ROS inhibitor might have other effects apart from the inhibition of ROS. Nevertheless, it remains an interesting theory to test, especially since I also found in Chapter 3 that Exonuclease III might be involved in the repair of quinolone-induced ROS damage whereas YafD might be involved in the repair of quinolone-induced ROS-independent damage.

7.3 How do bacteria repair quinolone-induced DNA damage?

As mentioned in the introduction (1.2.5), not much is known about how bacteria repair the damage caused by quinolones [12]. The only exceptions are the involvement of the SOS response, DNA repair proteins and Exo VII. By contrast, how eukaryotic cells repair the damage caused by topoisomerase inhibitors is well understood [123]. There are several eukaryotic proteins involved in the repair of trapped topoisomerases (or cleavage complexes) and most of them have a putative *E. coli* homolog (**Table 7.1**). In Chapter 3 and 4, I tested whether some of these *E. coli* homologs (ClpP, Exo III, YafD, YbhP and SbcD) participated in the repair of topoisomerase damage. I found that two of them (Exo III and YafD) were likely to be involved at some stage; however, none of them seemed to work as the eukaryotic counterpart. These results suggest that bacteria might not repair topoisomerase-related damage in a similar way as eukaryotes. It also suggests that bacteria might not have a TDP2-like protein or that perhaps Exo VII instead catalyses a reaction to release gyrase from DNA through a different mechanism. Eukaryotic topoisomerases (but not bacterial topoisomerases) can be stabilised on the DNA without

the presence of an inhibitor [224]. This could explain why eukaryotes might have more proteins specialised in the removal of trapped topoisomerases than bacteria.

It is also worth mentioning that quinolones and chemotherapeutic agents like doxorubicin work through a similar mode of action [225]. Besides, as shown in **Table 7.1**, not all the potential *E. coli* homologs of the eukaryotic proteins involved in the repair of topoisomerase cleavage complexes have been studied. Thus, it would be interesting to study more potential homologs, as further insights could be gained in cancer research, if bacteria are found to be using similar pathways of repair as eukaryotic cells.

Table 7.1. Eukaryotic proteins involved in repair of topoisomerase cleavage complexes and their putative homologs in *E. coli*.

Human protein	Putative *E. coli* homolog	Involved in the removal of trapped topoisomerase?
Proteasome	ClpP [153]	Probably not (Chapter 4)
	HslVU [154]	Not known
SPRTN	No significant similarity found*	-
TDP2	Exo III*	Probably not (Chapter 3)
	YafD*	Probably not (Chapter 3)
	YbhP*	Probably not (Chapter 3)
MRE11	SbcD [226]	Maybe [121] (Chapter 4)
	Yael*	Not known
RAD50	No significant similarity found*	-
NBS1	YfaA*	Not known
FEN1	Exo IX*	Not known
XPG	No significant similarity found*	Not known

*Proteins found by doing a BackPhyre or PSI-BLAST search comparing the human protein with all *E. coli* proteins.

7.4 The repair of quinolone-induced DNA damage and its role in antibiotic resistance

The link between the repair of quinolone-induced DNA damage and the acquisition of antibiotic resistance is not clear. There is evidence that treating bacteria with low levels of quinolones activates different stress responses (e.g., SOS response, oxidative damage response) that can increase the mutation rates and cause antibiotic-resistant mutations [77, 90]. DNA damage triggers those stress responses and the mutations might be a

consequence of the attempt of the bacterium to repair the DSBs caused by the quinolone-poisoned topoisomerases. Following this idea, several groups have tested whether proteins that participate in the SOS response (e.g., RecA, LexA, Pol II, Pol IV, and Pol V) affected QIAR [77, 105, 107, 111]. In all those studies, the lack of activity of RecA and LexA (the master regulators of the SOS response) decreased QIAR. However, the absence of the SOS-activated polymerases Pol II (PolB), Pol IV (DinB) and/or Pol V (UmuDC) did not affect QIAR in all the studies [111]. In Chapter 5, I studied one particular QIAR phenomenon, ciprofloxacin-induced chloramphenicol resistance. I found that mutants deficient in RecA or LexA did not become chloramphenicol resistant, whereas mutants without the SOS-activated polymerases could become chloramphenicol resistant. More interestingly, I observed that Exo VII was not involved in the acquisition of chloramphenicol resistance. Taken together, these results indicate that the SOS response is important in QIAR; however, the origin of the DNA breaks that cause the activation of the SOS response is not necessarily the removal of the trapped topoisomerase from the DNA, and the mutations are not necessarily caused by the SOS-activated polymerases (**Figure 7.1**).
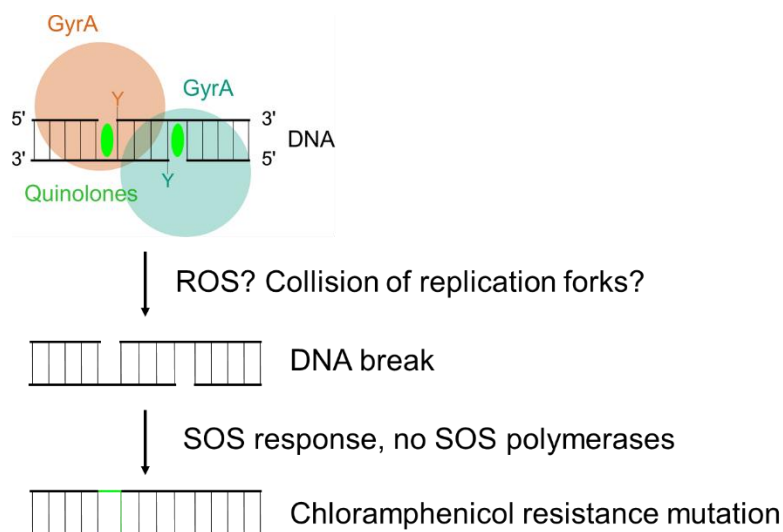
Figure 7.1. Proposed mechanism for the acquisition of chloramphenicol resistance induced by ciprofloxacin. The stabilisation of a topoisomerase on the DNA by the quinolone ciprofloxacin, leads to the accumulation of ROS and/or the collision of replication forks causing DNA breaks. The presence of the DNA breaks activates the SOS response, which, by an unknown mechanism independent of the SOS-activated polymerases Pol II, Pol IV, and Pol V, can make mutations conferring chloramphenicol resistance.

7.5   Is QIAR biologically and clinically relevant?

Several studies have claimed that QIAR is biologically relevant because low doses of quinolones caused an increase in the mutation rates of bacteria [77, 90]. Yet the biological and clinical relevance of this effect is still debated. It is argued that if population size is reduced (which happens even at low doses of antibiotics), the mutations caused by antibiotics may not be adequate to improve evolvability (that is, the ability of a population to generate adaptive genetic diversity) [227]. This is because evolvability is highly dependent on both the rate at which the genetic variety is produced and the size of the population. Frenoy & Bonhoeffer [228] showed that when cell death is not considered, antibiotic-induced mutagenesis is overestimated. Therefore, the studies that measured mutation rates without considering cell death might not be accurate. In contrast, *in vivo* experiments suggest that antibiotic-induced mutagenesis is crucial for development of resistance. Boshoff et al. [218] demonstrated that the absence of a SOS-regulated polymerase in *Mycobacterium tuberculosis* reduced the appearance of antibiotic-resistant bacteria after ciprofloxacin treatment. Cirz et al. [56] showed that *E. coli* cells unable to activate the SOS response could not evolve resistance to ciprofloxacin or to rifampin in a mouse model. Moreover, *E. coli* cells injected in mice that were co-treated with ciprofloxacin and an inhibitor of RecA had a reduced frequency of antibiotic resistance compared to the ciprofloxacin-only treatment [219].

Despite this amount of data, determining whether QIAR is due to increased survival or increased mutation rates remains a challenge. More *in vivo* research with proper controls (perhaps using the insect model *Galleria mellonella* as in Chapter 6) are needed to answer this question, especially as the inhibition of the SOS response has been identified as a potential therapeutic target [229]. Furthermore, as most countries have reported high resistance rates to quinolones and other antibiotics [4], it would be worth analysing whether QIAR is one of the reasons behind this.

7.6   Conclusions

Even though quinolones have been investigated for many years, some aspects of how quinolones work, like how they kill bacteria or how bacteria repair the damage caused by quinolones are still unclear. This lack of knowledge makes it difficult to understand downstream effects such as the appearance of mutations conferring antibiotic resistance. Despite this, I have been able to show that ciprofloxacin can induce mutations that confer chloramphenicol resistance via a response to DNA damage, the SOS response. The origin of this DNA damage is not necessarily the removal of trapped topoisomerases from

the DNA by Exo VII. However, I have confirmed that Exo VII (and probably Lon, Exo III, YafD and RecB) participate in the repair of quinolone-induced DNA damage. These findings may help us to understand better how quinolones work and how they can induce mutations in bacteria.

Abbreviations

Amp^R	Ampicillin resistance
AR	Antibiotic resistance
BHI	Brain Heart Infusion
Cam^R	Chloramphenicol resistance
dsDNA	Double-stranded DNA
E. coli	*Escherichia coli*
EDTA	Ethylenediaminetetraacetic acid
eGFP	Enhanced green fluorescent protein
En. faecalis	*Enterococcus faecalis*
En. gallinarum	*Enterococcus gallinarum*
Exo III	Exonuclease III
Exo VII	Exonuclease VII
FLP	Flippase
FRT	Flippase recognition target
G segment	Gate segment
G. mellonella	*Galleria mellonella*
Gyrase	DNA gyrase
HGT	Horizontal gene transfer
His	Histidine
HR	Homologous recombination
IR	Illegitimate recombination
Kan^R	Kanamycin resistance
L DNA	Linear DNA
LB	Luria-Bertani
MBP	Maltose-binding protein
MFA	Mutation frequency assay
MIC	Minimum inhibitory concentration
NER	Nucleotide excision repair
NHEJ	Non-homologous end-joining
QIAR	Quinolone-induced antimicrobial resistance
R DNA	Relaxed DNA
ROS	Reactive oxygen species
SC DNA	Supercoiled DNA
SDS-PAGE	Sodium dodecyl-sulphate polyacrylamide electrophoresis
ssDNA	Single-stranded DNA
SNP	Single-nucleotide polymorphism
SOC	Super Optimal broth with Catabolite repression
Spec^R	Spectinomycin resistance
T segment	Transported segment
TDP	Tyrosyl-DNA phosphodiesterase
Topo II	Topoisomerase II
Topo IV	Topoisomerase IV
UTI	Urinary tract infection
WT	Wild type

References

1. Andersson, D.I. and D. Hughes, *Microbiological effects of sublethal levels of antibiotics.* Nature Reviews Microbiology, 2014. **12**(7): p. 465-478.
2. Davies, J. and D. Davies, *Origins and evolution of antibiotic resistance.* Microbiol Mol Biol Rev, 2010. **74**(3): p. 417-33.
3. Ventola, C.L., *The antibiotic resistance crisis. Part 1: causes and threats.* Pharmacy and Therapeutics, 2015. **40**(4): p. 277-83.
4. WHO, *Global antimicrobial resistance and use surveillance system (GLASS) report 2021.* 2021.
5. O'Neill, J., *Tackling drug-resistant infections globally: final report and recommendations.* 2016.
6. Baquero, F. and B.R. Levin, *Proximate and ultimate causes of the bactericidal action of antibiotics.* Nat Rev Microbiol, 2021. **19**(2): p. 123-132.
7. Kapoor, G., S. Saigal, and A. Elongavan, *Action and resistance mechanisms of antibiotics: A guide for clinicians.* Journal of anaesthesiology, clinical pharmacology, 2017. **33**(3): p. 300-305.
8. Wald-Dickler, N., P. Holtom, and B. Spellberg, *Busting the Myth of "Static vs Cidal": A Systemic Literature Review.* Clin Infect Dis, 2018. **66**(9): p. 1470-1474.
9. Svetlov, M.S., N. Vázquez-Laslop, and A.S. Mankin, *Kinetics of drug-ribosome interactions defines the cidality of macrolide antibiotics.* Proc Natl Acad Sci U S A, 2017. **114**(52): p. 13673-13678.
10. Salamaga, B., et al., *Demonstration of the role of cell wall homeostasis in Staphylococcus aureus growth and the action of bactericidal antibiotics.* Proc Natl Acad Sci U S A, 2021. **118**(44).
11. Giroux, X., et al., *Maladaptive DNA repair is the ultimate contributor to the death of trimethoprim-treated cells under aerobic and anaerobic conditions.* Proceedings of the National Academy of Sciences, 2017. **114**(43): p. 11512-11517.
12. Drlica, K. and X. Zhao, *Bacterial death from treatment with fluoroquinolones and other lethal stressors.* Expert Review of Anti-infective Therapy, 2021. **19**(5): p. 601-618.
13. Drlica, K., et al., *Quinolone-mediated bacterial death.* Antimicrob Agents Chemother, 2008. **52**(2): p. 385-92.
14. Kohanski, M.A., et al., *A common mechanism of cellular death induced by bactericidal antibiotics.* Cell, 2007. **130**(5): p. 797-810.
15. Whitaker, A.M., et al., *Base excision repair of oxidative DNA damage: from mechanism to disease.* Front Biosci (Landmark Ed), 2017. **22**: p. 1493-1522.
16. Liu, Y. and J.A. Imlay, *Cell death from antibiotics without the involvement of reactive oxygen species.* Science, 2013. **339**(6124): p. 1210-3.
17. Keren, I., et al., *Killing by bactericidal antibiotics does not depend on reactive oxygen species.* Science, 2013. **339**(6124): p. 1213-6.
18. Imlay, J.A., *Diagnosing oxidative stress in bacteria: not as easy as you might think.* Curr Opin Microbiol, 2015. **24**: p. 124-31.
19. Dwyer, D.J., et al., *Antibiotics induce redox-related physiological alterations as part of their lethality.* Proceedings of the National Academy of Sciences, 2014. **111**(20): p. E2100.
20. Lobritz, M.A., et al., *Antibiotic efficacy is linked to bacterial cellular respiration.* Proc Natl Acad Sci U S A, 2015. **112**(27): p. 8173-80.
21. Machuca, J., et al., *Cellular Response to Ciprofloxacin in Low-Level Quinolone-Resistant Escherichia coli.* Frontiers in microbiology, 2017. **8**: p. 1370-1370.
22. Hoeksema, M., S. Brul, and B.H. Ter Kuile, *Influence of Reactive Oxygen Species on De Novo Acquisition of Resistance to Bactericidal Antibiotics.* Antimicrob Agents Chemother, 2018. **62**(6).

23. Hong, Y., et al., *Post-stress bacterial cell death mediated by reactive oxygen species.* Proc Natl Acad Sci U S A, 2019. **116**(20): p. 10064-10071.

24. Hong, Y., et al., *Reactive oxygen species play a dominant role in all pathways of rapid quinolone-mediated killing.* J Antimicrob Chemother, 2020. **75**(3): p. 576-585.

25. Van Acker, H. and T. Coenye, *The Role of Reactive Oxygen Species in Antibiotic-Mediated Killing of Bacteria.* Trends Microbiol, 2017. **25**(6): p. 456-466.

26. Munita, J.M. and C.A. Arias, *Mechanisms of Antibiotic Resistance.* Microbiol Spectr, 2016. **4**(2).

27. von Wintersdorff, C.J., et al., *Dissemination of Antimicrobial Resistance in Microbial Ecosystems through Horizontal Gene Transfer.* Front Microbiol, 2016. **7**: p. 173.

28. Blair, J.M.A., et al., *Molecular mechanisms of antibiotic resistance.* Nature Reviews Microbiology, 2015. **13**(1): p. 42-51.

29. Brauner, A., et al., *Distinguishing between resistance, tolerance and persistence to antibiotic treatment.* Nat Rev Microbiol, 2016. **14**(5): p. 320-30.

30. Sulaiman, J.E. and H. Lam, *Evolution of Bacterial Tolerance Under Antibiotic Treatment and Its Implications on the Development of Resistance.* Frontiers in Microbiology, 2021. **12**.

31. Webber, M.A. and L.J. Piddock, *The importance of efflux pumps in bacterial antibiotic resistance.* J Antimicrob Chemother, 2003. **51**(1): p. 9-11.

32. Delcour, A.H., *Outer membrane permeability and antibiotic resistance.* Biochim Biophys Acta, 2009. **1794**(5): p. 808-16.

33. Karczmarczyk, M., et al., *Mechanisms of fluoroquinolone resistance in Escherichia coli isolates from food-producing animals.* Appl Environ Microbiol, 2011. **77**(20): p. 7113-20.

34. Aldred, K.J., R.J. Kerns, and N. Osheroff, *Mechanism of quinolone action and resistance.* Biochemistry, 2014. **53**(10): p. 1565-74.

35. Feng, L., et al., *The pentapeptide-repeat protein, MfpA, interacts with mycobacterial DNA gyrase as a DNA T-segment mimic.* Proceedings of the National Academy of Sciences, 2021. **118**(11): p. e2016705118.

36. Hughes, D. and D.I. Andersson, *Selection of resistance at lethal and non-lethal antibiotic concentrations.* Curr Opin Microbiol, 2012. **15**(5): p. 555-60.

37. Drlica, K., *The mutant selection window and antimicrobial resistance.* J Antimicrob Chemother, 2003. **52**(1): p. 11-7.

38. Blázquez, J., et al., *Antimicrobials as promoters of genetic variation.* Curr Opin Microbiol, 2012. **15**(5): p. 561-9.

39. Liu, A., et al., *Selective advantage of resistant strains at trace levels of antibiotics: a simple and ultrasensitive color test for detection of antibiotics and genotoxic agents.* Antimicrob Agents Chemother, 2011. **55**(3): p. 1204-10.

40. Gullberg, E., et al., *Selection of resistant bacteria at very low antibiotic concentrations.* PLoS Pathog, 2011. **7**(7): p. e1002158.

41. Luria, S.E. and M. Delbrück, *Mutations of Bacteria from Virus Sensitivity to Virus Resistance.* Genetics, 1943. **28**(6): p. 491-511.

42. Luria, S.E., *Recent advances in bacterial genetics* Bacteriological reviews, 1947. **11**(1): p. 1-40.

43. Andersson, D.I., D. Hughes, and J.R. Roth, *The Origin of Mutants under Selection: Interactions of Mutation, Growth, and Selection.* EcoSal Plus, 2011. **4**(2).

44. Rosenberg, S.M., et al., *Stress-induced mutation via DNA breaks in Escherichia coli: a molecular mechanism with implications for evolution and medicine.* Bioessays, 2012. **34**(10): p. 885-92.

45. Fisher, R.A., B. Gollan, and S. Helaine, *Persistent bacterial infections and persister cells.* Nat Rev Microbiol, 2017. **15**(8): p. 453-464.

46. Dörr, T., K. Lewis, and M. Vulić, *SOS response induces persistence to fluoroquinolones in Escherichia coli.* PLoS Genet, 2009. **5**(12): p. e1000760.

47. Barrett, T.C., et al., *Enhanced antibiotic resistance development from fluoroquinolone persisters after a single exposure to antibiotic.* Nature communications, 2019. **10**(1): p. 1177-1177.

48. Zhang, X., et al., *Quinolone antibiotics induce Shiga toxin-encoding bacteriophages, toxin production, and death in mice.* J Infect Dis, 2000. **181**(2): p. 664-70.

49. Beaber, J.W., B. Hochhut, and M.K. Waldor, *SOS response promotes horizontal dissemination of antibiotic resistance genes.* Nature, 2004. **427**(6969): p. 72-4.

50. Ubeda, C., et al., *Antibiotic-induced SOS response promotes horizontal dissemination of pathogenicity island-encoded virulence factors in staphylococci.* Mol Microbiol, 2005. **56**(3): p. 836-44.

51. Lopatkin, A.J., et al., *Antibiotics as a selective driver for conjugation dynamics.* Nat Microbiol, 2016. **1**(6): p. 16044.

52. Souque, C., J.A. Escudero, and R.C. MacLean, *Integron activity accelerates the evolution of antibiotic resistance.* Elife, 2021. **10**.

53. Hocquet, D., et al., *Evidence for induction of integron-based antibiotic resistance by the SOS response in a clinical setting.* PLoS Pathog, 2012. **8**(6): p. e1002778.

54. López, E., et al., *Antibiotic-mediated recombination: ciprofloxacin stimulates SOS-independent recombination of divergent sequences in Escherichia coli.* Mol Microbiol, 2007. **64**(1): p. 83-93.

55. Bush, N.G., *The role of DNA gyrase in illegitimate recombination.* 2017, University of East Anglia.

56. Cirz, R.T., et al., *Inhibition of mutation and combating the evolution of antibiotic resistance.* PLoS Biol, 2005. **3**(6): p. e176.

57. Laureti, L., I. Matic, and A. Gutierrez, *Bacterial Responses and Genome Instability Induced by Subinhibitory Concentrations of Antibiotics.* Antibiotics (Basel), 2013. **2**(1): p. 100-14.

58. Gillespie, S.H., et al., *Effect of subinhibitory concentrations of ciprofloxacin on Mycobacterium fortuitum mutation rates.* J Antimicrob Chemother, 2005. **56**(2): p. 344-8.

59. Didier, J.P., et al., *Impact of ciprofloxacin exposure on Staphylococcus aureus genomic alterations linked with emergence of rifampin resistance.* Antimicrob Agents Chemother, 2011. **55**(5): p. 1946-52.

60. Nagel, M., et al., *Influence of ciprofloxacin and vancomycin on mutation rate and transposition of IS256 in Staphylococcus aureus.* Int J Med Microbiol, 2011. **301**(3): p. 229-36.

61. Lesher, G.Y., et al., *1,8-napthyridine derivates. A new class of chemotherapeutic agents.* J Med Pharm Chem, 1962. **91**: p. 1063-5.

62. Bisacchi, G.S., *Origins of the Quinolone Class of Antibacterials: An Expanded "Discovery Story".* J Med Chem, 2015. **58**(12): p. 4874-82.

63. WHO, *Critically Important Antimicrobials for Human Medicine, 5th ed.; World Health Organisation—WHO Advisory Group on Integrated Surveillance of Antimicrobial Resistance (AGISAR): Geneva, Switzerland.* 2017: p. pp. 48.

64. McKie, S.J., K.C. Neuman, and A. Maxwell, *DNA topoisomerases: Advances in understanding of cellular roles and multi-protein complexes via structure-function analysis.* Bioessays, 2021. **43**(4): p. e2000286.

65. Liu, L.F. and J.C. Wang, *Supercoiling of the DNA template during transcription.* Proc Natl Acad Sci U S A, 1987. **84**(20): p. 7024-7.

66. Funnell, B.E., T.A. Baker, and A. Kornberg, *Complete enzymatic replication of plasmids containing the origin of the Escherichia coli chromosome.* J Biol Chem, 1986. **261**(12): p. 5616-24.

67. Vanden Broeck, A., et al., *Cryo-EM structure of the complete E. coli DNA gyrase nucleoprotein complex.* Nat Commun, 2019. **10**(1): p. 4935.

68. Laponogov, I., et al., *Structural insight into the quinolone-DNA cleavage complex of type IIA topoisomerases.* Nat Struct Mol Biol, 2009. **16**(6): p. 667-9.

69.	Wohlkonig, A., et al., *Structural basis of quinolone inhibition of type IIA topoisomerases and target-mediated resistance.* Nat Struct Mol Biol, 2010. **17**(9): p. 1152-3.

70.	Bax, B.D., et al., *DNA Topoisomerase Inhibitors: Trapping a DNA-Cleaving Machine in Motion.* J Mol Biol, 2019. **431**(18): p. 3427-3449.

71.	Khodursky, A.B., E.L. Zechiedrich, and N.R. Cozzarelli, *Topoisomerase IV is a target of quinolones in Escherichia coli.* Proc Natl Acad Sci U S A, 1995. **92**(25): p. 11801-5.

72.	Jeong, K.S., et al., *Analysis of pleiotropic transcriptional profiles: a case study of DNA gyrase inhibition.* PLoS Genet, 2006. **2**(9): p. e152.

73.	Wentzell, L.M. and A. Maxwell, *The complex of DNA gyrase and quinolone drugs on DNA forms a barrier to the T7 DNA polymerase replication complex.* J Mol Biol, 2000. **304**(5): p. 779-91.

74.	Willmott, C.J., et al., *The complex of DNA gyrase and quinolone drugs with DNA forms a barrier to transcription by RNA polymerase.* J Mol Biol, 1994. **242**(4): p. 351-63.

75.	Chen, C.R., et al., *DNA gyrase and topoisomerase IV on the bacterial chromosome: quinolone-induced DNA cleavage.* J Mol Biol, 1996. **258**(4): p. 627-37.

76.	Zhao, X., et al., *Lethal action of quinolones against a temperature-sensitive dnaB replication mutant of Escherichia coli.* Antimicrob Agents Chemother, 2006. **50**(1): p. 362-4.

77.	Pribis, J.P., et al., *Gamblers: An Antibiotic-Induced Evolvable Cell Subpopulation Differentiated by Reactive-Oxygen-Induced General Stress Response.* Mol Cell, 2019. **74**(4): p. 785-800.e7.

78.	Henrikus, S.S., et al., *Single-molecule live-cell imaging reveals RecB-dependent function of DNA polymerase IV in double strand break repair.* Nucleic Acids Res, 2020. **48**(15): p. 8490-8508.

79.	Malik, M., X. Zhao, and K. Drlica, *Lethal fragmentation of bacterial chromosomes mediated by DNA gyrase and quinolones.* Mol Microbiol, 2006. **61**(3): p. 810-25.

80.	Piddock, L.J., R.N. Walters, and J.M. Diver, *Correlation of quinolone MIC and inhibition of DNA, RNA, and protein synthesis and induction of the SOS response in Escherichia coli.* Antimicrob Agents Chemother, 1990. **34**(12): p. 2331-6.

81.	Agarwal, R. and K.E. Duderstadt, *Multiplex flow magnetic tweezers reveal rare enzymatic events with single molecule precision.* Nature Communications, 2020. **11**(1): p. 4714.

82.	Malik, M., S. Hussain, and K. Drlica, *Effect of anaerobic growth on quinolone lethality with Escherichia coli.* Antimicrob Agents Chemother, 2007. **51**(1): p. 28-34.

83.	Shea, M.E. and H. Hiasa, *The RuvAB branch migration complex can displace topoisomerase IV.quinolone.DNA ternary complexes.* J Biol Chem, 2003. **278**(48): p. 48485-90.

84.	Pohlhaus, J.R. and K.N. Kreuzer, *Norfloxacin-induced DNA gyrase cleavage complexes block Escherichia coli replication forks, causing double-stranded breaks in vivo.* Mol Microbiol, 2005. **56**(6): p. 1416-29.

85.	Tsao, Y.P., et al., *Interaction between replication forks and topoisomerase I-DNA cleavable complexes: studies in a cell-free SV40 DNA replication system.* Cancer Res, 1993. **53**(24): p. 5908-14.

86.	Hsiang, Y.H., M.G. Lihou, and L.F. Liu, *Arrest of replication forks by drug-stabilized topoisomerase I-DNA cleavable complexes as a mechanism of cell killing by camptothecin.* Cancer Res, 1989. **49**(18): p. 5077-82.

87.	Strumberg, D., et al., *Conversion of topoisomerase I cleavage complexes on the leading strand of ribosomal DNA into 5'-phosphorylated DNA double-strand breaks by replication runoff.* Mol Cell Biol, 2000. **20**(11): p. 3977-87.

88. Cortés, F., J. Piñero, and T. Ortiz, *Importance of replication fork progression for the induction of chromosome damage and SCE by inhibitors of DNA topoisomerases.* Mutat Res, 1993. **303**(2): p. 71-6.

89. Goswami, M. and N. Jawali, *Glutathione-mediated augmentation of beta-lactam antibacterial activity against Escherichia coli.* J Antimicrob Chemother, 2007. **60**(1): p. 184-5.

90. Kohanski, M.A., M.A. DePristo, and J.J. Collins, *Sublethal antibiotic treatment leads to multidrug resistance via radical-induced mutagenesis.* Mol Cell, 2010. **37**(3): p. 311-20.

91. Dwyer, D.J., J.J. Collins, and G.C. Walker, *Unraveling the physiological complexities of antibiotic lethality.* Annu Rev Pharmacol Toxicol, 2015. **55**: p. 313-32.

92. Hong, Y., et al., *Contribution of reactive oxygen species to thymineless death in Escherichia coli.* Nat Microbiol, 2017. **2**(12): p. 1667-1675.

93. Drlica, K. and X. Zhao, *DNA gyrase, topoisomerase IV, and the 4-quinolones.* Microbiol Mol Biol Rev, 1997. **61**(3): p. 377-92.

94. Tamayo, M., et al., *Rapid assessment of the effect of ciprofloxacin on chromosomal DNA from Escherichia coli using an in situ DNA fragmentation assay.* BMC Microbiol, 2009. **9**: p. 69.

95. Turner, A.K., et al., *A whole-genome screen identifies Salmonella enterica serovar Typhi genes involved in fluoroquinolone susceptibility.* J Antimicrob Chemother, 2020. **75**(9): p. 2516-2525.

96. McDaniel, L.S., L.H. Rogers, and W.E. Hill, *Survival of recombination-deficient mutants of Escherichia coli during incubation with nalidixic acid.* J Bacteriol, 1978. **134**(3): p. 1195-8.

97. Liu, A., et al., *Antibiotic sensitivity profiles determined with an Escherichia coli gene knockout collection: generating an antibiotic bar code.* Antimicrob Agents Chemother, 2010. **54**(4): p. 1393-403.

98. de Campos-Nebel, M., I. Larripa, and M. González-Cid, *Topoisomerase II-mediated DNA damage is differently repaired during the cell cycle by non-homologous end joining and homologous recombination.* PLoS One, 2010. **5**(9).

99. Nakano, T., et al., *Nucleotide excision repair and homologous recombination systems commit differentially to the repair of DNA-protein crosslinks.* Mol Cell, 2007. **28**(1): p. 147-58.

100. Kreuzer, K.N., *DNA damage responses in prokaryotes: regulating gene expression, modulating growth patterns, and manipulating replication forks.* Cold Spring Harb Perspect Biol, 2013. **5**(11): p. a012674.

101. Cirz, R.T. and F.E. Romesberg, *Induction and inhibition of ciprofloxacin resistance-conferring mutations in hypermutator bacteria.* Antimicrob Agents Chemother, 2006. **50**(1): p. 220-5.

102. O'Sullivan, D.M., et al., *Mycobacterium tuberculosis DNA repair in response to subinhibitory concentrations of ciprofloxacin.* J Antimicrob Chemother, 2008. **62**(6): p. 1199-202.

103. Tattevin, P., L. Basuino, and H.F. Chambers, *Subinhibitory fluoroquinolone exposure selects for reduced beta-lactam susceptibility in methicillin-resistant Staphylococcus aureus and alterations in the SOS-mediated response.* Res Microbiol, 2009. **160**(3): p. 187-92.

104. López, E. and J. Blázquez, *Effect of subinhibitory concentrations of antibiotics on intrachromosomal homologous recombination in Escherichia coli.* Antimicrob Agents Chemother, 2009. **53**(8): p. 3411-5.

105. Long, H., et al., *Antibiotic treatment enhances the genome-wide mutation rate of target cells.* Proceedings of the National Academy of Sciences, 2016. **113**(18): p. E2498-E2505.

106. Yim, G., et al., *Modulation of Salmonella gene expression by subinhibitory concentrations of quinolones.* J Antibiot (Tokyo), 2011. **64**(1): p. 73-8.

107. Thi, T.D., et al., *Effect of recA inactivation on mutagenesis of Escherichia coli exposed to sublethal concentrations of antimicrobials.* J Antimicrob Chemother, 2011. **66**(3): p. 531-8.

108. Wang, P., et al., *Subinhibitory concentrations of ciprofloxacin induce SOS response and mutations of antibiotic resistance in bacteria.* Annals of Microbiology, 2010. **60**(3): p. 511-517.

109. Torres-Barceló, C., et al., *The SOS response increases bacterial fitness, but not evolvability, under a sublethal dose of antibiotic.* Proc Biol Sci, 2015. **282**(1816): p. 20150885.

110. Li, Y., et al., *Galleria mellonella - a novel infection model for the Mycobacterium tuberculosis complex.* Virulence, 2018. **9**(1): p. 1126-1137.

111. Song, L.Y., et al., *Mutational Consequences of Ciprofloxacin in Escherichia coli.* Antimicrobial agents and chemotherapy, 2016. **60**(10): p. 6165-6172.

112. Goswami, M., S.H. Mangoli, and N. Jawali, *Involvement of reactive oxygen species in the action of ciprofloxacin against Escherichia coli.* Antimicrob Agents Chemother, 2006. **50**(3): p. 949-54.

113. Kotova, V., A.S. Mironov, and G.B. Zavigel'skiĭ, *[Role of reactive oxygen species in the bactericidal action of quinolones--inhibitors of DNA gyrase].* Mol Biol (Mosk), 2014. **48**(6): p. 990-8.

114. Thomason, L.C., N. Costantino, and D.L. Court, *E. coli genome manipulation by P1 transduction.* Curr Protoc Mol Biol, 2007. **Chapter 1**: p. Unit 1.17.

115. Kieser, T., et al., *Practical streptomyces genetics.* 2000: John Innes Foundation.

116. Datsenko, K.A. and B.L. Wanner, *One-step inactivation of chromosomal genes in Escherichia coli K-12 using PCR products.* Proceedings of the National Academy of Sciences of the United States of America, 2000. **97**(12): p. 6640-6645.

117. Ryu, Y.S., et al., *A simple and effective method for construction of Escherichia coli strains proficient for genome engineering.* PloS one, 2014. **9**(4): p. e94266-e94266.

118. Andrews, J.M., *Determination of minimum inhibitory concentrations.* J Antimicrob Chemother, 2001. **48 Suppl 1**: p. 5-16.

119. Andrea, A., K.A. Krogfelt, and H. Jenssen, *Methods and Challenges of Using the Greater Wax Moth (Galleria mellonella) as a Model Organism in Antimicrobial Compound Discovery.* Microorganisms, 2019. **7**(3): p. 85.

120. Huang, S.N., et al., *Exonuclease VII repairs quinolone-induced damage by resolving DNA gyrase cleavage complexes.* Sci Adv, 2021. **7**(10).

121. Aedo, S. and Y.C. Tse-Dinh, *SbcCD-mediated processing of covalent gyrase-DNA complex in Escherichia coli.* Antimicrob Agents Chemother, 2013. **57**(10): p. 5116-9.

122. Sun, Y., et al., *A conserved SUMO pathway repairs topoisomerase DNA-protein cross-links by engaging ubiquitin-mediated proteasomal degradation.* Sci Adv, 2020. **6**(46).

123. Sun, Y., et al., *Excision repair of topoisomerase DNA-protein crosslinks (TOP-DPC).* DNA Repair (Amst), 2020. **89**: p. 102837.

124. Yang, S.W., et al., *A eukaryotic enzyme that can disjoin dead-end covalent complexes between DNA and type I topoisomerases.* Proceedings of the National Academy of Sciences of the United States of America, 1996. **93**(21): p. 11534-11539.

125. Cortes Ledesma, F., et al., *A human 5'-tyrosyl DNA phosphodiesterase that repairs topoisomerase-mediated DNA damage.* Nature, 2009. **461**(7264): p. 674-8.

126. Pommier, Y., et al., *Tyrosyl-DNA-phosphodiesterases (TDP1 and TDP2).* DNA Repair, 2014. **19**: p. 114-129.

127. Pouliot, J.J., et al., *Yeast gene for a Tyr-DNA phosphodiesterase that repairs topoisomerase I complexes.* Science, 1999. **286**(5439): p. 552-5.

128. Piddock, L.J. and R.N. Walters, *Bactericidal activities of five quinolones for Escherichia coli strains with mutations in genes encoding the SOS response or cell division.* Antimicrob Agents Chemother, 1992. **36**(4): p. 819-25.

129. Dillingham, M.S. and S.C. Kowalczykowski, *RecBCD enzyme and the repair of double-stranded DNA breaks.* Microbiol Mol Biol Rev, 2008. **72**(4): p. 642-71, Table of Contents.

130. Heisig, P., *Type II topoisomerases—inhibitors, repair mechanisms and mutations.* Mutagenesis, 2009. **24**(6): p. 465-469.

131. Mitelheiser, S., *DNA gyrase, quinolone drugs and supercoiling mechanism.* 2005, University of East Anglia.

132. Drlica, K., et al., *Bypassing fluoroquinolone resistance with quinazolinediones: studies of drug-gyrase-DNA complexes having implications for drug design.* ACS Chem Biol, 2014. **9**(12): p. 2895-904.

133. Germe, T., et al., *A new class of antibacterials, the imidazopyrazinones, reveal structural transitions involved in DNA gyrase poisoning and mechanisms of resistance.* Nucleic acids research, 2018. **46**(8): p. 4114-4128.

134. Kelley, L.A., et al., *The Phyre2 web portal for protein modeling, prediction and analysis.* Nature Protocols, 2015. **10**(6): p. 845-858.

135. Lovett, S.T., *The DNA Exonucleases of Escherichia coli.* EcoSal Plus, 2011. **4**(2).

136. Notredame, C., D.G. Higgins, and J. Heringa, *T-Coffee: A novel method for fast and accurate multiple sequence alignment.* J Mol Biol, 2000. **302**(1): p. 205-17.

137. Drlica, K., et al., *Quinolones: action and resistance updated.* Curr Top Med Chem, 2009. **9**(11): p. 981-98.

138. Wang, X., et al., *Contribution of reactive oxygen species to pathways of quinolone-mediated bacterial cell death.* J Antimicrob Chemother, 2010. **65**(3): p. 520-4.

139. Schellenberg, M.J., et al., *Mechanism of repair of 5'-topoisomerase II–DNA adducts by mammalian tyrosyl-DNA phosphodiesterase 2.* Nature Structural & Molecular Biology, 2012. **19**(12): p. 1363-1371.

140. Nitiss, J.L. and K.C. Nitiss, *Tdp2: a means to fixing the ends.* PLoS genetics, 2013. **9**(3): p. e1003370-e1003370.

141. Gorini, F., et al., *Towards a comprehensive view of 8-oxo-7,8-dihydro-2'-deoxyguanosine: Highlighting the intertwined roles of DNA damage and epigenetics in genomic instability.* DNA Repair (Amst), 2021. **97**: p. 103027.

142. Li, F., et al., *Apn2 resolves blocked 3' ends and suppresses Top1-induced mutagenesis at genomic rNMP sites.* Nat Struct Mol Biol, 2019. **26**(3): p. 155-163.

143. Lu, S., P.B. Killoran, and L.W. Riley, *Association of Salmonella enterica serovar enteritidis yafD with resistance to chicken egg albumen.* Infect Immun, 2003. **71**(12): p. 6734-41.

144. Aldred, K.J., A. Payne, and O. Voegerl, *A RADAR-based assay to isolate covalent DNA complexes in bacteria.* Antibiotics (Basel), 2019. **8**(1).

145. Ogiso, Y., et al., *Proteasome inhibition circumvents solid tumor resistance to topoisomerase II-directed drugs.* Cancer Res, 2000. **60**(9): p. 2429-34.

146. Mao, Y., et al., *26 S proteasome-mediated degradation of topoisomerase II cleavable complexes.* J Biol Chem, 2001. **276**(44): p. 40652-8.

147. Vaz, B., et al., *Metalloprotease SPRTN/DVC1 Orchestrates Replication-Coupled DNA-Protein Crosslink Repair.* Mol Cell, 2016. **64**(4): p. 704-719.

148. Hoa, N.N., et al., *Mre11 Is Essential for the Removal of Lethal Topoisomerase 2 Covalent Cleavage Complexes.* Mol Cell, 2016. **64**(3): p. 580-592.

149. Kametani, Y., et al., *FEN1 participates in repair of the 5'-phosphotyrosyl terminus of DNA single-strand breaks.* Carcinogenesis, 2016. **37**(1): p. 56-62.

150. Serrano-Benítez, A., F. Cortés-Ledesma, and J.F. Ruiz, *"An End to a Means": How DNA-End Structure Shapes the Double-Strand Break Repair Process.* Frontiers in Molecular Biosciences, 2020. **6**(153).

151. Li, X. and W.-D. Heyer, *Homologous recombination in DNA repair and DNA damage tolerance.* Cell Research, 2008. **18**(1): p. 99-113.

152. Gottesman, S., *Proteases and their targets in Escherichia coli.* Annual Review of Genetics, 1996. **30**(1): p. 465-506.

153. Kessel, M., et al., *Homology in structural organization between E. coli ClpAP protease and the eukaryotic 26 S proteasome.* J Mol Biol, 1995. **250**(5): p. 587-94.

154. Bochtler, M., et al., *The structures of HslU and the ATP-dependent protease HslU–HslV.* Nature, 2000. **403**(6771): p. 800-805.

155. Malik, M., J. Capecci, and K. Drlica, *Lon protease is essential for paradoxical survival of Escherichia coli exposed to high concentrations of quinolone.* Antimicrob Agents Chemother, 2009. **53**(7): p. 3103-5.

156. Theodore, A., K. Lewis, and M. Vulić, *Tolerance of Escherichia coli to Fluoroquinolone Antibiotics Depends on Specific Components of the SOS Response Pathway.* Genetics, 2013. **195**(4): p. 1265-1276.

157. Yamaguchi, Y., et al., *Effects of disruption of heat shock genes on susceptibility of Escherichia coli to fluoroquinolones.* BMC Microbiol, 2003. **3**: p. 16.

158. Newmark, K.G., et al., *Genetic analysis of the requirements for SOS induction by nalidixic acid in Escherichia coli.* Gene, 2005. **356**: p. 69-76.

159. Tamae, C., et al., *Determination of antibiotic hypersensitivity among 4,000 single-gene-knockout mutants of Escherichia coli.* Journal of bacteriology, 2008. **190**(17): p. 5981-5988.

160. Chayot, R., et al., *An end-joining repair mechanism in Escherichia coli.* Proc Natl Acad Sci U S A, 2010. **107**(5): p. 2141-6.

161. Wilkinson, M., et al., *Structural basis for the inhibition of RecBCD by Gam and its synergistic antibacterial effect with quinolones.* Elife, 2016. **5**.

162. Gur, E. and R.T. Sauer, *Recognition of misfolded proteins by Lon, a AAA(+) protease.* Genes Dev, 2008. **22**(16): p. 2267-77.

163. Langklotz, S. and F. Narberhaus, *The Escherichia coli replication inhibitor CspD is subject to growth-regulated degradation by the Lon protease.* Molecular Microbiology, 2011. **80**(5): p. 1313-1325.

164. Sonezaki, S., et al., *Overproduction and purification of Lon protease fromEscherichia coli using a maltose-binding protein fusion system.* Applied Microbiology and Biotechnology, 1994. **42**(2): p. 313-318.

165. Karlowicz, A., et al., *Defining the crucial domain and amino acid residues in bacterial Lon protease for DNA binding and processing of DNA-interacting substrates.* J Biol Chem, 2017. **292**(18): p. 7507-7518.

166. Sharma, P., et al., *The multiple antibiotic resistance operon of enteric bacteria controls DNA repair and outer membrane integrity.* Nature Communications, 2017. **8**(1): p. 1444.

167. Ghodke, H., et al., *Spatial and temporal organization of RecA in the Escherichia coli DNA-damage response.* Elife, 2019. **8**.

168. Keyamura, K., et al., *RecA protein recruits structural maintenance of chromosomes (SMC)-like RecN protein to DNA double-strand breaks.* J Biol Chem, 2013. **288**(41): p. 29229-37.

169. Shee, C., et al., *Engineered proteins detect spontaneous DNA breakage in human and bacterial cells.* Elife, 2013. **2**: p. e01222.

170. Uranga, L.A., et al., *The cohesin-like RecN protein stimulates RecA-mediated recombinational repair of DNA double-strand breaks.* Nature Communications, 2017. **8**(1): p. 15282.

171. Blattner, F.R., et al., *The complete genome sequence of Escherichia coli K-12.* Science, 1997. **277**(5331): p. 1453-62.

172. Grenier, F., et al., *Complete Genome Sequence of Escherichia coli BW25113.* Genome announcements, 2014. **2**(5): p. e01038-14.

173. Baba, T., et al., *Construction of Escherichia coli K-12 in-frame, single-gene knockout mutants: the Keio collection.* Molecular systems biology, 2006. **2**: p. 2006.0008-2006.0008.

174. Mi, H., et al., *Dimethyl Sulfoxide Protects Escherichia coli from Rapid Antimicrobial-Mediated Killing.* Antimicrob Agents Chemother, 2016. **60**(8): p. 5054-8.

175. Tashiro, Y., et al., *Generation of Small Colony Variants in Biofilms by Escherichia coli Harboring a Conjugative F Plasmid.* Microbes Environ, 2017. **32**(1): p. 40-46.

176. Dörr, T., M. Vulić, and K. Lewis, *Ciprofloxacin causes persister formation by inducing the TisB toxin in Escherichia coli.* PLoS Biol, 2010. **8**(2): p. e1000317.

177. Kiran Sidhu, M.T., Kirstin Van Mil, and Meghan Verstraete, *Treatment with sub-inhibitory kanamycin induces adaptive resistance to aminoglycoside antibiotics via the AcrD multidrug efflux pump in Escherichia coli K-12.* Journal of Experimental Microbiology and Immunology, 2012. **16**(11-16).

178. Pitruzzello, G., et al., *Multiparameter antibiotic resistance detection based on hydrodynamic trapping of individual E. coli.* Lab Chip, 2019. **19**(8): p. 1417-1426.

179. Dapa, T., et al., *The SOS and RpoS Regulons Contribute to Bacterial Cell Robustness to Genotoxic Stress by Synergistically Regulating DNA Polymerase Pol II.* Genetics, 2017. **206**(3): p. 1349-1360.

180. Minato, Y., et al., *Mutual potentiation drives synergy between trimethoprim and sulfamethoxazole.* Nat Commun, 2018. **9**(1): p. 1003.

181. Linde, H.J., et al., *In vivo increase in resistance to ciprofloxacin in Escherichia coli associated with deletion of the C-terminal part of MarR.* Antimicrob Agents Chemother, 2000. **44**(7): p. 1865-8.

182. Wang, X., et al., *Cryptic prophages help bacteria cope with adverse environments.* Nat Commun, 2010. **1**: p. 147.

183. Mehta, P., S. Casjens, and S. Krishnaswamy, *Analysis of the lambdoid prophage element e14 in the E. coli K-12 genome.* BMC microbiology, 2004. **4**: p. 4-4.

184. Ching, C. and M.H. Zaman, *Development and selection of low-level multi-drug resistance over an extended range of sub-inhibitory ciprofloxacin concentrations in Escherichia coli.* Scientific Reports, 2020. **10**(1): p. 8754.

185. Ruiz, C. and S.B. Levy, *Many chromosomal genes modulate MarA-mediated multidrug resistance in Escherichia coli.* Antimicrob Agents Chemother, 2010. **54**(5): p. 2125-34.

186. Suzuki, S., T. Horinouchi, and C. Furusawa, *Acceleration and suppression of resistance development by antibiotic combinations.* BMC Genomics, 2017. **18**(1): p. 328.

187. Duval, V., H. Nicoloff, and S.B. Levy, *Combined inactivation of lon and ycgE decreases multidrug susceptibility by reducing the amount of OmpF porin in Escherichia coli.* Antimicrob Agents Chemother, 2009. **53**(11): p. 4944-8.

188. Okusu, H., D. Ma, and H. Nikaido, *AcrAB efflux pump plays a major role in the antibiotic resistance phenotype of Escherichia coli multiple-antibiotic-resistance (Mar) mutants.* J Bacteriol, 1996. **178**(1): p. 306-8.

189. Martínez, J.L. and F. Rojo, *Metabolic regulation of antibiotic resistance.* FEMS Microbiol Rev, 2011. **35**(5): p. 768-89.

190. Hill, C.W., J.A. Gray, and H. Brody, *Use of the isocitrate dehydrogenase structural gene for attachment of e14 in Escherichia coli K-12.* J Bacteriol, 1989. **171**(7): p. 4083-4.

191. Edgar, R. and E. Bibi, *MdfA, an Escherichia coli multidrug resistance protein with an extraordinarily broad spectrum of drug recognition.* J Bacteriol, 1997. **179**(7): p. 2274-80.

192. Suarez, S.A. and A.C. Martiny, *Gene Amplification Uncovers Large Previously Unrecognized Cryptic Antibiotic Resistance Potential in E. coli.* Microbiol Spectr, 2021. **9**(3): p. e0028921.

193. Yasufuku, T., et al., *Correlation of overexpression of efflux pump genes with antibiotic resistance in Escherichia coli Strains clinically isolated from urinary tract infection patients.* J Clin Microbiol, 2011. **49**(1): p. 189-94.

194. Wolff, E., et al., *Polymerases leave fingerprints: analysis of the mutational spectrum in Escherichia coli rpoB to assess the role of polymerase IV in spontaneous mutation.* J Bacteriol, 2004. **186**(9): p. 2900-5.

195. Andersson, D.I. and D. Hughes, *Gene amplification and adaptive evolution in bacteria.* Annu Rev Genet, 2009. **43**: p. 167-95.

196. Hjort, K., H. Nicoloff, and D.I. Andersson, *Unstable tandem gene amplification generates heteroresistance (variation in resistance within a population) to colistin in Salmonella enterica.* Mol Microbiol, 2016. **102**(2): p. 274-289.

197. Bombelli, P., C.J. Howe, and F. Bertocchini, *Polyethylene bio-degradation by caterpillars of the wax moth Galleria mellonella.* Curr Biol, 2017. **27**(8): p. R292-r293.

198. Peleg, A.Y., et al., *Galleria mellonella as a model system to study Acinetobacter baumannii pathogenesis and therapeutics.* Antimicrob Agents Chemother, 2009. **53**(6): p. 2605-9.

199. Jander, G., L.G. Rahme, and F.M. Ausubel, *Positive correlation between virulence of Pseudomonas aeruginosa mutants in mice and insects.* J Bacteriol, 2000. **182**(13): p. 3843-5.

200. Purves, J., et al., *Comparison of the regulation, metabolic functions, and roles in virulence of the glyceraldehyde-3-phosphate dehydrogenase homologues gapA and gapB in Staphylococcus aureus.* Infect Immun, 2010. **78**(12): p. 5223-32.

201. Brennan, M., et al., *Correlation between virulence of Candida albicans mutants in mice and Galleria mellonella larvae.* FEMS Immunol Med Microbiol, 2002. **34**(2): p. 153-7.

202. Salamitou, S., et al., *The plcR regulon is involved in the opportunistic properties of Bacillus thuringiensis and Bacillus cereus in mice and insects.* Microbiology (Reading), 2000. **146**: p. 2825-2832.

203. Kavanagh, K. and E.P. Reeves, *Exploiting the potential of insects for in vivo pathogenicity testing of microbial pathogens.* FEMS Microbiol Rev, 2004. **28**(1): p. 101-12.

204. Cutuli, M.A., et al., *Galleria mellonella as a consolidated in vivo model hosts: New developments in antibacterial strategies and novel drug testing.* Virulence, 2019. **10**(1): p. 527-541.

205. Pereira, T.C., et al., *Recent Advances in the Use of Galleria mellonella Model to Study Immune Responses against Human Pathogens.* J Fungi (Basel), 2018. **4**(4).

206. Allonsius, C.N., et al., *The microbiome of the invertebrate model host Galleria mellonella is dominated by Enterococcus.* Animal Microbiome, 2019. **1**(1): p. 7.

207. Jarosz, J., *Gut flora of Galleria mellonella suppressing ingested bacteria.* Journal of Invertebrate Pathology, 1979. **34**(2): p. 192-198.

208. Waterhouse, D.F., *Axenic culture of was moths for digestion studies.* Annals of the New York Academy of Sciences, 1959. **77**(2): p. 283-289.

209. Dudziak, B., *Studies on the role of microorganisms in alimentation of Galleria mellonella larvae.* Ann. Univ. Mariae Curie-Skiodowska Sect. C, 1975. **30**: p. 15-22.

210. Ignasiak, K. and A. Maxwell, *Oxytetracycline reduces the diversity of tetracycline-resistance genes in the Galleria mellonella gut microbiome.* BMC Microbiology, 2018. **18**(1): p. 228.

211. Alghoribi, M.F., et al., *Galleria mellonella infection model demonstrates high lethality of ST69 and ST127 uropathogenic E. coli.* PloS one, 2014. **9**(7): p. e101547-e101547.

212. Jønsson, R., et al., *The wax moth Galleria mellonella as a novel model system to study Enteroaggregative Escherichia coli pathogenesis.* Virulence, 2017. **8**(8): p. 1894-1899.

213. Sugeçti, S., *Biochemical and immune responses of model organism Galleria mellonella after infection with Escherichia coli.* Entomologia Experimentalis et Applicata, 2021.

214. Lange, A., A. Schäfer, and J.S. Frick, *A Galleria mellonella oral administration model to study commensal-induced innate immune responses.* J Vis Exp, 2019(145).

215. Ignasiak, K.B., *Investigating antimicrobial resistance in the gut bacteria of insects feeding on plants.* 2016, University of East Anglia.

216. Moya-Andérico, L., et al., *Monitoring Gene Expression during a Galleria mellonella Bacterial Infection.* Microorganisms, 2020. **8**(11).

217. Crespo-Ortiz, M.d.P., M.E. Burbano, and M. Barreto, *Pathogenesis and in vivo interactions of human Streptococcus agalactiae isolates in the Galleria mellonella invertebrate model.* Microbial Pathogenesis, 2020. **147**: p. 104400.

218. Boshoff, H.I., et al., *DnaE2 polymerase contributes to in vivo survival and the emergence of drug resistance in Mycobacterium tuberculosis.* Cell, 2003. **113**(2): p. 183-93.

219. Alam, M.K., et al., *RecA Inhibitors Potentiate Antibiotic Activity and Block Evolution of Antibiotic Resistance.* Cell Chem Biol, 2016. **23**(3): p. 381-91.

220. Luther, M.K., et al., *Activity of daptomycin or linezolid in combination with rifampin or gentamicin against biofilm-forming Enterococcus faecalis or E. faecium in an in vitro pharmacodynamic model using simulated endocardial vegetations and an in vivo survival assay using Galleria mellonella larvae.* Antimicrob Agents Chemother, 2014. **58**(8): p. 4612-20.

221. Johnston, P.R. and J. Rolff, *Host and Symbiont Jointly Control Gut Microbiota during Complete Metamorphosis.* PLoS Pathog, 2015. **11**(11): p. e1005246.

222. Mitscher, L.A., *Bacterial topoisomerase inhibitors: quinolone and pyridone antibacterial agents.* Chem Rev, 2005. **105**(2): p. 559-92.

223. Bush, N.G., et al., *Quinolones: Mechanism, Lethality and Their Contributions to Antibiotic Resistance.* Molecules, 2020. **25**(23).

224. Morimoto, S., et al., *Type II DNA Topoisomerases Cause Spontaneous Double-Strand Breaks in Genomic DNA.* Genes, 2019. **10**(11): p. 868.

225. Pommier, Y., et al., *DNA Topoisomerases and Their Poisoning by Anticancer and Antibacterial Drugs.* Chemistry & Biology, 2010. **17**(5): p. 421-433.

226. Connelly, J.C. and D.R. Leach, *The sbcC and sbcD genes of Escherichia coli encode a nuclease involved in palindrome inviability and genetic recombination.* Genes Cells, 1996. **1**(3): p. 285-91.

227. Couce, A. and J. Blázquez, *Side effects of antibiotics on genetic variability.* FEMS Microbiology Reviews, 2009. **33**(3): p. 531-538.

228. Frenoy, A. and S. Bonhoeffer, *Death and population dynamics affect mutation rate estimates and evolvability under stress in bacteria.* PLoS Biol, 2018. **16**(5): p. e2005056.

229. Blázquez, J., J. Rodríguez-Beltrán, and I. Matic, *Antibiotic-Induced Genetic Variation: How It Arises and How It Can Be Prevented.* Annu Rev Microbiol, 2018. **72**: p. 209-230.

Appendix I

Table I. List of oligonucleotides.

Name	5'-3' sequence	Comments
yafD-pKD4_FW	CACCTATGCCATGCGCTATGTTGCCGGA CAACCTGCGGAAGTGTAGGCTGGAGCT GCTTC	Amplification fragment containing FRT and Cam^R
yafD-pKD4_RV	CGCCAAACGTTGGTCTGCCCTGTGGCA GACCTGACATACCATGGGAATTAGCCAT GGTCC	Amplification fragment containing FRT and Cam^R
ybhP-pKD4_FW	CCGACTACACTATTTCAATGAGATAAGA GGCAAAGACAGGGTGTAGGCTGGAGCT GCTTC	Amplification fragment containing FRT and Kan^R
ybhP-pKD4_RV	CTCCGCACTTAAAGGGGCATGATCAGAA AGGTGTCGCCATATGGGAATTAGCCATG GTCC	Amplification fragment containing FRT and Kan^R
xthA-pKD4_FW	CAACAGGCGGTAAGCAACGCGAAATTCT GCTACCATCCACGTGTAGGCTGGAGCT GCTTC	Amplification fragment containing FRT and Kan^R
xthA-pKD4_RV	GTTAATTCTCCTGACCCAGTTTGAGCCA GGAGAGCTGCATGGGAATTAGCCATGG TCC	Amplification fragment containing FRT and Kan^R
yafD_H1_FW	CTATGCCATGCGCTATGTTG	Confirmation of *yafD* deletion
yafD_H2_RV	CTGTGGCAGACCTGACATAC	Confirmation of *yafD* deletion
ybhP_H1_FW	GAGATAAGAGGCAAAGACAGG	Confirmation of *ybhP* deletion
ybhP_H2_RV	CATGATCAGAAAGGTGTCGC	Confirmation of *ybhP* deletion
xthA_H1_FW	CGGTAAGCAACGCGAAATTC	Confirmation of *xthA* deletion
xthA_H2_RV	GTTAATTCTCCTGACCCAG	Confirmation of *xthA* deletion
yafD-pET28_FW	TTGTATTTCCAGGGCGTGCGAAAAAACA CCTATGCCATGCGCTAT	Amplification of the insert with *yafD* in pET28-MHL
yafD-pET28_RV	CAAGCTTCGTCATCATTATTTATCAGGCT TGCCGGGACTG	Amplification of the insert with *yafD* in pET28-MHL
ybhP-pET28_FW	TGTATTTCCAGGGCATGCCCGATCAAAC ACAACAATTTTCG	Amplification of the insert with *ybhP* in pET28-MHL
ybhP-pET28_RV	CAAGCTTCGTCATCATCATAAATGAATCT CCGCAC	Amplification of the insert with *ybhP* in pET28-MHL
xthA-pET28_FW	TTGTATTTCCAGGGCATGAAATTTGTCTC TTTTAATATCAACGGCCTGCGC	Amplification of the insert with *xthA* in pET28-MHL
xthA-pET28_RV	CAAGCTTCGTCATCATTAGCGGCGGAAG GTC	Amplification of the insert with *xthA* in pET28-MHL
T7-pET28_FW	AATTAATACGACTCACTATAGGG	Confirmation of insertion in pET28-MHL and pOPIN
T7-pET28_RV	ATGCTAGTTATTGCTCAGCGG	Confirmation of insertion in pET28-MHL

pCS6_T7_FW	CATACTCCCGCCATTCAGAGAAG	Confirmation of T7 in pCS6
pCS6_T7_RV	GAGACTTAGCGCAAGCCATGATG	Confirmation of T7 in pCS6
T7-pOPIN_RV	GGTTATGCTAGTTACATATGGG	Confirmation of insertion in pOPIN
yafD-pOPIN_FW	AAGTTCTGTTTCAGGGCCCGGTGCGAAAAAACACCTATGCCAT	Amplification of the insert with *yafD* in pOPIN
yafD-pOPIN_RV	ATGGTCTAGAAAGCTTTATTATTATTTATCAGGCTTGCCGGG	Amplification of the insert with *yafD* in pOPIN
TDP2-pOPIN_FW	AAGTTCTGTTTCAGGGCCCGATGGAGTTGGGGGAGTTGCCT	Amplification of the insert with *TDP2* in pOPIN
TDP2-pOPIN_RV	ATGGTCTAGAAAGCTTTATTATTACAATATTATATCTAAGTTGC	Amplification of the insert with *TDP2* in pOPIN
xseA-pKD4_FW	GGTTACTATCGACTGAATAACCTGCTGATTTAGAATTTGATCTCGCTCACGTGTAGGCTGGAGCTGCTTC	Amplification fragment containing FRT and Kan^R
xseA-pKD4_RV	CAGCACGGGCATGGCTTGATATCGAAAAAACGCGTTGAATTCGTGCTGGCATGGGAATTAGCCATGGTCC	Amplification fragment containing FRT and Kan^R
recB-pKD4_FW	AGCGCGTTGCAGCAAACAATGCCCCTGATGAGTGAAAAGAGTGTAGGCTGGAGCTGCTTC	Amplification fragment containing FRT and Kan^R
recB-pKD4_RV	TTGTGCTCCACAGCTTCCAGTAATTGCTTTTGCAATTTCAATGGGAATTAGCCATGGTCC	Amplification fragment containing FRT and Kan^R
recC-pKD4_FW	TGCATTGCCCGAATCGTCAGTAGTCAGGAGCCGCTGTGTAGGCTGGAGCTGCTTC	Amplification fragment containing FRT and Kan^R
recC-pKD4_RV	GTAAGCGGATAGATTGCGCAATTTTTATACAGCACATGGGAATTAGCCATGGTCC	Amplification fragment containing FRT and Kan^R
sbc-pKD4_FW	ACATCTGTTTGGGTATAATCGCGCCCATGCTTTTTCGCCAGGGAACCGTTGTGTAGGCTGGAGCTGCTTC	Amplification fragment containing FRT and Kan^R
sbc-pKD4_RV	CAAGGCCAAGAGATAATTCGCCCCTCTGTATTCATTATCCTGCTGAATAGATGGGAATTAGCCATGGTCC	Amplification fragment containing FRT and Kan^R
clpP-pKD4_FW	AGGTTACAATCGGTACAGCAGGTTTTTTCAATTTTATCCAGGAGACGGAAGTGTAGGCTGGAGCTGCTTC	Amplification fragment containing FRT and Kan^R
clpP-pKD4_RV	AGCGTTGTGCCGCCCTGGATAAGTATAGCGGCACAGTTGCGCCTCTGGCAATGGGAATTAGCCATGGTCC	Amplification fragment containing FRT and Kan^R
lon-pKD4_FW	ATCTGATTACCTGGCGGAAATTAAACTAAGAGAGAGCTCTGTGTAGGCTGGAGCTGCTTC	Amplification fragment containing FRT and Kan^R
lon-pKD4_RV	TGCCAGCCCTGTTTTTATTAGTGCATTTTGCGCGAGGTCAATGGGAATTAGCCATGGTCC	Amplification fragment containing FRT and Kan^R
recA-pKD4_FW	ATATCCTTACAACTTAAAAAAGCAAAAGGGCCGCAGATGCGACCGTGTAGGCTGGAGCTGCTTC	Amplification fragment containing FRT and Kan^R

recA-pKD4_RV	GCTTCAACAGAACATATTGACTATCCGG TATTACCCGGCATGACAGGAGCATATGA ATATCCTCCTTA	Amplification fragment containing FRT and Kan^R
recA-H1_FW	ATTGACTATCCGGTATTACCCGGCA	Confirmation of *recA* deletion
recA-H2_RV	GCCGCAGATGCGACCCTTGTGTATC	Confirmation of *recA* deletion
sbc_FW	TTGGGTATAATCGCGCCCAT	Confirmation of *sbcCD* deletion
sbc_RV	CAAGGCCAAGAGATAATTCG	Confirmation of *sbcCD* deletion
xseA-H1_FW	GGGTTACTATCGACTGAATAAC	Confirmation of *xseA* deletion
xseA-H2_RV	CACGGGCATGGCTTGATATCG	Confirmation of *xseA* deletion
clp_FW	GTTACAATCGGTACAGCAGG	Confirmation of *clpP* deletion
clp_RV	CTGGATAAGTATAGCGGCAC	Confirmation of *clpP* deletion
recB-2788_FW	GCGCGTTGCAGCAAACAATG	Confirmation of *recB* deletion
recB-2788_RV	AGCGGGCGTAGCTGTTTGTG	Confirmation of *recB* deletion
recC-2790_FW	GGCAGGTCAACCGAATGCAG	Confirmation of *recC* deletion
recC-2790_RV	CCCAAAGGGCAACTAACAAC	Confirmation of *recC* deletion
lon-H1_FW	TCGTGTCATCTGATTACCTG	Confirmation of *lon* deletion
lon-H2_RV	CGATCCGCCATCTAACTTAG	Confirmation of *lon* deletion
pBAD_FW	ATGCCATAGCATTTTTATCC	Confirmation of Gam in pBAD
pBAD_RV	GATTTAATCTGTATCAGG	Confirmation of Gam in pBAD
pOPIN-Lon_FW	AAGTTCTGTTTCAGGGCCCGATGAATCC TGAGCGTTCTGA	Amplification of the insert with *lon* in pOPIN
pOPIN-Lon_RV	ATGGTCTAGAAAGCTTTACTATTTTGCAG TCACAACCT	Amplification of the insert with *lon* in pOPIN
DsRed2-RecB_FW	GTTCCTGTAAGAATTATGAGTGATGTCG CCGAG	Amplification of the insert with *recB* in DsRed2-pBAD
eGFP-RecB_FW	GTACAAGTAAGAATTATGAGTGATGTCG CCGAG	Amplification of the insert with *recB* in eGFP-pBAD
DsRed2-RecB_RV	GCCAAGCTTCGAATTTTACGCCTCCTCC AGGGTCA	Amplification of the insert with *recB* in DsRed2-pBAD and eGFP-pBAD
dinB-pKD4_FW	TCTCAAACCCTGAAATCACTGTATACTTT ACCAGTGTTGAGAGGTGAGCAGTGTAG GCTGGAGCTGCTTC	Amplification fragment containing FRT and Kan^R
dinB-pKD4_RV	CAGTGATACCCTCATAATAATGCACACC AGAATATACATAATAGTATACAATGGGAA TTAGCCATGGTCC	Amplification fragment containing FRT and Kan^R

polB-pKD4_FW	CAAACGAAACCAGGCTATACTCAAGCCT GGTTTTTTGATGGATTTTCAGCGTGTAG GCTGGAGCTGCTTC	Amplification fragment containing FRT and Kan^R
polB-pKD4_RV	AAAGCATTCGTCACGCATCAAAATGGTA TCTGGCGAACTCTTTTTTTTGCATGGGA ATTAGCCATGGTCC	Amplification fragment containing FRT and Kan^R
umuD-pkD4_FW	CAAGAACAGACTACTGTATATAAAAACA GTATAACTTCAGGCAGATTATTGTGTAG GCTGGAGCTGCTTC	Amplification fragment containing FRT and Kan^R
umuD-pKD4_RV	CACCGTCTCACAGCTGGCATAAAACGC GTTTACATCACAGAGGGCAAACAATGGG AATTAGCCATGGTCC	Amplification fragment containing FRT and Kan^R
dinB-H1_FW	CCAGTGTTGAGAGGTGAGCA	Confirmation of *dinB* deletion
dinB-H2_RV	CCCTCATAATAATGCACACCAG	Confirmation of *dinB* deletion
polB-H1_FW	CAGGCTATACTCAAGCCTGG	Confirmation of *polB* deletion
polB-H2_RV	GCAAAGCATTCGTCACGCATC	Confirmation of *polB* deletion
umuD-H1_FW	GATCTGCTGGCAAGAACAGAC	Confirmation of *umuD* deletion
umuD-H2_RV	GCGTTTACATCACAGAGGGC	Confirmation of *umuD* deletion
lexA.A1_FW	TGAATGGCGAATGGCATTCAAGCCGAAT GCTGATTTCCTGCTGCGCGTCAGCGGG ATGGCG	Amplification of fragment A
lexA.A2_FW	GTCAGCGGGATGGCGATGAAAGATATC GGCATTATG	Amplification of fragment A2
lexA.A2_RV	TTACAGCCAGTCGCCGTTGCGAATA	Amplification of fragment A2 and A
lexA.B1_FW	GGCGACTGGCTGTAAGAGCTGCTTCGA AGTTCCTATACT	Amplification of fragment B1 and B
lexA.B1_RV	GTTCCTATTCCGAAGTTCC	Amplification of fragment B1
lexA.B2_RV	AATACCGCATCAGGCGATGAAAAACAAA CCGCGACGCCAGGCGGCATCGCGGTCT CAGAGATATGGTTCCTATTCCGAAG	Amplification of fragment B
pUC19.lexA_FW	ATTCAAGCCGAATGCTGATTTCCTG	Confirmation of the *lexA*(S119A) cassette in pUC19
pUC19.lexA_RV	AAACCGCGACGCCAGGCGGCAT	Confirmation of the *lexA*(S119A) cassette in pUC19
lexA_A_H1KanR_FW	GATCCTTCCTTATTCAAGCCGAATGCTG ATTTCCTGCTGCGCGTCAGCGGGATGG CG	Amplification of fragment lexA1
lexA_A_H1KanR_RV	GCCCAGTCATAGCCGAATA	Amplification of fragment lexA1
lexA_B_H2KanR_FW	CTATTCGGCTATGACTGGGCACAACAGA CAATCG	Amplification of fragment lexA2

lexA_B_H2K anR_RV	GATGAAAAACAAACCGCGACGCCAGGC GGCATCGCGGTCTCAGAGATATGCATAT GAATATCCTCCT	Amplification of fragment lexA2
lexA_FW	GGAATGAAAGCGTTAACGGC	Confirmation of the *lexA*(S119A) cassette in *E. coli* cells
lexA600_RV	ACCAGCGTACGGGCTAATGCCT	Confirmation of the *lexA*(S119A) cassette in *E. coli* cells
marR-pKD4_FW	CAATATTATCCCCTGCAACTAATTACTTG CCAGGGCAACTAATGTGTAGGCTGGAG CTGCTTC	Amplification fragment containing FRT and Kan^R
marR-pKD4_RV	GGTAATAGCGTCAGTATTGCGTCTGGAC ATCGTCATACCTCATGGGAATTAGCCAT GGTCC	Amplification fragment containing FRT and Kan^R
marR170-pKD4_FW	GTTTAAGGTGCTCTGCTCTATCCGCTGC GCGGCGTGTATTACTCGTGTAGGCTGG AGCTGCTTC	Amplification fragment containing FRT and Kan^R
marR170-pKD4_RV	CTTGGTGCAGGTCCTGGCCAACTAATTG ATGGCATTGTATGGGAATTAGCCATGGT CC	Amplification fragment containing FRT and Kan^R
marR-H1_FW	GCAACTAATTACTTGCCAGGGC	Confirmation of *marR* deletion
marR-H2_RV	GTATTGCGTCTGGACATCGT	Confirmation of *marR* deletion
e14-H1_FW	GGCTCTATTATTCTCTCCGC	Confirmation of e14 deletion
e14-mid_FW	CCGGTTGCGTTTAATAATGC	Confirmation of e14 deletion
e14-H2_RV	CTTCAGTCCAACCCATATGG	Confirmation of e14 deletion
e14_lit-pKD4_FW	GTATATACTACCTAGCCCAACAATGTAG AGGTTAACGAAAAGTGTAGGCTGGAGCT GCTTC	Amplification fragment containing FRT and Kan^R
e14_A-pKD4_RV	AAACTAAAAAGTCCACTTTAAGCGAGCG GCGGACAGCCATGGGAATTAGCCATGG TCC	Amplification fragment containing FRT and Kan^R
e14_C-pKD4_FW	CCCTTGTACCGTTAAGGTACAAGTATCT TGAAGGTTCGTGTAGGCTGGAGCTGCTT C	Amplification fragment containing FRT and Kan^R
e14_ymfM-pKD4_RV	CATCCCATACATAGCCGGTTAATTTAGT GCTCATGACCGACCTATGGGAATTAGCC ATGGTCC	Amplification fragment containing FRT and Kan^R
e14_lit_FW	CCTAGCCCAACAATGTAGAG	Confirmation of *lit* deletion
e14_A-H2_RV	GCATCTCAACGCCACATTGA	Confirmation of *lit* deletion
e14_C-H1_FW	CCCTTGTACCGTTAAGGTAC	Confirmation of *ymfML* deletion
e14_ymfM_RV	GCAACCATCCCATACATAGC	Confirmation of *ymfML* deletion
Tyrosine oligos	**Sequence (5'-3')**	**Comments**
Y-18	Y-TCCGTTGAAGCCTGCTTT(FITC)	

Y-19-3PT	Y-TCCGTTGAAGCCT*G*C*T*[FlcdT]T*T*T
P-18	TCCGTTGAAGCCTGCTTT(FITC)
P-19-3PT	TCCGTTGAAGCCT*G*C*T*[FlcdT]T*T*T

Kan[R]- kanamycin resistance, Cam[R]- chloramphenicol resistance, FRT- flippase recognition target, FlcdT - fluorescein-conjugated deoxythymidine, FITC - fluorescein isothiocyanate, * - phosphorothioate bond.

Appendix II

Supporting material for Chapter 4
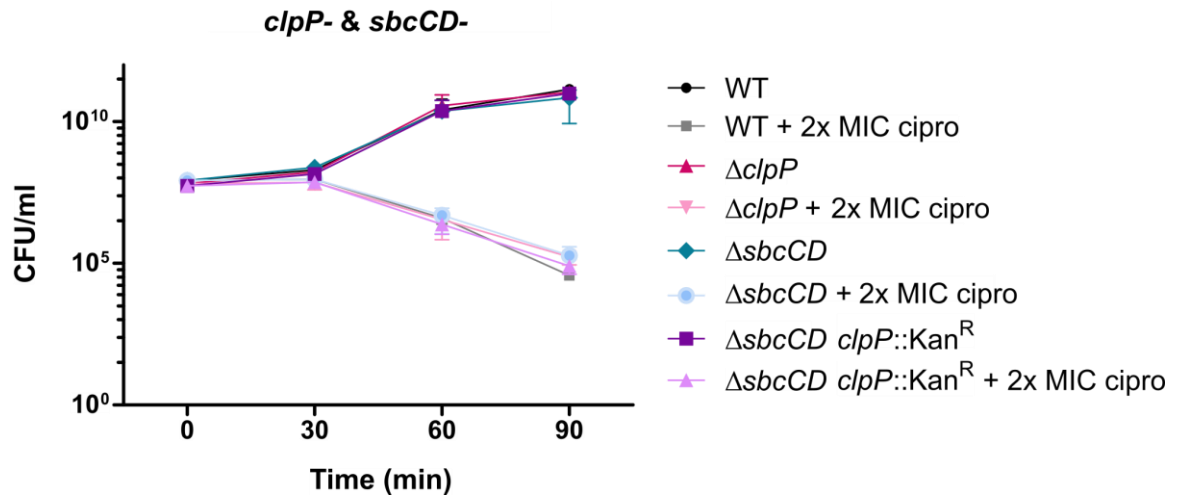
Figure I. Survival assay of WT, *clpP* and *sbcCD* mutants. Cells were grown until log phase and then split into two cultures: one was treated with 2x MIC of ciprofloxacin (0.054 µg/mL) and the other was left untreated. 0, 30, 60 and 90 min after the addition of the drug, a sample from each culture was taken and plated on LB to count the number of colony forming units (CFU) per mL. Each point in the graph represents the average CFU/ml of two replicates. The error bars show the standard deviation.

Appendix III

Supporting material for Chapter 5

Table II. List of all mutations found in the samples sent for sequencing.

Locus with mutations	wt	wt_1_CamR	wt_2_noCamR	wt_2_1_CamR	wt_2_2_CamR	wt_2_3_CamR	mito_1_CamR	mito_2_noCamR	mito_2_CamR	dinB_1_noCamR	dinB_1_CamR	dpu	dpu_1_noCamR	dpu_1_CamR
polB												63428 to 65777 del	63428 to 65777 del	63428 to 65777 del
dinB										250897 to 251953 del	250897 to 251953 del	250897 to 251953 del	250897 to 251953 del	250897 to 251953 del
mdfA/ybjGHIJLM/rcdA/grxA/					882813 to 891459 amp	882194 to 890596 amp			880532 to 888336 amp	883417 to 886545 amp	883417 to 888538 amp			882051 to 890231 amp
icd					1196220 C>T, 1196232 C>T, 1196245 TTA>CTG	1196220 C>T, 1196232 C>T, 1196245 TTA>CTG	1196220 C>T, 1196232 C>T, 1196245 TTA>CTG		1196220 C>T, 1196232 C>T, 1196245 TTA>CTG, 1196277 CGCGAAA>TGCCAAG, 1196292 C>T, 1196304 G>A, 1196316 T>A,					

Locations and types of mutations in the samples

Gene	1	2	3	4	5	6	7	8	9	10	11	12
e14				1196296 to 1211412 del	1196291 to 1211412 del	1196293 to 1211412 del		1196325 A>G 1196367 to 1211412 del				
umuD									1230770 to 1231186 del	1230770 to 1231186 del	1230770 to 1231186 del	
insH21									1300590 to 1300693 del			
marR	1619090 T>TGCAACTAATTACTTGCCAGG							1619165 CGCTTAATCCATA>C		1619290 to 1619447 del		
IS1H									1978502 to 1978974 del	1979142 to 1979270 del	1978502 1978567 del	1979203 1979269 del
gatC	2173360 ACC>A								2173360 ACC>A	2173360 ACC>A	2173360 ACC>A	2173360 ACC>A
ung		2716940 C>T										
glpR	3560455 C>CG								3560455 C>CG	3560455 C>CG	3560455 C>CG	3560455 C>CG
yibA									3767031 T>A			
intergenic_region	4296380 A>ACG	4296380 A>ACG	4296380 A>ACG	4296380 A>ACG	4296380 A>ACG	4296380 A>ACG	4296380 A>ACG	4296380 A>ACG	4296380 A>ACG	4296380 A>ACG	4296380 A>ACG	4296380 A>ACG

Appendix IV

Bush, N.G., Diez-Santos, I., Abbott, L. R., & Maxwell, A. *Quinolones: mechanism, lethality and their contributions to antibiotic resistance.* Molecules, 2020. **25**(23).

Quinolones: Mechanism, Lethality and Their Contributions to Antibiotic Resistance

Natassja G. Bush **† [ID]**, **Isabel Diez-Santos** **† [ID]**, **Lauren R. Abbott and Anthony Maxwell *** **[ID]**

Department of Biological Chemistry, John Innes Centre, Norwich Research Park, Norwich NR4 7UH, UK; tash.bush@jic.ac.uk (N.G.B.); Isabel.Diez-Santos@jic.ac.uk (I.D.-S.); lra10@leicester.ac.uk (L.R.A.)

* Correspondence: tony.maxwell@jic.ac.uk; Tel.: +44-16-0345-0771

† These authors contributed equally to this work.

Abstract: Fluoroquinolones (FQs) are arguably among the most successful antibiotics of recent times. They have enjoyed over 30 years of clinical usage and become essential tools in the armoury of clinical treatments. FQs target the bacterial enzymes DNA gyrase and DNA topoisomerase IV, where they stabilise a covalent enzyme-DNA complex in which the DNA is cleaved in both strands. This leads to cell death and turns out to be a very effective way of killing bacteria. However, resistance to FQs is increasingly problematic, and alternative compounds are urgently needed. Here, we review the mechanisms of action of FQs and discuss the potential pathways leading to cell death. We also discuss quinolone resistance and how quinolone treatment can lead to resistance to non-quinolone antibiotics.

---

1. Introduction

The quinolone antibiotics (Figure 1) are the most successful class of topoisomerase inhibitors to date. They are synthetic antimicrobials with the initial compound, nalidixic acid, being discovered as a by-product of chloroquine synthesis in 1962 [1,2]. They are used to treat bacterial infections caused by both Gram-positive and Gram-negative bacteria, including, but not limited to, urinary tract infections (UTIs), pyelonephritis, gastroenteritis, sexually-transmitted diseases, such as Gonorrhoea, tuberculosis [3], prostatitis, community-acquired pneumonia and skin and soft-tissue infections [4,5]. However, due to an increase in resistance and issues surrounding toxicity, their use in the treatment of mild infections has been contraindicated [6]. The global rise in antibiotic resistance has galvanised research into new antibiotics against both well-established targets and new targets. It has also sparked further research into antibiotics whose mode of killing is less well-established, as well as how bacteria become resistant to them. This is certainly true in the case of quinolones. In this review, the current knowledge on the mode of action of quinolones, how they kill bacteria and known pathways to resistance will be discussed. Moreover, we will review the current literature on sublethal quinolone exposure leading to resistance to quinolone and non-quinolone antibiotics.
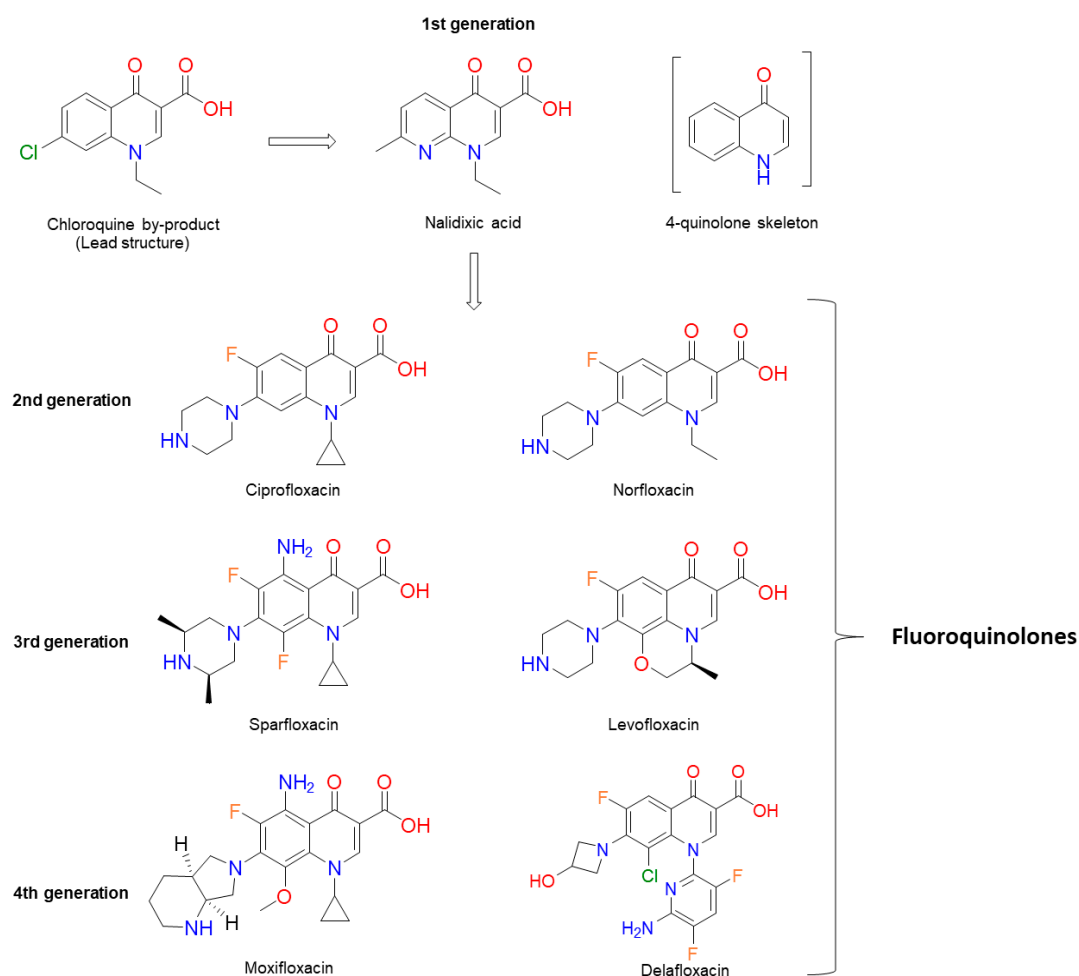
Figure 1. Chemical structures of several significant fluoroquinolones. Nalidixic acid (the first "quinolone") is shown, along with the chloroquine by-product inspiring its synthesis. Note that nalidixic acid lacks the 4-quinolone core and instead contains a 1,8-naphthyridine nucleus.

2. Background on Quinolones

The discovery of nalidixic acid (Figure 1) was reported in 1962 during the analogue synthesis of a lead structure: 7-chloro-1-ethyl-1,4-dihydro-4-oxo-3-quinolinecarboxylic acid, which was detected as an impurity in the synthesis of chloroquine (an antimalarial agent). From the analogues produced, nalidixic acid was notable due to its moderate antibacterial activity against Gram-negative species (except against *Pseudomonas aeruginosa*), including *Escherichia coli*, both in vitro and in vivo [1]. Several years later, nalidixic acid was released for clinical use for the treatment of uncomplicated UTIs [7]. This sparked the synthesis of additional analogues, although with little improvement over nalidixic acid in terms of spectrum of activity and serum concentration [1,8,9]. Other analogues included oxolinic acid, which was also introduced to the clinic, and these compounds, along with nalidixic acid (although, in relation to its structure, nalidixic acid is a 1,8 naphthyridone and not a true quinolone [1,2]), are considered first-generation quinolones [4,10,11]. There are many proposals concerning how the generations of quinolones should be defined. Of particular note, there is the suggestion of quinolone generations characterised by their structure, mechanism and their killing pathway [12], and there is the classification by structure, in vitro activity and clinical use [13]. In this review, we are referring to the quinolone generations classified by their clinical uses and spectrum of antibacterial activity outlined by Andriole [11]. Continued optimisation of the quinolones led to a fluorine atom being substituted onto carbon 6 (C-6) of the quinolone scaffold (Figure 3), producing a fluoroquinolone (FQ). The first fluoroquinolone was Flumequine, which, after brief use in the clinic, was abandoned due

to ocular toxicity [13,14]. Another key modification that enhanced potency was the incorporation of a piperazine ring onto C-7 [2,15–18]. This C-7 addition, along with the C-6 fluorine, formed the second-generation quinolones, which have a broader scope of activity and better bioavailability, as well as improved pharmacokinetic and pharmacodynamic properties [8,16,19–21]. They were also less toxic and were less susceptible to single point mutations that led to high levels of resistance seen against the first-generation quinolones [7,8,17,22]. The second-generation quinolone class began with norfloxacin (Figure 1) [15], which proved to be effective in the treatment of genitourinary and gastrointestinal tract infections, as well as increased activity against *P. aeruginosa* [15,16,21–23]. However, it was ciprofloxacin (Figure 1) that was the first quinolone that showed effective systemic activity [8,17,24,25]. Ciprofloxacin is listed as a first-line treatment for low-risk febrile neutropenia within cancer patients and a second-line treatment for cholera, as well as being employed clinically against a range of UTIs, such as those caused by *Pseudomonas aeruginosa* [26]. It has also been demonstrated to be effective in the treatment of Enterobacteriaceae-induced osteomyelitis, prostatitis and septicaemia [8].

Following the success of ciprofloxacin, the observed structure-activity relationships (SARs) were explored further (Figure 3). This medicinal chemistry effort produced a wide range of newer-generation FQs (third and fourth generations) that have even broader spectra of activity, greater efficacy and a lower prevalence of resistance [27]. Sparfloxacin and moxifloxacin (Figure 1) are the better-known compounds of the third and fourth generations, respectively, and are amongst the first quinolones to show significant potency against Gram-positive bacteria [11]. Furthermore, *Mycobacterium tuberculosis*, the bacterial species that causes tuberculosis (TB; currently the world's deadliest bacterial infectious disease to date), is susceptible to the FQs, and both moxifloxacin and levofloxacin (a second-generation quinolone) have been used in the treatment of multidrug-resistant (MDR) infections [3,28]. Despite their success, some promising FQs, such as trovafloxacin and grepafloxacin (Figure 2), have had to be withdrawn from the clinic due to safety concerns [8,29,30]. However, many have remained in the clinic, with ciprofloxacin continuing to be one of the most clinically important antibiotics to date. In fact, the World Health Organisation has categorised ciprofloxacin (amongst other FQs) as a critically important antibiotic [31].
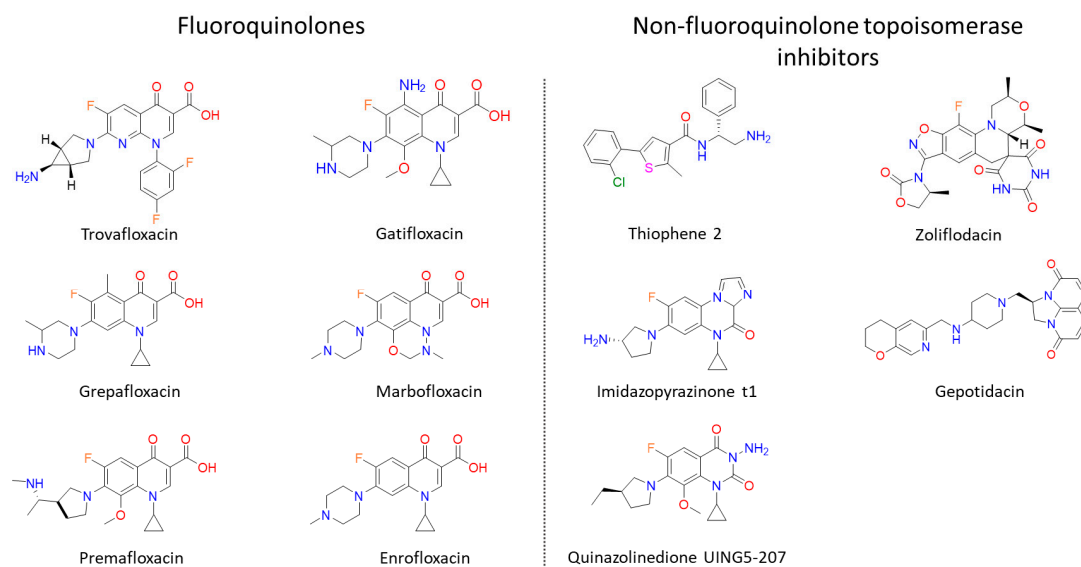
Figure 2. Structures of "new" fluoroquinolones and non-fluoroquinolone topoisomerase inhibitors discussed in the text. Gepotidacin and Zoliflodacin (Novel Bacterial Topoisomerase Inhibitors) are both in phase III clinical trials. Thiophene 2: *N*-(2-amino-1-phenylethyl)-5-(2-chlorophenyl)-2-methylthiophene-3-carboxamide, Imidazopyrazinone t1: 7-((3~[S])-3-azanylpyrrolidin-1-yl)-.5-cyclopropyl-8-fluoranyl-imidazo (1,2-a)quinoxalin-4-one and Quinazolinedione UING5-207: 3-Amino-1-cyclopropyl-7-((3R)-3-ethyl-1-pyrrolidinyl)-6-fluoro-8-methoxy-2,4(1H,3H)-quinazolinedione.
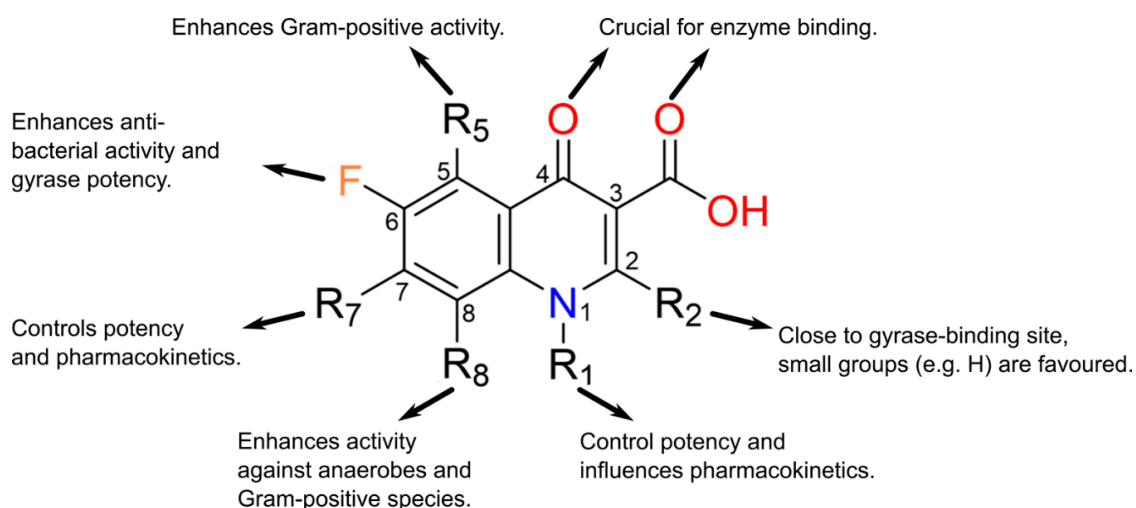
Figure 3. The observed structure-activity relationships (SARs) of quinolone core substitutions. Most often R5 = H, but sparfloxacin (a discontinued 3rd-generation fluoroquinolone (FQ)) has R5 = NH$_2$ (diagram adapted from [32], with permission).

A major reason for the comparative success of FQs is that they target the bacterial type II topoisomerases, DNA gyrase (gyrase) and DNA topoisomerase IV (topo IV) [33–35]. DNA topoisomerases are enzymes that catalyse the interconversion of different topological forms of DNA (e.g., relaxed-supercoiled and catenated-decatenated) and are crucial for several DNA-associated processes, such as replication and transcription [36]. All topoisomerases can relax DNA, but only gyrase can introduce negative supercoiling [37–39]. Gyrase is present and essential in all bacteria but absent from higher eukaryotes (e.g., humans), making it an ideal target for antibacterials; however, gyrase does occur in plants and plasmodial parasites [40,41]. Eukaryotes possess a related enzyme, DNA topoisomerase II (topo II), but it is sufficiently different from bacterial gyrase and topo IV such that these enzymes can be selectively targeted. Gyrase and topo IV are both heterotetramers, consisting of GyrA and GyrB (A$_2$B$_2$) in the case of gyrase and ParC and ParE (C$_2$E$_2$) in the case of topo IV [35]. Through extensive structural and mechanistic studies, the mechanisms of action of gyrase (Figure 4) and topo IV are well-understood [35,42]. As with all type II topoisomerases, the mechanism entails the binding of two segments of DNA, a G (or Gate) segment and a T (or Transported) segment. The enzyme cleaves the G segment in both strands of the DNA, leaving a four-base stagger, involving amino acid residues in both subunits and entailing the formation of covalent bonds between the 5′ ends of the broken DNA and the active site tyrosines in GyrA or ParC [35,42]. This allows passage of the T segment through the G-segment break (strand passage), enabling the alterations in DNA topology, such as relaxation or decatenation. In the case of gyrase, the T and G segments are located close together on the same piece of DNA, enabling vectorial strand passage and, thus, the introduction of negative supercoils. The mechanism requires the hydrolysis of two ATP molecules [43,44], although the exact timing and role of the ATP is yet to be determined.
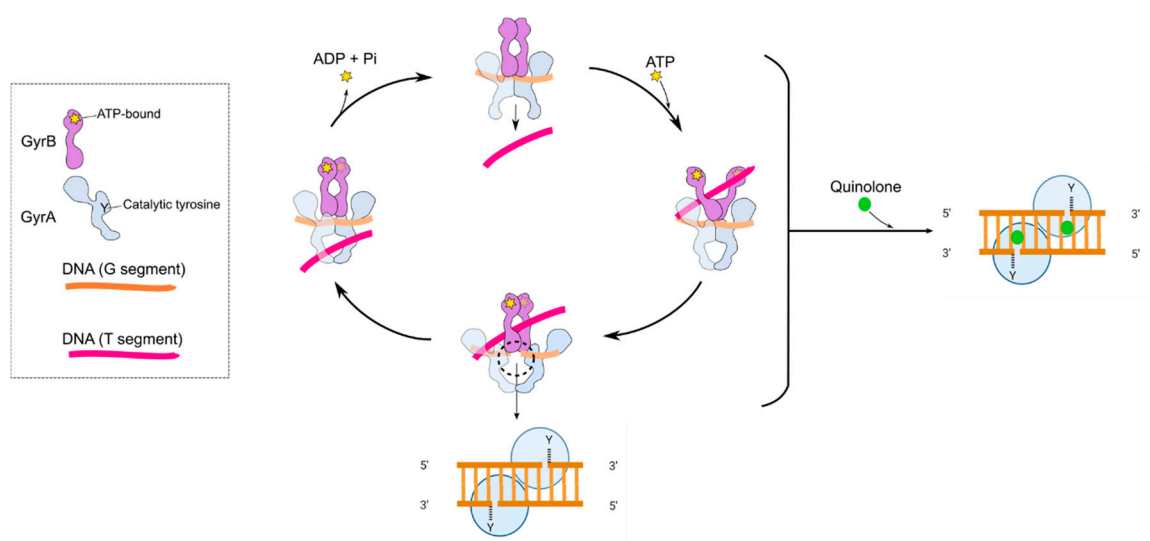
Figure 4. Cartoon showing the proposed mechanism of DNA supercoiling by DNA gyrase and how quinolones interfere with this mechanism by stabilising the cleavage complex. The inset shows the GyrA (blue) and GyrB (purple) subunits. Y indicates the position of the active site tyrosine, and the star indicates the position of the ATP-binding site. The G segment (orange) binds across the GyrA dimer interface. The GyrA C-terminal domain wraps the DNA (not shown) to present the T segment (pink) in a positive node. ATP binds to the N-terminal domain of GyrB, which closes the GyrB clamp (also known as the N-gate), capturing the T segment. The G segment is transiently cleaved, the GyrB domains rotate (not shown), the DNA gate widens and the T segment is transported through the cleaved G segment. The G segment is re-ligated, and the T segment exits through the GyrA C-gate. The hydrolysis of ATP and the leaving of ADP + Pi resets the enzyme for another cycle, although the exact timing of these reactions is unknown. The black-dashed circle and lower inset show the cleavage complex. The right-hand panel shows the binding of quinolones (green spheres) in the cleavage complex.

The quinolones inhibit DNA supercoiling and relaxation by binding to both gyrase and DNA and stabilising the gyrase-DNA-cleaved complex [33,34]. This is also true for topo IV, which is the primary target in a number of Gram-positive species [45,46]. However, this is often dependent on the specific quinolone, and some quinolones have been shown to target both enzymes equally [5,7,47–49]. A thorough review by Cheng et al. [50] provides more information about the differential targeting of gyrase and topo IV by quinolones and the consequences thereof.

The quinolones have been shown to have interactions with both subunits of the enzyme (GyrA and GyrB for gyrase and ParC and ParE for topo IV). Research into the nature of FQ binding has led to several potential mechanisms and the suggestion that it may involve several steps [51,52]. Crystal structures published in 2009 and 2010 indicated a convincing model that is likely to represent the principle and most stable mode of binding [53–55]. In this model, the drug is seen to be intercalated between DNA bases at the DNA-cleavage site (Figure 5); intercalation of quinolones into DNA were proposed from earlier works [56–58]. The intercalation model represents a now well-established explanation for FQ binding, in which the drug binds at the DNA gate region of the enzyme whilst partially intercalating into the substrate DNA (Figure 5). It appears that the drugs may take advantage of the modified DNA structure at the cleavage site to intercalate between DNA bases at the sites of breakage. Within X-ray crystal structures, one FQ molecule has been found to intercalate between the bases at each DNA break, inducing a kink. The C-7 substituent of the FQ protrudes out of the DNA slightly, avoiding unfavourable clashes with the DNA bases on either side. This model also explains the increased action of the FQs over the first-generation quinolones, where the fluorine substituent likely perturbs the electronic balance of the partially aromatic structure and strengthens pi-stacking interactions with the DNA bases [54]. The carbonyl substituents at C-3 and -4 contribute essential contacts and underpin the formation of a water-metal ion bridge. This water-metal ion

bridge was found to mediate the interactions between the drug and the target enzyme; this consists of a noncatalytic Mg^{2+} ion in an octahedral complex with four water molecules and the FQ C-3/C-4 carbonyl oxygens. Two of these water ligands interact with enzyme residues, S83 and D87, in GyrA (using *E. coli* numbering), completing the bridge. Interactions between position 466 in GyrB and the C-7 ring of the FQ are also important for binding of the compound [52,59–61]. These interactions between the quinolones and the topoisomerase-DNA complex trap the topoisomerase on the DNA, making the enzyme unable to supercoil or relax the DNA. This topoisomerase-DNA-quinolone complex also transforms the enzyme into a poisonous protein that blocks the replication [62,63] and transcription machinery [64], potentially causing lethal double-strand breaks [45,46,64–66].
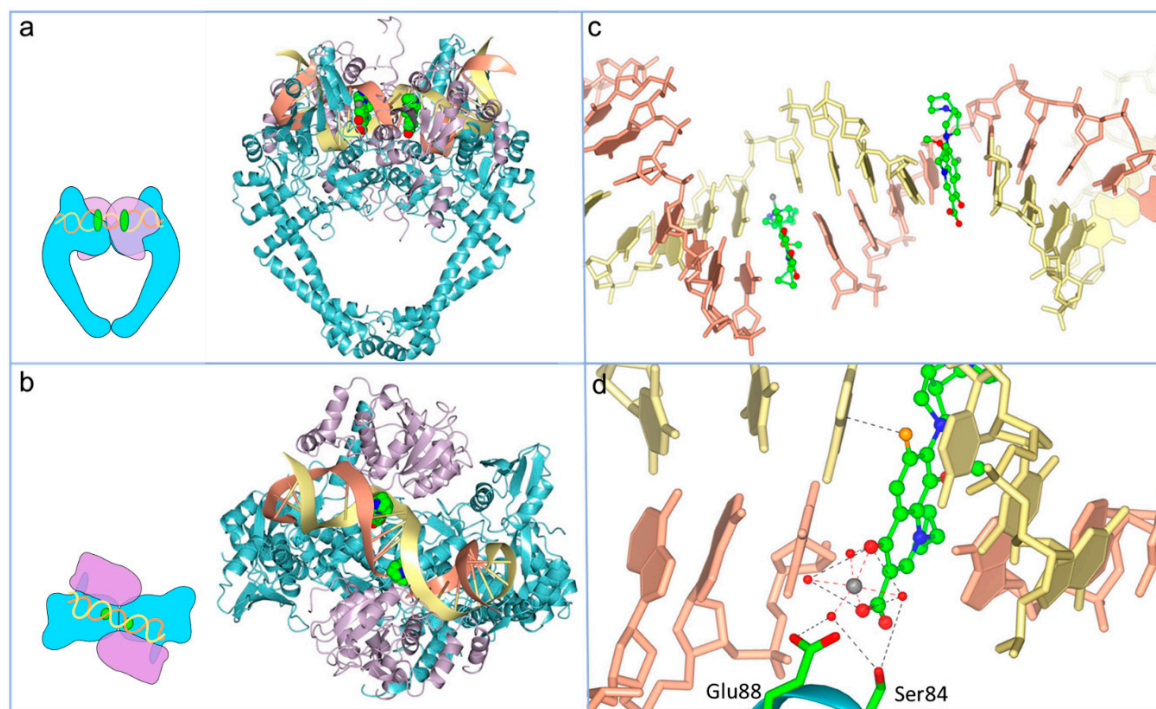
Figure 5. Overview of moxifloxacin binding to the topo IV-DNA complex (Protein Data Bank (PDB): 2XKK; [55]; figure modified with permission). (**a**) Front-faced view of moxifloxacin (Van der Waals model, green carbons) bound within the cleavage complex of *Acinetobacter baumannii* topo IV ParE (purple ribbons) N-terminal domain, fused to a ParC (blue ribbons) C-terminal domain and complexed with a 34-base pair (bp) heteroduplex DNA (yellow and coral ribbons). (**b**) View of the same complex from above. (**c**) Detail of moxifloxacin (ball and stick, green carbons) partially intercalated into the DNA bases at the break sites, spaced 4-bp apart. (**d**) Water-metal ion bridge formed between moxifloxacin, a noncatalytic Mg^{2+} (grey sphere), four water molecules (red spheres) and S84 and G88 of ParC.

3. Quinolone Lethality

Quinolones kill bacteria slowly or quickly, depending on their concentrations. At concentrations that are twice the minimum inhibitory concentration (MIC) value, bacteria are killed after an overnight quinolone treatment; whereas, at concentrations 5–10 times the MIC value, bacteria die after a few hours of quinolone exposure [67,68]. How slow or rapid killing happens is not fully understood. We know that the first stage in quinolone lethality is the binding of the quinolone to a topoisomerase-DNA cleavage complex. Cleavage complexes contain broken DNA that cannot be resealed by the same topoisomerase if the quinolone is present. However, cleavage complexes and their "hidden" DNA breaks are reversible, so there must be additional events that cause bacterial death [65]. Depending on whether the cleavage complex is processed, it is thought that bacterial death can arise in two different ways. If the cleavage complex is not processed, DNA replication and transcription are blocked, eventually leading to cell death: slow death. If the cleavage complex is processed (either by removing

the gyrase from the DNA with an unknown protein or because the gyrase subunits dissociate) and the broken DNA is not repaired, it causes chromosome fragmentation, which quickly kills the cell: rapid death. The presence of broken DNA and, perhaps, cleavage complexes also cause the accumulation of intracellular ROS (reactive oxygen species), which can lead to more DNA breaks (Figure 6) [50,69]. The quinolone-induced DNA damage can be repaired (at least in part), which, as we will mention later, can have important consequences for the survival of the cell to quinolone and non-quinolones antibiotics.
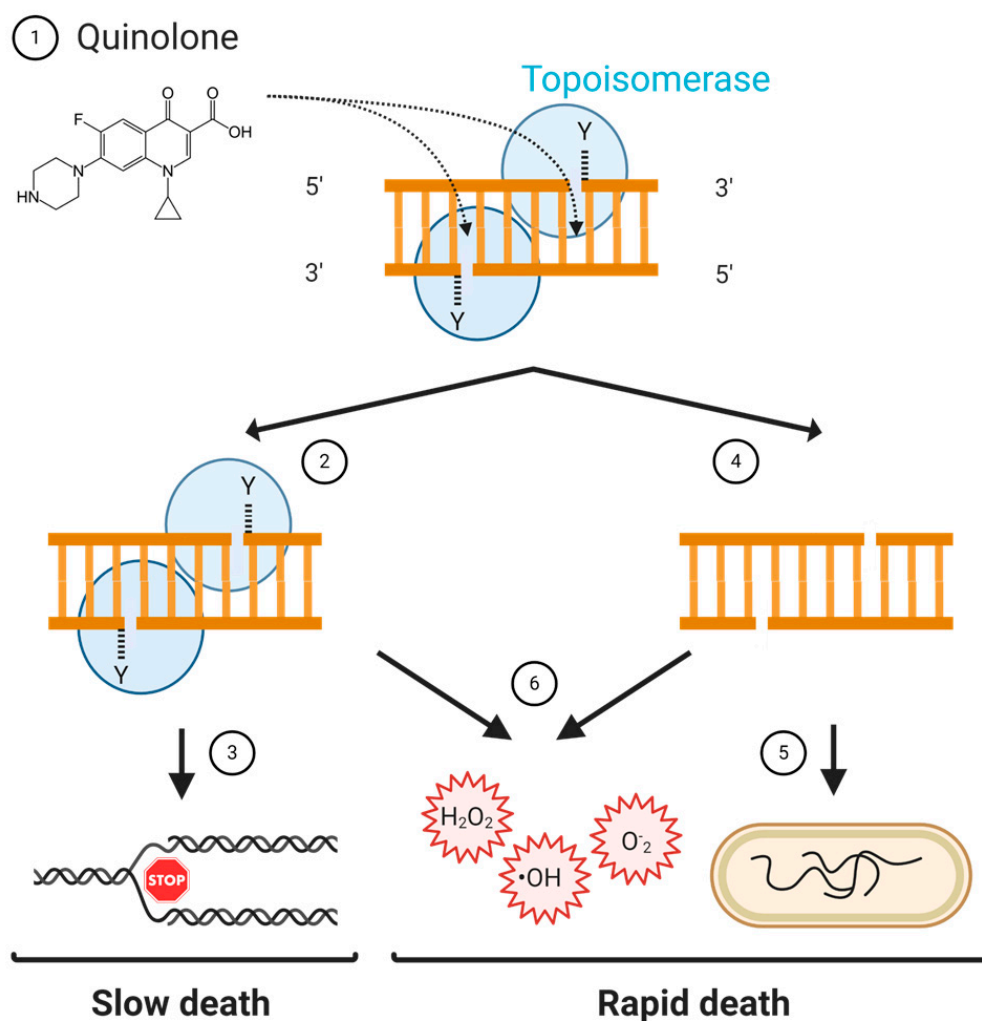
Figure 6. Model of quinolone lethality. (1) Quinolones stabilise the topoisomerase-DNA cleavage complex in which there is a double-strand break. (2) If the cleavage complex is not resolved, (3) replication and transcription cannot happen, which causes slow bacterial cell death. (4) If the topoisomerase is removed, the double-strand break is free, and if left unrepaired, (5) it leads to the fragmentation of the chromosome, which causes rapid bacterial cell death. (6) The stabilised cleavage complex, or the removal of the topoisomerase from the cleavage complex, might lead to the accumulation of reactive oxygen species (ROS) that can cause rapid bacterial cell death.

3.1. Slow Death

3.1.1. Block of Replication and Transcription

At low concentrations, quinolones block replication and transcription by inhibiting gyrase and topo IV, which are essential enzymes during replication and transcription [48,70]. Replication fork progression causes positive supercoils to build up ahead of the fork [71,72]. These positive supercoils

need to be resolved, as a build-up will cause a large amount of torsional stress [73] that can stall replication. To relieve the torsional stress, the replication fork may rotate causing the development of precatenanes behind the fork [71,74–76]. These precatenanes can become tangled and knotted if left unresolved, leading to incomplete segregation at the end of replication [71,76]. Gyrase acts ahead of the replication fork, removing positive supercoils so that replication and transcription can continue unhindered. Topo IV, on the other hand, works behind the replication fork, unlinking precatenanes that could prevent cell division [77]. The main components of the replication and transcription machinery, the DNA and RNA polymerases, are blocked by gyrase-quinolone-DNA complexes [63,64], and the same happens to replication forks [78]. However, stopping replication had little effect on the lethal activity of the quinolones [79], and it is therefore unlikely to be the cause of quinolone-induced death. In fact, quinolone-induced death correlated with the release of DNA breaks from gyrase-cleavage complexes [65]. These lethal DNA breaks do not come from the blockage of replication [80,81] but happen after the trapped gyrase is removed from the DNA.

In contrast to quinolones, drugs that stabilise eukaryotic topoisomerase-DNA complexes can generate lethal DNA breaks when replication forks collide with cleavage complexes and the trapped topoisomerase has not been removed from the DNA [82,83]. Camptothecin, a stabiliser of the eukaryotic topoisomerase I-DNA cleavage complex, inhibits DNA replication and generates DNA breaks [82,84]. It also causes the formation of double-strand breaks when the replication fork collides with the cleavage complex [83,85]. A similar situation might happen with topo II-DNA cleavage complexes, as m-AMSA, an inhibitor of topo II, is less lethal in the presence of a DNA synthesis inhibitor, which indicates that its lethality depends on the replication of DNA [86].

3.1.2. Inhibition of DNA and RNA Synthesis

The main consequence of the arrest of replication forks and transcription bubbles is the inhibition of DNA and RNA synthesis. DNA and RNA synthesis rates quickly decrease in the presence of quinolones [62,65,87], and this correlates with the inhibition of growth [87,88]. However, the quinolone-induced inhibition of DNA synthesis is reversible—that is, DNA synthesis resumes upon the removal of the drug, so, like inhibition of replication, it is unlikely to cause cell death [89]. Nevertheless, it has been proposed that quinolone slow killing (which happens when bacteria are given long quinolone treatments at twice the MIC) might be caused by secondary events stimulated by the inhibition of replication [51].

3.2. Rapid Death

3.2.1. Processing of the Quinolone-Poisoned Gyrase

As mentioned before, quinolones can quickly kill bacterial cells at concentrations over the MIC, and this lethality mostly appears when the quinolone-poisoned gyrase subunits disassociate or are removed from the DNA. There are three ways in which a poisoned topoisomerase can be removed from the DNA that differ in the need for protein synthesis and aerobic conditions [90]. First-generation quinolones, such as oxolinic or nalidixic acid, are not lethal in the presence of a protein-synthesis inhibitor (e.g., chloramphenicol) or under anaerobic conditions, and therefore, they belong to the protein synthesis, aerobic-dependent pathway. Norfloxacin, a second-generation quinolone, is not lethal in the presence of chloramphenicol, but it is lethal under anaerobic conditions and, thus, belongs to the protein synthesis-dependent, aerobic-independent pathway. Ciprofloxacin, a second-generation quinolone, and other second- and third-generation quinolones, are lethal regardless of protein synthesis or aerobiosis, so they belong to the protein synthesis, aerobic-independent pathway [65,90].

In principle, gyrase-cleavage complexes could be removed by a protein (e.g., either a nuclease that cleaves next to the gyrase-DNA bond, a protease that processes the topoisomerase or a protein that specifically breaks the bond between the gyrase and the DNA) or by the dissociation of the gyrase subunits. For the first-generation quinolones that belong to the protein synthesis-dependent pathway,

it is expected that said protein would be needed to be lethal. Whereas FQs like ciprofloxacin, which are lethal regardless of continued protein synthesis, might be lethal due to dissociation of the gyrase subunits. We will discuss these alternatives in the following sections.

3.2.2. Nuclease and Protease Activity

Chen et al. [65] first suggested that there is a bacterial protein (or proteins) that can release the poisoned gyrase from the DNA. This suggestion was based on the observation that first-generation quinolones were not lethal if the synthesis of proteins was inhibited. This means that the lethality of first-generation quinolones depends on the presence of a protein that removes the gyrase from the DNA and that releases the lethal double-strand breaks, i.e., that protein would be responsible for killing by quinolones. Malik et al. [66] tried to find that protein by doing rounds of treatments with quinolones to find mutants that were bacteriostatic but not bacteriolytic. They were not able to map the mutations, and they suggested that multiple genes might be involved. To date, that protein(s) has not been found, although there are potential candidates that we will mention later.

In eukaryotes, several proteins are known to remove trapped topoisomerase-DNA complexes [91]. Notably TDP1 and TDP2, Tyrosyl-DNA-Phosphodiesterases 1 and 2, are well-characterised DNA repair proteins that remove the 3′ or 5′ tyrosyl-DNA adducts with eukaryotic topo I and topo II, respectively [92]. It is interesting to note that, in contrast to what has been hypothesised in bacteria (that there is a protein that can remove gyrase from the DNA and cause lethal breaks), in eukaryotes, this type of protein is involved in repair and not in killing [91,93–95]. This might be because the lethality of topoisomerase poisons in eukaryotes comes from DNA breaks that occur when replication forks collide. Whereas, with prokaryotes, the lethality mostly comes after the poisoned topoisomerases are removed from the DNA, releasing double-strand breaks, and, less importantly, when the replication forks are stalled. This means that if the poisoned topoisomerases are not processed in eukaryotes, they will be much more lethal than in prokaryotes. In any case, it is likely that the proteins that participate in the processing of poisoned gyrase are involved in both the killing and the repair, as the cleavage complexes need to be removed to be lethal and to be repaired.

Some evidence points to SbcCD and RuvAB as protein complexes that can remove poisoned topoisomerases in bacteria [81,96]. SbcCD is a nuclease complex that can make double-stranded breaks to release a protein attached to the DNA [97]. The deletion of *sbcCD* increased the sensitivity of cells to oxolinic acid but not to ciprofloxacin, and cells without *sbcCD* had more cleavage complexes in the presence of quinolones than wild-type cells, suggesting that SbcCD was needed to remove the gyrase [96]. However, it has not been tested directly (for example, by incubating purified SbcCD with DNA and gyrase) whether SbcCD can indeed cut the DNA near gyrase-bound DNA ends. The second protein complex, RuvAB, has helicase activity and was shown to remove topo IV-norfloxacin-DNA complexes [81]. Purified RuvAB was able to reverse cleavage complexes in vitro without the help of any other protein. How RuvAB causes the reversal of cleavage complexes is not known.

3.2.3. Gyrase Subunit Dissociation

The second proposed mechanism to remove poisoned gyrase is the dissociation of gyrase subunits. When Chen et al. [65] found that second-generation quinolones, like ciprofloxacin, killed bacteria in the absence of protein synthesis, they hypothesised that it happened through the dissociation of gyrase subunits. As mentioned above, gyrase is a heterotetrametric enzyme (A_2B_2) formed of two GyrA and two GyrB subunits. If the GyrA subunits, somehow without the help of another protein, dissociate and leave the DNA, the lethal double-stranded breaks would be exposed. Malik et al. [66] tested this hypothesis by using a GyrA(A67S) mutant that presumably had an unstable GyrA-GyrA interface. They found that when they used nalidixic acid, cells were killed in the presence of chloramphenicol, and extracted nucleoids were fragmented (as happens with second-generation quinolones) [66]. This indicated that the mutation in GyrA caused a first-generation quinolone to stabilise the cleavage complex in a similar way to second-generation quinolones. However, even if gyrase subunits can

dissociate because of the presence of a second-generation quinolone, their GyrA subunits would still be covalently bound to the DNA. Thus, further processing of GyrA would be needed to completely release it from the DNA.

3.2.4. Chromosome Fragmentation

The final event of rapid quinolone killing is the fragmentation of the chromosome. Chromosome fragmentation has been observed in cells exposed to high concentrations of gatifloxacin, ciprofloxacin or oxolinic acid by measuring the sedimentation of the DNA [66] or by visualising the fragmentation of the nucleoids under the microscope [98]. As chromosome fragmentation is a hallmark of cell death [99], it is likely that it is a direct and quick cause of bacterial killing.

3.2.5. Reactive Oxygen Species (ROS) Formation

Apart from chromosome fragmentation, rapid quinolone killing has also been associated with the accumulation of intracellular reactive oxygen species (ROS). These are natural by-products of aerobic metabolism, and some examples include peroxide (H_2O_2), superoxide radical ($O_2^{\bullet-}$) and hydroxyl radicals ($^\bullet OH$). Bactericidal antibiotics presumably increase ROS levels by disrupting the membrane, which causes the activation of the Krebs cycle [100]. In the Krebs cycle, reduced cofactors are formed. The reduced cofactors travel down the electron transport chain, where they can release electrons to oxygen molecules producing O_2. Superoxide oxidises iron-sulphur clusters of respiratory dehydrogenases, which causes the release of iron. The iron, which is kept reduced by cellular reductants, then reduces H_2O_2 to $^\bullet OH$, which can damage the DNA by oxidising DNA bases, creating aberrant base pairs, often leading to mutations [101]. When ROS accumulate in the cell, bacteria respond through the *oxyR*, *soxRS* and *rpoS* regulons. These regulons control the transcription of genes that degrade O_2 (e.g., *sod* or superoxide dismutase) or that degrade H_2O_2 (e.g., *kat* or catalase) [102].

Several groups have shown a correlation between quinolone lethality and the accumulation of ROS [69,103,104]. They have done this by measuring levels of ROS and lethality after treating cells with quinolones and inhibitors of ROS or using strains overproducing or lacking enzymes that regulate oxidative stress (e.g., *sod* and *kat*). For example, Dwyer et al. [105] showed that, after norfloxacin treatment, ROS-related genes were upregulated, there was an increase in $^\bullet OH$ and no killing was observed when a ROS neutralizer was used. More recently, Hong et al. [69] found that all types of quinolones were lethal because of the accumulation of ROS.

Initially, there was some controversy about whether quinolones could indeed kill cells by the accumulation of ROS. Liu et al. [106] showed that quinolones did not increase the levels of ROS, and Keren et al. [107] found no correlation between ROS formation and quinolone lethality [106,107]. The disparities between these results and the ones from Dwyer et al. [105] were addressed in an exhaustive review [103], and since then, several studies have shown that ROS account, at least in part, for the lethality of quinolones [69,104,108]. Still, there are many unanswered questions around the ROS formation theory. For example, how do quinolones induce the formation of ROS? Norfloxacin treatment increases the production of metabolites of the Krebs cycle, which might trigger the formation of ROS [109], but the toxic effects of quinolones happen when they stabilise a cleavage complex, and the steps between the formation of quinolone-stabilised cleavage complexes and the formation of ROS have not been unravelled. Additionally, can quinolones induce the formation of enough ROS to kill the cell? The accumulation of intracellular ROS theoretically can only inhibit growth, and the mechanisms that cause cell death after ROS formation are not fully known [110,111]. Nevertheless, it is been shown that ROS can convert single-stranded DNA breaks into double-stranded breaks [112] and that the accumulation of ROS can be self-amplifying [104], so it is possible that ROS cause sufficient DNA damage to kill the cell.

3.3. Repair of Quinolone-Induced DNA Damage

Quinolones induce DNA damage that can kill the cells, but this damage can also be repaired [45]. The repair of quinolone-induced DNA damage was observed in quinolone-treated bacterial cultures that became denser after removing the drug [66]. This increase in density suggested that DNA breaks were resealed, as the longer the DNA is, the more viscous the solution is. Additionally, nucleoids of quinolone-treated cells became less fragmented after removing the quinolones [98], and the deletion of DNA repair proteins increased the susceptibility of bacteria to quinolones [113–115].

It is not clear how bacteria repair quinolone-induced damage. Due to the mechanism of quinolone killing and how eukaryotes repair poisoned topoisomerase-DNA cleavage complexes, it is possible that bacteria first have to remove the topoisomerase trapped on the DNA (for example, through the nuclease SbcCD or the helicase RuvAB). This would release the double-strand breaks and would activate stress responses such as the SOS response [51]. The SOS response is a cellular response to DNA damage that is controlled by the auto-repressor LexA and the activator RecA [116]. The SOS response is activated by all quinolones [88], but it is not the only stress response activated by quinolones. Pribis et al. [117] showed that, when exposed to sublethal ciprofloxacin, a subpopulation of cells undergoes SOS and the accumulation of ROS, which then activates the σ^S response. This is a general stress response that regulates the transcription of hundreds of genes, including genes involved in DNA repair. All these stress responses lead to the repair of DNA breaks through error-free (e.g., homologous recombination or nucleotide excision repair) or error-prone (e.g., translesion synthesis) DNA damage repair pathways [116,118]. Error-free repair pathways do not cause mutations, whereas the error-prone repair can generate mutations. This is one of the reasons why quinolones can trigger the appearance of mutations that cause quinolone antimicrobial resistance.

4. Resistance to Quinolones

Antibacterial resistance towards the FQ drugs has arisen following its widespread use as a medication in both humans and animals [119–121]. In particular, during 2001–2006, the prevalence of FQ-resistant *E. coli* isolates in the UK increased from 6% to 20%. This then decreased slightly, to 17%, by 2010 [122]. Furthermore, even higher quinolone resistance rates of Enterobacteriaceae (such as *E. coli*) have been recorded across the globe; in 2015, it was reported that up to 30% of community-associated isolates from across the United States showed FQ nonsusceptibility [123]. Elsewhere resistance rates are very variable but can be as high as almost 100%, particularly in Asia [124,125]. The rising resistance towards FQs threatens their efficacy against a range of diseases, and scientific efforts have focused on understanding the mechanisms behind resistance and the different ways to combat the bacterial infections. The mechanisms include the upregulation of efflux pumps, a reduced ability to uptake the drug, plasmid-mediated resistance or actual mutations in the gyrase or topo IV genes (Figure 7) [49,61].

4.1. Mutations in DNA Gyrase and Topo IV

The mutations in gyrase and topo IV that confer resistance to quinolones are often found in a region termed the quinolone resistance-determining region (QRDR), which is between amino acids 67 and 106 in GyrA (*E. coli* numbering) or 63 and 102 in ParC [126]. There is also a QRDR found in GyrB between amino acids 426 and 447 and in ParE between amino acids 420 and 441, with the two most common mutations found to be D426N and L447E (*E. coli* numbering) [55,127–129]. However, the most prevalent quinolone-resistance mutations are found in GyrA. These mutations cluster near the active site tyrosines at the dimer interface [130]. Due to their specific interactions with the quinolone through the water-metal ion bridge, the residues most commonly mutated in ciprofloxacin-resistant strains are serine and aspartic acid/glutamic acid on helix IV in GyrA/ParC [5,7,49,61]. Resistance-conferring mutations outside the traditional QRDR have also been identified. For example, an A51V mutation results in a six-fold increase in ciprofloxacin resistance [131]. Furthermore, there have been reports of the decreased gene expression of topo IV in *Staphylococcus aureus*, increasing its MIC to premafloxacin

(Figure 2) and ciprofloxacin by two–eight-fold. This was found to be caused by a point mutation in the promoter of the *grlB* (*parE*) gene, which reduced the expression of the gene, conferring an increase in the MIC [132].
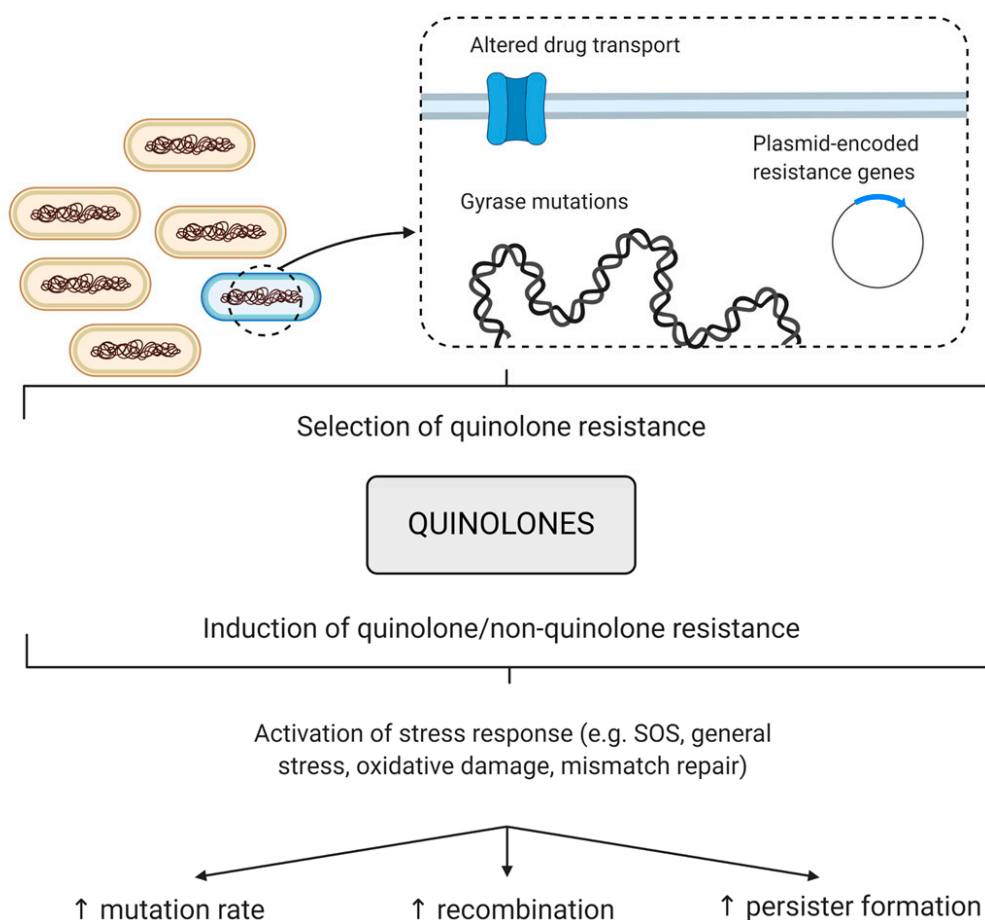
Figure 7. Contributions of quinolones to antibiotic resistance. Quinolones can select for quinolone resistance, which is caused by the upregulation of efflux pumps, mutations in DNA gyrase or DNA topoisomerase IV genes or plasmid-encoded resistance genes. Quinolones can also induce resistance to quinolones and non-quinolones antibiotics, presumably by the activation of a stress response that then increases the mutation, recombination or persister formation rates.

4.2. Plasmid-Mediated Quinolone Resistance (PMQR)

Early in the history of quinolones, it was reported that they were able to eliminate plasmids from bacteria [133–135], suggesting that they were unlikely to be subject to plasmid-mediated resistance. However, plasmid-mediated resistance to FQs has now been discovered. The first plasmid gene found to introduce bacterial protection against FQs was named *qnrA*, which was followed by the isolation of several related genes, including *qnrB* and *qnrS* [61,136]. Each gene codes for a different Qnr protein, and QnrA was the first of these to be characterised. QnrA was assigned to a family of proteins known as the pentapeptide repeat proteins (PRPs), due to their series of five amino acid tandem repeats throughout the total sequence of 218 amino acids [137]. Additional PRPs, including MfpA and McbG, were also shown to aid in FQ resistance [138–140]. MfpA was the first of the proteins to produce a successful crystal structure, and this revealed a 3D form that appeared to mimic the structure of DNA [141]. The beta-helix-like structure was also observed with other PRPs, such as Qnr proteins (e.g., AhQnr from *Aeromonas hydrophila* [142]). McbG was initially discovered to protect *E. coli* gyrase against Microcin B17, a natural antibacterial peptide toxin produced by Enterobacteriaceae. These bacteria produce McbG to defend their own gyrase during the production of the toxin [140,143].

The PRPs (and similar plasmid-encoded resistance proteins) likely evolved as defence mechanisms against natural threats, such as competing bacteria. The PRP structure suggests that their primary function is to mimic DNA when binding competitively to DNA-dependent enzymes, thus preventing the binding of inhibitors. Current research efforts are aimed at revealing molecular mechanisms of protection by PRPs, with current data indicating that subtle sequence variation can cause significant functional differences. For instance, not all PRPs can protect gyrase or topo IV against FQs [140]; conversely, Qnr cannot protect against Microcin B17 [140,144].

A second PMQR mechanism was revealed with the detection of the AAC(6′)-Ib-cr mutant protein. AAC(6′)-Ib-cr is an aminoglycoside 6′-N-acetyltransferase enzyme containing two point mutations, W102R and D179Y, that introduce the ability to acetylate (and so deactivate) some FQs [145]. The D179Y alteration is believed to aid in favourable pi-stacking interactions during enzyme-FQ binding, and the W102R mutation is thought to position the FQ, perhaps through hydrogen bonds with the C-3/C-4 oxygen atoms. Acetylation occurs at the amino nitrogen of the piperazine ring within second-generation FQs and may impact binding with the target enzyme [145].

4.3. Altered Drug Transport

Other identified chromosomal mutations that confer quinolone resistance include those involved with the uptake of the drug, the upregulation of efflux pumps and in the regulons that control the expression of these. In Gram-negative bacteria, modifications of the bacterial membrane either structurally by the reduction of the number of porins (via OmpA and OmpX) in the cell membrane or through the alteration of the porins themselves have been reported [7,146–149]. Additionally, the overexpression of various efflux pumps (also found in Gram-positive species) can lead to increased resistance [7,61,150,151]. Efflux describes the process by which bacteria are able to expel harmful compounds (such as antibiotics) using active transport proteins known as efflux pumps. Alterations to efflux genes can arise from both chromosomal mutations and via plasmids, which typically involve changes in regulatory proteins and de-repression of the efflux systems [5,151,152]. Efflux pumps span the membranes of both Gram-negative and Gram-positive species, and the overexpression of these proteins lowers the cytoplasmic concentration of drugs retained in the cell [153]. Efflux effects can cause low-level resistance alone but present an advantage for the evolutionary selection of high-resistance strains [154,155]. These efflux pumps can be classified into five families; those that are most relevant to FQ resistance are the major facilitator superfamily (MFS) in Gram-negative and -positive species and the resistance-nodulation-division superfamily (RND) in Gram-negative species [152,156].

Efflux pumps can have a range of substrate specificities. For example, FQ efflux systems tend to be broad-ranged and able to transport many drugs and toxic compounds. This means that, often, mutations in these efflux pumps can cause resistance to FQs and other drugs at the same time (cross-resistance) [153,157]. Many FQ-resistant strains carrying such efflux mutations are typically resistant to multiple drugs. Two examples of plasmid-based efflux mutants that induce FQ resistance are *oqxAB* and *qepA*, isolated from animal and clinical samples, respectively [158]. Many chromosomal efflux mutants have also been detected, including *norA*, *norB* and *norC*, within *St. aureus* strains. The corresponding pumps are multidrug transporters, though they do display some specificity towards the structure of FQ that they bind. NorA only transports the more hydrophilic FQs (such as norfloxacin and ciprofloxacin), whilst NorB and NorC transport norfloxacin, ciprofloxacin and the less hydrophilic compounds (such as moxifloxacin and levofloxacin) [159]. Interestingly, the overexpression of NorA not only causes low-level resistance, but it also increases the evolvability of ciprofloxacin resistance in *St. aureus* [154]. In *E. coli*, the overexpression of efflux pumps is often linked to mutations in MarRA, SoxRS and Rob regulons, which are involved in the regulation of these efflux pumps, as well as many other pathways in the cell [7,61,147,160–163].

5. Quinolone-Induced AMR

Along with the increase in FQ resistance that is seen with FQ use, there is also evidence that FQs may increase resistance to non-FQ antibiotics [164–168], particularly under sublethal or sub-MIC exposure. Treatments with sublethal FQs have been shown to increase mutation, recombination and persister formation rates, often leading to an increase in the frequency of resistance to non-quinolone antibiotics (Figure 7) [169–175].

5.1. Treatment with Quinolones Increases Resistance to Non-Quinolone Antibiotics (QIAR)

There is growing evidence, particularly from the livestock and veterinary sectors, that FQ use can lead to an increase in antibiotic-resistant isolates [176]. This resistance can be FQ resistance, resistance to non-FQ antimicrobials or multidrug resistance. Pereira et al. [166] looked at the resistance profiles of *E. coli* isolates from pre-weaned calves that were treated with enrofloxacin (Figure 2) or the cephalosporin ceftiofur for diarrhoea and respiratory diseases. They found that 77% of the isolates from the FQ-treated calves showed resistance to three or more antimicrobials, including ciprofloxacin, streptomycin, tetracycline, ampicillin, ceftiofur and chloramphenicol. In the study, only the calves treated with the FQ were significantly more likely to have non-susceptible *E. coli* isolates [166]. Similarly, a study on healthy chickens found an increase in the number of isolates resistant to doxycycline, amoxicillin and enrofloxacin in the commensal *E. coli* populations after treatment with enrofloxacin [164]. This was mirrored in more recent studies on commensal *E. coli* isolates from chickens and turkeys that were treated with enrofloxacin [167,168]. In the former study, multidrug resistance was identified in *E. coli* isolates from chickens treated with the FQ for *Salmonella* sp. infections [168], whilst, in the latter, *E. coli* isolates from turkeys treated with enrofloxacin were found to be resistant to ampicillin, despite ampicillin not being used in the study [167]. Further evidence comes from *Sa*. Typhimurium clinical isolates from pigs, which showed multidrug resistance following a single treatment of marbofloxacin (Figure 2) below the mutant prevention concentration [177]. This phenomenon is not peculiar to isolates from livestock; a strain of multidrug resistant *Sa. enteritidis* was isolated after a patient with a splenic abscess was treated with ciprofloxacin [178]. One of the first studies done in vitro looked at the resistance profiles of *Salmonella* spp. after repeated exposure to FQs and β-lactams. They found that mutants generated after treatments with various FQs showed reduced susceptibility to a wide range of the antibiotics tested (seven different antibiotics). This was in contrast to mutants generated under treatment with β-lactams, which showed reduced susceptibility to fewer antibiotics (five antibiotics) [179]. Similarly, it has been shown that the treatment of methicillin-resistant *St. aureus* with sublethal FQ further enhances methicillin resistance [169]. A similar effect is seen with *E. coli*, as cells become resistant to quinolone and non-quinolone antibiotics after exposure to sublethal FQ [180]. Alongside these studies that show increases in resistance to non-quinolone antibiotics after FQ treatment, there is also evidence that sublethal treatment with quinolones increases mutation rates, mutation frequencies and recombination [170–175].

5.2. Sublethal FQ Treatment Increases Mutation Rate

Quinolones are potent inducers of the SOS response [45,181–183]. As mentioned above, the SOS response is the bacterial response to DNA damage. It is regulated by RecA, a recombinase that is activated when there is DNA damage, and LexA, the repressor of the SOS regulon that autocleaves when RecA is active. The autocleavage of LexA results in the derepression of the SOS regulon that controls the expression of ~50 genes in *E. coli*, including three error-prone polymerases (PoI II, Pol IV and Pol V) that can introduce mutations [116]. Thus, it is not that surprising that quinolones could potentially increase the mutation rate. Indeed, many studies have shown that after the treatment with sublethal concentrations of FQs, there is an increase in mutation rate and mutation frequency [169–174,183–187].

Ysern et al. [183] were the first to show that the quinolones increase mutagenesis through the induction of the SOS response. They suggested that the mutagenic effect was through the upregulation

of Pol V. In 2005, Gillespie et al. [174] demonstrated that the treatment of *Mycobacterium fortuitum* with sub-MIC ciprofloxacin was able to increase the mutation rate by 72–120-fold. A more systematic study of the role of SOS in the mutagenic effect of quinolones was performed by Cirz et al. [184]. Using a neutropenic murine thigh infection model, they found that, in pathogenic *E. coli*, LexA, the repressor of the SOS response, was required for the evolution of the resistance induced by treatment with ciprofloxacin. They concluded that the homologous recombination pathway was important in the repair of ciprofloxacin-induced DNA damage and that LexA cleavage was induced during the repair. This then caused the upregulation of the three error-prone polymerases, which, together, generated the mutations that conferred resistance [184]. The same group went on to show that this was also the case in *P. aeruginosa* [173] and *St. aureus* [172]. LexA, RecA and error-prone DNA polymerases were also found to be upregulated in *M. tuberculosis* when treated with sublethal doses of ciprofloxacin [175]. Some groups, however, have suggested that upregulation of the error-prone polymerases is not the only mutagenic pathway induced by treatments with sublethal quinolones. Song et al. [188] showed that, when all three of the error-prone polymerases were deleted, ciprofloxacin-induced deletions still occurred. Long et al. [189] suggested that the increased mutagenesis observed with norfloxacin was not only due to the error-prone polymerases but, also, by indirect effects of the antibiotic on the mismatch-repair system and DNA-oxidative repair mechanisms. Oxidative stress has also been suggested as the main mutagenic pathway of a range of antibiotics, including norfloxacin, by Kohanski et al. [165]. They demonstrated that treating *E. coli* MG1655 with sublethal concentrations of norfloxacin in vitro caused multidrug resistance, which was abolished by the use of the ROS scavenger thiourea.

5.3. Sublethal FQ Treatment Stimulates Recombination

Sub-MIC treatment with quinolones have also been shown to increase genetic recombination. Ciprofloxacin has been demonstrated to stimulate homologous recombination in *E. coli* [170]. This was shown to be RecA-dependent and only partially reliant on induction of the SOS response; an uncleavable LexA mutant reduced the recombination but did not abolish it [170]. Sublethal ciprofloxacin was also demonstrated to induce nonhomologous recombination. This recombination was surprisingly independent of the SOS response but did require the other recombination pathways, RecBCD or RecFOR [171]. This study also looked at the effect of sublethal ciprofloxacin on conjugative transfer. Although they found no significant increase in the transfer of a conjugative plasmid, they did see an increase in horizontal gene transfer of an antibiotic-resistance gene from the plasmid to the genome [171]. Along these lines, three different FQs where shown to stimulate generalised transduction in *Sa.* Typhimurium. This was demonstrated through the transfer of a kanamycin resistance gene from a multidrug-resistant strain to susceptible strains through a P22-like bacteriophage [190].

5.4. Sublethal FQ Stimulates the Formation of Persisters

Another factor is how sublethal FQs has been shown to increase the presence of persister cells in the population [113,191–194]. Persisters are cells that can survive lethal concentrations of antibiotics due to phenotypic (but not genetic) changes. How persisters manage to survive antibiotic action is not clear, though it has been suggested that they do it by inactivating the drug target or lowering the drug uptake [195]. Persister cells have been demonstrated to form as a result of induction of the SOS response [113,192,193] or through a cellular response to starvation [194]. This persister population has also been shown to allow long-term survival to the exposure to the quinolone by allowing mutations to accumulate within the population that are then selected for by the antibiotic [113,191].

How sublethal FQs induce mutation appears to be complex, much like the lethality of quinolones and the repair of quinolone-induced DNA damage. There appear to be several pathways that lead to an increase in mutation. However, mutation seems to be a consequence of repair, and this mutagenesis does not increase the evolvability of the bacteria [196]. More work is needed to understand the role FQs play in mutagenesis, as a better understanding of how these drugs induce mutation may enable strategies to be put in place that will reduce their role in the acquisition of antibiotic resistance.

6. Future Prospects

The significant rise in FQ resistance over the last 20 years has mirrored the poorly controlled usage of this broad-ranged drug class [197]. However, this period has also seen the discontinuation of many FQs due to serious adverse side effects, such as several third-generation analogues, including grepafloxacin and sparfloxacin. To tackle FQ resistance, sensible usage guidelines must be followed worldwide. There are some restrictions in place at present, like the prohibited prescription of ciprofloxacin for complicated UTIs, but controls must become more widespread to make a greater impact [198]. There have recently been restrictions placed on the use of FQs for mild bacterial infections, but this is due to potential side effects and not for antimicrobial resistance reasons [199]. Alongside this, the evidence that the misuse and sublethal exposure of FQs is potentially leading to an increase in mutagenesis and resistance to other antibiotics is of concern. A systematic review into the extent of the problem is underway [200].

The continued discovery of novel antibiotics that are potent against non-resistant and resistant strains of bacteria (especially those with MDR) is key in the fight against resistance. Though somewhat diminished, the development of FQs is still ongoing, with a few pharmaceutical companies currently conducting research on the synthesis of novel FQs. Delafloxacin (Figure 1) is an example of a FQ recently approved for clinical use [201]. The structure of delafloxacin has three distinct features: a 3-hydroxyazetidine ring substituent at C-7, a chlorine atom at C-8 and a bi-fluorinated aromatic ring at N-1. Overall, the structure is more acidic than other FQs, meaning the compound is more likely to be deprotonated (at its C-3 carboxyl group) at a neutral pH. It has been demonstrated to be effective against quinolone- and methicillin-resistant *St. aureus* due to its improved cellular uptake in acidic conditions [202,203]. Furthermore, delafloxacin shows dual targeting, meaning it inhibits both gyrase and topo IV with equal affinity, in contrast to older FQs (with the exception of those with C-8 methoxy groups). Dual targeting is believed to reduce the likelihood of drug resistance, as seen with moxifloxacin [204–207]. The exact explanation for this dual affinity is not necessarily clear. It was suggested that the C-8 methoxy substituent of moxifloxacin allows for dual targeting [208]; however, the lack of this group in delafloxacin suggests that it could not be caused by the methoxy group alone. However, it may simply be due to different FQs having differential affinities for gyrase and topo IV, depending upon their side groups, and the particular arrangement of amino acids in the binding pockets of the enzymes. Further crystal structures of the quinolone-enzyme-DNA complex should illuminate this.

The search for FQ alternatives is also incredibly important for combatting resistance. The screening of both natural and synthetic compounds against gyrase and topo IV provides the opportunity for the discovery of such inhibitors. For instance, an allosteric-binding pocket was discovered within gyrase when a thiophene-based compound (Figure 2) showed significant inhibition during high-throughput screens at GSK [209]. An even more potent analogue was developed from this compound, though it was found to be toxic in animal trials. Usefully, the thiophene compounds also stabilise the gyrase-DNA cleavage complex and do not show any cross-resistance with quinolones [209], suggesting that further investigation is warranted. Such discoveries provide the rationale for future research on compound designs and highlight the importance of screening. The determination of the structures of several gyrase and topo IV enzymes bound to antibiotic compounds raises the possibility of computational drug design methods being used in the search for new agents.

The quinazolinediones are a class of compounds that are structurally similar to FQs but lack the C-4 carboxyl substituent required for water-metal ion bridge formation [210] (Figure 2). It was hoped that these molecules may be unaffected by the two key target enzyme mutations and possess significant inhibition activity. Unfortunately, challenges have been found with their low potency and concurrent human topo II poisoning. This poisoning of the homologous human enzymes has indicated the quinazolinediones' potential as anticancer agents, however [5]. The discovery of imidazopyrazinones (IPYs; Figure 2) as gyrase inhibitors that bind in a similar way to quinolones but

have a different resistance profile are examples of other compounds that may hold promise as future antibiotics [211,212].

Another class of new topoisomerase inhibitor are the NBTIs (Novel Bacterial Topoisomerase Inhibitors). These compounds, which include the spiropyrimidinetriones and the triazaacenaphthylenes, bind adjacent to the quinolone-binding pocket and are not subject to the resistance mutations in the QRDR. They inhibit the enzyme by intercalating into the DNA at the dimer interface, stabilizing a pre-cleaved state, which increases the prevalence of single-stranded DNA breaks. Two of these NBTIs, gepotidacin and zoliflodacin, are in phase III clinical trials for the treatment of uncomplicated gonorrhoea (ClinicalTrials.gov Identifier: NCT04010539 and ClinicalTrials.gov Identifier: NCT03959527 respectively).

The understanding of low-level resistance mechanisms, such as PMQR, also provides helpful insight into the development of novel antibacterial drugs. For instance, the use of efflux pump inhibitors, in combination with FQs, has significant potential in the treatment of FQ-resistant species [213,214].

Although the induction of resistance by FQ treatment seems to be multifactorial, many groups have suggested that a combinatorial approach may be the way forward to reduce the mutagenic effects. Some have suggested the use of drugs that inhibit RecA or stop the cleavage of LexA [186,215]. This would reduce the mutagenesis but, with targeting RecA, also potentiate the quinolones themselves [186,216]. This has also been shown to potentially re-sensitise quinolone-resistant mutants [217]. Other groups have argued for the use for antioxidants agents such as N-acetylcysteine, which has been shown to reduce ROS and SOS induction without reducing the antimicrobial activity of ciprofloxacin [218].

As well as understanding resistance mechanisms, more work is needed to elucidate the exact path of quinolone lethality and repair. The exact mechanisms that lead to bacterial death, especially the role of ROS in lethality need to be found. The same is true of the mechanisms of repair; we still do not know what proteins remove quinolone-poisoned topoisomerases, despite these proteins having been known in eukaryotes for decades. Moreover, the role of the SOS response and other stress responses, like oxidative damage repair or general stress repair, need to be clarified. Additionally, different quinolones kill in different ways, and it is likely that their damage is repaired through different pathways. Answering all these fundamental questions will help us to better understand how quinolones work and what specific components of their lethality and repair pathways should be targeted in order to avoid the appearance of quinolone and non-quinolone resistance.

Conflicts of Interest: The authors declare no conflict of interest. The funders had no role in the design of this study or the decision to publish.

References

1. Lesher, G.Y.; Froelich, E.J.; Gruett, M.D.; Bailey, J.H.; Brundage, R.P. 1,8-Naphthyridone derivatives. A new class of chemotherapeutic agents. *J. Med. Pharm. Chem.* **1962**, *91*, 1063–1065. [CrossRef]

2. Bisacchi, G.S. Origins of the quinolone class of antibacterials: An expanded "Discovery Story". *J. Med. Chem.* **2015**, *58*, 4874–4882. [CrossRef]

3. Gillespie, S.H. The role of moxifloxacin in tuberculosis therapy. *ERR* **2016**, *25*, 19–28. [CrossRef]

4. Oliphant, C.M.; Green, G.M. Quinolones: A comprehensive review. *Am. Fam. Physician* **2002**, *65*, 455–464.

5. Aldred, K.J.; Kerns, R.J.; Osheroff, N. Mechanism of quinolone action and resistance. *Biochemistry* **2014**, *53*, 1565–1574. [CrossRef]

6. EMEA/H/A-31/1452. *Quinolone-and Fluoroquinolone-Containing Medicinal Products*; European Commision: Amsterdam, The Netherlands, 2018.

7.	Correia, S.; Poeta, P.; Hébraud, M.; Capelo, J.L.; Igrejas, G. Mechanisms of quinolone action and resistance: Where do we stand? *J. Med. Microbiol.* **2017**, *66*, 551–559. [CrossRef]

8.	Emmerson, A.M.; Jones, A.M. The quinolones: Decades of development and use. *J. Antimicrob. Chemother.* **2003**, *51*, 13–20. [CrossRef]

9.	Appelbaum, P.C.; Hunter, P.A. The fluoroquinolone antibacterials: Past, present and future perspectives. *Int. J. Antimicrob. Agents* **2000**, *16*, 5–15. [CrossRef]

10.	Collin, F.; Karkare, S.; Maxwell, A. Exploiting bacterial DNA gyrase as a drug target: Current state and perspectives. *Appl. Microbiol. Biotechnol.* **2011**, *92*, 479–497. [CrossRef]

11.	Andriole, V.T. The quinolones: Past, present, and future. *Clin. Infect. Dis.* **2005**, *41*, S113–S119. [CrossRef]

12.	Drlica, K.; Zhao, X.; Malik, M.; Hiasa, H.; Mustaev, A.; Kerns, R. Fluoroquinolone Resistance. In *Bacterial Resistance to Antibiotics—From Molecules to Man*; Bonev, B.B., Brown, N.M., Eds.; John Wiley & Sons: Hoboken, NJ, USA, 2019; pp. 125–161. [CrossRef]

13.	Ball, P. Quinolone generations: Natural history or natural selection? *J. Antimicrob. Chemother.* **2000**, *46*, 17–24. [CrossRef]

14.	Rohlfing, S.R.; Gerster, J.R.; Kvam, D.C. Bioevaluation of the antibacterial flumequine for urinary tract use. *Antimicrob. Agents Chemother.* **1976**, *10*, 20–24. [CrossRef]

15.	Ito, A.; Hirai, K.; Inoue, M.; Koga, H.; Suzue, S.; Irikura, T.; Mitsuhashi, S. In vitro antibacterial activity of AM-715, a new nalidixic acid analog. *Antimicrob. Agents Chemother.* **1980**, *17*, 103–108. [CrossRef]

16.	Wolfson, J.S.; Hooper, D.C. Norfloxacin: A new targeted fluoroquinolone antimicrobial agent. *Ann. Intern. Med.* **1988**, *108*, 238–251. [CrossRef]

17.	Wolfson, J.S.; Hooper, D.C. Fluoroquinolone antimicrobial agents. *Clin. Microbiol. Rev.* **1989**, *2*, 378–424. [CrossRef]

18.	Van Bambeke, F.; Michot, J.M.; Van Eldere, J.; Tulkens, P.M. Quinolones in 2005: An update. *Clin. Microbiol. Infect.* **2005**, *11*, 256–280. [CrossRef]

19.	Adhami, Z.N.; Wise, R.; Weston, D.; Crump, B. The pharmacokinetics and tissue penetration of norfloxacin. *J. Antimicrob. Chemother.* **1984**, *13*, 87–92. [CrossRef]

20.	Aznar, J.; Caballero, M.C.; Lozano, M.C.; de Miguel, C.; Palomares, J.C.; Perea, E.J. Activities of new quinoline derivatives against genital pathogens. *Antimicrob. Agents Chemother.* **1985**, *27*, 76–78. [CrossRef]

21.	Holmes, B.; Brogden, R.N.; Richards, D.M. Norfloxacin. *Drugs* **1985**, *30*, 482–513. [CrossRef]

22.	Hooper, D.C.; Wolfson, J.S.; Souza, K.S.; Tung, C.; McHugh, G.L.; Swartz, M.N. Genetic and biochemical characterization of norfloxacin resistance in *Escherichia coli*. *Antimicrob. Agents Chemother.* **1986**, *29*, 639–644. [CrossRef]

23.	Norrby, S.R.; Jonsson, M. Antibacterial activity of norfloxacin. *Antimicrob. Agents Chemother.* **1983**, *23*, 15–18. [CrossRef]

24.	Schacht, P.; Chyský, V.; Gruenwaldt, G.; Hullmann, R.; Weuta, H.; Arcieri, G.; Griffith, E.; O'Brien, B.; Branolte, J.; Bruck, H.; et al. Worldwide clinical data on efficacy and safety of ciprofloxacin. *Infection* **1988**, *16*, S29–S43. [CrossRef]

25.	Segev, S.; Yaniv, I.; Haverstock, D.; Reinhart, H. Safety of long-term therapy with ciprofloxacin: Data analysis of controlled clinical trials and review. *Clin. Infect. Dis.* **1999**, *28*, 299–308. [CrossRef]

26.	World Health Organization. *WHO Model List of Essential Medicines, 20th List (March 2017, Amended August 2017)*; World Health Organization: Geneva, Switzerland, 2017.

27.	Mitscher, L.A. Bacterial topoisomerase inhibitors: Quinolone and pyridone antibacterial agents. *Chem. Rev.* **2005**, *105*, 559–592. [CrossRef]

28.	Ahuja, S.D.; Ashkin, D.; Avendano, M.; Banerjee, R.; Bauer, M.; Bayona, J.N.; Becerra, M.C.; Benedetti, A.; Burgos, M.; Centis, R.; et al. Multidrug resistant pulmonary tuberculosis treatment regimens and patient outcomes: An individual patient data meta-analysis of 9153 patients. *PLoS Med.* **2012**, *9*, e1001300. [CrossRef]

29.	Lucena, M.I.; Andrade, R.J.; Rodrigo, L.; Salmerón, J.; Alvarez, A.; Lopez-Garrido, M.J.; Camargo, R.; Alcantára, R. Trovafloxacin-induced acute hepatitis. *Clin. Infect. Dis.* **2000**, *30*, 400–401. [CrossRef]

30.	Mandell, L.; Tillotson, G. Safety of fluoroquinolones: An update. *Can. J. Infect. Dis.* **2002**, *13*, 54–61. [CrossRef]

31.	WHO. *Critically Important Antimicrobials for Human Medicine*, 5th ed.; World Health Organisation—WHO Advisory Group on Integrated Surveillance of Antimicrobial Resistance (AGISAR): Geneva, Switzerland, 2017; p. 48.

32. Domagala, J.M. Structure-activity and structure-side-effect relationships for the quinolone antibacterials. *J. Antimicrob. Chemother.* **1994**, *33*, 685–706. [CrossRef]

33. Gellert, M.; Mizuuchi, K.; O'Dea, M.H.; Itoh, T.; Tomizawa, J.-I. Nalidixic acid resistance: A second genetic character involved in DNA gyrase activity. *Proc. Natl. Acad. Sci. USA* **1977**, *74*, 4772–4776. [CrossRef]

34. Sugino, A.; Peebles, C.L.; Kreuzer, K.N.; Cozzarelli, N.R. Mechanism of action of nalidixic acid: Purification of Escherichia coli nalA gene product and its relationship to DNA gyrase and a novel nicking-closing enzyme. *Proc. Natl. Acad. Sci. USA* **1977**, *74*, 4767–4771. [CrossRef]

35. Bush, N.G.; Evans-Roberts, K.; Maxwell, A. DNA Topoisomerases. *EcoSal Plus* **2015**, *6*. [CrossRef]

36. Bates, A.D.; Maxwell, A. *DNA Topology*, 2nd ed.; Oxford University Press: New York, NY, USA, 2005; p. 216.

37. Gellert, M.; Mizuuchi, K.; O'Dea, M.H.; Nash, H.A. DNA gyrase: An enzyme that introduces superhelical turns into DNA. *Proc. Natl. Acad. Sci. USA* **1976**, *73*, 3872–3876. [CrossRef]

38. Wang, J.C. DNA Topoisomerases. *Annu. Rev. Biochem.* **1996**, *65*, 635–692. [CrossRef]

39. Berger, J.M. Type II DNA topoisomerases. *Curr. Opin. Struct. Biol.* **1998**, *8*, 26–32. [CrossRef]

40. Dar, M.A.; Sharma, A.; Mondal, N.; Dhar, S.K. Molecular cloning of apicoplast-targeted *Plasmodium falciparum* DNA gyrase genes: Unique intrinsic ATPase activity and ATP-independent dimerization of PfGyrB subunit. *Eukaryot. Cell* **2007**, *6*, 398–412. [CrossRef]

41. Wall, M.K.; Mitchenall, L.A.; Maxwell, A. *Arabidopsis thaliana* DNA gyrase is targeted to chloroplasts and mitochondria. *Proc. Natl. Acad. Sci. USA* **2004**, *101*, 7821–7826. [CrossRef]

42. Corbett, K.D.; Berger, J.M. Structure, molecular mechanisms, and evolutionary relationships in DNA topoisomerases. *Annu. Rev. Biophys. Biomol. Struct.* **2004**, *33*, 95–118. [CrossRef]

43. Roca, J.; Wang, J.C. The capture of a DNA double helix by an ATP-dependent protein clamp: A key step in DNA transport by type II DNA topoisomerases. *Cell* **1992**, *71*, 833–840. [CrossRef]

44. Wang, J. Moving one DNA double helix through another by a type II DNA topoisomerase: The story of a simple molecular machine. *Q. Rev. Biophys.* **1998**, *31*, 107–144. [CrossRef]

45. Drlica, K.; Zhao, X. DNA gyrase, topoisomerase IV, and the 4-quinolones. *Microbiol. Mol. Biol. Rev.* **1997**, *61*, 377–392. [CrossRef]

46. Hooper, D.C.; Jacoby, G.A. Topoisomerase inhibitors: Fluoroquinolone mechanisms of action and resistance. *Cold Spring Harb. Perspect. Med.* **2016**, *6*, a025320. [CrossRef]

47. Ferrero, L.; Cameron, B.; Manse, B.; Lagneaux, D.; Crouzet, J.; Famechon, A.; Blanche, F. Cloning and primary structure of *Staphylococcus aureus* DNA topoisomerase IV: A primary target of fluoroquinolones. *Mol. Microbiol.* **1994**, *13*, 641–653. [CrossRef]

48. Khodursky, A.B.; Zechiedrich, E.L.; Cozzarelli, N.R. Topoisomerase IV is a target of quinolones in *Escherichia coli. Proc. Natl. Acad. Sci. USA* **1995**, *92*, 11801–11805. [CrossRef]

49. Redgrave, L.S.; Sutton, S.B.; Webber, M.A.; Piddock, L.J. Fluoroquinolone resistance: Mechanisms, impact on bacteria, and role in evolutionary success. *Trends Microbiol.* **2014**, *22*, 438–445. [CrossRef]

50. Cheng, G.; Hao, H.; Dai, M.; Liu, Z.; Yuan, Z. Antibacterial action of quinolones: From target to network. *Eur. J. Med. Chem.* **2013**, *66*, 555–562. [CrossRef]

51. Drlica, K.; Hiasa, H.; Kerns, R.; Malik, M.; Mustaev, A.; Zhao, X. Quinolones: Action and resistance updated. *Curr. Top. Med. Chem.* **2009**, *9*, 981–998. [CrossRef]

52. Mustaev, A.; Malik, M.; Zhao, X.; Kurepina, N.; Luan, G.; Oppegard, L.M.; Hiasa, H.; Marks, K.R.; Kerns, R.J.; Berger, J.M.; et al. Fluoroquinolone-gyrase-DNA complexes: Two modes of drug binding. *J. Biol. Chem.* **2014**. [CrossRef]

53. Bax, B.D.; Chan, P.F.; Eggleston, D.S.; Fosberry, A.; Gentry, D.R.; Gorrec, F.; Giordano, I.; Hann, M.M.; Hennessy, A.; Hibbs, M.; et al. Type IIA topoisomerase inhibition by a new class of antibacterial agents. *Nature* **2010**, *466*, 935–940. [CrossRef]

54. Laponogov, I.; Sohi, M.K.; Veselkov, D.A.; Pan, X.-S.; Sawhney, R.; Thompson, A.W.; McAuley, K.E.; Fisher, L.M.; Sanderson, M.R. Structural insight into the quinolone–DNA cleavage complex of type IIA topoisomerases. *Nat. Struct. Mol. Biol.* **2009**, *16*, 667–669. [CrossRef]

55. Wohlkonig, A.; Chan, P.F.; Fosberry, A.P.; Homes, P.; Huang, J.; Kranz, M.; Leydon, V.R.; Miles, T.J.; Pearson, N.D.; Perera, R.L.; et al. Structural basis of quinolone inhibition of type IIA topoisomerases and target-mediated resistance. *Nat. Struct. Mol. Biol.* **2010**, *17*, 1152–1153. [CrossRef]

56. Tornaletti, S.; Pedrini, A.M. Studies on the interaction of 4-quinolones with DNA by DNA unwinding experiments. *Biochim. Biophys. Acta* **1988**, *949*, 279–287. [CrossRef]

57. Tornaletti, S.; Pedrini, A.M. DNA unwinding induced by nalidixic acid binding to DNA. *Biochem. Pharmacol.* **1988**, *37*, 1881–1882. [CrossRef]

58. Shen, L.L. A reply: "Do quinolones bind to DNA?"—Yes. *Biochem. Pharmacol.* **1989**, *38*, 2042–2044. [CrossRef]

59. Aldred, K.J.; Breland, E.J.; Vlckova, V.; Strub, M.P.; Neuman, K.C.; Kerns, R.J.; Osheroff, N. Role of the water-metal ion bridge in mediating interactions between quinolones and *Escherichia coli* topoisomerase IV. *Biochemistry* **2014**, *53*, 5558–5567. [CrossRef] [PubMed]

60. Aldred, K.J.; McPherson, S.A.; Turnbough, C.L., Jr.; Kerns, R.J.; Osheroff, N. Topoisomerase IV-quinolone interactions are mediated through a water-metal ion bridge: Mechanistic basis of quinolone resistance. *Nucleic Acids Res.* **2013**, *41*, 4628–4639. [CrossRef] [PubMed]

61. Hooper, D.C.; Jacoby, G.A. Mechanisms of drug resistance: Quinolone resistance. *Ann. N. Y. Acad. Sci.* **2015**, *1354*, 12–31. [CrossRef]

62. Snyder, M.; Drlica, K. DNA gyrase on the bacterial chromosome: DNA cleavage induced by oxolinic acid. *J. Mol. Biol.* **1979**, *131*, 287–302. [CrossRef]

63. Wentzell, L.M.; Maxwell, A. The complex of DNA gyrase and quinolone drugs on DNA forms a barrier to the T7 DNA polymerase replication complex. *J. Mol. Biol.* **2000**, *304*, 779–791. [CrossRef]

64. Willmott, C.J.R.; Critchlow, S.E.; Eperon, I.C.; Maxwell, A. The complex of DNA gyrase and quinolone drugs with DNA forms a barrier to transcription by RNA polymerase. *J. Mol. Biol.* **1994**, *242*, 351–363. [CrossRef]

65. Chen, C.-R.; Malik, M.; Snyder, M.; Drlica, K. DNA gyrase and topoisomerase IV on the bacterial chromosome: Quinolone-induced DNA cleavage. *J. Mol. Biol.* **1996**, *258*, 627–637. [CrossRef]

66. Malik, M.; Zhao, X.; Drlica, K. Lethal fragmentation of bacterial chromosomes mediated by DNA gyrase and quinolones. *Mol. Microbiol.* **2006**, *61*, 810–825. [CrossRef] [PubMed]

67. Carret, G.; Flandrois, J.P.; Lobry, J.R. Biphasic kinetics of bacterial killing by quinolones. *J. Antimicrob. Chemother.* **1991**, *27*, 319–327. [CrossRef] [PubMed]

68. Drlica, K.; Malik, M.; Kerns, R.J.; Zhao, X. Quinolone-mediated bacterial death. *Antimicrob. Agents Chemother.* **2008**, *52*, 385–392. [CrossRef] [PubMed]

69. Hong, Y.; Li, Q.; Gao, Q.; Xie, J.; Huang, H.; Drlica, K.; Zhao, X. Reactive oxygen species play a dominant role in all pathways of rapid quinolone-mediated killing. *J. Antimicrob. Chemother.* **2020**, *75*, 576–585. [CrossRef] [PubMed]

70. Jeong, K.S.; Xie, Y.; Hiasa, H.; Khodursky, A.B. Analysis of pleiotropic transcriptional profiles: A case study of DNA gyrase inhibition. *PLoS Genet.* **2006**, *2*, e152. [CrossRef] [PubMed]

71. Postow, L.; Crisona, N.J.; Peter, B.J.; Hardy, C.D.; Cozzarelli, N.R. Topological challenges to DNA replication: Conformations at the fork. *Proc. Natl. Acad. Sci. USA* **2001**, *98*, 8219–8226. [CrossRef]

72. Schvartzman, J.B.; Stasiak, A. A topological view of the replicon. *EMBO Rep.* **2004**, *5*, 256–261. [CrossRef]

73. Seol, Y.; Neuman, K.C. The dynamic interplay between DNA topoisomerases and DNA topology. *Biophys. Rev.* **2016**, *8*, 101–111. [CrossRef]

74. Peter, B.J.; Ullsperger, C.; Hiasa, H.; Marians, K.J.; Cozzarelli, N.R. The structure of supercoiled intermediates in DNA replication. *Cell* **1998**, *94*, 819–827. [CrossRef]

75. Sogo, J.M.; Stasiak, A.; Martínez-Robles, M.a.L.; Krimer, D.B.; Hernández, P.; Schvartzman, J.B. Formation of knots in partially replicated DNA molecules. *J. Mol. Biol.* **1999**, *286*, 637–643. [CrossRef]

76. Cebrián, J.; Castán, A.; Martínez, V.; Kadomatsu-Hermosa, M.J.; Parra, C.; Fernández-Nestosa, M.J.; Schaerer, C.; Hernández, P.; Krimer, D.B.; Schvartzman, J.B. Direct evidence for the formation of precatenanes during DNA replication. *J. Biol. Chem.* **2015**, *290*, 13725–13735. [CrossRef] [PubMed]

77. Sissi, C.; Palumbo, M. In front of and behind the replication fork: Bacterial type IIA topoisomerases. *Cell. Mol. Life Sci.* **2010**, *67*, 2001–2024. [CrossRef] [PubMed]

78. Pohlhaus, J.R.; Kreuzer, K.N. Norfloxacin-induced DNA gyrase cleavage complexes block *Escherichia coli* replication forks, causing double-stranded breaks in vivo. *Mol. Microbiol.* **2005**, *56*, 1416–1429. [CrossRef] [PubMed]

79. Zhao, X.; Malik, M.; Chan, N.; Drlica-Wagner, A.; Wang, J.-Y.; Li, X.; Drlica, K. Lethal action of quinolones against a temperature-sensitive *dnaB* replication mutant of *Escherichia coli*. *Antimicrob. Agents Chemother.* **2006**, *50*, 362–364. [CrossRef] [PubMed]

80. Gutierrez, A.; Stokes, J.M.; Matic, I. Our evolving understanding of the mechanism of quinolones. *Antibiotics* **2018**, *7*, 32. [CrossRef] [PubMed]

81. Shea, M.E.; Hiasa, H. The RuvAB branch migration complex can displace topoisomerase IV·quinolone·DNA ternary complexes. *J. Biol. Chem.* **2003**, *278*, 48485–48490. [CrossRef] [PubMed]

82. Hsiang, Y.-H.; Lihou, M.G.; Liu, L.F. Arrest of replication forks by drug-stabilized topoisomerase I-DNA cleavable complexes as a mechanism of cell killing by camptothecin. *Cancer Res.* **1989**, *49*, 5077–5082.

83. Tsao, Y.P.; Russo, A.; Nyamuswa, G.; Silber, R.; Liu, L.F. Interaction between replication forks and topoisomerase I-DNA cleavable complexes: Studies in a cell-free SV40 DNA replication system. *Cancer Res.* **1993**, *53*, 5908–5914.

84. Hsiang, Y.H.; Hertzberg, R.; Hecht, S.; Liu, L.F. Camptothecin induces protein-linked DNA breaks via mammalian DNA topoisomerase I. *J. Biol. Chem.* **1985**, *260*, 14873–14878.

85. Strumberg, D.; Pilon, A.A.; Smith, M.; Hickey, R.; Malkas, L.; Pommier, Y. Conversion of topoisomerase I cleavage complexes on the leading strand of ribosomal DNA into 5′-phosphorylated DNA double-strand breaks by replication runoff. *Mol. Cell. Biol.* **2000**, *20*, 3977–3987. [CrossRef]

86. Cortés, F.; Piñero, J.; Ortiz, T. Importance of replication fork progression for the induction of chromosome damage and SCE by inhibitors of DNA topoisomerases. *Mutat. Res. Lett.* **1993**, *303*, 71–76. [CrossRef]

87. Chow, R.T.; Dougherty, T.J.; Fraimow, H.S.; Bellin, E.Y.; Miller, M.H. Association between early inhibition of DNA synthesis and the MICs and MBCs of carboxyquinolone antimicrobial agents for wild-type and mutant [*gyrA nfxB(ompF) acrA*] *Escherichia coli* K-12. *Antimicrob. Agents Chemother.* **1988**, *32*, 1113–1118. [CrossRef]

88. Piddock, L.J.; Walters, R.N.; Diver, J.M. Correlation of quinolone MIC and inhibition of DNA, RNA, and protein synthesis and induction of the SOS response in *Escherichia coli*. *Antimicrob. Agents Chemother.* **1990**, *34*, 2331–2336. [CrossRef] [PubMed]

89. Deitz, W.H.; Cook, T.M.; Goss, W.A. Mechanism of action of nalidixic acid on *Escherichia coli*. 3. Conditions required for lethality. *J. Bacteriol.* **1966**, *91*, 768–773. [CrossRef] [PubMed]

90. Malik, M.; Hussain, S.; Drlica, K. Effect of anaerobic growth on quinolone lethality with *Escherichia coli*. *Antimicrob. Agents Chemother.* **2007**, *51*, 28–34. [CrossRef] [PubMed]

91. Sun, Y.; Saha, S.; Wang, W.; Saha, L.K.; Huang, S.-Y.N.; Pommier, Y. Excision repair of topoisomerase DNA-protein crosslinks (TOP-DPC). *DNA Repair* **2020**, *89*, 102837. [CrossRef]

92. Pommier, Y.; Huang, S.-y.N.; Gao, R.; Das, B.B.; Murai, J.; Marchand, C. Tyrosyl-DNA-phosphodiesterases (TDP1 and TDP2). *DNA Repair* **2014**, *19*, 114–129. [CrossRef]

93. Cortes Ledesma, F.; El Khamisy, S.F.; Zuma, M.C.; Osborn, K.; Caldecott, K.W. A human 5′-tyrosyl DNA phosphodiesterase that repairs topoisomerase-mediated DNA damage. *Nature* **2009**, *461*, 674–678. [CrossRef]

94. Pouliot, J.J.; Robertson, C.A.; Nash, H.A. Pathways for repair of topoisomerase I covalent complexes in *Saccharomyces cerevisiae*. *Genes Cells* **2001**, *6*, 677–687. [CrossRef]

95. Pouliot, J.J.; Yao, K.C.; Robertson, C.A.; Nash, H.A. Yeast gene for a Tyr-DNA phosphodiesterase that repairs topoisomerase I complexes. *Science* **1999**, *286*, 552–555. [CrossRef]

96. Aedo, S.; Tse-Dinh, Y.-C. SbcCD-mediated processing of covalent gyrase-DNA complex in *Escherichia coli*. *Antimicrob. Agents Chemother.* **2013**, *57*, 5116–5119. [CrossRef] [PubMed]

97. Connelly, J.C.; de Leau, E.S.; Leach, D.R.F. Nucleolytic processing of a protein-bound DNA end by the *E. coli* SbcCD (MR) complex. *DNA Repair* **2003**, *2*, 795–807. [CrossRef]

98. Tamayo, M.; Santiso, R.; Gosalvez, J.; Bou, G.; Fernández, J.L. Rapid assessment of the effect of ciprofloxacin on chromosomal DNA from *Escherichia coli* using an in situ DNA fragmentation assay. *BMC Microbiol.* **2009**, *9*, 69. [CrossRef] [PubMed]

99. Andryukov, B.G.; Somova, L.M.; Timchenko, N.F. Molecular and genetic characteristics of cell death in prokaryotes. *Mol. Gen. Microbiol. Virol.* **2018**, *33*, 73–83. [CrossRef]

100. Van Acker, H.; Coenye, T. The role of reactive oxygen species in antibiotic-mediated killing of bacteria. *Trends Microbiol.* **2017**, *25*, 456–466. [CrossRef]

101. Whitaker, A.M.; Schaich, M.A.; Smith, M.R.; Flynn, T.S.; Freudenthal, B.D. Base excision repair of oxidative DNA damage: From mechanism to disease. *Front. Biosci. (Landmark Ed.)* **2017**, *22*, 1493–1522. [CrossRef]

102. Imlay, J.A. Pathways of oxidative damage. *Annu. Rev. Microbiol.* **2003**, *57*, 395–418. [CrossRef]

103. Dwyer, D.J.; Collins, J.J.; Walker, G.C. Unraveling the physiological complexities of antibiotic lethality. *Annu. Rev. Pharmacol. Toxicol.* **2015**, *55*, 313–332. [CrossRef]

104. Hong, Y.; Zeng, J.; Wang, X.; Drlica, K.; Zhao, X. Post-stress bacterial cell death mediated by reactive oxygen species. *Proc. Natl. Acad. Sci. USA* **2019**, *116*, 10064–10071. [CrossRef]

105. Dwyer, D.J.; Kohanski, M.A.; Hayete, B.; Collins, J.J. Gyrase inhibitors induce an oxidative damage cellular death pathway in *Escherichia coli*. *Mol. Syst. Biol.* **2007**, *3*, 91. [CrossRef]

106. Liu, Y.; Imlay, J.A. Cell death from antibiotics without the involvement of reactive oxygen species. *Science* **2013**, *339*, 1210–1213. [CrossRef] [PubMed]

107. Keren, I.; Wu, Y.; Inocencio, J.; Mulcahy, L.R.; Lewis, K. Killing by bactericidal antibiotics does not depend on reactive oxygen species. *Science* **2013**, *339*, 1213–1216. [CrossRef] [PubMed]

108. Foti, J.J.; Devadoss, B.; Winkler, J.A.; Collins, J.J.; Walker, G.C. Oxidation of the guanine nucleotide pool underlies cell death by bactericidal antibiotics. *Science* **2012**, *336*, 315–319. [CrossRef] [PubMed]

109. Belenky, P.; Ye, J.D.; Porter, C.B.M.; Cohen, N.R.; Lobritz, M.A.; Ferrante, T.; Jain, S.; Korry, B.J.; Schwarz, E.G.; Walker, G.C.; et al. Bactericidal antibiotics induce toxic metabolic perturbations that lead to cellular damage. *Cell Rep.* **2015**, *13*, 968–980. [CrossRef] [PubMed]

110. Imlay, J.A. The molecular mechanisms and physiological consequences of oxidative stress: Lessons from a model bacterium. *Nat. Rev. Microbiol.* **2013**, *11*, 443–454. [CrossRef] [PubMed]

111. Imlay, J.A. Diagnosing oxidative stress in bacteria: Not as easy as you might think. *Curr. Opin. Microbiol.* **2015**, *24*, 124–131. [CrossRef] [PubMed]

112. Hong, Y.; Li, L.; Luan, G.; Drlica, K.; Zhao, X. Contribution of reactive oxygen species to thymineless death in *Escherichia coli*. *Nat. Microbiol.* **2017**, *2*, 1667–1675. [CrossRef]

113. Dörr, T.; Lewis, K.; Vulić, M. SOS response induces persistence to fluoroquinolones in *Escherichia coli*. *PLoS Genet.* **2009**, *5*, e1000760. [CrossRef]

114. Henderson, M.L.; Kreuzer, K.N. Functions that protect *Escherichia coli* from tightly bound DNA-protein complexes created by mutant EcoRII methyltransferase. *PLoS ONE* **2015**, *10*, e0128092. [CrossRef]

115. McDaniel, L.S.; Rogers, L.H.; Hill, W.E. Survival of recombination-deficient mutants of *Escherichia coli* during incubation with nalidixic acid. *J. Bacteriol.* **1978**, *134*, 1195–1198. [CrossRef]

116. Kreuzer, K.N. DNA damage responses in prokaryotes: Regulating gene expression, modulating growth patterns, and manipulating replication forks. *Cold Spring Harb. Perspect. Biol.* **2013**, *5*, a012674. [CrossRef] [PubMed]

117. Pribis, J.P.; García-Villada, L.; Zhai, Y.; Lewin-Epstein, O.; Wang, A.Z.; Liu, J.; Xia, J.; Mei, Q.; Fitzgerald, D.M.; Bos, J.; et al. Gamblers: An antibiotic-induced evolvable cell subpopulation differentiated by reactive-oxygen-induced general stress response. *Mol. Cell* **2019**, *74*, 785–800.e7. [CrossRef] [PubMed]

118. Storvik, K.A.M.; Foster, P.L. RpoS, the stress response sigma factor, plays a dual role in the regulation of *Escherichia coli*'s error-prone DNA polymerase IV. *J. Bacteriol.* **2010**, *192*, 3639–3644. [CrossRef] [PubMed]

119. Davies, J.; Davies, D. Origins and evolution of antibiotic resistance. *Microbiol. Mol. Biol. Rev.* **2010**, *74*, 417–433. [CrossRef] [PubMed]

120. Fair, R.J.; Tor, Y. Antibiotics and bacterial resistance in the 21st century. *Perspect. Med. Chem.* **2014**, *6*, 25–64. [CrossRef]

121. Phillips, I.; Casewell, M.; Cox, T.; De Groot, B.; Friis, C.; Jones, R.; Nightingale, C.; Preston, R.; Waddell, J. Does the use of antibiotics in food animals pose a risk to human health? A critical review of published data. *J. Antimicrob. Chemother.* **2004**, *53*, 28–52. [CrossRef]

122. Livermore, D.M.; Hope, R.; Reynolds, R.; Blackburn, R.; Johnson, A.P.; Woodford, N. Declining cephalosporin and fluoroquinolone non-susceptibility among bloodstream Enterobacteriaceae from the UK: Links to prescribing change? *J. Antimicrob. Chemother.* **2013**, *68*, 2667–2674. [CrossRef]

123. Spellberg, B.; Doi, Y. The rise of fluoroquinolone-resistant *Escherichia coli* in the community: Scarier than we thought. *J. Infect. Dis.* **2015**, *212*, 1853–1855. [CrossRef]

124. Dalhoff, A. Global fluoroquinolone resistance epidemiology and implictions for clinical use. *Interdiscip. Perspect. Infect. Dis.* **2012**, *2012*, 37. [CrossRef]

125. Kim, E.S.; Hooper, D.C. Clinical importance and epidemiology of quinolone resistance. *Infect. Chemother.* **2014**, *46*, 226–238. [CrossRef]

126. Yoshida, H.; Bogaki, M.; Nakamura, M.; Nakamura, S. Quinolone resistance-determining region in the DNA gyrase *gyrA* gene of *Escherichia coli*. *Antimicrob. Agents Chemother.* **1990**, *34*, 1271–1272. [CrossRef] [PubMed]

127. Avalos, E.; Catanzaro, D.; Catanzaro, A.; Ganiats, T.; Brodine, S.; Alcaraz, J.; Rodwell, T. Frequency and geographic distribution of *gyrA* and *gyrB* mutations associated with fluoroquinolone resistance in clinical *Mycobacterium tuberculosis* isolates: A systematic review. *PLoS ONE* **2015**, *10*, e0120470. [CrossRef] [PubMed]

128. Gensberg, K.; Jin, Y.F.; Piddock, L.J. A novel *gyrB* mutation in a fluoroquinolone-resistant clinical isolate of *Salmonella* Typhimurium. *FEMS Microbiol. Lett.* **1995**, *132*, 57–60. [CrossRef] [PubMed]

129. Yoshida, H.; Bogaki, M.; Nakamura, M.; Yamanaka, L.M.; Nakamura, S. Quinolone resistance-determining region in the DNA gyrase *gyrB* gene of *Escherichia coli*. *Antimicrob. Agents Chemother.* **1991**, *35*, 1647–1650. [CrossRef]

130. Morais Cabral, J.H.; Jackson, A.P.; Smith, C.V.; Shikotra, N.; Maxwell, A.; Liddington, R.C. Crystal structure of the breakage-reunion domain of DNA gyrase. *Nature* **1997**, *388*, 903–906. [CrossRef] [PubMed]

131. Friedman, S.M.; Lu, T.; Drlica, K. Mutation in the DNA gyrase A gene of *Escherichia coli* that expands the quinolone resistance-reterrming region. *Antimicrob. Agents Chemother.* **2001**, *45*, 2378–2380. [CrossRef]

132. Ince, D.; Hooper, D.C. Quinolone resistance due to reduced target enzyme expression. *J. Bacteriol.* **2003**, *185*, 6883–6892. [CrossRef]

133. Michel-Briand, Y.; Uccelli, V.; Laporte, J.-M.; Plesiat, P. Elimination of plasmids from Enterobacteriaceae by 4-quinolone derivatives. *J. Antimicrob. Chemother.* **1986**, *18*, 667–674. [CrossRef]

134. Weisser, J.; Wiedemann, B. Elimination of plasmids by enoxacin and ofloxacin at near inhibitory concentrations. *J. Antimicrob. Chemother.* **1986**, *18*, 575–583. [CrossRef]

135. Weisser, J.; Wiedemann, B. Inhibition of R-plasmid transfer in *Escherichia coli* by 4-quinolones. *Antimicrob. Agents Chemother.* **1987**, *31*, 531–534. [CrossRef]

136. Martínez-Martínez, L.; Pascual, A.; Jacoby, G.A. Quinolone resistance from a transferable plasmid. *Lancet* **1998**, *351*, 797–799. [CrossRef]

137. Vetting, M.W.; Hegde, S.S.; Fajardo, J.E.; Fiser, A.; Roderick, S.L.; Takiff, H.E.; Blanchard, J.S. Pentapeptide repeat proteins. *Biochem.* **2006**, *45*, 1–10. [CrossRef] [PubMed]

138. Jacoby, G.A.; Chow, N.; Waites, K.B. Prevalence of plasmid-mediated quinolone resistance. *Antimicrob. Agents Chemother.* **2003**, *47*, 559–562. [CrossRef] [PubMed]

139. Montero, C.; Mateu, G.; Rodriguez, R.; Takiff, H. Intrinsic resistance of *Mycobacterium smegmatis* to fluoroquinolones may be influenced by new pentapeptide protein MfpA. *Antimicrob. Agents Chemother.* **2001**, *45*, 3387. [CrossRef]

140. Collin, F.; Maxwell, A. The microbial toxin microcin B17: Prospects for the development of new antibacterial agents. *J. Mol. Biol.* **2019**, *431*, 3400–3426. [CrossRef]

141. Hegde, S.S.; Vetting, M.W.; Roderick, S.L.; Mitchenall, L.A.; Maxwell, A.; Takiff, H.E.; Blanchard, J.S. A fluoroquinolone resistance protein from *Mycobacterium tuberculosis* that mimics DNA. *Science* **2005**, *308*, 1480–1483. [CrossRef]

142. Xiong, X.; Bromley, E.H.C.; Oelschlaeger, P.; Woolfson, D.N.; Spencer, J. Structural insights into quinolone antibiotic resistance mediated by pentapeptide repeat proteins: Conserved surface loops direct the activity of a Qnr protein from a gram-negative bacterium. *Nucleic Acids Res.* **2011**, *39*, 3917–3927. [CrossRef]

143. Garrido, M.C.; Herrero, M.; Kolter, R.; Moreno, F. The export of the DNA replication inhibitor Microcin B17 provides immunity for the host cell. *EMBO J.* **1988**, *7*, 1853–1862. [CrossRef]

144. Jacoby, G.A.; Corcoran, M.A.; Hooper, D.C. Protective effect of Qnr on agents other than quinolones that target DNA gyrase. *Antimicrob. Agents Chemother.* **2015**, *59*, 6689–6695. [CrossRef]

145. Robicsek, A.; Strahilevitz, J.; Jacoby, G.A.; Macielag, M.; Abbanat, D.; Hye Park, C.; Bush, K.; Hooper, D.C. Fluoroquinolone-modifying enzyme: A new adaptation of a common aminoglycoside acetyltransferase. *Nat. Med.* **2006**, *12*, 83–88. [CrossRef]

146. Heisig, P.; Tschorny, R. Characterization of fluoroquinolone-resistant mutants of *Escherichia coli* selected in vitro. *Antimicrob. Agents Chemother.* **1994**, *38*, 1284–1291. [CrossRef] [PubMed]

147. Everett, M.J.; Jin, Y.F.; Ricci, V.; Piddock, L.J. Contributions of individual mechanisms to fluoroquinolone resistance in 36 *Escherichia coli* strains isolated from humans and animals. *Antimicrob. Agents Chemother.* **1996**, *40*, 2380–2386. [CrossRef] [PubMed]

148. Bolla, J.-M.; Alibert-Franco, S.; Handzlik, J.; Chevalier, J.; Mahamoud, A.; Boyer, G.; Kieć-Kononowicz, K.; Pagès, J.-M. Strategies for bypassing the membrane barrier in multidrug resistant Gram-negative bacteria. *FEBS Lett.* **2011**, *585*, 1682–1690. [CrossRef] [PubMed]

149. Fernández, L.; Hancock, R.E.W. Adaptive and mutational resistance: Role of porins and efflux pumps in drug resistance. *Clin. Microbiol. Rev.* **2012**, *25*, 661–681. [CrossRef]

150. Alekshun, M.N.; Levy, S.B. Regulation of chromosomally mediated multiple antibiotic resistance: The mar regulon. *Antimicrob. Agents Chemother.* **1997**, *41*, 2067–2075. [CrossRef]

151. Alekshun, M.N.; Levy, S.B. Molecular Mechanisms of Antibacterial Multidrug Resistance. *Cell* **2007**, *128*, 1037–1050. [CrossRef]

152. Davin-Regli, A.; Bolla, J.-M.; James, C.E.; Lavigne, J.-P.; Chevalier, J.; Garnotel, E.; Molitor, A.; Pages, J.-M. Membrane permeability and regulation of drug "influx and efflux" in enterobacterial pathogens. *Curr. Drug Targets* **2008**, *9*, 750–759. [CrossRef]

153. Van Bambeke, F.; Balzi, E.; Tulkens, P.M. Antibiotic efflux pumps. *Biochem. Pharmacol.* **2000**, *60*, 457–470. [CrossRef]

154. Papkou, A.; Hedge, J.; Kapel, N.; Young, B.; MacLean, R.C. Efflux pump activity potentiates the evolution of antibiotic resistance across *Staphylococcus aureus* isolates. *Nat. Commun.* **2020**, *11*, 3970. [CrossRef]

155. Schmalstieg, A.M.; Srivastava, S.; Belkaya, S.; Deshpande, D.; Meek, C.; Leff, R.; van Oers, N.S.C.; Gumbo, T. The antibiotic resistance arrow of time: Efflux pump induction is a general first step in the evolution of mycobacterial drug resistance. *Antimicrob. Agents Chemother.* **2012**, *56*, 4806–4815. [CrossRef]

156. Hernández, A.; Sánchez, M.B.; Martínez, J.L. Quinolone resistance: Much more than predicted. *Front. Microbiol.* **2011**, *2*, 22. [CrossRef] [PubMed]

157. Piddock, L.J.V.; Hall, M.C.; Walters, R.N. Phenotypic characterization of quinolone-resistant mutants of Enterobacteriaceae selected from wild type, *gyrA* type and multiplyresistant (*marA*) type strains. *J. Antimicrob. Chemother.* **1991**, *28*, 185–198. [CrossRef] [PubMed]

158. Strahilevitz, J.; Jacoby, G.A.; Hooper, D.C.; Robicsek, A. Plasmid-mediated quinolone resistance: A multifaceted threat. *Clin. Microbiol. Rev.* **2009**, *22*, 664–689. [CrossRef] [PubMed]

159. Costa, S.S.; Viveiros, M.; Amaral, L.; Couto, I. Multidrug efflux pumps in *Staphylococcus aureus*: An update. *Open Microbiol J.* **2013**, *7*, 59–71. [CrossRef] [PubMed]

160. Goldman, J.D.; White, D.G.; Levy, S.B. Multiple antibiotic resistance (mar) locus protects *Escherichia coli* from rapid cell killing by fluoroquinolones. *Antimicrob. Agents Chemother.* **1996**, *40*, 1266–1269. [CrossRef]

161. Kern, W.V.; Oethinger, M.; Jellen-Ritter, A.S.; Levy, S.B. Non-target gene mutations in the development of fluoroquinolone resistance in *Escherichia coli*. *Antimicrob. Agents Chemother.* **2000**, *44*, 814–820. [CrossRef]

162. Maneewannakul, K.; Levy, S.B. Identification for mar mutants among quinolone-resistant clinical isolates of *Escherichia coli*. *Antimicrob. Agents Chemother.* **1996**, *40*, 1695–1698. [CrossRef]

163. Oethinger, M.; Podglajen, I.; Kern, W.V.; Levy, S.B. Overexpression of the marA or soxS regulatory gene in clinical topoisomerase mutants of *Escherichia coli*. *Antimicrob. Agents Chemother.* **1998**, *42*, 2089–2094. [CrossRef]

164. Jurado, S.; Medina, A.; de la Fuente, R.; Ruiz-Santa-Quiteria, J.A.; Orden, J.A. Resistance to non-quinolone antimicrobials in commensal *Escherichia coli* isolates from chickens treated orally with enrofloxacin. *Jpn. J. Vet. Res.* **2015**, *63*, 195–200.

165. Kohanski, M.A.; DePristo, M.A.; Collins, J.J. Sublethal antibiotic treatment leads to multidrug resistance via radical-induced mutagenesis. *Mol. Cell* **2010**, *37*, 311–320. [CrossRef]

166. Pereira, R.V.; Siler, J.D.; Ng, J.C.; Davis, M.A.; Grohn, Y.T.; Warnick, L.D. Effect of on-farm use of antimicrobial drugs on resistance in fecal *Escherichia coli* of preweaned dairy calves. *J. Dairy Sci.* **2014**, *97*, 7644–7654. [CrossRef] [PubMed]

167. Chuppava, B.; Keller, B.; El-Wahab, A.A.; Meißner, J.; Kietzmann, M.; Visscher, C. Resistance of *Escherichia coli* in turkeys after therapeutic or environmental exposition with enrofloxacin depending on flooring. *Int. J. Environ. Res. Public Health* **2018**, *15*, 1993. [CrossRef] [PubMed]

168. Li, J.; Hao, H.; Dai, M.; Zhang, H.; Ning, J.; Cheng, G.; Shabbir, M.A.B.; Sajid, A.; Yuan, Z. Resistance and virulence mechanisms of *Escherichia coli* selected by Enrofloxacin in Chicken. *Antimicrob. Agents Chemother.* **2019**, *63*, e01824-18. [CrossRef] [PubMed]

169. Tattevin, P.; Basuino, L.; Chambers, H.F. Subinhibitory fluoroquinolone exposure selects for reduced beta-lactam susceptibility in methicillin-resistant *Staphylococcus aureus* and alterations in the SOS-mediated response. *Res. Microbiol.* **2009**, *160*, 187–192. [CrossRef] [PubMed]

170. Lopez, E.; Blazquez, J. Effect of subinhibitory concentrations of antibiotics on intrachromosomal homologous recombination in *Escherichia coli*. *Antimicrob. Agents Chemother.* **2009**, *53*, 3411–3415. [CrossRef] [PubMed]

171. Lopez, E.; Elez, M.; Matic, I.; Blazquez, J. Antibiotic-mediated recombination: Ciprofloxacin stimulates SOS-independent recombination of divergent sequences in *Escherichia coli*. *Mol. Microbiol.* **2007**, *64*, 83–93. [CrossRef] [PubMed]

172. Cirz, R.T.; Jones, M.B.; Gingles, N.A.; Minogue, T.D.; Jarrahi, B.; Peterson, S.N.; Romesberg, F.E. Complete and SOS-mediated response of *Staphylococcus aureus* to the antibiotic ciprofloxacin. *J. Bacteriol.* **2007**, *189*, 531–539. [CrossRef]

173. Cirz, R.T.; O'Neill, B.M.; Hammond, J.A.; Head, S.R.; Romesberg, F.E. Defining the *Pseudomonas aeruginosa* SOS response and its role in the global response to the antibiotic ciprofloxacin. *J. Bacteriol.* **2006**, *188*, 7101–7110. [CrossRef]

174. Gillespie, S.H.; Basu, S.; Dickens, A.L.; O'Sullivan, D.M.; McHugh, T.D. Effect of subinhibitory concentrations of ciprofloxacin on *Mycobacterium fortuitum* mutation rates. *J. Antimicrob. Chemother.* **2005**, *56*, 344–348. [CrossRef]

175. O'Sullivan, D.M.; Hinds, J.; Butcher, P.D.; Gillespie, S.H.; McHugh, T.D. *Mycobacterium tuberculosis* DNA repair in response to subinhibitory concentrations of ciprofloxacin. *J. Antimicrob. Chemother.* **2008**, *62*, 1199–1202. [CrossRef]

176. Marshall, B.M.; Levy, S.B. Food animals and antimicrobials: Impacts on human health. *Clin. Microbiol. Rev.* **2011**, *24*, 718–733. [CrossRef] [PubMed]

177. Lee, S.J.; Park, N.H.; Mechesso, A.F.; Lee, K.J.; Park, S.C. The phenotypic and molecular resistance induced by a single-exposure to sub-mutant prevention concentration of marbofloxacin in *Salmonella* Typhimurium isolates from swine. *Vet. Microbiol.* **2017**, *207*, 29–35. [CrossRef] [PubMed]

178. Pers, C.; Søgaard, P.; Pallesen, L. Selection of multiple resistance in *Salmonella enteritidis* during treatment with ciprofloxacin. *Scand. J. Infect. Dis.* **1996**, *28*, 529–531. [CrossRef] [PubMed]

179. Cebrian, L.; RodríGuez, J.C.; Escribano, I.; Royo, G. Effect of exposure to fluoroquinolones and beta-lactams on the in vitro activity of other groups of antibiotics in *Salmonella* spp. *APMIS* **2006**, *114*, 523–528. [CrossRef]

180. Ching, C.; Zaman, M.H. Development and selection of low-level multi-drug resistance over an extended range of sub-inhibitory ciprofloxacin concentrations in *Escherichia coli*. *Sci. Rep.* **2020**, *10*, 8754. [CrossRef]

181. Piddock, L.J.V.; Wise, R. Induction of the SOS response in *Escherichia coli* by 4-quinolone antimicrobial agents. *FEMS Microbiol. Lett.* **1987**, *41*, 289–294. [CrossRef]

182. Lewin, C.S.; Howard, B.M.A.; Ratcliff, N.T.; Smith, J.T. 4-Quinolones and the SOS response. *J. Med. Microbiol.* **1989**, *29*, 139–144. [CrossRef]

183. Ysern, P.; Clerch, B.; Castaño, M.; Gibert, I.; Barbé, J.; Llagostera, M. Induction of SOS genes in *Escherichia coli* and mutagenesis in *Salmonella typhimurium* by fluoroquinolones. *Mutagenesis* **1990**, *5*, 63–66. [CrossRef]

184. Cirz, R.T.; Chin, J.K.; Andes, D.R.; de Crecy-Lagard, V.; Craig, W.A.; Romesberg, F.E. Inhibition of mutation and combating the evolution of antibiotic resistance. *PLoS Biol.* **2005**, *3*, e176. [CrossRef]

185. Cirz, R.T.; Romesberg, F.E. Induction and inhibition of ciprofloxacin resistance-conferring mutations in hypermutator bacteria. *Antimicrob. Agents Chemother.* **2006**, *50*, 220–225. [CrossRef]

186. Thi, T.D.; López, E.; Rodríguez-Rojas, A.; Rodríguez-Beltrán, J.; Couce, A.; Guelfo, J.R.; Castañeda-García, A.; Blázquez, J. Effect of *recA* inactivation on mutagenesis of *Escherichia coli* exposed to sublethal concentrations of antimicrobials. *J. Antimicrob. Chemother.* **2011**, *66*, 531–538. [CrossRef] [PubMed]

187. Blazquez, J.; Rodriguez-Beltran, J.; Matic, I. Antibiotic-induced genetic variation: How it arises and how it can be prevented. *Annu. Rev. Microbiol.* **2018**, *72*, 209–230. [CrossRef] [PubMed]

188. Song, L.Y.; Goff, M.; Davidian, C.; Mao, Z.; London, M.; Lam, K.; Yung, M.; Miller, J.H. Mutational consequences of ciprofloxacin in *Escherichia coli*. *Antimicrob. Agents Chemother.* **2016**, *60*, 6165–6172. [CrossRef] [PubMed]

189. Long, H.; Miller, S.F.; Strauss, C.; Zhao, C.; Cheng, L.; Ye, Z.; Griffin, K.; Te, R.; Lee, H.; Chen, C.-C.; et al. Antibiotic treatment enhances the genome-wide mutation rate of target cells. *Proc. Natl. Acad. Sci. USA* **2016**, *113*, E2498–E2505. [CrossRef] [PubMed]

190. Bearson, B.L.; Brunelle, B.W. Fluoroquinolone induction of phage-mediated gene transfer in multidrug-resistant Salmonella. *Int. J. Antimicrob. Agents* **2015**, *46*, 201–204. [CrossRef]

191. Barrett, T.C.; Mok, W.W.K.; Murawski, A.M.; Brynildsen, M.P. Enhanced antibiotic resistance development from fluoroquinolone persisters after a single exposure to antibiotic. *Nat. Commun.* **2019**, *10*, 1177. [CrossRef]

192. Goneau, L.W.; Yeoh, N.S.; MacDonald, K.W.; Cadieux, P.A.; Burton, J.P.; Razvi, H.; Reid, G. Selective target inactivation rather than global metabolic dormancy causes antibiotic tolerance in uropathogens. *Antimicrob. Agents Chemother.* **2014**, *58*, 2089–2097. [CrossRef]

193. Theodore, A.; Lewis, K.; Vulić, M. Tolerance of *Escherichia coli* to fluoroquinolone antibiotics depends on specific components of the SOS response pathway. *Genetics* **2013**, *195*, 1265–1276. [CrossRef]

194. Gutierrez, A.; Jain, S.; Bhargava, P.; Hamblin, M.; Lobritz, M.A.; Collins, J.J. Understanding and sensitizing density-dependent persistence to quinolone antibiotics. *Mol. Cell* **2017**, *68*, 1147–1154.e3. [CrossRef]

195. Fisher, R.A.; Gollan, B.; Helaine, S. Persistent bacterial infections and persister cells. *Nat. Rev. Microbiol.* **2017**, *15*, 453–464. [CrossRef]

196. Torres-Barceló, C.; Kojadinovic, M.; Moxon, R.; MacLean, R.C. The SOS response increases bacterial fitness, but not evolvability, under a sublethal dose of antibiotic. *Proc. R. Soc. B* **2015**, *282*, 20150885. [CrossRef] [PubMed]

197. Almalki, Z.S.; Yue, X.; Xia, Y.; Wigle, P.R.; Guo, J.J. Utilization, Spending, and Price Trends for Quinolones in the US Medicaid Programs: 25 Years' Experience 1991–2015. *Pharmacoecon. Open* **2017**, *1*, 123–131. [CrossRef] [PubMed]

198. Durkin, M.J.; Keller, M.; Butler, A.M.; Kwon, J.H.; Dubberke, E.R.; Miller, A.C.; Polgreen, P.M.; Olsen, M.A. An assessment of inappropriate antibiotic use and guideline adherence for uncomplicated urinary tract infections. *Open Forum Infect. Dis.* **2018**, *5*. [CrossRef] [PubMed]

199. Richards, G.A.; Brink, A.J.; Feldman, C. Rational use of the fluoroquinolones. *S. Afr. Med. J. S. Afr. Med. Tydskr.* **2019**, *109*, 378–381. [CrossRef] [PubMed]

200. Ching, C.; Orubu, E.S.F.; Wirtz, V.J.; Zaman, M.H. Bacterial antibiotic resistance development and mutagenesis following exposure to subminimal inhibitory concentrations of fluoroquinolones in vitro: A systematic literature review protocol. *BMJ Open* **2019**, *9*, e030747. [CrossRef] [PubMed]

201. Jorgensen, S.C.J.; Mercuro, N.J.; Davis, S.L.; Rybak, M.J. Delafloxacin: Place in therapy and review of microbiologic, clinical and pharmacologic properties. *Infect. Dis. Ther* **2018**, *7*, 197–217. [CrossRef]

202. Chan, P.F.; Huang, J.; Bax, B.D.; Gwynn, M.N. Recent developments in inhibitors of bacterial type IIA topoisomerases. In *Antibiotics: Targets, Mechanisms and Resistance*; Gualerzi, C.O., Brandi, L., Fabbretti, A., Pon, C.L., Eds.; Wiley-VCH Verlag GmbH & Co: Weinheim, Germany, 2014; pp. 263–297.

203. Candel, F.J.; Peñuelas, M. Delafloxacin: Design, development and potential place in therapy. *Drug Design Dev. Ther.* **2017**, *11*, 881–891. [CrossRef]

204. Houssaye, S.; Gutmann, L.; Varon, E. Topoisomerase mutations associated with *in vitro* selection of resistance to moxifloxacin in *Streptococcus pneumoniae*. *Antimicrob. Agents Chemother.* **2002**, *46*, 2712–2715. [CrossRef]

205. Li, X.; Zhao, X.; Drlica, K. Selection of *Streptococcus pneumoniae* mutants having reduced susceptibility to moxifloxacin and levofloxacin. *Antimicrob. Agents Chemother.* **2002**, *46*, 522–524. [CrossRef]

206. Takei, M.; Fukuda, H.; Kishii, R.; Hosaka, M. Target preference of 15 duinolones against *Staphylococcus aureus*, based on antibacterial activities and target inhibition. *Antimicrob. Agents Chemother.* **2001**, *45*, 3544–3547. [CrossRef]

207. Varon, E.; Janoir, C.; Kitzis, M.D.; Gutmann, L. ParC and GyrA may be interchangeable initial targets of some fluoroquinolones in *Streptococcus pneumoniae*. *Antimicrob. Agents Chemother.* **1999**, *43*, 302–306. [CrossRef] [PubMed]

208. Kishii, R.; Takei, M.; Fukuda, H.; Hayashi, K.; Hosaka, M. Contribution of the 8-methoxy group to the activity of gatifloxacin against type II topoisomerases of *Streptococcus pneumoniae*. *Antimicrob. Agents Chemother.* **2003**, *47*, 77–81. [CrossRef]

209. Chan, P.F.; Germe, T.; Bax, B.D.; Huang, J.; Thalji, R.K.; Bacqué, E.; Checchia, A.; Chen, D.; Cui, H.; Ding, X.; et al. Thiophene antibacterials that allosterically stabilize DNA-cleavage complexes with DNA gyrase. *Proc. Natl. Acad. Sci. USA* **2017**, *114*, E4492–E4500. [CrossRef]

210. Drlica, K.; Mustaev, A.; Towle, T.R.; Luan, G.; Kerns, R.J.; Berger, J.M. Bypassing fluoroquinolone resistance with quinazolinediones: Studies of drug–gyrase–DNA complexes having implications for drug design. *ACS Chem. Biol.* **2014**, *9*, 2895–2904. [CrossRef] [PubMed]

211. Germe, T.; Vörös, J.; Jeannot, F.; Taillier, T.; Stavenger, R.A.; Bacqué, E.; Maxwell, A.; Bax, B.D. A new class of antibacterials, the imidazopyrazinones, reveal structural transitions involved in DNA gyrase poisoning and mechanisms of resistance. *Nucleic Acids Res.* **2018**, *46*, 4114–4128. [CrossRef] [PubMed]

212. Jeannot, F.; Taillier, T.; Despeyroux, P.; Renard, S.; Rey, A.; Mourez, M.; Poeverlein, C.; Khichane, I.; Perrin, M.-A.; Versluys, S.; et al. Imidazopyrazinones (IPYs): Non-quinolone bacterial topoisomerase inhibitors showing partial cross-resistance with quinolones. *J. Med. Chem.* **2018**, *61*, 3565–3581. [CrossRef]

213. Askoura, M.; Mottawea, W.; Abujamel, T.; Taher, I. Efflux pump inhibitors (EPIs) as new antimicrobial agents against *Pseudomonas aeruginosa*. *Libyan J. Med.* **2011**, *6*. [CrossRef]

214. Lomovskaya, O.; Warren, M.S.; Lee, A.; Galazzo, J.; Fronko, R.; Lee, M.; Blais, J.; Cho, D.; Chamberland, S.; Renau, T.; et al. Identification and characterization of inhibitors of multidrug resistance efflux pumps in *Pseudomonas aeruginosa*: Novel agents for combination therapy. *Antimicrob. Agents Chemother.* **2001**, *45*, 105–116. [CrossRef]

215. Mo, C.Y.; Manning, S.A.; Roggiani, M.; Culyba, M.J.; Samuels, A.N.; Sniegowski, P.D.; Goulian, M.; Kohli, R.M. Systematically altering bacterial SOS activity under stress reveals therapeutic strategies for potentiating antibiotics. *mSphere* **2016**, *1*, e00163-16. [CrossRef]

216. Klitgaard, R.N.; Jana, B.; Guardabassi, L.; Nielsen, K.L.; Løbner-Olesen, A. DNA damage repair and drug efflux as potential targets for reversing low or intermediate ciprofloxacin resistance in *E. coli* K-12. *Front. Microbiol.* **2018**, *9*, 1438. [CrossRef]

217. Recacha, E.; Machuca, J.; Díaz de Alba, P.; Ramos-Güelfo, M.; Docobo-Pérez, F.; Rodriguez-Beltrán, J.; Blázquez, J.; Pascual, A.; Rodríguez-Martínez, J.M. Quinolone resistance reversion by targeting the SOS response. *mBio* **2017**, *8*, e00971-17. [CrossRef] [PubMed]

218. Rodríguez-Rosado, A.I.; Valencia, E.Y.; Rodríguez-Rojas, A.; Costas, C.; Galhardo, R.S.; Rodríguez-Beltrán, J.; Blázquez, J. N-acetylcysteine blocks SOS induction and mutagenesis produced by fluoroquinolones in *Escherichia coli*. *J. Antimicrob. Chemother.* **2019**, *74*, 2188–2196. [CrossRef] [PubMed]

Publisher's Note: MDPI stays neutral with regard to jurisdictional claims in published maps and institutional affiliations.